TRANSCRIPTIONAL ADAPTATION OF ADIPOSE TISSUE IN DAIRY COWS IN RESPONSE TO ENERGY OVERFEEDING

BY

PENG JI

DISSERTATION

Submitted in partial fulfillment of the requirements
for the degree of Doctor of Philosophy in Animal Sciences
in the Graduate College of the
University of Illinois at Urbana-Champaign, 2011

Urbana, Illinois

Doctoral Committee:

Professor James K. Drackley, Chair and Director of Research
Associate Professor Juan J. Loor, Director of Research
Professor Walter L. Hurley
Assistant Professor Yuan-Xiang Pan

ABSTRACT

In experiment 1, 18 multiparous non-pregnant non-lactating Holstein dairy cows were fed either moderate energy diet (MoE, NE_L = 1.62 Mcal/kg DM) or controlled energy diet (LoE, NE_L = 1.35 Mcal/kg DM) for 8 weeks and sacrificed. Compared with LoE animals, MoE cows had markedly increased visceral adipose mass (Nikkhah et al., unpublished data). Higher dietary energy plane significantly increased lipogenic gene expression in both visceral and subcutaneous adipose tissue (AT). Visceral AT (including mesenteric and omental fat; MES and OAT) exhibited higher mRNA profile for genes associated with utilization of long-chain fatty acid (LCFA), whereas subcutaneous AT (SUBQ) had greater gene expression related with *de novo* FA synthesis. Visceral AT, particularly MES, showed greater mRNA expression of pro-inflammatory cytokines, chemokines, and acute-phase protein. In conclusion, overfeeding energy may increase visceral AT secretion of pro-inflammatory cytokines by stimulating fat accumulation in visceral AT depots. (For the contents in chapter 3 and 4)

In experiment 2, mRNA samples of MES and SUBQ collected from a subset of animals (5 cows from each treatment) that used in experiment 1 was utilized to conduct transcriptomic study through microarray technique. The microarray platform contains 13k annotated bovine oligonucleotides. A FDR value of 0.2 was used as the cut-off threshold for determination of differentially expressed genes (DEG). Totally 409 and 310 DEGs were identified due to either adipose depot effect or dietary energy effect. Bioinformatics analysis revealed that gene sets associated with extracellular matrix, vasculature development and cytoskeleton formation were differentially expressed between MES and SUBQ. Overfeeding energy had significant impact on the genes in the pathway of MAPK signaling and apoptosis, and response to external stimuli. (For the contents in chapter 5)

In experiment 3, 14 Holstein dairy cows (≥ 2 parity, a subset from another study) were fed the same controlled energy diet during far-off dry period (-50 to -22 d) and randomly assigned to either moderate energy diet (Overfed, NE_L = 1.47 Mcal/kg DM) or controlled energy diet (Controlled, NE_L = 1.24 Mcal/kg DM) during close-up dry period (-21 d until parturition). Compared with Controlled group, Overfed animals had lower and higher serum NEFA in pre- and postpartum respectively, higher prepartal insulin and close-up DMI, and greater postpartal hepatic lipid storage and BHBA production. No difference in milking performance was found between the two groups. AT biopsy was carried out on -10, 7 and 21 d relative to parturition date for RNA extraction and gene expression analysis through quantitative PCR (qPCR). Energy overfeeding increased prepartal lipogenic genes and pre- and early postpartal lipolytic related gene (*ATGL* and *ABHD5*) expression in subcutaneous AT, but decreased *PDE3B* expression during periparturient period. Part of AT from biopsy of -10 and 7 d was used for tissue explant and challenged with hyperphysiological bovine insulin *in vitro*. Over-consumption of dietary energy increased and decreased insulin-stimulated IRS1 tyrosine phosphorylation in AT in pre- and postpartum, respectively, which may contribute to differentially regulated lipolysis in these overfed animals. (For contents in chapter 6)

Keywords: Transcrition, Adipose tissue, Transition period, Dairy cow, Energy overfeeding

ACKNOWLEDGEMENTS

I give the deepest gratitude to my advisors, Dr. James K. Drackley and Dr. Juan J. Loor, for their guidance and financial support throughout my graduate study, especially for their great patience with me during my first year in U.S. This is one of my best experiences to study in their laboratories. I thank Dr. Walter L. Hurley and Dr. Yuan-Xiang Pan for serving as my committee. Their suggestions, encouragements and consideration gave me a lot of help while composing the thesis. I thank Dr. Michael F. Hutjens, whose enthusiasm and whole-souled dedication to students and dairy industry is the best class per se. I also want to give my thanks to Dr. Massimo Bionaz for teaching me the whole set of lab technique, his seriousness and passion to scientific research always inspired me to learn more.

I thank Dr. Jan E. Novakofski for his advice on the research. I appreciate all the help from dairy farm staff, who make the experiments more propitious. I thank HiDee Ekstrom for her secretarial support during the past three years.

It is such a wonderful experience to recognize all graduate fellows and post-doctors in two laboratories, and had your friendship accompanying me through the Ph.D. study. I thank Dr. Nicole Janovick, Dr. Kasey Moyes, Dr. Bruce Richards, Dr. Guido Invernizzi, Joel Vasquez, Johan Osorio, Sonia Moisa, Shaoyu Luan, Arnulfo Pineda, Dr. Daniel Graugnard, Jawad Khan, Aisha Naeem, Dr. Kathiravan Periasamy, Jackie Ploetz, Kate Cowles, Phil Cardoso, Juan Castro, Jing Li, Shuowen Chen, Haji Akbar, Khuram Shahzad, Wes Hornback.

I also want to give my special thanks to my dear friends: Dr. James E. Pettigrew and Mrs Cinda Pettigrew, Dr. Minho Song and his family, Juliana Soares and Ferdinando Almeida, Dr.

Tung M. Che and his family, Dr. Pedro Urriola and his family, Nicola Serao and his family, Jeong Jae Lee and Soo Rin Kim, Ju Lan Chun, Mrs Xianhui Fu and her family, Fang Yang and Han Jiang, Shaoyu Luan and his family, and all the fellows in Chinese Tiger Soccer team. I always feel lucky to know you. You and the times we shared will be missed.

Finally, to my dearest family, my mother Mrs. Xia Wu, my wife Yanhong Liu and our baby in her belly, and my father-in-law Mr. Zhixiu Liu and mother-in-law Mrs. Xiuyun Mao, I owe you so much that cannot be expressed. I will try my best to take good care of you, to be a good son, husband and father.

University of Illinois at Urbana-Champaign (UIUC) is such a place that you always can easily find someone to answer your questions, no matter it is a puzzle of your research or the confusion you met in your life. I am very happy to spend the most valuable years of my student life here.

Peng Ji
August 11, 2011

TABLE OF CONTENTS

LIST OF TABLES viii

LIST OF FIGURES x

LIST OF ABBREVIATIONS xii

CHAPTER 1. LITERATURE REVIEW 1

Overview 1
Adipose Tissue Development in Ruminants: Hyperplasia and Hypertrophy 3
Transcriptional Control of Adipogenesis 5
Specific Characteristics of Lipid Metabolism in AT of Ruminants 9
Visceral vs. Subcutaneous Adipose Tissue 11
Difference in Cellularity 11
Difference in Lipogenic Capacity 12
Difference in Lipolytic Activity 14
Visceral Obesity, Inflammation, and Metabolic Disease 15
Physiological Adaptation and Lipid Metabolism During the Transition Period 18
Homeorhetic Control During the Transition Period 18
Hormonal Adaptation 19
Dry Matter Intake and Energy Balance 21
Adipose Tissue Metabolism 25
Hyperlipidemia and Liver Dysfunction 28
Insulin Resistance Symptom 32
Effect of Prepartal Plane of Dietary Energy on Lipid Metabolism During the Transition Period 39
Prepartal Dietary Energy Plane 40
Hypothesis of Current Research 43
Literature Cited 44

CHAPTER 2. OVERFEEDING ENERGY UPREGULATES PPARγ-CONTROLLED ADIPOGENIC NETWORKS AND INDUCIBLE ADIPOCYTOKINES IN VISCERAL AND SUBCUTANEOUS ADIPOSE DEPOTS OF HOLSTEIN COWS 60

Abstract 60
Introduction 61
Materials and Methods 63
Results and Discussion 69
Summary and Conclusions 84
Literature Cited 84
Tables and Figures 93

CHAPTER 3. INFLAMMATION- AND LIPID METABOLISM-RELATED GENE NETWORK SIGNATURES IN VISCERAL AND SUBCUTANEOUS ADIPOSE DEPOTS OF DAIRY COWS 108

Abstract 108
Introduction 109
Materials and Methods 111
Results and Discussion 116
Summary and Conclusions 122
Literature Cited 123
Tables and Figures 127

CHPATER 4. TRANSCRIPTIONAL CHANGES IN MESENTERIC AND SUBCUTANEOUS ADIPOSE TISSUE FROM HOLSTEIN COWS IN RESPONSE TO PLANE OF DIETARY ENERGY 134

Abstract 134
Introduction 135
Materials and Methods 137
Results 146
Discussion 150
Literature Cited 160
Tables and Figures 166

CHAPTER 5. PREPARTAL PLANE OF DIETARY ENERGY CHANGED INSULIN SIGNALING TRANSDUCTION AND TRANSCRIPTIONAL ADAPTATION OF ADIPOSE TISSUE OF DAIRY COWS DURING TRANSITION PERIOD 176

Abstract 176
Introduction 178
Materials and Methods 181
Results 186
Discussion 189
Conclusions 205
Literature Cited 205
Tables and Figures 213

CHAPTER 6. SUMMARY AND CONCLUSIONS 228

Literature Cited 235

APPENDIX A. STUDY OF HEPATIC LIPID ACCUMULATION, FIBROSIS AND AGGREGATION OF MATURE MACROPHAGES VIA HISTOCHEMICAL AND IMMUNOHISTOCHEMICAL TECHNIQUE 236

VITA 252

LIST OF TABLES

Table Page

2.1 DMI, BW, BCS, visceral organ mass, visceral adipost tissue mass and serum metabolites in cows either overfed energy (OVE, NEL = 1.62 Mcal/kg DM) or fed the controlled energy diet (CON, NEL = 1.35 Mcal/kg DM). 93

2.2 Ingredients and nutrient composition of diets (% of DM) 94

2.3 GenBank accession number, hybridization position, sequence, and amplicon size of primers use to analyze gene expression by qPCR 95

2.4 Gene symbol, name and percentage of mRNA abundance among all genes investigated in each treatment 96

2.5 Correlation analysis of SCD and THRSP mRNA level with net energy intake. 98

S2.1 Sequencing results using BLASTN from NCBI (http://blast.ncbi.nlm.nih.gov/Blast.cgi) 99

S2.2 Sequencing results obtained from PCR products 100

S2.3 qPCR performances among 29 genes measured in adipose tissues....101

3.1 Ingredients and nutrient composition of diets (% of DM) 127

3.2 Gene symbol, name and percentage of mRNA abundance among all genes investigated in each adipose tissue site 128

3.3 Correlation analysis of SCD and LEP mRNA level with BCS and tissue weight. 130

4.1 DEG (FDR ≤ 0.2) with expression difference ≥ 2-fold between dietary treatments (OVE vs. CON) 166

4.2 DEG (FDR ≥ 0.2) with expression difference ≥ 2-fold between tissues (MAT vs. SAT) 167

4.3 Fold change consistency of genes investigated in qPCR and microarray 169

5.1 Ingredient and nutrient composition of diets 213

5.2 Effect of close-up overfeeding energy on DMI, NE_L, blood metabolites and production of dairy cows 214

S5.1 Gene symbol, full name and subcellular localization and mRNA abundance for genes investigated 215

S5.2 GenBank accession number, hybridization position, sequence, and amplicon size of primers used to analyze gene expression in qPCR 217

LIST OF FIGURES

Figure Page

2.1 Main effect of dietary energy intake on mRNA expression of genes involved in lipid metabolism. 102

2.2 Main effect of dietary energy intake on mRNA expression of transcriptional regulator genes. 103

2.3 Main effect of dietary energy intake on mRNA expression of cytokines. 104

2.4 Putative network and changes in transcription profile of genes in CON vs. OVE cows 105

S2.1 Panel A, average expression stability M of remaining genes tested in the pairwise comparison. Panel B, optimal number of ICG for normalization. 107

3.1 Main effect of adipose site on mRNA expression of genes involved in lipid metabolism 131

3.2 Main effect of adipose site level on mRNA expression of transcriptional regulator genes 132

3.3 Main effect of adipose site on mRNA expression of cytokines. 133

4.1 Most representative cellular component (Cc) in GO analyses among DEG in either diet or tissue comparison. 170

4.2 Most representative molecular functions (Mf) in GO analyses among DEG in either diet or tissue comparison. 171

4.3 Most representative biological process (Bp) in GO analyses among DEG in either diet or tissue comparison. 172

4.4 The FLUX and IMPACT of main- and sub-categories of KEGG PATHWAY database due to main effects of fat depots (SAT vs. MAT) or dietary energy plane (OVE vs. CON). 173

4.5 The FLUX, IMPACT and the DEGs for the most over-represented KEGG pathway in comparison of fat depots (MAT vs. SAT) 174

4.6 The FLUX, IMPACT and the DEGs for the most over-represented KEGG pathway in comparison of dietary energy plane (OVE vs. CON). 175

5.1 Daily DMI (kg/d) from -21 to 28 d relative to parturition for cows either fed controlled energy diet (CON, n = 7) or moderate energy diet (OVE, n = 7) during close-up dry period (-21 d to parturition). 219

5.2 Daily milk yield (kg/d) from parturition until 30 d in lactation.....219

5.3 Weekly whole-body energy balance (% of requirements) from -3 to 4 wk relative to parturition. 220

5.4 Liver lipid and triglyceride content (wt % of the wet tissue wt) at -10, 7 and 21 d relative to parturition.....220

5.5 Temporal concentrations of serum insulin and metabolites from -14 to 21 d relative to parturition.....221

5.6 Relative mRNA expressions of genes involved in insulin signaling pathway in adipose tissue of transition dairy cows in response to close-up energy overfeeding.....222

5.7 Relative mRNA expressions of genes associated with *de novo* FA synthesis (*ACLY*, *ACACA*, *FASN* and *SCD*), cytosolic acetate activation (*ACSS2*) and cytosolic NADPH production (*G6PD* and *IDH1*) in adipose tissue of transition dairy cows in response to close-up energy overfeeding 223

5.8 Relative mRNA expressions of genes associated with LCFA import and activation (*LPL* and *ACSL1*), TAG synthesis (*GPAM* and *DGAT2*) and glyceroneogenesis (*PCK1*) in adipose tissue of transition dairy cows in response to close-up energy overfeeding.....224

5.9 Relative mRNA expressions of genes associated with lipolysis in adipose tissue of transition dairy cows in response to close-up energy overfeeding. 225

5.10 Relative mRNA expressions of transcriptional factors (*CEBPA*, *PPARG* and *SREBF1*) and fasting induced adipose factor (*ANGPTL4*) in adipose tissue of transition dairy cows in response to close-up energy overfeeding.....226

5.11 IRS1 tyrosine phosphorylation (IRS1-pY) in vitro.....227

LIST OF ABBREVIATIONS

ABHD5 (*ABHD5*)	adipose triglyceride lipase activator protein (gene symbol, italicized, the same as below)
ACACA (*ACACA*)	acetyl CoA carboxylase
ACLY (*ACLY*)	ATP citrate lyase
ACS	acetyl CoA synthetase
ACSS2 (*ACSS2*)	cytosolic acetyl-CoA synthetase
ACTB (*ACTB*)	actin, beta
ADFP (*ADFP*)	adipose differentiation-related protein
ADIPOQ (*ADIPOQ*)	adiponectin
ADRB1 (*ADRB1*)	β-adrenergic receptor 1
ADRB2 (*ADRB2*)	β-adrenergic receptor 2
ADRB3 (*ADRB3*)	β-adrenergic receptor 3
AGPAT (*AGPAT*)	1-acylglycerol-3-phosphate O-acyltransferase
AKT (*AKT*)	serine/threonine protein kinase Akt
AMP	adenosine monophosphate
ANGPTL4 (*ANGPTL4*)	angiopoietin-like 4
ApoB(100)	apolipoprotein B(100)
ApoE	apolipoprotein E
AT	adipose tissue
ATGL (*ATGL*)	adipose triglyceride lipase
ATP	adenosine-5'-triphosphate
BCA	bicinchoninic acid
BCS	body condition score
BHBA	B-hydroxybutyrate
bHLH	basic helix–loop–helix
BW	body weight
C	carbon
°C	degrees celsius
Ca	calcium
C/EBP	CCAAT/enhancer binding protein
cAMP	cyclic adenosine monophosphate
CCK	cholecystokinin
CCL2 (*CCL2*)	chemokine (C-C motif) ligand 2
CCL5 (*CCL5*)	chemokine (C-C motif) ligand 5

CD14	cluster of differentiation 14
CD68	cluster of differentiation 68
cDNA	complementary deoxyribonucleic acid
CEBPα (*CEBPA*)	CCAAT/enhancer binding protein, alpha
ChIP	chromatin immunoprecipitation
ChoRE	carbohydrate response element
ChREBP (*MLXIPL*)	carbohydrate response element binding protein
CoA	coenzyme A
CON	controlled-energy diet
CP	crude protein
CPT-1	carnitine palmitoyltransferase I
CRP	C-reactive protein
Ct	the threshold cycle
d	Day
DAG	diacylglycerol
DGAT2 (*DGAT2*)	diacylglycerol O-acyltransferase 2
DIM	day in milk
dl	deciliter
DLK1 (*DLK1*)	delta-like 1 homolog
DM	dry matter
DMEM	Dulbecco's Modified Eagle Medium
DMI	dry matter intake
DNA	deoxyribonucleic acid
DNS	*de novo* FA synthesis
EBW	empty body weight
ECM	energy corrected milk yield
ED_{50}	the hormone concentration required to produce a half-maximal
ELISA	enzyme-linked immunosorbent assay
ELOVL6 (*ELOVL6*)	elongation of long chain fatty acids
F4/80	transmembrane protein on cell-surface of mature macrophage
FA	fatty acid
FASN (*FASN*)	fatty acid synthase
FATP	fatty acid transport protein
FCM	fat-corrected milk yield
g	gram
G6PDH (*G6PDH*)	glucose-6-phosphate dehydrogenase

GCR	glucose clearance rate
GH	growth hormone
GHR (*GHR*)	growth hormone receptor
GI	gastrointestinal tract
GIP	glucose-dependent insulinotropic polypeptide
GLP-1	glucagon-like peptide 1-amide
GLUT1 (*GLUT1*)	glucose transporter 1
GLUT4 (*GLUT4*)	glucose transporter 4
GPAM (*GPAM*)	mitochondrial glycerol-3-phosphate acyltransferase
GPAT	glycerol-3-phosphate acyltransferase
GSC	ground shelled corn
GTT	glucose tolerance test
h	hour
H	hydrogen
HCl	hydrochloric acid
HMG-CoA	3-hydroxy-3-methylglutaryl-coenzyme A
ICG	internal control gene
IDH1 (*IDH1*)	NADP-isocitrate dehydrogenase 1
IL-1β (*IL1B*)	interleukin-1 beta
IL-6 (*IL6*)	interleukin-6
IL6R (*IL6R*)	interleukin-6 receptor
iNOS	inducible nitric oxidase
IPA	Ingenuity Pathway Analysis
IR	insulin resistance
INSR (*INSR*)	insulin receptor
IRS1 (*IRS1*)	insulin receptor substrate 1
IRS1-pY	IRS1 tyrosine phosphorylation
IRS2 (*IRS2*)	insulin receptor substrate 2
KEAP1 (*KEAP1*)	kelch-like ECH-associated protein 1
kg	kilogram
L	liter
LCFA	long chain fatty acid
LDL	low-density lipoprotein
LEP (*LEP*)	leptin
LIPE (*LIPE*)	hormone-sensitive lipase
LPIN1 (*LPIN1*)	lipin 1

LPL (*LPL*)	lipoprotein lipase
LPS	lipopolysaccharide
LXR	liver X receptor
m	meter
M	molar
MAPK	Mitogen-activated protein kinase
Mcal	megacalorie
MAT	mesenteric adipose tissue
MCP-1 (*CCL2*)	monocyte chemoattractant protein
MD	NADP-malate dehydrogenase
MD-2	lymphocyte antigen 96
ME	metabolizable energy
mEq	milliequivalent
mg	milligram
Mg	magnesium
MIB	maximum insulin binding
min	minute
MJ	megajoule
ml	milliliter
mm	millimeter
mM	millimolar
mmol	millimole
Mn	manganese
mRNA	messenger ribonucleic acid
MRP63 (*MRP63*)	mitochondrial ribosomal protein 63
MTP	microsomal triglyceride transfer protein
MW	mature weight
MyD88 (*MYD88*)	myeloid differentiation factor 88
n	number of samples
N	nitrogen
Na	sodium
NADH	nicotinamide adenine dinucleotide
NADPH	nicotinamide adenine dinucleotide phosphate
NCBI	National Center for Biotechnology Information
NDF	Neutral detergent fiber
NEB	negative energy balance

NEFA	non-esterified fatty acids
NE_L	net energy for location
NFC	nonfiber carbohydrate
NFκB	nuclear factor kappa-light-chain-enhancer of activated B cells
nmol	nanomole
NRC	National Research Council
NO	nitric oxide
NTC	non-template control
OAT	omental adipose tissue
OVE	overfed-energy diet
PA	phosphatidic acid
PAP	phosphatidate phosphatases
PBS	phosphate buffered saline
PCK1 (*PCK1*)	phosphoenolpyruvate carboxykinase 1
PDE3B (*PDE3B*)	phosphodiesterase 3B
PDH	pyruvate dehydrogenase
PDV	portal drained visceral
PEPCK (*PEPCK*)	phosphoenolpyruvate carboxykinase
PGD	6-phosphogluconate dehydrogenase
PI3Ks	phosphatidylinositol 3-kinases
PKA	protein kinase A
PPARγ (*PPARG*)	peroxisome proliferator-activated receptor gamma
PPRE	PPAR responsive elements
PRL	prolactin
qPCR	quantitative polymerase chain reaction
r	correlation coefficient
R	restricted intake
RBP4 (*RBP4*)	retinol binding protein-4
rbST	recombinant bovine somatotropin
RES	restricted intake
RIN	RNA integrity
R_{max}	the maximal response to insulin
RNA	ribonucleic acid
RPS9 (*RPS9*)	ribosomal protein S9
RT	reverse transcription
RXR	retinoic X receptor

SAA3 (*SAA3*)	acute-phase serum amyloid A3
SAT	subcutaneous adipose tissue
SC	dry ground corn replaced 21% of the corn silage
SCD (*SCD*)	stearoyl CoA desaturase
SE	standard error
SN	sympathetic nervous system
SRE	sterol regulatory elements
SRS	Statistical Analysis System
SREBP1c (*SREBF1*)	sterol regulatory element binding transcription factor 1c
T_3	3,5,3'-triiodothyronine
TAG	triglyceride
TCA	tricarboxylic acid
TF	transcriptional factors
TH	thyroid hormone
THRSP (*THRSP*)	thyroid hormone responsive SPOT 14
TIR	Toll/IL-1 receptor
TLR4 (*TLR4*)	toll-like receptor 4
TMR	total mixed ration
TNFα (*TNF*)	tumor necrosis factor alpha
TR	thyroid hormone receptor
TRIM41 (*TRIM41*)	tripartite motif-containing 41
TRα	isomer of TR
TZD	thiazolidinediones
VAT	visceral adipose tissue
VLDL	very low density lipoprotein
wk	week
wt	weight
Zfp423 (*ZNF423*)	zinc-finger protein

CHAPTER 1

LITERATURE REVIEW

Overview

To maintain a certain amount of body fat as a reserve of energy is essential for wild animals, as it helps animals to survive food scarcity and fierce climate change. However, for domestic animals, which are relatively well-protected from extreme weather and food shortage, body fat has been bestowed new significance based on its intrinsic interest. For beef cattle, body fatness was directly associated with economical values. Those cattle that produce more intramuscular fat rather than subcutaneous fat bring more profits to producers. For dairy cows, adipose tissue (AT) plays a critical role as an energy source to support lactation in high producing cows; however, over-mobilization of body fat during negative energy balance (NEB) in early lactation may induce fatty liver disease and ketosis, which may compromise milk production for the entire lactation (Vernon et al., 1984; Drackley, 1999; Grummer, 1993). The transition period, generally defined as 3 wk before and after parturition, is characterized by the occurrence of marked metabolic changes of AT in dairy cows, such as decreased insulin response and sensitivity, greatly suppressed lipogenesis, and intense lipolysis. Although metabolic activity of AT during this crucial period has been illustrated in several studies (McNamara and Hillers, 1986; McNamara et al., 1995; Vernon, 1996), the underlying molecular mechanisms that regulate and adapt to these metabolic changes have not been clearly established.

The discovery of leptin in 1994 (Zhang et al., 1994) led to the recognition of an endocrine function of AT. Since then, a great number of protein products have been demonstrated to be

secreted or specifically secreted from AT during different physiological states. Many of these products are pro-inflammatory cytokines, chemokines, and signaling molecules that function in endocrine, paracrine, or autocrine manners to regulate immune response, food intake, and metabolism (Tilg and Moschen, 2008; Ouchi et al., 2011). Studies in human and rodent animals have revealed that endocrine functions of AT exhibit depot-specific characteristics, and that visceral obesity is closely associated with a variety of metabolic diseases including insulin resistance and non-alcholic fatty liver disease (Tilg and Moschen, 2008; Palou et al., 2009). However, the depot-specific metabolic and endocrine characteristics and their association with metabolic disorders have been much less documented in ruminant animals.

Many nutritional strategies have been utilized in the dairy industry to regulate AT metabolism in dairy cows with the purpose of maximizing milk production and minimizing metabolic disorders. For example, recombinant bovine somatotropin (rbST) has been administered after mid-lactation to redirect nutrients from deposition in peripheral tissues to milk production. On the other hand, despite variation of results, niacin has been supplemented during the periparturient period to prevent fatty liver and ketosis through decreasing AT lipolysis. Energy status of the whole animal is an important factor that regulates lipid metabolism of AT. Particularly during the transition period, several studies from our laboratory have shown that the plane of prepartal dietary energy intake was able to manipulate lipid metabolic profiles during periparturient period (Dann et al., 2006; Douglas et al., 2006). However, the molecular response and adaptation of AT to dietary energy plane prepartum have not been illustrated before. In addition, despite the intensive research in human and rodent AT metabolism, the ruminant-specific AT metabolic characteristics need to be established.

To study the metabolic activity of AT during different physiological states in animals requires that major metabolic pathways, such as lipolysis, lipogenesis, and NADPH production be clarified. Enzymes primarily control the nutrient flux through these pathways. Although enzyme activity, which is subjected to regulation from different levels, is the predominant driving force that regulates metabolic activity, transcriptional change is the one representing relatively long-term adaptations. Quantitative polymerase chain reaction (qPCR) and microarray are two main genomic tools utilized to study mRNA expression. Hence, utilization of tissue biopsy coupled with these genomic tools may shed light on tissue metabolic adaptation to various physiological states and nutritional regulation.

Adipose Tissue Development in Ruminants: Hyperplasia and Hypertrophy

Adipose tissue is present in all mammalian species. White AT is the only tissue in the body that can markedly change its mass after adult size is reached. The cellular development associated with AT growth involves both cellular hyperplasia (increase in number) and hypertrophy (increase in size or volume), of which the two types of adipose expension were collectively termed adipogenesis. Adipogenesis typically involves: the determination stage, namely hyperplasia; the conversion of a pluripotent stem cell to the preadipocyte, which cannot be distinguished morphologically from its precursor cell but has lost the potential to differentiate into other cell types; and the terminal differentiation stage, during which the preadipocyte takes on the characteristics of the mature adipocyte by acquiring the machinery necessary for lipid transport and synthesis, insulin sensitivity, and the secretion of adipocyte-specific proteins. Hypertrophy occurs during the differentiation state, and is the result of triglyceride (TAG) accumulation in existing adipocytes primarily due to a positive energy balance (Rosen and MacDougald, 2006; Hausman et al., 2009).

The development of AT during the growth of animals is defined as an increase in adipocytes by number (hyperplasia) and/or by volume (hypertrophy). Hood (1982) summarized that the development of AT in ruminants (especially for beef cattle) occurred in three phases: an initial period of hyperplasia, a period of combined hyperplasia and hypertrophy, and a period when fattening occurs only by hypertrophy. Age, breed, physiological status of the animal, and potential limitation of adipocyte size seemed to be crucial factors in determining the major pathway driving adipogenesis. Hood (1982) pointed out that the age at which cell division is complete in AT varies among species and tissue sites. Hyperplasia is generally confined to early stages of postnatal development. Hood and Allen (1973a) found that bovine adipocyte hyperplasia in subcutaneous and perirenal depots were nearly complete at ~8 mo of life. Hood and Thornton (1979) found that although hyperplasia remains active in sheep AT until approximately 11 mo of age, hypertrophy was the predominant type of growth of body fat as demonstrated by the good relationships between both carcass weights and internal depot fat and the volume of adipose cells in the corresponding depots. Moreover, Cianzio et al. (1985) found that fat deposition in mesenteric and subcutaneous depots of steers during the growing phase occurred mainly via hypertrophy.

The great differences in total fat content and distribution of fat among breeds had been observed in early studies (e.g., 20 mo-old Holstein vs. Hereford cattle in Truscott et al., 1980; Holstein vs. Hereford×Angus steers in Hood and Allen, 1973b). Dairy cattle generally have less subcutaneous fat than beef cattle at a given weight (Allen et al., 1976). Truscott et al. (1980) reported that 20-mo-old Hereford cattle had more subcutaneous AT than Holsteins because of an increased number of adipose cells. Robelin (1981) studied the development of AT (subcutaneous, intermuscular, and internal) in male cattle (Friesian and Charolais) growing from 15 to 65% of

the mature weight. In each fat tissue, adipose cells became 15 times larger from 15 to 65% of mature weight, whereas total adipose cell number increased only 1.8-fold during this period. However, a significant hyperplasia occurred at near 45% of mature weight, when mean cell diameter reached approximately 80 to 90 μm. In all fat depots, a pattern of two-phase development was observed, which began with an increase in small-sized adipocytes (hyperplasia) and then followed by the filling of these cells (hypertorphy) (Robelin, 1981). For mature dairy cows, McNamara et al. (1995) and Smith and McNamara (1990) observed an obvious trend for increased adipocyte number per gram of subcutaneous AT from early lactation until 120 DIM. However, a reciprocal decrease in size (represented by diameter) and volume of adipose cell occurred during the same period. Thereafter, changes in adipocyte size in semi-adult and adult ruminants, including lactating ruminants, may account for the majority of changes in body fat mass, despite the possibility of changes in absolute cell number *pari passu*.

Transcriptional Control of Adipogenesis

Adipocytes derive from multipotent mesenchymal stem cells. The conversion of the stem cell to mature, lipid-filled adipoctye is termed adipogenesis, also known as hyperplasia, which was described as proceeding in two phases of development (Hausman et al., 1999; Rosen and MacDougald, 2006). The first phase is known as determination, which includes the commitment process of a pluripotent stem cell to a preadipocyte. Preadipocytes cannot be distinguished morphologically from their precursor cells, but have lost the potential to differentiate into other cell types. Preadipocytes possess proliferating capability and can enlarge AT mass by increasing cell numbers. However, once preadipocytes go into the second phase, namely terminal differentiation, they lose the capability of proliferation (Sethi and Vidal-Puig, 2007). During differentiation, preadipocytes take on the characteristics of mature adipocytes by a change in

morphology from fibroblastic to the unilocular appearance of lipid-filled fat cells (Gregoire et al., 1998). Meanwhile, differentiation is also characterized by the expression of a series of transcription factors in a sequential cascade, which finally results in the expression of genes related with lipogenesis, FA transport, increased insulin sensitivity, endocrine function, and increased lipogenic capacity (Ailhaud et al., 1992).

The cumulative consideration of the experiments has led to a model for a transcriptional cascade in regulating preadipocyte differentiation (adipogenesis) and adipocyte function. This network of transcription factors coordinates expression of hundreds of proteins responsible for establishing the mature adipocyte. The center event of this network is the activation of C/EBPs and PPARγ, which are essential in regulating the entire terminal differentiation process. In particular, PPARγ is considered the master regulator of adipogenesis and enables the precursor cell to express any known aspect of the adipocyte phenotype (Rosen et al., 2002). In this model, the transient activation of C/EBPβ and δ precedes and induces expression of PPARγ (Wu et al., 1996) and C/EBPα (Cao et al., 1991), which is likely through direct binding to C/EBP binding sites in the promoter regions of these two genes (Christy et al., 1991; Zhu et al., 1995; Clarke et al., 1997; Fajas et al., 1997). PPARγ was reported to be responsible for induction of C/EBPα (Rosen et al., 1999), whereas the expression of C/EBPα was suggested to be required for maintaining expression of PPARγ in the mature fat cell (Wu et al., 1999). In vitro studies demonstrated that the failure to express C/EBPα results in insulin resistance in cell culture systems and the loss of ability to develop WAT in vivo (Wu et al., 1999; Linhart et al., 2001). In addition to the above mentioned network between C/EBP family and PPARγ, the insulin-induced expression of SREBF1c was identified as a parallel pathway that was prior to and contributed to expression and activity of PPARγ (Kim and Spiegelman, 1996). The underlying mechanism of

SREBF1 on PPARγ expression was reported to be through a SREBP binding site in the promoter of PPARγ (Fajas et al., 1999), and contributing to production of an endogenous PPARγ ligand, which is still unknown yet, was suggested to be the method that SREBF1 increased PPARγ activity (Kim et al., 1998a). A brief introduction about how these TF function, including PPARγ, C/EBPα, and SREBF1 and their target genes, is given below.

PPARγ: PPARγ is a nuclear receptor that has been implicated in not only adipogenesis, but also insulin sensitivity of adipocytes. Four mRNA isoforms of PPARγ arise from differential promoter action and alternative splicing (Feve, 2005). However, the mRNA of PPARγ3 and 4 yield proteins identical to that of PPARγ1, hence only PPARγ1 and 2 receptors are finally translated (Gurnell, 2005). Both are expressed in adipocytes, but PPARγ2 is the form that is involved in differentiation by regulating gene expression (Rosen and Spiegelman, 2001; Lehrke and Lazar, 2005). PPARγ is not only crucial for adipogenesis but is also required for maintenance of the differentiated state (Rosen and MacDougald, 2006). After binding of small lipophilic ligands activated PPARγ exerts function to regulate gene expression through forming heterodimers with retinoic X receptor (RXR), and then binding to specific PPAR responsive elements (PPRE) in enhancer regions of target genes to initiate transcription activity (Osumi et al., 1991; Tugwood et al., 1992). Target genes directly regulated by PPARγ that are involved in this pathway include lipoprotein lipase (LPL; Schoonjans et al., 1996), fatty acid transport protein (FATP; Frohnert et al., 1999), oxidized LDL receptor1 (Chui et al., 2005), and phosphoenolpyruvate carboxykinase (PEPCK; Tontonoz et al., 1995) as well as others (see review in Lehrke and Lazar, 2005). Additionally, PPARγ was reported to induce expression of GLUT4, despite absence of a PPRE sequence in that gene (Wu et al., 1996).

C/EBPα: C/*EBPα* induces many adipocyte genes directly and in vivo studies indicate an important role for this factor in development of AT. Overexpression of C/EBPα in 3T3-L1 preadipocytes induces the differentiation into mature fat, and the expression of C/EBPα antisense RNA in these cells blocks this process (Lin and lane, 1994). Animals that carry a homozygous deletion of the C/EBPα gene have dramatically reduced fat accumulation in WAT and brown AT pads (Wang et al., 1995). Despite the important role of C/EBPα in adipogenesis, it cannot function efficiently without the presence of PPARγ. However, cells lacking C/EBPα are capable of adipogenesis, but are not insulin sensitive (Wu et al., 1999).

SREBF1: SREBF1 is a basic helix-loop-helix transcription factor and is regulated in adipogenesis (Tontonoz et al., 1993). There are three SREBF isoforms (SREBF1a, -1c and -2). SREBF1a and -1c are transcribed from the same gene, by a distinct promoter, and SREBF1c is the predominant isoform in AT (Eberlé et al., 2004). Activated SREBF1 enters into the nucleus and binds to specific DNA sequences in the promoters of its target genes. So far the identified sequences include sterol regulatory elements (SRE; Briggs et al., 1993) and classic palindromic E-boxes (Kim et al., 1995). The promoter regions of many lipogenic genes contain SREBF binding and activation sites, which vary considerably and are tentatively designated SRE-like sequences (Mater et al., 1999). SREBF1c is inactive in binding to SRE-reporter genes, but is active for E-box binding sequences and SRE-like sequences in lipogenic gene promoters (Tontonoz et al., 1993; Mater et al., 1999) and so is implicated in transcriptional regulation of adipocyte differentiation. The identified target genes include acetyl CoA carboxylase (*ACACA*), fatty acid synthase *(FASN*), stearoyl CoA desaturase (*SCD*), ATP citrate lyase (*ACLY*), malic enzyme, *PPARG*, *LPL*, acetyl CoA synthetase (*ACS*), glycerol-3-phosphate acyltransferase (*GPAT*), and *SREBF1* itself (see review in Shimano, 2001). Although SREBF1c was identified

as a pro-adipogenic TF by inducing PPARγ expression and possibly by generating PPARγ ligands (Kim et al., 1998a), it also mediates the induction of lipid biosynthesis by insulin in adipocytes (Kim et al., 1998b). Its essentiality in lipogenesis was doubted in several studies, in which SREBF1c$^{-/-}$ mice still possessed normal fat mass, and SREBP1c binding to the functional SRE/E-box site on the FASN promoter in adipocytes was not verified (Shimano et al., 1997; Sekiya et al., 2007).

Specific Characteristics of Lipid Metabolism in AT of Ruminants

In humans and rodents, liver is the major organ of *de novo* FA synthesis (DNS) (Hillgartner et al., 1995; Bernlohr et al., 2002; Bergen and Mersmann, 2005). In contrast, DNS capacity in liver represented about 1% of the rate in AT in non-lactating ruminants (ovine and bovine), assessed by comparing the incorporation rate of radiolabeled acetate *in vitro* in tissue slices of cattle (Hood et al., 1972; Ingle et al., 1972b) and sheep (Hanson and Ballard, 1967; Ingle et al., 1972a), or by tracking [1-^{14}C] acetate in sheep *in vivo* in which AT accounted for ~92% of DNS (Ingle et al., 1972a). Thus, AT is the predominant site of lipogenic activity in ruminants.

Unlike humans and rodents for which glucose is the major precursor for DNS (Bergen and Mersmann, 2005), acetate is the principle substrate for DNS in AT of ruminants as determined in early studies (Hanson and Ballard, 1967; Hood et al., 1972). The normal blood glucose concentration in ruminants is comparatively lower than in rodents, and such a characteristic of AT helps spare glucose for other more important organs, such as brain. The supporting evidence was demonstrated from several aspects: (1) The incorporation rate of radiolabeled acetate was ~6-7 times higher (>20 times higher, if glucose was present in the media) than glucose in AT slices from either lamb or calf (perirenal and omental, Ingle et al.,

1972b); similar results were obtained with AT slices from mature sheep (Vernon, 1976). (2) The activity of cytosolic acetyl-CoA synthetase (encoded by *ACSS2* gene in bovine), which was considered to be the isoform primarily involved in DNS, was found to be greater in ovine and bovine AT than in rat AT (Hanson and Ballard, 1967). (3) Ingle et al. (1972b) found that the low glucose incorporation rate into FA in AT slices of growing calves, even in the absence of acetate, coincided with the relative low activity of ACLY in comparison with nonruminant tissues. It was reported that ACLY activity in sheep AT is less than 20% of that of rat AT measured under identical conditions (Hanson and Ballard, 1967). ACLY catalyzes conversion of cytosolic citrate into oxaloacetate and acetyl-CoA, which represent the important step in DNS from carbohydrate carbon sources. Thus, the low activity of ACLY implicated a minor contribution of glucose carbon to DNS. (4) The low activity of pyruvate dehydrogenase (PDH) in bovine AT was hypothesized to be another important limiting factor that resulted in the low glucose utilization rate in DNS; however, research did not give sufficient direct supporting evidence for this possibility, which is only implicated through the high lactate output by ruminant AT (Khachadurian et al., 1966; Yang and Baldwin, 1973).

The DNS process requires an adequate supply of cytosolic reducing equivalents in the form of NADPH. For synthesis of each molecule of palmitic acid by the DNS pathway, eight and fourteen molecules of acety-CoA and NADPH are needed, respectively. In rodents, NADPH required for DNS is primarily derived from glucose oxidation via the pentose phosphate pathway, which accounted for 50% of requirement, and the citrate cleavage pathway contributed the remainder (Flatt and Ball, 1964; Rognstad and Katz, 1966). In ruminants, glucose-6-phosphate dehydrogenase (G6PDH) and 6-phosphogluconate dehydrogenase (PGD), two enzymes catalyzing NADPH-producing reactions in the pentose phosphate pathway, were active in AT.

However, due to the lack of substantial incorporation rates of glucose, NADP-malate dehydrogenase, which converts cytosolic malate to pyruvate with production of NADPH, was measured in very low activity in AT in early studies (Ingle et al., 1972b). This finding undercut the importance of the citrate cleavage pathway for NADPH production. Ingle and coworkers (1972b) observed the enzymatic activity of cytosolic NADP-isocitrate dehydrogenase (IDH) was ~4-6 times higher than G6PDH and PGD in AT (perirenal, omental, and epididymal) of growing calves. Cytosol IDH converts isocitrate to α-ketoglutarate and produces 1 molecule of NADPH, which was first proposed to play a significant role in supplying NADPH for lipogenesis in ruminant mammary gland (Bauman et al., 1976). Thus, IDH rather than the citrate cleavage cycle may represent a much more important pathway for production of the cytosolic NADPH pool to support lipogenesis in ruminant AT as well.

Visceral vs. Subcutaneous Adipose Tissue

Difference in Cellularity

Faulconnier et al. (2007) found that neither the nature of the diet (grass based or maize silage based) or nor grazing pattern had a significant effect on cell volume (size) or adipocyte number of three adipose sites (perirenal, intermuscular, and subcutaneous) from Charolais steers. Adipocyte volume varied significantly among AT depots, and was globally greater in the visceral depot (perirenal) than in intermuscular or subcutaneous AT. Eguinoa et al. (2003) reported that in both Pirenaican and Holstein heifers, the hierarchy of adipocyte size in different fat depots was omental AT > perirenal AT > subcutaneous AT > intermuscular AT, which was similar to trends that had been observed before (Haugebak et al., 1974; Hood, 1982; Cianzio et al., 1985, Mendizabal et al., 1999). Growth modality (proliferation vs. differentiation) of the various AT

depots may be regulated by many factors, including precursor cell population, blood vessel enrichment (blood flow), and innervation density. An inverse relationship was observed between the sympathetic nervous system innervation and the propensity for adipocyte proliferation (DiGirolamo et al., 1998). In rodents, the richest density of sympathetic nervous system innervation is in mesenteric AT (MAT) and the poorest is in inguinal (subcutaneous) fat; the hyperplasic capacity was just the opposite (Rebuffe-Scrive, 1991). Although no data are available for ruminants, these characteristics probably apply as well.

Difference in Lipogenic Capacity

Hood and Allen (1973a, 1975) reported that subcutaneous AT (SAT) slices from 14-mo-old steers of Holstein and Hereford × Angus breeds incorporated significantly more [1-^{14}C] acetate for lipogenesis than did perirenal AT (expressed per 10^6 cells basis), even though the SAT had relatively smaller adipocytes. Baldwin et al. (2007) observed a similar result in that acetate incorporation rates across depots (based on wet tissue weight) followed the order of SAT > omental AT (OAT) > MAT in beef steers. Consistently, the activities of enzymes (per 10^5 cell) catalyzing NADPH production reactions (IDH, G6PD, and PGD) were relatively higher in SAT than in perirenal AT in two breeds. Ingle et al. (1970b) found that the lipogenic activity per 100 mg tissue of internal AT (omental and perirenal) was greater than that in SAT sites (rump, shoulder, and abdominal) in lambs, which was measured by incorporation rate of radiolabeled acetate in tissue slices. In contrast, the SAT sites had the greatest lipogenic capacity in mature sheep and steers, averaging two- to threefold higher than the internal depots. Such results indicated that maturity is an important factor that influences lipogenic capacity among adipose depots. Faulconnier et al. (2007) observed depot-specific difference in activities of lipogenic enzymes, with greater activities (FASN, G3PDH, G6PDH, and LPL, expressed per 10^6

adipocytes) in SAT and/or perirenal AT than in intermuscular AT from Charolais steers. Moreover, perirenal AT was found to have greater cell volume and adipocyte number than either intermuscular or subcutaneous AT, which was independent of diet (either grass-based diet or maize silage-based isoenergetic diet; Faulconnier et al., 2007). Eguinoa et al. (2003) demonstrated that the abdominal depots (omental and perirenal) had a greater adipose size and, in general, greater lipogenic enzyme activities per cell (G3PDH, FASN, MD, G6PDH, and IDH) than the subcutaneous and intermuscular carcass depots in either Holstein or Pirenaican bulls and heifers. However, for a given cell size, enzyme activities varied over a large range due to different depot origins. Subcutaneous depots had greater FASN, G6PDH, and MD activities than omental and perirenal AT, when adipocyte size was equalized (Eguinoa et al., 2003). In cellular aspects, the average adipose cell volumes in ruminant fat depots usually decrease in the following order: omental and perirenal > subcutaneous > intermuscular > intramuscular, as mentioned before. Thus, compared with visceral fat, the SAT has smaller cell size or volume and higher *de novo* lipogenic activity when cell size was taken into account.

However, this does not warrant the sweeping conclusion that SAT has higher capacity for TAG synthesis than does visceral AT (VAT). Lipoprotein lipase, which liberates FA from TAG in circulating chylomicrons and VLDL, was observed to be higher in both activity and mRNA expression in internal fat depots (omental and perirenal) than in SAT in male calves (Hocquette et al., 1998). Greater LPL mRNA abundance was also detected in perirenal AT and OAT than in SAT in both German Holstein and Charolais, but Holstein deposited more internal fat mass than Charolais (Wegner et al., 2002). The LPL system is subject to regulation at many levels, involving gene expression, synthesis and degradation of protein, translocation, and activation/inactivation by serum factors. However, LPL activity depends primarily on a balance

between synthesis and degradation, which can be reflected by differences in mRNA abundance (Cryer, 1987). Expression of LPL was reported to be greater with increased adipocyte size, and independent of AT depot in sheep (Barber et al., 2000). Thus, this is in consistent with the previous finding that VAT, being composed of larger adipocytes, is more capable of uptake of FA from circulation.

The underlying rationale for differences in formation of the intracellular FA pool may be attributed to the nutrient supply from blood between VAT depots and SAT. Blood flow to carcass depots is less than that to abdominal depots in ruminants (Gregory et al., 1986), and the attachment to the digestive tract enabled VAT more access to preformed (mainly dietary) FA through FA taken up before drainage of the portal vein; hence the greater lipogenic capacity expressed by SAT may be a compensatory mechanism for a reduced nutrient supply. This may also explain the early finding that FA of dietary origin have a greater tendency to be deposited in abdominal rather than carcass AT depots (Christie, 1978).

Difference in Lipolytic Activity

In rodents, the mRNA expression of hormone-sensitive lipase (HSL) and adipose triglyceride lipase (ATGL), the two proteins primarily involved in stimulated lipolysis and basal lipolysis, was greater in the retroperitoneal AT, followed by MAT, and lowest in SAT (inguinal fat) (Palou et al., 2009). Both stimulated lipolysis and basal lipolysis release glycerol during hydrolysis of FA from TAG. The activity of glycerol kinase in bovine AT was very low (Hood et al., 1972; Metz et al., 1973). Hence, measuring glycerol release rate was representative of lipolysis in bovine AT. Most studies, however, found similar rates of basal and stimulated lipolysis in abdominal AT and SAT. The maximum (i.e., catecholamine-stimulated) lipolytic rate of adipocytes and the sensitivity of adipocytes to catecholamines are both enhanced during

lactation in ruminants (Bauman and Currie, 1980; McNamara, 1995), but not in rats (Vernon, 1996) or pigs (Parmley et al., 1996). The response and sensitivity to catecholamines during lactation were increased similarly in both OAT and SAT in sheep; however, the underlying mechanism may differ between two sites. Increased number of β-adrenergic receptors was probably the primary factor within OAT, whereas an increase in the maximum activity and amount of adenylate cyclase appeared to be the major factor in SAT (Vernon et al., 1995).

Visceral Obesity, Inflammation, and Metabolic Disease

The metabolic characteristics and endocrine function of AT have been extensively studied in humans and rodent animal models due to the prevalence of obesity and a series of accompanying metabolic diseases. Accumulating evidence indicates that a state of chronic inflammation, which is strongly associated with obesity and in particular visceral obesity, has a crucial role in the pathogenesis of obesity-related metabolic dysfunction including insulin resistance, dyslipidaemia, and fatty liver disease (Xu et al., 2003; Weisberg et al., 2003; Lehrke and Lazar., 2004). A broad spectrum of adipocytokines involved in inflammation, chemotaxis for immune cells, and immune response were found to be secreted from AT, either by adipocytes, stromal-vascular cells, or recruited immune cells, and some of the adipocytokines exhibited depot-specific characteristics (Ouchi et al., 2011). In obese humans, the increased plasma concentrations of C-reactive protein (CRP) and IL-6 are predictive of the development of type 2 diabetes in various populations (Visser et al., 1999; Pradhan et al., 2001). Franckhauser et al. (2008) demonstrated that chronic overexpression of IL-6 resulted in insulin resistance, liver inflammation, and hyperinsulinaemia. Increased secretion of TNFα and iNOS was reported to attenuate adipocyte insulin sensitivity in an autocrine or paracrine manner through inhibition of insulin-stimulated phosphorylation of insulin receptor substrate 1 (IRS1) in muscle and AT

(Hotamisligil et al., 1994; Uysal et al., 1997; Unoki et al., 2008). TNFα and IL-6 also increase lipolysis and have been implicated in the hypertriglyceridemia and increased serum NEFA associated with obesity (Zhang et al., 2002). Adiponectin was identified as an adipocyte-specific adipokine (Hu et al., 1996), and its circulating concentration was reported to be negatively correlated with insulin sensitivity of AT. Visceral AT was reported to produce more pro-inflammatory cytokines including TNFα and IL-6 and less adiponectin than SAT (Hamdy et al., 2006; Schäffler and Schölmerich, 2010). Recently RBP4 was found to be secreted by both adipocytes and macrophages (Broch et al., 2010) and preferentially produced by VAT in obesity and insulin resistance (Klöting et al., 2007). The adipocyte expression of RBP4 was reported to be inversely related to the insulin-sensitive glucose transporter, SLC2A4 (Yang et al., 2005). RBP4 released by adipocytes had inhibitory effects on tyrosine-phosphorylation of IRS1 in an autocrine or paracrine manner (Ost et al., 2007).

Another signature change in obese humans and animal models of obesity is the infiltration of a large number of macrophages, which is highly involved in the systemic inflammation and insulin resistance (Xu et al., 2003). Weisberg et al. (2003) showed that the accumulation of macrophages (represented by expression of CD68 or F4/80) is positively correlated with adipocyte size in human SAT and both VAT and SAT in mice. Bruun et al. (2005) found higher mRNA expression of macrophage specific markers (CD68 and CD14) in VAT than SAT and higher in obese individuals than leaner controls. Moreover, the transcription profile of monocyte chemoattractant protein (MCP-1), secreted as a chemotactic recruiter of immune cells, showed the same expression pattern as those macrophage marker genes. Thus, such results indicated that the accumulation of AT macrophages is proportional to adiposity and is more abundant in VAT than SAT. Activated macrophages release stereotypical profiles of cytokines

and biologically active molecules such as NO, TNF-a, IL-6, and IL-1 (Gordon, 1998), which exacerbate the inflammation status.

Collectively, these findings have led to the notion that metabolic dysfunction due to excess AT mass may partly result from an imbalance in the expression of pro- and anti-inflammatory adipokines and increased infiltration of immune cells, which accelerate the secretion of pro-inflammatory cytokines. Visceral AT is more subject to the infiltration of macrophages, hence visceral obesity is more detrimental to systemic insulin sensitivity and predisposes to increased risk of metabolic disease. The increased release of cytokines from VAT is directly drained to the liver through the portal vein, which may be more detrimental to liver function and health than products released from SAT.

Dairy cows easily overconsume dietary energy during the dry period (Dann et al., 2006; Douglas et al., 2006). Baldwin et al. (2004) found that VAT mass markedly increased during late lactation. Nikkhah et al. (2008) reported that 8 wk of overfeeding energy significantly increased visceral fat mass including mesenteric, omental, and perirenal AT of non-pregnant non-lactating dairy cows compared with animals fed a controlled-energy diet. Mukesh et al. (2009) examined the mRNA expression of major pro-inflammatory cytokines, acute phase proteins, and chemokines in MAT and SAT of dairy cows before and after a 2-h LPS challenge *in vitro*. Before the challenge, MAT had higher expression of *SAA3* than SAT and both depots had increased mRNA abundance of *TNF* and *IL6* after LPS challenge for 2 h, with a more pronounced increase in MAT. Bradford et al. (2009) observed that subcutaneous injection of recombinant bovine TNFα (rbTNFα) to late-lactation cows for 7 d decreased feed intake by 15%, increased hepatic *TNF* mRNA and protein, and increased liver TAG content compared with control animals. Taken together, evidence obtained from rodent and human studies seems to hold

true in ruminant animals; visceral obesity resulting from overfeeding energy may be responsible, at least partly, for fatty liver and other metabolic disorders.

Physiological Adaptation and Lipid Metabolism During the Transition Period

Homeorhetic Control During the Transition Period

The transition period in the dairy cow was defined as the period from 3 wk before to 3 wk after parturition (Grummer, 1995; Drackley, 1999), which is also known as the periparturient period. This period is primarily characterized by systemic homeorhetic change. Homeorhesis was first elaborated by Bauman and Currie (1980) to describe "the orchestrated or coordinated regulation in metabolism of peripheral tissues and nutrient partitioning to support a dominant physiological state". Three key features of homeorhetic regulation as described by Bauman and Currie (1980) were: (1) its chronic nature (e.g., hours or days instead of seconds or minutes); (2) its simultaneous influence on multiple tissues with apparently unrelated functions; and (3) its mediation through altered responses to homeostatic signals. In dairy cows, homeorhetic control during the transition period is associated with a complex series of synchronized metabolic and endocrine adjustments that are initiated during the last few weeks of gestation and continue through the first several weeks of lactation (Bauman and Currie, 1980). The rapid growth of the fetus during late pregnancy and copious milk synthesis during the onset and development of lactation are potent "pulling" forces that drive nutrients away from peripheral tissues (e.g., AT and skeletal muscle), which usually exhibit reduced sensitivity to insulin and increased sensitivity to adrenergic agents (Guesnet et al, 1987; Vernon and Finley, 1988). Such drastic physiological changes from the periparturient period to early lactation have significant impact on

the nutritional (Grummer, 1993), metabolic (Bell, 1995; Drackley, 1999), and immune (Goff and Horst, 1997) status of dairy cows.

Hormonal Adaptation

An important aspect of homeorhetic regulation during the transition period is the marked change in hormonal environment. Since fetal development and mammary gland growth overlap during the last trimester of gestation (Bauman and Currie, 1980), the progressive change in hormones was believed to play crucial roles to initiate and sustain lactogenesis, "switch on" parturition, regulate nutrient partitioning, and alter peripheral tissue (e.g., AT and skeletal muscle) responsiveness to certain hormones (e.g., insulin and catecholamines; Bell, 1995). Insulin, as the major homeostatic hormone, functions primarily to stimulate lipogenesis and glucose utilization (low rate in ruminants) and to inhibit lipolysis in bovine AT. Plasma insulin concentration peaks at parturition, but is maintained at lower concentrations postpartum than prepartum (Grum et al., 1996). Thus, the increasing concentration of circulating NEFA during late gestation should be, at least partly, attributed to the decreased insulin. Although the insulin response of AT was demonstrated to be compromised prepartum (Petterson et al., 1994), drenching cows with propylene glycol for the last 9 d prepartum was observed to increase insulin and decrease NEFA release (Studer et al., 1993). Glucagon concentrations increased postpartum, which paralleled the period of decreased plasma glucose concentration (Hammon et al., 2009). Glucagon primarily affects hepatic gluconeogenesis in ruminants by stimulating conversion of propionate to glucose (Faulkner and Pollock, 1990; Donkin and Armentano, 1995), and infusion of glucagon into early lactating cows increased hepatic mRNA expression for pyruvate carboxylase (She et al., 1999). Conversely, insulin decreases gluconeogenesis; intravenous infusion of insulin into sheep

decreased glucose synthesis rate (Brockman, 1990). Hence, the decreased insulin/glucagon ratio is an important adaptation that favors hepatic gluconeogenesis.

The plasma concentrations of progesterone begin to decrease gradually during the last few weeks of gestation, then decline immediately a few days before calving and are maintained at very low levels postpartum (Bauman and Currie, 1980; Bell, 1995). Meanwhile, estrogen (estradiol-17β) concentration in blood increases prepartum and peaks within the last week of pregnancy, which is followed by a transient spike of prolactin (PRL) in circulation within a few days around parturition (Kuhn, 1977; Bell, 1995). The coordinated change of these three hormones was considered to be homeorhetic control over lactogenesis and milk synthesis in the mammary gland (Kuhn, 1977). Prolactin functions to enhance mammary lipid synthesis through activation of key enzymes, such as ACC, LPL, and PDH (Field and Coore, 1976; Barber et al., 1992a; Hang and Rillema, 1997), whereas it was reported to reduce activity of lipogenic enzymes in AT (ACC, FAS, and LPL) of rodents (Barber et al., 1992b). Although in ruminants the transient surge of PRL and its similar structure and overlapping function with GH and placental lactogens does not warrant PRL a crucial role in regulation of nutrient partitioning, how much PRL may affect lipogenesis in AT of dairy cows during the transition period and whether this is attributed to progressively decreased insulin response postpartum still needs further investigation.

Theblood concentration of GH rises during late gestation, peaks at calving and declines to a moderately increased level postpartum in comparison with other lactation periods (Bell, 1995; Grum et al., 1996). It is well established that GH has a directing effect on nutrient repartitioning (Bauman and Vernon, 1993). It dramatically stimulates lipolysis through increased AT response to catecholamines when the animal is in negative energy balance, whereas it reduces nutrient

utilization by AT and redirects them for milk synthesis during positive energy balance (Sechen et al., 1989). In study of AT in culture, GH supplementation decreased ACC active state with no change in total activity (Vernon et al., 1991), which may be implicated as one aspect of GH inhibition on lipogenesis. Thus, the opposite effect of GH on AT metabolism compared with insulin may be dominant during early lactation.

Dry Matter Intake and Energy Balance

The transition period, particularly the last week of gestation, is characterized by a potentially dramatic exponential decline (20 to 40%) in dry matter intake (DMI) that begins at about the last 3 wk of gestation, reaches a nadir around calving, and slowly recovers after parturition (Ingvartsen and Anderson, 2000; Hayirli et al., 2002). Paradoxically, the drastic increase in demand of energy from either fetal growth or lactogenesis occurs during this period. The fetus acquires approximately 60% of the birth weight during the last 2 month of gestation, however the apparent efficiency of utilization of metabolizable energy is only about 10 to 25% (Bauman and Currie, 1980). As calculated by Bell (1995), the energy required for fetal growth at 250 d of pregnancy is 2.3 Mcal/d. Lactogenesis is conveniently considered to be a two stage process. The first stage involves mammary differentiation and limited synthesis and secretion of pre-colostrum for several weeks before parturition; while the second stage is associated with the onset of copious milk secretion shortly before calving and for several days postpartum, which requires significantly greater amounts of nutrients than the first stage. Based on the calculation by Bell (1995), the net energy required for lactation (30 kg/d milk yield) of Holstein cows at 4 d postpartum was approximately 26 Mcal/d, whereas 15 kg/d DMI can only provide 23 Mcal/d as NE_L, if conversion of ME to NE_L is assumed to be 60%. Thus, during the transition period, the concurrence of DMI depression and increased energy demand results in NEB and increased

mobilization of body reserves, which is may be detrimental to both lactation performance and health of dairy cows if severe.

Mechanisms that result in the depression of DMI are still largely unclear. Numerous factors have been reported to affect DMI during the transition period, which can be generally categorized as animal factors, dietary nutrients, and endocrine influence (NRC 2001). Hayirli et al. (2002) reported that the average DMI (expressed as a percentage of BW) for heifers and cows during the last 3 wk of pregnancy were 1.69 and 1.88%, respectively. Additionally, the duration of DMI depression is longer for cows than for heifers. However, Ingvartsen et al. (1997) observed a similar pattern of DMI decline for heifers and multiparous cows. Prepartum body condition score (BCS) was reported to be inversely related to DMI and appetites of obese dairy cows (Treacher et al., 1986; Hayirli et al., 2002). In addition, obese cows (BCS >4) were prone to mobilize body reserves to a greater extent and more rapidly than cows with lower BCS, and in turn were more susceptible to fatty liver and ketosis (Reid et al., 1986). Ingvartsen et al. (1995) reported a positive relation between prepartum weight gain and lipid mobilization postpartum in dairy cows as well. Thus, the above evidence indicates that overconditioning in the dry period potentially predisposes dairy cows to more severe NEB postpartum due to more pronounced decrease in DMI.

Leptin is produced and secreted primarily by adipocytes (Maffei et al., 1995), and its plasma concentration is positively correlated with body reserves in rodents (Frederich et al., 1995) and humans (Caro et al., 1996). The mechanism by which leptin inhibits feed intake is through decreased availability of neuropeptide Y, a potent stimulator of appetite in rodents and a main target of leptin for binding to dorso- and ventromedial nuclei of the hypothalamus and the arcuate nucleus, as reported in ovine (Dyer et al., 1997; Henry et al., 1999). Positive correlations

were detected between plasma leptin concentration and BCS (Ehrhardt et al., 2000), adipocyte volume (Chilliard et al., 1998), and feeding level (Chilliard et al., 1998) in sheep and cattle. However, the effect of leptin in regulation of DMI does not seem to be maintained during the periparturient period in dairy cows. Janovick et al. (2009) observed a constantly higher plasma leptin concentration in cows overfed energy than in a controlled-energy group during late gestation (from 28-d prepartum), but DMI was not decreased until ~10 d before calving. Reist et al. (2003) found the opposite result in that cows that consumed more concentrate form 1 to 10 wk postpartum had higher leptin concentration along with higher and faster recovery of DMI.

Increased secretion of pro-inflammatory cytokines (e.g., TNFα, IL1β, IL6) due to obesity, particularly visceral obesity, was demonstrated to be closely associated with systemic chronic low-grade inflammation, reduced appetite, fatty liver disease, and insulin resistance in human and rodent studies (Xu et al., 2003; Steppan and Lazar, 2004; Tilg and Moschen, 2008). In lactating dairy cows, subcutaneous injection of recombinant bovine TNFα (rb TNFα) drastically reduced DMI by 34% and increased plasma NEFA and haptoglobin concentration (Kushibiki et al., 2003). During the dry period, dairy cows readily overconsume energy and gain BCS (Dann et al., 2006). In an earlier study from our lab, we found that overfeeding dietary energy to non-pregnant dry cows significantly increased visceral AT mass compared with those that received a controlled-energy diet, which was not reflected by gain in BCS (Nikkhah et al., 2008). It is well-established that cows that are fat at parturition or overfed prior to parturition are particularly at risk to severe NEB and tend to eat less relative to requirements and so mobilize more fat than thinner cows (Grummer, 1993). Serum TNFα concentration is also increased by obesity in sheep (Daniels et al., 2003). Hence, we speculate that overconditioned cows prepartum may have higher circulating concentrations of pro-inflammatory cytokines, which is detrimental to liver

health and interferes with DMI postpartum. Such speculation is consistant with the phenomenon that obese cows experience a longer time to recover DMI postpartum and are more susceptible to fatty liver. However, this speculation may just highlight a factor that potentially exacerbates NEB and DMI depression rather than explains the reason for decreased DMI during the transition period.

Glucose-dependent insulinotropic polypeptide (GIP), glucagon-like peptide 1-amide (GLP-1), and cholecystokinin (CCK) are well-established gut hormones secreted by the small intestine in response to luminal nutrient concentrations in non-ruminant animals (Hansen et al., 2004). All three gut peptides can decrease DMI in rodents directly through effects on hypothalamic recptors or indirectly by reducing gut motility (Holst, 1997). In addition, increased GLP-1 and GIP secretion were reported to stimulate insulin secretion in sheep (McCarthy et al., 1992; Faulkner and Martin, 1999). Decreased DMI was associated with increases in plasma CCK, GLP-1, and GIP when rumen-protected fat was supplemented at 3.5% of dietary DM to mid-lactation cows (Relling and Reynolds, 2007a). However, during the transition period, dairy cows were found to be resistant to these gut hormones. A gradual increase in GIP, GLP-1, and CCK was related with the similar increase in DMI within 19 days postcalving (Relling and Reynolds, 2007b). Several reasons may be potentially involved in this phenomenon for early lactating dairy cows. (1) These gut peptide may be more associated with digestion rather than restricting DMI when blood glucose and insulin were in relative low concentrations during early lactation, as suggested by Ingvartsen and Anderson (2000). (2) In addition, certain threshold values probably need to be attained to trigger the mechanism to inhibit appetite, which may be associated with gut fill or lipid content of diet, because the concentrations of these peptides detected in the

Transition cow study (Relling and Reynolds, 2007b) were all lower than in study of mid-lactation cows (Relling and Reynolds, 2007a).

Drackley (1999) reported that coefficients of variation for DMI during the 1st wk postpartum range from 30 to 40%, whereas they are only 6 to 10% for DMI after peak lactation. Hence, many other factors (such as health problems and genetics) coupled with variation from individual animals also contribute to the large DMI variation during this crucial period. Additionally, variability may also indicate the complex crosstalk among different factors that affect transition period DMI.

Adipose Tissue Metabolism

Adipose tissue is one of the major targets of homeorhetic control during the transition period. The NEB and transition period-associated hormonal changes result in pronounced alterations in lipid metabolism, glucose utilization, and sensitivities to homeostatic and homeorhetic stimulation, which have been well-discussed in several elegant reviews (McNamara, 1991; Grummer, 1993; Vernon, 2005). As shown through measuring [2-^{14}C] acetate incorporation rate *in vitro*, *de novo* FA synthesis in AT was significantly decreased in late pregnancy (15 d prepartum) compared to that at 120 and 240 DIM; however, the activity was almost completely suppressed during early lactation (McNamara et al., 1995). The reduced acetate incorporation may be due to marked decreases in both mRNA expression of lipogenic genes (*ACACA* and *FASN*) and enzymatic activity of ACC during the transition period (Travers et al., 1997; Janovick et al., 2009; Sadri et al., 2010b). ACC controls the flux of lipogenic precursor, malonyl-CoA, and is the rate-limiting enzyme of the FA biosynthesis pathway. The activity of lipoprotein lipase, the major enzyme in the pathway of preformed lipid uptake, was also decreased with initiation of lactation (McNamara, 1997).

The dramatic restriction of lipogenesis in AT may result from the combination of multiple factors. Insulin is the key hormone that stimulates lipogenesis through both transcriptional activation and allosteric regulation of lipogenic enzymes such as ACC. Hypoinsulinemia and decreased adipose sensitivity to insulin should be one of the primary reasons for decreased lipogenesis. The competition for substrates by mammary gland for lactation may contribute as another factor. Bionaz and Loor (2008) observed a similar pattern of marked up-regulation and/or relative mRNA abundance in mammary gland during early lactation for genes associated with FA uptake (*LPL* and *CD36*), long-chain (*ACSL1*) and short-chain intracellular FA activation, de novo FA synthesis (*ACACA* and *FASN*), and TAG synthesis. The suppression in lipogenesis is probably due in part to increased plasma GH during early lactation. Growth hormone can markedly decrease AT response to the lipogenic effect of insulin and promote lipolysis during NEB periods (Bauman and Vernon, 1993). Additionally, McNamara (1995) found that dairy cows of high genetic merit experienced more pronounced suppression of lipogenesis during early lactation than animals of average genetic merit. Hence, the suppressed lipogenesis in AT may be not only a short-term homeorhetic adaptation to lactation but also a genetic adaptation to continuously improved milk production of cows.

Another signature change of AT peripartum is the dramatic increase in both basal and catecholamine-stimulated lipolytic activity (McNamara and Hillers, 1986), which compensates for the slowly increased DMI to support milk production. The activity of HSL, the major enzyme that primarily mediates β-agonist stimulated lipolysis, was observed to be increased during lactation and peaked at 30 to 60 DIM, then remained elevated until 240 DIM (McNamara et al., 1987; Smith and McNamara, 1990). Recent evidence showed that mRNA expression of HSL was increased during lactation with the highest value appearing at 90 DIM (Sumner and

McNamara, 2007). Genes encoding three β-adrenergic receptors were upregulated in AT during the lactation period (30, 90, and 27 DIM) compared to those at 30 d prepartum, which contributes to the increased responsiveness to catecholamine (Sumner and McNamara, 2007). Similarly, the lipolysis rate postpartum was affected by genetic merit. Adipose tissue biopsied from cows of high genetic merit exhibited increased basal and stimulated lipolytic rates, implying that high producing cows tend to mobilize more body reserves to support milk production (McNamara and Hillers, 1986).

The increased blood NEFA is not simply due to the elevated lipolytic activity, but also exacerbated by reduced re-esterification of NEFA in AT after parturition (McNamara, 1991). Rukkwamsuk et al. (1999) found that both basal and stimulated (addition of glucose or glucose plus insulin) esterification rate of SAT was markedly decreased postpartum (tested at 0.5, 1, and 3 wk post-calving) compared with that during the last week prepartum.

Two studies shed light on the metabolic activity of VAT during different stages of lactation. Baldwin et al. (2004) demonstrated that VAT lost 2/3 of its weight during the first 120 d of lactation, and rebounded during late lactation. When this was expressed as a percentage of empty body weight (EBW), the VAT accounted for approximately 4.8% of EBW at 14 DIM, but was reduced to ~2.1% of EBW at 120 DIM. Another earlier study from Butler-Hogg et al. (1984) showed that, in dairy cattle, the VAT (represented by mesenteric fat) changed in the same pattern as that of subcutaneous AT and intermuscular AT across various physiological stages. The absolute weight of both MAT and SAT markedly declined from the onset of lactation and reached the nadir, at about half of the weight at point of calving, at mid-lactation, then replenished and maximized during the dry period, which was about 7-fold the weight at mid-lactation. Reynolds et al. (2003) showed that the net portal drained visceral (PDV) release of

NEFA increased moderately at late pregnancy and dramatically after parturition, of which the release rate at 11 d postpartum was more than 4-fold that at 19 d before parturition. Since most dietary FA is channeled through lymphatic circulation rather than the portal vein, the increased NEFA release from PDV was primarily due to lipolysis of visceral fat. Thus, these results clearly demonstrated that VAT is also markedly mobilized and replenished during the lactation cycle. As we discussed previously, overconditioned cows during the dry period tend to mobilize more fat in early lactation and are subject to higher risk of fatty liver disease. It is rational to propose that, due to the direct portal drainage and increased portal blood flow in early lactation (Reynold et al., 2003), the drastically increased lipolysis in VAT of these fat cows is one of the major factors that predisposes them to inferior liver health compared with thinner cows.

Hyperlipidemia and Liver Dysfunction

The liver plays a pivotal role in controlling nutrient partitioning. The requirements for glucose and metabolizable energy increase two- to threefold from 21 d before to 21 d after parturition (Drackley et al., 2001). On the other hand, the blood flow through portal vein and liver increased during early lactation to more than double the average rates before calving (Reynolds et al., 2003). The liver machinery must respond quickly to this sharply increased demand for glucose and energy for milk production and adapt to the overwhelming influx of nutrients.

Liver cells take up NEFA from blood in proportion to its concentration (Thompson et al., 1975), which is an important adaptation strategy to support its own function and service other tissues by converting NEFA to the water-soluble fuels, ketone bodies. However, sustained hyperlipidemia that overloads hepatocytes with lipid in excess of liver capacity to metabolize it will result in fatty liver. Reynolds et al. (2003) showed that the hepatic uptake rate of blood

NEFA was elevated at 11 d lactation (115.8 mmol/h) by more than 5-fold of the rate at 19 d before parturition (21 mmol/h). Based on physiologically representative parameters from previous studies, Drackley et al. (2001) calculated that during the periparturient period 525 g/d of NEFA could be available for esterification and 583 g of TAG would be produced in liver per day. Upon uptake into hepatocytes, NEFA can either be oxidized completely to CO_2 and provide energy or be oxidized incompletely to ketone bodies and exported for other organs and peripheral tissues, or it can be esterified to TAG and secreted in the form of VLDL. Synthesis of TAG in excess of the rate of VLDL output leads to accumulation of TAG in liver. Hence, increased VLDL export or FA oxidation may help to alleviate lipid accumulation in liver. Multiple factors have been demonstrated to influence the fate of NEFA metabolism in hepatocytes. Drackley et al. (1991) incubated liver slices *in vitro* and observed that the proportion of total palmitate uptake that was oxidized was inversely related with the whole-animal energy balance and physiological state rather than with changes in substrate delivery, whereas the proportion of NEFA that was esterified decreased coordinately with NEB.

Carnitine palmitoyltransferase I (CPT-1) is the primary regulator of translocation of LCFA from the cytoplasm into the mitochondria, which partitions LCFA between esterification and oxidation. Being associated with mitochondrial outer membrane, CPT-1 translocates LCFA into the inner mitochondrial membrane space by binding with carnitine. Its activity is subject to inhibition by malonyl-CoA to prevent a futile cycle between lipogenesis and β-oxidation. The total activity of CPT-1 was 49% greater at 1 d postpartum than 21 d prepartum (Douglas et al., 2006). In a later study, Dann and Drackley (2005) analyzed mitochondrial CPT-1 activity during the periparturient period through longitudinal liver biopsies. The authors found that CPT-1 activity was positively correlated with liver total lipid, liver TAG content, liver TAG to glycogen

ratio, and serum NEFA concentration. Sensitivity to malonyl-CoA did not differ across the periparturient period, in contrast to data from rodents. Insulin decreased the activity of CPT-1 and increased affinity of CPT-1 for malonyl-CoA (Grantham and Zammit, 1988). In addition, insulin's inhibitory effect on CPT-1 is also related to its stimulatory action on activity of ACC and the formation of malonyl-CoA. Zammit (1999) reported that the sensitivity of CPT-1 to malonyl-CoA's inhibition effect decreased with the decline of insulin concentration in a rodent model. Thus, the hypoinsulinemia after parturition may contribute to increased FA oxidation and ketogenesis. Hence, maintaining a high activity of CPT-1 is important to attenuate hepatic TAG accumulation. However, Mizutani et al. (1999) observed a significant decrease in CPT-1 activity in dairy cows with fatty liver disease compared with healthy animals. Recently, in an in vitro study of bovine hepatocyte culture, Xu et al. (2011) found that both transcription and translation of CPT-1 were significantly up-regulated when the NEFA concentration in media increased from 0 to 1.2 mmol/L, but were markedly down-regulated when the NEFA concentration increased from 1.2 to 4.8 mmol/L. Thus, the decreased mRNA and protein level due to the suppressive effect of high NEFA concentration may have contributed to diverting FA to esterification and accelerated the development of fatty liver postpartum.

Carnitine is required for CPT-1 to import LCFA into mitochondria for oxidation. Drackley et al. (1991) showed that supplemental L-carnitine in liver slice culture medium increased oxidation of palmitate to CO_2 by more than 2 fold *in vitro*. Carlson et al. (2006) showed that abomasal L-carnitine infusion decreased the liver lipid concentration in feed-restricted cows, which was mediated through increased β-oxidation. In a following study, dietary supplementation of L-carnitine (6, 50, and 100 g/d as low, medium, and high level) from -14 d to 21 d relative to calving date decreased liver total lipid and TAG accumulation on d 10 after

calving, and increased liver glycogen during early lactation probably through increased hepatic conversion of Ala to glucose (Carlson et al., 2007). However, supplementation of L-carnitine simultaneously increased the plasma BHBA concentration in both studies, which may have resulted from the excess production of acetyl-CoA that overloads the capacity of the TCA cycle to metabolize it due to high NADH/NAD ratio.

Peroxisomal β-oxidation is an alternative pathway in liver that produces heat rather than mitochondrial ATP formation. Grum et al. (1994) found that peroxisomal β-oxidation represented nearly 50% of the total capacity for the initial cycle of β-oxidation of palmitate in liver homogenates from dairy cows. In addition, peroxisomal β-oxidation was reported to be negatively correlated with hepatic TAG content at 1 d postpartum (Grum et al., 1996). Hence, peroixsomal β-oxidation provided an additional channel to alleviate hepatic lipid accumulation without the risk of induction of ketosis. The regulation and modulation of this pathway may warrant further research.

Export of NEFA in the form of lipoprotein (VLDL) serves as another outlet to prevent hepatic lipid overload; however, the secretion of TAG in VLDL is much lower in ruminant animals than in many non-ruminants (Pullen et al., 1989). In a review by Drackley et al. (2001), the authors summarized two aspects of limitations primarily involved in low VLDL formation in dairy cows during periparturient period. First, the relatively low concentration of apolipoprotein (apo) B in both plasma and liver of dairy cows during early lactation limited the secretion of VLDL. Moreover, the TAG in newly formed VLDL is primarily derived from a TAG pool within the microsomal compartment, which is highly associated with the rate of *de novo* lipogenesis. *De novo* lipogenesis is low in ruminant liver (Grummer, 1993), which may result in a smaller pool of microsomal TAG and restricted supply of secretory TAG for VLDL synthesis.

Bernabucci et al. (2004) examined the mRNA expression of ApoB(100), ApoE, and microsomal TAG transfer protein (MTP) of liver tissue at -35, 3, and 35 d relative to parturition. Plasma VLDL was decreased after calving. Compared with values of d -35, the ApoB mRNA expression was lower, whereas MTP and APoE mRNA were higher on d 3 pospartum. A negative correlation (r = -0.57) was observed between ApoB mRNA abundance and plasma NEFA concentration. MTP is responsible for transfer of TAG into VLDL particle. Thus, the results indicated that increased NEFA influx may compromise hepatic VLDL output by reducing ApoB synthesis rather than recruitment of TAG into VLDL particles.

Insulin Resistance Symptom

Insulin resistance (IR) was described as the state in which a physiological level of plasma insulin failed to produce an equivalent normal biological response (Kahn, 1978). Kahn (1978) described how to evaluate IR by insulin responsiveness and sensitivity, of which responsiveness is defined as the maximal response to insulin (R_{max}), and sensitivity is defined as the hormone concentration required to produce a half-maximal response (ED_{50}), implying the tissue responsiveness to insulin. The mechanism of IR may result from defects at different levels in either pancreatic β-cell or insulin-sensitive tissues and organs: (1) prior to interaction that includes decreased insulin from pancreas and/or increased insulin degradation rates; (2) at receptor level of interaction, which can derive from the reduced receptor number and/or binding affinity; (3) at post-receptor level, that is associated with defects in insulin signal transduction intracellularly. Such defects can be due to the reduced expression of certain kinases in the pathway, decreased availability of glucose transporter (GLUT4), and/or compromised post-translational regulation of molecules (such as phosphorylation of insulin receptor substrates) to transmit signal (Hayirli, 2006). In general, defects prior to interaction result in hypoinsulinemia,

defects at the receptor level causes decreased insulin responsiveness, and compromised intracellular signal transduction results in low insulin sensitivity (Kahn, 1978).

As discussed previously, insulin is the key anabolic hormone that regulates lipid, carbohydrate, and protein metabolism in AT, skeletal muscle, and liver. Insulin resistance causes disturbance in regulation of nutrient metabolism. Although in ruminant AT significantly less glucose is used for lipogenesis (Ingle, 1972b), glucose is still required as a source of glycerol 3-phosphate synthesis and provision of NADPH mainly through the pentose phosphate pathway for FA synthesis (Bauman, 1976). Thus, IR may result in decreased incorporation of glucose through GLUT4 in AT and decreased *de novo* FA synthesis due to decreased supply of reducing equivalents. Furthermore, insulin can promote mRNA expression of *LPL* and lipogenic genes, such as *ACACA* and *FASN*, either mediated through SREBF1 or by direct interaction with insulin responsive elements on the promoter region of genes. Additionally, insulin suppress lipolysis in AT through activation of PDE3B, which decreases the concentration of cAMP that reduces PKA activity and consequently reduces activation of HSL (Degerman et al., 1997). Hence, during insulin resistant states, decreased lipogenesis, decreased re-esterification, and increased lipolysis will occur in AT.

Insulin resistance was previously observed in humans and rodents during late pregnancy and early lactation, which was characterized as decreased sensitivity and /or responsiveness to insulin's effect on restricting hepatic gluconeogenesis, decreasing lipolysis, increasing lipogenesis, and increasing glucose incorporation rate by AT and muscle. During late pregnancy, the fetus utilized approximately 42-50% of total glucose production in ewes (Prior and Christenson, 1978). Such IR was considered as an important facet of metabolic adaptation

through homeorhetic control to prioritize nutrient utilization for fetus growth and mammary gland differentiation (Hauguel et al., 1987; Ryan et al., 1985; Leturque et al., 1987).

Petterson et al. (1993) found a prominent reduction in whole-body sensitivity to insulin's effects on glucose utilization in sheep as evidenced by increased ED_{50}. In a following study, Petterson et al. (1994) reported decreased insulin responsiveness of lipolysis and NEFA mobilization in late-pregnant sheep. Several other studies observed an even more pronounced state of IR in early lactation, which is usually associated with even lower concentrations of plasma insulin. Vernon et al. (1981) measured lipid metabolism and insulin binding affinity in AT biopsied from different physiological states through in vitro tissue culture study. The insulin effects on rate of FA synthesis and acylglycerol glycerol synthesis in AT were significantly decreased in late pregnancy (105 to 135 d) and reached a nadir in early lactation (18 to 50 d). Activity of LPL in AT was lower in late pregnancy and early lactation than other physiological states. McNamara and Hillers (1986) observed that basal and norepinephrine-stimulated glycerol release of SAT were all increased during lactation compared with late pregnancy, and the elevation was more prominent in early lactation. In a tissue culture study by McNamara et al. (1995), lipogenic activity of AT collected during late pregnancy (15 d before parturition) was markedly lower than in AT during mid- and late-lactation; however, AT biopsied during early lactation (15 and 60 d postpartum) almost completely lost lipogenic capacity as measured through acetate incorporation. Faulkner and Pollock (1990) found no effect on glucose metabolism, but insulin-induced suppression of plasma NEFA and glycerol was reduced in ewes during early lactation. Taken together, these studies suggested that both late pregnancy and early lactation are usually marked by IR in peripheral tissues, with more pronounced IR status in early

lactation, thereby promoting FA release and spring glucose to support pregnancy and milk production.

Although the predominant mechanism is still unclear, as mentioned before, defects at different levels can contribute to transition period IR. First, decreased insulin secretion in the periparturient period is one of the factors contributing to hyperlipidemia. During the last few weeks before parturition, plasma NEFA concentrations gradually increased and were markedly stimulated around calving, accompanied by decreased DMI; meanwhile insulin concentration was sharply decreased postpartum (Ingvartsen and Andersen, 2000). Although DMI depression was considered as a primary factor to induce lipolysis and hypoinsulinemia, preliminary evidence has shown that long-term exposure to NEFA substantially increased TAG accumulation and inhibited glucose-stimulated insulin secretion though decreasing glucose oxidation in rat islets (Zhou and Grill, 1994; Shimabukuro et al., 1998). The inhibitory effect on insulin secretion was improved by adding an insulin-sensitizing drug, trogliazone, into the incubation medium (Shimabukuro et al., 1998). It seems that increased TAG accumulation induced IR in islets as well. It has been observed that plasma insulin increment was significantly lower in sheep during late pregnancy (105 d and 135 d of gestation) than in non-pregnant non-lactating sheep after hyperglycemic clamp (Regnault et al., 2004). This finding also supported the impaired pancreatic response to secreting insulin during the transition period. However, hypoinsulinemia during the transition period cannot fully explain the IR status, because euglycemic hyperinsulinemia cannot totally recover insulin sensitivity in glucose utilization by AT and muscle in early lactating sheep (Faulkner and Pollock, 1990).

To date GLUT4 is the only reported insulin-sensitive glucose transporter and is highly expressed in AT and muscle. Insulin stimulation causes GLUT4 translocation from intracellular

storage to the plasma membrane and uptake of glucose. Balage et al. (1997) detected decreased GLUT4 protein in muscles of lactating goats in comparison with muscles from non-lactating animals. Sadri et al. (2010a) reported the mRNA expression of *GLUT4* and *GLUT1* were significantly (although slightly) lower in AT of early lactating dairy cows compared with those from dry cows. The elevated NEFA during early lactation probably has an adverse effect on AT insulin sensitivity. Van Epps-Fung et al. (1997) found a 50% reduction in insulin-induced glucose transport in 3T3-L1 adipocyte cultures that were exposed to 1 mmol/L of palmitate, myristate, and stearate overnight; inhibition of insulin action was specific to GLUT4 translocation after 4 h of adipocyte culture with 0.3 mmol/L palmitate. Although there was no corresponding data about bovine adipocytes, either 1 mmol/L of FA or 0.3 mmol/L palmitate are within the physiological range for dairy cows during early lactation. Hence, decreased insulin sensitivity of peripheral tissues for glucose utilization could be, at least partly, attributed to reduced transcription of *GLUT4* during the transition period.

Travers et al. (1997) reported that gene expression and enzymatic activity of ACC was reduced approximately 3-fold and 25- to 30-fold, respectively, in OAT and SAT of sheep during late pregnancy and remained low into lactation when compared with non-pregnant, non-lactating animals. In addition, Janovick et al. (2009) and Sadri et al. (2010b) observed the significant reduction in mRNA of lipogenic genes (*ACACA* and *FASN*) in SAT of dairy cows after parturition in comparison with the dry period. ACC is the rate-limiting enzyme in controlling the flux of FA in *de novo* synthesis. Thus, the compromised transcription and post-translational regulation of major lipogenic genes may be responsible for the pronounced suppression of lipogenic activity during the transition period.

The alteration at receptor level is another possible reason for reduced insulin response and/or sensitivity of AT. Vernon et al. (1981) observed a decreased rate of FA synthesis and LPL activity in AT of sheep during late pregnancy and early lactation, which paralleled a decline in number of high-affinity insulin receptors and total insulin receptors and reduced receptor binding affinity in AT. Guesnet et al. (1991) also reported that the number of total insulin receptors was decreased by 62% and insulin was inefficient in stimulating lipogenesis in ewes during early lactation.

However, defects at receptor level have not always been the case. In another two studies, Flint et al. (1979) and Vernon and Taylor (1988) reported that neither in rat nor sheep was there any change in the number or affinity of insulin receptors in AT, but blunted adipose sensitivity to insulin-stimulated lipogenesis and glucose utilization was observed between lactation and non-lactation periods. They proposed that alteration in insulin sensitivity during lactation was due to defects in post-receptor signal transduction after binding of the hormone to its receptor. IRS1 and IRS2 are the major insulin receptor substrates that mediate intracellular insulin signal transduction. In earlier studies, overexpression of human IRS1 in rat adipose cells increased the amount of surface GLUT4 even in the absence of insulin (Quon et al., 1994). Recent evidence showed that AT isolated from IRS1-deficient mice exhibited reduced insulin-induced glucose transport (Tamemoto et al., 1994). Similar results were obtained by a short-term in vivo whole-body reduction of IRS1 expression. These animals displayed IR and blunted insulin-induced GLUT4 translocation in muscle and AT (Araujo et al., 2005). In contrast, neither insulin- nor exercise-stimulated glucose uptake into isolated muscles of IRS2-null mice differed from that in wild-type animals (Withers et al., 1998). Taken together, the preliminary evidence showed that IRS1 is the major substrate type leading to stimulation of glucose transport in peripheral tissues.

The function of IRS1 and other mediators in ruminant peripheral tissues during the periparturient period warrants further research.

Intriguingly, Vernon and Taylor (1988) and Vernon and Finley (1988) found that AT collected from early lactating sheep was initially refractory to insulin stimulation of lipogenesis and glucose utilization within the first 24 h of in vitro incubation with different insulin concentrations. However, both lipogenic activity and glucose uptake were markedly induced after the initial 24-h lag phase. Travers et al. (1997) observed that mRNA, enzymatic activity, and active enzyme proportion of ACC in both OAT and SAT from late-pregnant and early lactating sheep were significantly increased after a lag period of 32 to 48 h in incubation with insulin plus dexamethasone. These data may indicate that transition IR could be recovered by long-term exposure to insulin stimulation. In addition, such results probably indicate that other hormones may interfere with AT response and/or sensitivity to insulin. During late gestation serum concentrations of the hormones estradiol, progesterone, and PRL affect the sensitivity of peripheral tissues to insulin. Ryan and Enns (1988) demonstrated that estradiol increased maximum insulin binding (MIB), whereas progesterone and cortisol decreased glucose transport and MIB. Prolactin and placental lactogen decreased glucose transport without changing MIB in AT. Growth hormone is another important hormone in regulation of nutrient partitioning. Bauman and Vernon (1993) stated that GH promoted lipolysis and reduced glucose utilization in AT during NEB in early lactation. However, the underlying mechanisms by which these hormones regulate peripheral tissue insulin sensitivity and/or responsiveness are still unclear.

Another focus of attention concerning transition IR is unrestricted lipolysis in AT. However, the accumulating evidence seems to support that the increased lipolytic activity is more due to increased sensitivity to lipolytic stimulators rather than reduced sensitivity to

antilipolytic effects of insulin. Petterson et al. (1994) demonstrated that pregnancy reduced AT responsiveness but not the sensitivity to the antilipolytic effect of insulin, which implied that the cellular basis probably was altered activity or content of certain key enzyme(s). Hypoinsulinemia certainly favors lipolysis during the transition period; additionally, McNamara and Murray (2001) reported increased sympathetic nervous system activity as grossly evaluated by norepinephrine concentration in AT in early lactating rats compared with non-pregnant, non-lactating control animals. Recently, the same group reported that the mRNA expression of genes encoding β-adrenergic receptors (*ADRB1*, *ADRB2*, and *ADRB3*), HSL (*LIPE*), and perilipin (*PLIN*) were all increased during different lactation stages (30, 90, and 270 DIM) compared with expression at 30 d prepartum, and the highest expression value generally occurred at 90 DIM accompanied by the highest blood NEFA concentration (Sumner and McNamara, 2007). Thus, I propose that reduced insulin sensitivity in AT during the transition period may be specific to its effect on glucose utilization and lipogenesis, but not to antilipolysis.

Effect of Prepartal Plane of Dietary Energy on Lipid Metabolism during the Transition Period

During late gestation and early lactation, the flow of nutrients to fetus and mammary tissues is accorded a high degree of metabolic priority. This priority coincides with decreased responsiveness and sensitivity of extrahepatic tissue to insulin (Nieuwenhuizen et al. 1998), which was considered to play a key role in development of hepatic lipidosis and ketosis (Holtenius, 1993). Different nutritional strategies have been pursued with purposes of (1) increasing hepatic TAG secretion in the form of VLDL, such as supplementation of choline into the diet during the transition period, (2) decreasing lipolysis of AT through supplementing niacin,

or (3) improving insulin sensitivity of peripheral tissues by administration of insulinotropic agents like chromium or insulin-sensitizing drugs such as TZD. On the other hand, the DMI depression and the lag time between slowly increased DMI and sharply increased milk yield during early lactation results in the development of NEB, hypoglycemia, hyperlipidemia, and presumably hypoinsulinemia. Grummer (1995) suggested that prepartum DMI was positively correlated with postpartum DMI and affected postpartum performance and health, and that increasing prepartal dietary energy density could improve DMI and energy balance. However, other researchers demonstrated that controlled prepartal energy intake could improve postpartal DMI and liver TAG accumulation (Tesfa et al., 1999; Dann et al., 2006; Douglas et al., 2006; Janovick and Drackley, 2010). Moreover, the dietary energy plane during far-off and close-up period was shown to exert different influences on postpartal DMI and lipid metabolism (Holcomb et al., 2001; Dann et al., 2006).

Prepartal Dietary Energy Plane

Increasing highly fermentable carbohydrates has been the most commonly used approach to increase energy density of the diet. In a large herd experiment, Mashek and Beede (2000) provided dry cows either a basal diet (Control, NE_L = 1.52 Mcal/kg DM) or a diet supplemented with corn grain (SC; dry ground corn replaced 21% of the corn silage, NE_L = 1.63 Mcal/kg DM) during the close-up period. Cows fed SC had lower plasma BHBA and tended to have increased insulin concentration prepartum compared with cows fed the basal diet. Increasing dietary nonfiber carbohydrate (NFC) could stimulate the production of propionate, which as the primary gluconeogenic precursor in ruminants can have a stimulatory effect on insulin secretion. Moreover, in the process of gluconeogenesis, propionate converges to the TCA cycle by formation of succinyl-CoA, which can inhibit activity of HMG-CoA synthase through

succinylation (Hegardt, 1999). HMG-CoA controls the regulatory step in conversion of acetyl-CoA to ketone bodies (Hegardt, 1999). However, plasma NEFA was not changed due to dietary energy intake during the entire transition period. Furthermore, supplementation of SC did not affect blood metabolites postpartum in that study and DMI information was not provided (Mashek and Beede, 2000). Minor et al. (1998) showed that overfeeding energy (NE_L = 1.63 Mcal/kg DM) during the last 19 d prior to expected calving increased DMI prepartum and tended to increase plasma glucose concentration compared to animals fed a control diet (NE_L = 1.34 Mcal/kg DM). In addition, overfeeding energy prepartum significantly decreased plasma NEFA and BHBA concentration prepartum and tended to decrease liver TAG content. However, it is hard to tell the effect of prepartum dietary energy intake on postpartum lipid metabolism, because the treatments were applied through postpartum as well.

Other studies have demonstrated that restricting NE_L intake to 100% or less of NRC (2001) recommendations prepartum resulted in more stable transition of DMI during the periparturient period and reduced BCS loss postpartum. Douglas et al. (2006) showed that irrespective of the energy sources (moderate grain or fat supplementation), cows that were restricted in NE_L intake to 80% of NRC (2001) requirements from -60 d to parturition had higher DMI and NE_L intake during the first 21 d postpartum than cows fed at ad libitum (160% of requirement) during dry period. Restricted cows had lower plasma NEFA and BHBA and lower total lipid and TAG in liver postpartum, but cows from both restricted and overfed groups had similar insulin levels postpartum, which implicate different sensitivity of AT to antilipolytic effect of insulin postpartum. In a recent study, Janovick and Drackley (2010) fed dry cows a moderate energy diet (NE_L = 1.63 Mcal/kg) for either ad libitum intake (OVR) or restricted intake (RES) to supply 150 or 80% of requirements, or fed a controlled-energy diet (CON; NE_L

= 1.21 Mcal/kg) for ad libitum intake through the entire 60-d dry period. Due to the inclusion of 32% of DM as chopped wheat straw, the energy intake of cows fed the controlled energy diet was limited to about 100% of requirement by bulkiness. The results showed that multiparous cows in the OVR group lost more BCS postpartum than those in RES and CON groups due to the lower DMI (as % of BW) during the first 3 wk postpartum. It seems that cows (especially multiparous cows) overfed during the dry period experienced more pronounced DMI depression and changes in energy balance, and mobilized more body fat to support lactation postpartum. Controlled energy intake during the dry period prevented the marked changes in DMI and energy intake postpartum and decreased lipid mobilization.

Rukkwamsuk et al. (1999) observed that overfeeding energy (96 MJ/d of NE_L) during the dry period significantly increased AT esterification rate prepartum, blood NEFA, and liver TAG content within first 3 wk postpartum compared with those indices from cows fed a controlled energy diet (44 MJ/d). Although a marked drop in esterification rate of AT was observed postpartum in both groups, AT from overfed cows showed reduced sensitivity to glucose- or glucose plus insulin-stimulated esterification. Thus, overfeeding energy during the dry period predisposes dairy cows to accumulate fat in AT prepartum and to higher risk to liver lipidosis due to increased mobilization of AT postpartum.

In the study of Dann et al. (2006), 74 multiparous cows were randomly assigned to different combination of far-off [NE_L intake = 80% (RES), 100% (CON) and 150% (OVR) of NRC (2001) requirements] and close-up [NE_L intake = 80% (CCON) and 150% (COVR) of NRC (2001) requirements] dietary energy planes. Overall results showed that the energy plane of far-off diet rather than energy intake during the close-up period had more pronounced impact on performance and lipid metabolism within 10 d postpartum. Cows fed RES and CON had greater

DMI and energy balance and lower serum NEFA and BHBA during the first 10 d of lactation in comparison with cows overfed energy (OVR) during the far-off period. The OVR cows had the highest serum insulin concentration and simultaneously the highest serum NEFA concentration during the close-up period regardless of the close-up dietary treatment, which the authors presumed as an indication of IR of the overfed cows. During the first 10 day of lactation, serum insulin and glucose concentrations were numerically lower in cows fed CON than animals in OVR. Moreover, restriction of energy intake during close-up period numerically decreased serum NEFA concentration during early lactation for cows that received CON or RES during far-off period. However, there was no effect of close-up energy restriction on serum NEFA in early lactation for cows overfed during far-off period, which probably resulted in the lack of statistical significance of close-up diet effect on postpartum serum NEFA concentration. Such results implicate a compromised insulin sensitivity of AT in cows overfed energy during close-up period.

Hypothesis of Current Research

Previous researches from our group repeatedly found that, compared with controlled-energy or restricted-energy feeding, prepartum overfeeding energy in form of NFC feeds either during entire dry period (Douglas et al., 2006; Janovick et al., 2011) or in close-up period (Richards et al., 2009) increased concentrations of blood insulin and glucose prepartum and increased concentrations of blood NEFA and BHBA, hepatic lipid accumulation and occurancy of metabolic disorders postpartum. Such symptoms indicated overfed cows experienced reduced insulin efficiency in stimulating peripheral glucose utilization prepartum and increased body fat mobilization postpartum. Similar responses were typically observed in cases of obesity induced

type II diabetes in non-ruminant subjects (McGarry, 2002; Jin et al., 2005). In these diabeteic subjects, AT is refractory to insulin's effects, which contributes to hyperglycemia and dyslipidemia. More recent evidence suggested that AT of obese individuals release more pro-inflammatory cytokines to blood, which result in the low grade inflammation in other organs, especially in liver, and induce the hepatic dysfunction and fatty liver disease (Tilg and Moschen, 2008). In non-ruminant animals, visceral AT has been reported to be different from SAT as compose of greater proportion of immune cells, higher lipolytic activity and more active in endocrine functions (Lionetti et al., 2009). However, how prepartum plane of dietary energy regulates AT metabolism of transition dairy cows and whether visceral AT respond differently to energy overfeeding compared with SAT in dairy cows is still largely unclear. Based on the evidences from other species, we hypothesize that prepartum overfeeding dietary energy increase preparturient BCS and exacerbated insulin resistance of AT in transition dairy cow, which is responsible for dramaticly increased lipolysis when concentration of blood insulin was reduced postpartum. Compared with SAT, visceral AT may secret more pro-inflammatory cytokines in response to energy overfeeding, which drains directly to liver from portal vein and compromise liver function postpartum.

LITERATURE CITED

Ailhaud, G., P. Grimaldi, and R. Negrel. 1992. Cellular and molecular aspects of adipose tissue development. Annu. Rev. Nutr. 12:207-233.

Allen, C. E., D. C. Beitz, D. A. Cramer, and R. G. Kauffman. 1976. Biology of fat in meat animals. Madison: U. Wisconsin; North Central Regional Research Publication No. 234.

Araujo, E. P., C. T. De Souza, A. L. Gasparetti, M. Ueno, A. C. Boschero, M. J. A. Saad, and L. A. Velloso. 2005. Short-term in vivo inhibition of insulin receptor substrate-1 expression leads to insulin resistance, hyperinsulinemia, and increased adiposity. Endocrinology 146:1428-1437.

Balage, M., J. F. Hocquette, B. Graulet, P. Ferré, and J. Grizard. 1997. Skeletal muscle glucose transporter (GLUT-4) protein is decreased in lactating goats. Anim. Sci. 65:257-265.

Baldwin, R. L., K. R. McLeod, and A. V. Capuco. 2004. Visceral tissue growth and proliferation during the bovine lactation cycle. J. Dairy Sci. 87:2977-86.

Baldwin, R. L., K. R. McLeod, J. P. McNamara, T. H. Elsasser, and R. G. Baumann. 2007. Influence of abomasal carbohydrates on subcutaneous, omental, and mesenteric adipose lipogenic and lipolytic rates in growing beef steers. J. Anim. Sci. 85:2271-2282.

Barber, M. C., R. J. Ward, S. E. Richards, A. M. Salter, P. J. Buttery, R. G. Vernon, and M. T. Travers. 2000. Ovine adipose tissue monounsaturated fat content is correlated to depot-specific expression of the stearoyl-CoA desaturase gene. J. Anim. Sci. 78:62–68.

Barber, M. C., M. T. Travers, E. Finley, D. J. Flint, and R. G. Vernon. 1992a. Growth-hormone-prolactin interactions in the regulation of mammary and adipose-tissue acetyl-CoA carboxylase activity and gene expression in lactating rats. Biochem. J. 285:469-475.

Barber, M. C., R. A. Clegg, E. Finley, R. G. Vernon, and D. J. Flint. 1992b. The role of growth hormone, prolactin and insulin-like growth factors in the regulation of rat mammary gland and adipose tissue metabolism during lactation. J. Endocrinol. 135:195-202.

Bauman, D. E. 1976. Intermediary metabolism of adipose tissue. Fed. Proc. 35:2308-2313.

Bauman, D. E., and W. B. Currie. 1980. Partitioning of nutrients during pregnancy and lactation: a review of mechanisms involving homeostasis and homeorhesis. J. Dairy Sci. 63:1514-1529.

Bauman. D. E., and R. G. Vernon. 1993. Effects of exogenous bovine somatotropin on lactation. Annu. Rev. Nutr. 13:437-461.

Bell, A. W. 1995. Regulation of organic nutrient metabolism during transition from late pregnancy to early lactation. J. Anim. Sci. 73:2804-2819.

Bergen, W. G., and H. J. Mersmann. 2005. Comparative aspects of lipid metabolism: impact on contemporary research and use of animal models. J. Nutr. 135:2499-2502.

Bernabucci, U., B. Ronchi, L. Basiricò, D. Pirazzi, F. Rueca, N. Lacetera, and A. Nardone. 2004. Abundance of mRNA of apolipoprotein b100, apolipoprotein e, and microsomal triglyceride transfer protein in liver from periparturient dairy cows. J. Dairy Sci. 87:2881-2888.

Bernlohr, D. A., A. E. Jenkins, and A. A. Bennars. 2002. Adipose tissue metabolism and lipid metabolism. In: Vance, D. E., and J. E. Vance. editors. Biochemistry of lipids, lipoproteins and membranes. 4th ed. p.263–289.

Bionaz, M., and J. J. Loor. 2008. Gene networks driving bovine milk fat synthesis during the lactation cycle. BMC Genomics. 9:366-387.

Bradford, B. J., L. K. Mamedova, J. E. Minton, J. S. Drouillard, and B. J. Johnson. 2009. Daily injection of tumor necrosis factor-{alpha} increases hepatic triglycerides and alters transcript abundance of metabolic genes in lactating dairy cattle. J Nutr. 139:1451-1456.

Briggs, M. R., C. Yokoyama, X. Wang, M. S. Brown, and J. L. Goldstein. 1993. Nuclear protein that binds sterol regulatory element of low density lipoprotein receptor promoter. I. Identification of the protein and delineation of its target nucleotide sequence. J. Biol. Chem. 268:14490–14496.

Broch, M., R. Ramírez, M. T. Auguet, M. J. Alcaide, C. Aguilar, A. Garcia-Espana, and C. Richart. 2010. Macrophages are novel sites of expression and regulation of retinol binding protein-4 (RBP4). Physiol. Res. 59:299–303.

Brockman, R. P. 1990. Effect of insulin on the utilization of propionate in gluconeogenesis in sheep. Br. J. Nutr. 64:95-101.

Bruun, J. M., A. S. Lihn, S. B. Pedersen, and B. Richelsen. 2005. Monocyte chemoattractant protein-1 release is higher in visceral than subcutaneous human adipose tissue (AT): implication of macrophages resident in the AT. J. Clin. Endocrinol. Metab. 90:2282-2289.

Butler-Hogg, B. W., J. D. Wood, and J. A. Bines. 1985. Fat partitioning in British Friesian cows: the influence of physiological state on dissected body composition. J. Agric. Sci., Camb. 104:519-528.

Cao, Z., R. M. Umek, and S. L. McKnight. 1991. Regulated expression of three C/EBP isoforms during adipose conversion of 3T3-L1 cells. Genes Dev. 5:1538-1552.

Carlson, D. B., J. W. McFadden, A. D. Angelo, J. C. Woodworth, and J. K. Drackley. 2007. Dietary L-carnitine affects periparturient nutrient metabolism and lactation in multiparous cows. J. Dairy Sci. 90:3422-3441.

Carlson, D. B., N. B. Litherland, H. M. Dann, J. C. Woodworth, and J. K. Drackley. 2006. Metabolic effects of abomasal L-carnitine infusion and feed restriction in lactating Holstein cows. J. Dairy Sci. 89:4819-4934.

Caro, J. F., M. K. Sinha, J. W. Kolaczynski, P. L. Zhang, and R. V. Considine. 1996. Leptin: the tale of an obesity gene. Diabetes 45:1455–1462.

Chilliard, Y., A. Ferlay, C. Delavaud, and F. Bocquier. 1998. Plasma leptin in underfed or overfed adult Holstein and Charolais cows, and its relationship with adipose tissue cellularity. Int. J. Obes. 22 (Suppl.3):171.

Christie, W. W. 1978. The composition, structure and function of lipids in the tissues of ruminant animals. Prog. Lipid Res. 17:111–205.

Christy, R. J., K. H. Kaestner, D. E. Geiman, and M. D. Lane. 1991. CCAAT/ enhancer binding protein gene promoter: binding of nuclear factors during differentiation of 3T3-L1 preadipocytes. Proc. Natl. Acad. Sci. USA 88:2593–2597.

Chui, P. C., H. P. Guan, M. Lehrke, and M. A. Lazar. 2005. PPARgamma regulates adipocyte cholesterol metabolism via oxidized LDL receptor 1. J. Clin. Invest. 115:2244–2256.

Cianzio, D. S., D. G. Topel, G. B. Whitehurst, D. C. Beitz, and H. L. Self. 1985. Adipose tissue growth and cellularity: changes in bovine adipocyte size and number. J Anim Sci. 60:970-976.

Clarke, S. L., C. E. Robinson, and J. M. Gimble. 1997. CAAT/enhancer binding proteins directly modulate transcription from the peroxisome proliferatoractivated receptor gamma2 promoter. Biochem. Biophys. Res. Commun. 240:99–103.

Cryer, A. 1987. Comparative biochemistry and physiology of lipoprotein lipase. Page 277-327. In: Borensztajn J, editor. Lipoprotein Lipase. Chicago: Evener.

Daniels, J. A., T. H. Elsasser, C. D. Morrison, D. H. Keisler, B. K. Whitlock, B. Steele, D. Pugh, and J. L. Sartin. 2003. Leptin, tumour necrosis factor-a (TNF), and CD14 in ovine adipose tissue and changes in circulating TNF in lean and fat sheep. J. Anim. Sci. 81:2590–2599.

Dann, H. M., and J. K. Drackley. 2005. Carnitine palmitoyltransferase I in liver of periparturient dairy cows: effects of prepartum intake, postpartum induction of ketosis, and periparturient disorders. J. Dairy Sci. 88:3851-3859.

Dann, H. M., N. B. Litherland, J. P. Underwood, M. Bionaz, A. D'Angelo, J. W. McFadden, and J. K. Drackley. 2006. Diets during far-off and close-up dry periods affect periparturient metabolism and lactation in multiparous cows. J Dairy Sci 89:3563-3577.

Degerman, E., P. Belfrage, and V. C. Manganiello. 1997. Structure, localization, and regulation of cGMP-inhibited phosphodiesterase (PDE3). J. Biol. Chem. 272:6823–6826.

DiGirolamo, M., J. B. Fine, K. Tagra, and R. Rossmanith.1998. Qualitative regional differences in adipose tissue growth and cellularity in male Wistar rats fed ad libitum. Am. J. Physiol. 274:R1460–R1467.

Donkin, S. S., and L. E. Armentano. 1995. Insulin and glucagon regulation of gluconeogenesis in preruminating and ruminating bovine. J. Anim. Sci. 73:546-551.

Douglas, G. N., T. R. Overton, H. G. Bateman, II, H. M. Dann, and J. K. Drackley. 2006. Prepartal plane of nutrition, regardless of dietary energy source, affects periparturient metabolism and dry matter intake in Holstein cows. J. Dairy Sci. 89:2141–2157.

Drackley, J. K. 1999. Biology of Dairy Cows During the Transition Period: the Final Frontier? J. Dairy Sci. 82:2259-2273.

Drackley, J. K., D. C. Beitz, and J. W. Young. 1991. Regulation of in vitro palmitate oxidation in liver from dairy cows during early lactation. J. Dairy Sci. 74:1884-1892.

Drackley, J. K., T. R. Overton, and G. N. Douglas. 2001. Adaptations of glucose and long-chain fatty acid metabolism in liver of dairy cows during the periparturient period. J. Dairy Sci. 84:E100-E112.

Dyer, C. J., J. M. Simmons, R. L. Matteri, and D. H. Keisler. 1997. Leptin receptor mRNA is expressed in ewe anterior pituitary and adipose tissues and is differentially expressed in hypothalamic regions of well-fed and feed-restricted ewes. Domest. Anim. Endocrinol. 14:119-128.

Ehrhardt, R. A., R. M. Slepetis, J. Siegal-Willott, M. E. Van Amburgh, A. W. Bell, and Y. R. Boisclair. 2000. Development of a specific radioimmunoassay to measure physiological changes of circulating leptin in cattle and sheep. J. Endocrinol. 166:519-528.

Eberlé. D., K. Clément, D. Meyre, M. Sahbatou, M. Vaxillaire, A. Le Gall, P. Ferré, A. Basdevant, P. Froguel, and F. Foufelle. 2004. SREBF-1 gene polymorphisms are associated with obesity and type 2 diabetes in French obese and diabetic cohorts. Diabetes 53:2153-2157.

Eguinoa, P., S. Brocklehurst, A. Arana, J. A. Mendizabal, R. G. Vernon, and A. Purroy. 2003. Lipogenic enzyme activities in different adipose depots of Pirenaican and Holstein bulls and heifers taking into account adipocyte size. J Anim Sci 81:432-440.

Fajas, L., D. Auboeuf, E. Raspé, K. Schoonjans, A. -M. Lefebvre, R. Saladin, J. Najib, M. Laville, J.-C. Fruchart, S. Deeb, A. Vidal-Puig, J. Flier, M.R. Briggs, B. Staels, H. Vidal, and J. Auwerx. 1997. The organization, promoter analysis, and expression of the human PPARg gene. J. Biol. Chem. 272:18779-18789.

Fajas, L., K. Schoonjans, L. Gelman, J. B. Kim, J. Najib, G. Martin, J. C. Fruchart, M. Briggs, B. M. Spiegelman, and J. Auwerx. 1999. Regulation of peroxisome proliferator-activated receptor gamma expression by adipocyte differentiation and determination factor 1/sterol regulatory element binding protein 1: implications for adipocyte differentiation and metabolism. Mol. Cell. Biol. 19:5495–5503.

Faulconnier, Y., I. Ortigues-Marty, C. Delavaud, D. Dozias, R. Jailler, D. Micol, and Y. Chilliard. 2007. Influence of the diet and grazing on adipose tissue lipogenic activities and plasma leptin in steers. Animal 1:1263-1271.

Faulkner, A., and P. A. Martin. 1999. Insulin secretion and intestinal peptides during lactation in sheep. J. Dairy Res. 66:45–52.

Faulkner, A., and H. T. Pollock. 1990. Metabolic responses to euglycaemic hyperinsulinaemia in lactating and non-lactating sheep in vivo. J. Endocrinol. 124:59-66.

Feve, B. 2005. Adipogenesis: cellular and molecular aspects. Best Pract. Res. Clin. Endocrinol. Metab.19:483-499.

Field, B., and H. G. Coore. 1976. Control of rat mammary-gland pyruvate dehydrogenase by insulin and prolactin. Biochem. J. 156:333-337.

Flatt, J. P., and E. G. Ball. 1964. Studies on the metabolism of adipose tissue. XV. An evaluation of the major pathways of glucose catabolism as influenced by insulin and epinephrine. J. Biol. Chem. 239:675-685.

Flint, D. J., P. A. Sinnett-Smith, R. A.Clegg, and R. G. Vernon. 1979. Role of insulin receptors in the changing metabolism of adipose tissue during pregnancy and lactation in the rat. Biochem. J. 182:421-427.

Franckhauser, S., I. Elias, V. Rotter Sopasakis, T. Ferré, I. Nagaev, C. X. Andersson, J. Agudo, J. Ruberte, F. Bosch, and U. Smith. 2008. Overexpression of Il6 leads to hyperinsulinaemia, liver inflammation and reduced body weight in mice. Diabetologia 51:1306-1316.

Frederich, R. C., A. Hamann, S. Anderson, B. Lollmann, B. B. Lowell, and J. S. Flier. 1995. Leptin levels reflect body lipid content in mice: evidence for diet-induced resistance to leptin action. Nature Med. 1:1311-1314.

Frohnert, B. I., T. Y. Hui, and D. A. Bernlohr. 1999. Identification of a functional peroxisome proliferator-responsive element in the murine fatty acid transport protein gene. J. Biol. Chem. 274:3970-3977.

Goff, J. P., and R. L. Horst. 1997. Physiological changes at parturition and their relationship to metabolic disorders. J. Dairy Sci. 80:1260-1268.

Gordon, S. 1998. The role of the macrophage in immune regulation. Res. Immunol. 149:685-688.

Grantham, B. D., and V. A. Zammit. 1988. Role of carnitine palmitoyltransferase I in the regulation of hepatic ketogenesis during the onset and reversal of chronic diabetes. Biochem. J. 249:409-419.

Gregoire, F. M., C. M. Smas, and H. S. Sul. 1998. Understanding adipocyte differentiation. Physiol. Rev. 78:783-809.

Gregory, N. G., R. J. Christopherson, and D. Lister. 1986. Adipose tissue capillary blood flow in relation to fatness in sheep. Res. Vet. Sci. 40:352-356.

Grum, D. E., J. K. Drackley, R. S. Younker, D. W. LaCount, and J. J. Veenhuizen. 1996. Nutrition during the dry period and hepatic lipid metabolism of periparturient dairy cows. J. Dairy Sci. 79:1850-1864.

Grum, D. E., L. R. Hansen, and J. K. Drackley. 1994. Peroxisomal β-oxidation of fatty acid in bovine and rat liver. Comp. Biochem. Physiol. 109B:281-292.

Grummer, R. R. 1993. Etiology of lipid-related metabolic disorders in periparturient dairy cows. J. Dairy Sci. 76:3882-3896.

Grummer, R. R. 1995. Impact of changes in organic nutrient metabolism on feeding the transition dairy cow. J. Dairy Sci. 73:2820-2833.

Guesnet, P., M. Massoud, and Y. Demarne. 1987. Effects of pregnancy and lactation on lipolysis of ewe adipocytes induced by beta-adrenergic stimulation. Mol. Cell. Endocrinol. 50:177-181.

Guesnet, M. Ph., M. J. Massoud, and Y. Demarne. 1991. Regulation of adipose tissue metabolism during pregnancy and lactation in the ewe: the role of insulin. J. Anim. Sci. 69:2057-2065.

Gurnell, M. 2005. Peroxisome proliferator-activated receptor gamma and the regulation of adipocyte function: lessons from human genetic studies. Best Pract. Res. Clin. Endocrinol. Metab.19:501-523.

Hamdy, O., S. Porramatikul, and E. Al-Ozairi. 2006. Metabolic obesity: the paradox between visceral and subcutaneous fat. Curr. Diabetes Rev. 2:367-73.

Hammon, H. M., G. Stürmer, F. Schneider, A. Tuchscherer, H. Blum, T. Engelhard, A. Genzel, R. Staufenbiel, and W. Kanitz. 2009. Performance and metabolic and endocrine changes with emphasis on glucose metabolism in high-yielding dairy cows with high and low fat content in liver after calving. J. Dairy Sci.92:1554-1566.

Hang, J., and J. A. Rillema. 1997. Prolactin's effects on lipoprotein lipase (LPL) activity and on LPL mRNA levels in cultured mouse mammary gland explants. Proc. Soc. Exp. Biol. Med. 214:161-166.

Hansen, L., B. Hartmann, H. Mineo, and J. J. Holst. 2004. Glucagon like peptide-1 secretion is influenced by perfusate glucose concentration and by a feedback mechanism involving somatostatin in isolated perfused porcine ileum. Regul. Peptides. 118:11-18.

Hanson, R. W., and F. J. Ballard. 1967. The relative significance of acetate and glucose as precursor for lipid synthesis in liver and adipose tissue from ruminants. Biochem. J. 105:529-536.

Haugebak, C. D., H. B. Hedrick, and J. M. Asplund. 1974. Adipose tissue accumulation and cellularity in growing and fattening lambs. J. Anim. Sci. 39:1016-1025.

Hauguel, S., M. Gilbert, and J. Girard. 1987. Pregnancy-induced insulin resistance in liver and skeletal muscles of the conscious rabbit. Am. J. Physiol. 252:E165-E169.

Hausman, D. B., G. J. Hausman, and R. J. Martin. 1999. Endocrine regulation of fetal adipose tissue metabolism in the pig: interaction of porcine growth hormone and thyroxine. Obesity Res. 7:76-82.

Hausman, G. J., M. V. Dodson, K. Ajuwon, M. Azain, K. M. Barnes, L. L. Guan, Z. Jiang, S. P. Poulos, R. D. Sainz, S. Smith, M. Spurlock, J. Novakofski, M. E. Fernyhough, and W. G. Bergen. 2009. Board-invited review: the biology and regulation of preadipocytes and adipocytes in meat animals. J Anim Sci 87:1218-1246.

Hayirli, A. 2006. The role of exogenous insulin in the complex of hepatic lipidosis and ketosis associated with insulin resistance phenomenon in postpartum dairy cattle. Vet. Res. Commun. 30:749-774.

Hayirli, A., R. R. Grummer, E. V. Nordheim, and P. M. Crump. 2002. Animal and dietary factors affecting feed intake during the prefresh transition period in Holsteins. J. Dairy Sci. 85:3430-3443.

Hegardt, F. G. 1999. Mitochondrial 3-hydroxy-3-methylglutaryl-CoA synthase: a control enzyme in ketongenesis. Biochem. J. 338:569-582.

Henry, B. A., J. W. Goding, W. S. Alexander, A. J. Tilbrook, B. J. Canny, F. Dunshea, A. Rao, A. Mansell, and I. J. Clarke. 1999. Central administration of leptin to ovariectomized ewes inhibits food intake without affecting the secretion of hormones from the pituitary gland: evidence for a dissociation of effects on appetite and neuroendocrine function. Endocrinology 140:1175-1182.

Hillgartner, F. B., L. S. Salati, and A. G. Goodridge. 1995. Physiological and molecular mechanisms involved in nutritional regulation of fatty acid synthesis. Physiol Rev. 75:47-76.

Hocquette, J. F., B. Graulet, and T. Olivecrona. 1998. Lipoprotein lipase activity and mRNA levels in bovine tissues. Comp. Biochem. Physiol. 121:201-212.

Holcomb, C. S., H. H. Van Horn, H. H. Head, M. B. Hall, and C. J. Wilcox. 2001. Effects of prepartum dry matter intake and forage percentage on postpartum performance of lactating dairy cows. J Dairy Sci. 84:2051-2058.

Holst, J. J. 1997. Enteroglucagon. Annu. Rev. Physiol. 59:257-271.

Holtenius, P. 1993. Hormonal regulation related to the development of fatty liver and ketosis. Acta. Vet. Scand. Suppl. 89:55-60.

Hood R. L., and C. E. Allen. 1973b. Comparative methods for the expression of enzyme data in porcine adipose tissue. Comp. Biochem. Physiol. 44B:677-686.

Hood R. L., and C. E. Allen. 1973a. Cellularity of bovine adipose tissue. J. Lipid Res. 14:605-610.

Hood, R. L. 1982. Relationships among growth, adipose cell size, and lipid metabolism in ruminant adipose tissue. Fed. Proc. 41:2555-2561.

Hood, R. L., and R. F. Thornton. 1979. The cellularity of ovine adipose tissue. Aust. J. Agric. Res. 30:153-161.

Hood, R. L., E. H. Thompson, and C. E. Allen. 1972. The role of acetate, propionate, and glucose as substrates for lipogenesis in bovine tissues. Int. J. Biochem. 3:598-606.

Hotamisligil, G. S., A. Budavari, D. Murray, and B. M. Spiegelman. 1994. Reduced tyrosine kinase activity of the insulin receptor in obesity-diabetes. Central role of tumor necrosis factor-α. J. Clin. Invest. 94:1543-1549.

Hu, E., P. Liang, and B. M. Spiegelman. 1996. AdipoQ is a novel adipose-specific gene dysregulated in obesity. J. Biol. Chem. 271:10697-10703.

Ingle, D. L., D. E. Bauman, and U. S. Garrigus. 1972a. Lipogenesis in the ruminant: in vivo site of fatty acid synthesis in sheep. J. Nutr. 102:617-623.

Ingle, D. L., D. E. Bauman, and U. S. Garrigus. 1972b. Lipogenesis in the ruminant: in vitro study of tissue sites, carbon source and reducing equivalent generation for fatty acid synthesis. J. Nutr. 102:609-616.

Ingvartsen, K. L., A. Danfær, P. H. Andersen, and J. Foldager. 1995. Prepartun feeding of dairy cattle: a review of the effect on prepartum metabolism, feed intake, production and health. Pages 83 in Book of Abstracts of the 46th Annual Meeting of the EAAP, Pragh. J.A.M. Arendonk, ed.Wageningen Press, Wageningen.

Ingvartsen, K. L., J. Foldager, and O. Aaes. 1997. Effect of prepartum TMR energy concentration on feed intake, milk yield, and energy balance in dairy heifers and cows. J. Dairy Sci. 80:211(Abstr.).

Ingvartsen, K. L., and J. B. Andersen. 2000. Integration of metabolism and intake regulation: a review focusing on periparturient animals. J. Dairy Sci. 83:1573-1597.

Janovick, N. A., J. J. Loor, P. Ji, R. E. Everts, H. A. Lewin, S. L. Rodriguez-Zas, And J. K. Drackley. 2009. Overfeeding energy prepartum dramatically affects peripartal expression of mRNA transcriptions in subcutaneous adipose tissue compared with controlling energy intake prepartum. J. Dairy Sci. 92(E-Suppl.):557. (Abstr.)

Janovick, N. A., and J. K. Drackley. 2010. Prepartum dietary management of energy intake affects postpartum intake and lactation performance by primiparous and multiparous Holstein cows. J Dairy Sci 93:3086-3102.

Jin, H.-B., Z.-Y. Gu, C.-H. Yu, and Y.-M. Li. 2005. Association of nonalcoholic fatty liver disease with type 2 diabetes: Clinical features and independent risk factors in diabetic fatty liver patients. Hepatobiliary Pancreat Dis. Int. 4:389–392.

Kahn, C. R. 1978. Insulin resistance, insulin, insensitivity, and insulin unresponsiveness: A necessary distinction. Metabolism 27:1893-1902.

Khachadurian, A. K., B. Adrouni, and H. Yacoubian. 1966. Metabolism of adipose tissue in the fat tail of the sheep in vivo. J. Lipid Res. 7:427-436.

Kim, J. B., and B. M. Spiegelman. 1996. ADD1/SREBP1 promotes adipocyte differentiation and gene expression linked to fatty acid metabolism. Genes Dev. 10:1096-1107.

Kim, J. B., G. D. Spotts, Y. D. Halvorsen, H. M. Shih, T. Ellenberger, H. C. Towle, and B. M. Spiegelman. 1995. Dual DNA binding specificity of ADD1/SREBP1 controlled by a single amino acid in the basic helix-loop-helix domain. Mol. Cell Biol.15:2582-2588.

Kim, J. B., H. M. Wright, M. Wright, and B. M. Spiegelman. 1998a. ADD1/SREBP1 activates PPAR gamma through the production of endogenous ligand. Proc. Natl. Acad. Sci. USA. 95:4333-4337.

Kim, J. B., P. Sarraf, M. Wright, K. M. Yao, E. Mueller, G. Solanes, B. B. Lowell, and B. M. Spiegelman. 1998b. Nutritional and insulin regulation of fatty acid synthetase and leptin gene expression through ADD1/SREBP1. J. Clin. Invest. 101:1-9.

Klöting, N., T. E. Graham, J. Berndt, S. Kralisch, P. Kovacs, C. J. Wason, M. Fasshauer, M. R. Schön, M. Stumvoll, M. Blüher, and B. B. Kahn. 2007. Serum retinol-binding protein is more highly expressed in visceral than in subcutaneous adipose tissue and is a marker of intra-abdominal fat mass. Cell Metab. 6:79-87.

Kuhn, N. J.1977. Lactogenesis: The search for trigger mechanisms in different species. Page 165 in Comparative aspects of lactation. M. Peaker, edi. Academic press, New York, NY.

Kushibiki, S., K. Hodate, H. Shingu, Y. Obara, E. Touno, M. Shinoda, and Y. Yokomizo. 2003. Metabolic and lactational responses during recombinant bovine tumor necrosis factor-alpha treatment in lactating cows. J. Dairy Sci. 86:819-827.

Lehrke, M. and M. A. Lazar. 2004. Inflamed about obesity. Nature Med.10:126–127.

Lehrke, M., and M. A. Lazar. 2005. The many faces of PPARgamma. Cell 123:993-999.

Leturque, A., S. Hauguel, P. Fed, and J. Girard. 1987. Glucose metabolism in pregnancy. Biol. Neonate. 51:64-69.

Linhart, H.G., K. Ishimura-Oka, F. DeMayo, T. Kibe, D. Repka, B. Poindexter, R. J. Bick, and G. J. Darlington. 2001. C/EBPalpha is required for differentiation of white, but not brown, adipose tissue. Proc. Natl. Acad. Sci. USA. 98:12532-12537.

Lionetti, L., M. P. Mollica, A. Lombardi, G. Cavaliere, G. Gifuni, and A. Barletta. 2009. From chronic overnutrition to insulin resistance: The role of fat-storing capacity and inflammation. Nutr. Metab. Cardiovas. 19:146-152.

Maffei, M., H. Fei, G. H. Lee, C. Dani, P. Leroy, Y. Zhang, R. Proenca, R. Negrel, G. Ailhaud, and J. M. Friedman. 1995. Increased expression in adipocytes of ob RNA in mice lesions of the hypothalamus and with mutations at the db locus. Proc. Natl. Acad. Sci. 92:6957-6960.

Mashek, D. G., and D. K. Beede. 2000. Peripartum responses of dairy cows to partial substitution of corn silage with corn grain in diets fed during the late dry period. J. Dairy Sci. 83:2310-2318.

Mater, M. K., A. P. Thelen, D. A. Pan, and D. B. Jump. 1999. Involvement of SREBP1c in the polyunsaturated fatty acid regulation of hepatic S14 gene transcription. J. Biol. Chem. 274:32725-32732.

McCarthy, J. P., A. Faulkner, P. A. Martin, and D. J. Flint. 1992. Changes in the plasma concentration of gastric inhibitory polypeptide and other metabolites in response to feeding in sheep. J. Endocrinol. 134:235-240.

McGarry, J. D. 2002. Dysregulation of fatty acid metabolism in the etiology of type 2 diabetes. Diabetes. 51:7-18.

McNamara, J. P. 1991. Regulation of adipose tissue metabolism in support of lactation. J. Dairy Sci. 74:706-719.

McNamara, J. P. 1995. Role and regulation of adipose tissue metabolism during lactation. J. Nutr. Biochem. 6:120-129.

McNamara, J. P. 1997. Adipose tissue metabolism during lactation: where do we go from here? Proc. Nutr. Soc. 56:149-167.

McNamara, J. P., and C. E. Murray. 2001. Sympathetic nervous system activity in adipose tissues during pregnancy and lactation of the rat. J. Dairy Sci. 84:1382-1389.

McNamara, J. P., and J. K. Hillers. 1986. Regulation of bovine adipose tissue metabolism during lactation. 2. Lipolysis response to milk production and energy intake. J. Dairy Sci. 69:3042-3050.

McNamara, J. P., D. C. McFhrland, and S. Bai. 1987. Regulation of bovine adipose tissue metabolism during lactation. 3. Adaptations in hormone sensitive and lipoprotein lipases. J. Dairy Sci. 70:1377.

McNamara, J. P., J. H. Harrison, R. L. Kincaid, and S. S. Waltner. 1995. Lipid metabolism in adipose tissue of cows fed high fat diets during lactation. J. Dairy Sci. 78:2782-2796.

Mendizabal, J. A., P. Alberti, P. Eguinoa, A. Arana, B. Soret, and A. Purroy. 1999. Adipocyte size and lipogenic enzyme activities in different adipose tissue in steers of local Spanish breeds. Anim. Sci. 69:115–121.

Metz, S. H. M., I. Mulder, and S. G. Van Den Bergh. 1973. Regulation of lipolysis in bovine adipose tissue by the degree of saturation of plasma albumin with fatty acids. Biochim. Biophys. Acta 306:42-50.

Minor, D. J., S. L. Trower, B. D. Strang, R. D. Shaver, and R. R. Grummer. 1998. Effects of nonfiber carbohydrate and niacin on periparturient metabolic status and lactation of dairy cows. J. Dairy Sci. 81:189-200.

Mizutani. H., T. Sako, Y. Toyoda, T. Kawabata, N. Urumuhang, H. Koyama, and S. Motoyoshi. 1999. Preliminary studies on hepatic carnitine palmitoyltransferase in dairy cattle with or without fatty liver. Vet. Res. Commun. 23:475-480.

Mukesh, M., M. Bionaz, D. E. Graugnard, J. K. Drackley, and J. J. Loor. 2009. Adipose tissue depots of Holstein cows are immune responsive: inflammatory gene expression in vitro. Domest. Anim. Endocrinol. 38:168-178.

Nieuwenhuizen, A. G., G. A. Schuiling, A. Bonen, A. M. Paans, W. Vaalburg, and T. R. Koiter. 1998. Glucose consumption by various tissues in pregnant rats: effects of a 6-day euglycaemic hyperinsulinaemic clamp. Acta Physiol. Scand. 164:325-34.

Nikkhah, A., J. J. Loor, R. J. Wallace, D. E. Graugnard, J. Vasquez, B. Richards, and J. K. Drackley. 2008. Moderate excesses of dietary energy markedly increase visceral adipose tissue mass in non-lactating dairy cows. J. Dairy Sci. 91(E-Suppl. 1):LB4. (Abstr.)

NRC. 2001. Nutrient Requirements of Dairy Cattle. 7th rev. ed. National Academy Press, Washington, DC.

Ost, A., A. Danielsson, M. Lidén, U. Eriksson, F. H. Nystrom, and P. Strålfors. 2007. Retinol-binding protein-4 attenuates insulin-induced phosphorylation of IRS1 and ERK1/2 in primary human adipocytes. FASEB J. 21:3696-3704.

Osumi, T., J. K. Wen, and T. Hashimoto. 1991. Two cis-acting regulatory sequences in the peroxisome proliferator-responsive enhancer region of rat acyl-CoA oxidase gene. Biochem. Biophys. Res. Commun. 175:866-871.

Ouchi, N., J. L. Parker, J. J. Lugus, and K. Walsh. 2011. Adipokines in inflammation and metabolic disease. Nature Rev. Immunol. 11:85-97.

Palou, M., T. Priego, J. Sánchez, A. M. Rodríguez, A. Palou, and C. Picó. 2009. Gene expression patterns in visceral and subcutaneous adipose depots in rats are linked to their morphologic features. Cell. Physiol. Biochem. 24:547-556.

Parmley, K. L. S., C. R. Machado, and J. P. McNamara. 1996. Rates of lipid metabolism in adipose tissue of pigs adapt to lactational state and dietary energy restriction. J. Nutr. 126:1644-1656.

Petterson, J. A., F. R. Dunshea, R. A. Ehrhardt, and A. W. Bell. 1993. Pregnancy and undernutrition alter glucose metabolic responses to insulin in sheep. J. Nutr. 123:1286-1295.

Petterson, J. A., R. Slepetis, R. A. Ehrhardt, F. R. Dunshea, and A. W. Bell. 1994. Pregnancy but not moderate undernutrition attenuates insulin suppression of fat mobilization in sheep. J. Nutr. 124:2431-2436.

Pradhan, A. D., J. E. Manson, N. Rifai, J. E. Buring, and P. M. Ridker. 2001. C-reactive protein, interleukin 6, and risk of developing type 2 diabetes mellitus. J. Amer. Med. Assoc. 286:327-334.

Prior, R. L., and R. K. Christenson. 1978. Insulin and glucose effects on glucose metabolism in pregnant and nonpregnant ewes. J. Anim. Sci. 46:201-210.

Pullen, D. L., D. L. Palmquist, and R. S. Emery. 1989. Effect on days of lactation and methionine hydroxy analog on incorporation of plasma fatty acids into plasma triglycerides. J. Dairy Sci. 72:49-58.

Quon, M. J., A. J. Butte, M. J. Zarnowski, G. Sesti, S. W. Cushman, and S. I. Taylor. 1994. Insulin receptor substrate 1 mediates the stimulatory effect of insulin on GLUT4 translocation in transfected rat adipose cells. J. Biol. Chem. 269:27920-27924.

Rebuffe-Scrive, M. 1991. Neuroregulation of adipose tissue: molecular and hormonal mechanisms. Int. J. Obesity. 15:83-86.

Regnault, T. R., H. V. Oddy, C. Nancarrow, N. Sriskandarajah, and R. J. Scaramuzzi. 2004. Glucose-stimulated insulin response in pregnant sheep following acute suppression of plasma non-esterified fatty acid concentrations. Reprod. Biol. Endocrinol. 2:64-74.

Reid, I. M., C. J. Roberts, R. J. Treacher, and L. A. Williams. 1986. Effect of body condition at calving on tissue mobilization, development of fatty liver, and blood chemistry of dairy cows. Anim. Prod. 43:7-15.

Reist, M., D. Erdin, D. von Euw, K. tschuemperlin, H. Leuenberger, C. Delavaud, Y. Chilliard, H. M. Hammon, N. Kuenzi, and J. W. Blum. 2003. Concentrate feeding strategy in lactating dairy cows: metabolic and endocrine changes with emphasis on leptin. J. Dairy Sci. 86:1690-1706.

Relling, A. E., and C. K. Reynolds. 2007a. Plasma concentrations of gut peptides in dairy cattle increase after calving. J. Dairy Sci. 90:325-330.

Relling, A. E., and C. K. Reynolds. 2007b. Feeding rumen-inert fats differing in their degree of saturation decreases intake and increases plasma concentrations of gut peptides in lactating dairy cows. J. Dairy Sci. 90:1506-1515.

Reynolds, C. K., P. C. Aikman, B. Lupoli, D. J. Humphries, and D. E. Beever. 2003. Splanchnic metabolism of dairy cows during the transition from late gestation through early lactation. J. Dairy Sci. 86:1201-1217.

Richards, B. F., N. A. Janovick, K. M. Moyes, D. E. Beever, and J. K. Drackley. 2009. Comparison of a controlled-energy high-fiber diet fed throughout the dry period to a two-stage far-off and close-up dietary strategy. J. Dairy Sci. 92(E-Suppl.):140. (Abstract)

Robelin, J. 1981. Cellularity of bovine adipose tissues: developmental changes from 15 to 65 percent mature weight. J. Lipid Res. 22:452-457.

Rognstad, R., and J. Katz. 1966. The balance of pyridine nucleotides and ATP in adipose tissue. Proc. Nat. Acad. Sci. 55:1148-1156.

Rosen, E. D., and B. M. Spiegelman. 2001. PPARgamma: a nuclear regulator of metabolism, differentiation, and cell growth. J. Biol. Chem. 276:37731-37734.

Rosen, E. D., C. H. Hsu, X. Wang, S. Sakai, M. W. Freeman, F. J. Gonzalez, and B. M. Spiegelman. 2002. C/EBPalpha induces adipogenesis through PPARgamma: a unified pathway. Genes Dev. 16:22-26.

Rosen, E. D., P. Sarraf, A. E. Troy, G. Bradwin, K. Moore, D. S. Milstone, B. M. Spiegelman, and R. M. Mortensen. 1999. PPAR gamma is required for the differentiation of adipose tissue in vivo and in vitro. Mol. Cell. 4:611-617.

Rosen, E. D., and O. A. MacDougald. 2006. Adipocyte differentiation from the inside out. Nature Rev. Mol. Cell Biol. 7:885-896.

Rukkwamsuk, T., T. A. M. Kruip, G. A. L. Meijer, and T. Wensing. 1999. Hepatic fatty acid composition in periparturient dairy cows with fatty liver lnduced by intake of a high energy diet in the dry period. J. Dairy Sci. 82:280-287.

Ryan, E. A., and L. Enns. 1988. Role of gestational hormones in the induction of insulin resistance. J. Clin. Endocrinol. Metab. 67:341-347.

Ryan, E. A., M. J. O'Sullivan, and J. S. Skyler. 1985. Insulin action during pregnancy. Studies with the euglycemic clamp technique. Diabetes 34:380-389.

Sadri, H., M. Mielenz, I. Morel, R. M. Bruckmaier, and H. A. van Dorland. 2010b. Plasma leptin and mRNA expression of lipogenesis and lipolysis-related factors in bovine adipose tissue around parturition. J. Anim. Physiol. Anim. Nutr (Berl). doi: 10.1111/j.1439-0396.2010.01111.x. [Epub ahead of print]

Sadri, H., R. M. Bruckmaier, H. R. Rahmani, G. R. Ghorbani, I. Morel, and H. A. van Dorland. 2010a. Gene expression of tumour necrosis factor and insulin signalling-related factors in subcutaneous adipose tissue during the dry period and in early lactation in dairy cows. J. Anim. Physiol. Anim. Nutr. (Berlin) 94:e194-e202.

Schäffler, A., and J. Schölmerich. 2010. Innate immunity and adipose tissue biology. Trends Immunol. 31:228-235.

Schoonjans, K., J. Peinado-Onsurbe, A. M. Lefebvre, R. A. Heyman, M. Briggs, S. Deeb, B. Staels, and J. Auwerx. 1996. PPARalpha and PPARgamma activators direct a distinct tissue-specific transcriptional response via a PPRE in the lipoprotein lipase gene. EMBO J. 15:5336-5348.

Sechen, S. I., S. N. McCutcheon, and D. E. Bauman. 1989. Response to metabolic challenges in early lactation dairy cows during treatment with bovine somatotropin. Domest. Anim. Endocrinol. 6:141-154.

Sekiya, M., N. Yahagi, T. Matsuzaka, Y. Takeuchi, Y. Nakagawa, H. Takahashi, H. Okazaki, Y. Iizuka, K. Ohashi, T. Gotoda, S. Ishibashi, R. Nagai, T. Yamazaki, T. Kadowaki, N. Yamada, J. Osuga, and H. Shimano. 2007. SREBP-1-independent regulation of lipogenic gene expression in adipocytes. J. Lipid Res. 48:1581-1591.

Sethi J. K., and A. J. Vidal-Puig. 2007. Adipose tissue function and plasticity orchestrate nutritional adaptation. 48:1253-1262.

She, P., G. L. Lindberg, A. R. Hippen, D. C. Beitz, and J. W. Young. 1999. Regulation of messenger ribonucleic acid expression for gluconeogenic enzymes during glucagon infusions into lactating cows. J. Dairy Sci. 82:1153-1163.

Shimabukuro, M., Y. T. Zhou, Y. Lee, and R. H. Unger. 1998. Troglitazone lowers islet fat and restores beta cell function of Zucker diabetic fatty rats. J. Biol. Chem. 273:3547-3550.

Shimano, H. 2001. Sterol regulatory element-binding proteins (SREBPs): transcriptional regulators of lipid synthetic genes. Prog. Lipid Res. 40:439-452.

Shimano, H., I. Shimomura, R. E. Hammer, J. Herz, J. L. Goldstein, M. S. Brown, J. D. Horton. 1997. Elevated levels of SREBP-2 and cholesterol synthesis in livers of mice homozygous for a targeted disruption of the SREBP-1 gene. J. Clin. Invest. 100:2115-2124.

Smith, T. R., and J. P. McNamara. 1990. Regulation of bovine adipose tissue metabolism during lactation. 6. Cellularity and hormone-sensitive lipase activity as affected by genetic merit and energy intake. J. Dairy Sci. 73:772-783.

Steppan, C. M., and M. A. Lazar. 2004. The current biology of resistin. J. Int. Med. 255:439-447.

Studer, V. A., R. R. Grummer, and S. J. Bertics. 1993. Effect of prepartum propylene glycol administration on periparturient fatty liver in dairy cows. J. Dairy Sci. 76:2931-2939.

Sumner, J. M., and J. P. McNamara. 2007. Expression of lipolytic genes in the adipose tissue of pregnant and lactating Holstein dairy cattle. J. Dairy Sci. 90:5237-5246.

Tamemoto, H., T. Kadowaki, K. Tobe, T. Yagi, H. Sakara, T. Hayakawa, Y. Terauchi, K. Ueki, Y. Kaburagi, S. Satoh, H. Sekihara, S. Yoshioka, H. Horikoshi, Y. Furuta, Y. Ikawa, M. Kasuga, Y. Yazaki, and S. Alzawa. 1994. Insulin resistance and growth retardation in mice lacking insulin receptor substrate-1. Nature 372:182-186.

Tesfa, A. T., M. Tuori, L. Syrjälä-Qvist, R. Pösö, H. Saloniemi, K. Heinonen, K. Kivilahti, T. Saukko, and L. A. Lindberg. 1999. The influence of dry period feeding on liver fat and postpartum performance of dairy cows. Anim. Feed Sci. Technol. 76:275–295.

Thompson, G. E., J. W. Gardner, and A. W. Bell. 1975. The oxygen consumption, fatty acid and glycerol uptake of the liver in fed and fasted sheep during cold exposure. Q. J. Exp. Physiol. 60:107-121.

Tilg, H., and A. R. Moschen. 2008. Insulin resistance, inflammation, and non-alcholic fatty liver disease. Trends Endocrinol. Metab. 19:371-379.

Tontonoz, P., E. Hu, J. Devine, E. G. Beale, and B. M. Spiegelman. 1995. PPAR gamma 2 regulates adipose expression of the phosphoenolpyruvate carboxykinase gene. Mol. Cell. Biol. 15:351-357.

Tontonoz, P., J. B. Kim, R. A. Graves, and B. M. Spiegelman. 1993. ADD1: a novel helix-loop-helix transcription factor associated with adipocyte determination and differentiation. Mol. Cell. Biol. 13:4753-4759.

Travers, M. T., R. G. Vernon, and M. C. Barber. 1997. Repression of the acetyl-CoA carboxylase gene in ovine adipose tissue during lactation: the role of insulin responsiveness. J. Mol. Endocrinol. 19:99-107.

Treacher, R. J., I. M. Reid, and C. J. Roberts. 1986. Effect of body condition at calving on the health and performance of dairy cows. Anim. Prod. 43:1-6.

Truscott, T. G., J. D. Wood, and H. R. Denny. 1980. Growth and cellularity of fat depots in British Friesian and Hereford cattle. Proc. 26th Eur. Meet. Meat Res. Workers 1:6-9.

Tugwood, J. D., I. Issemann, R. G. Anderson, K. R. Bundell, W. L. McPheat, and S. Green. 1992. The mouse peroxisome proliferator activated receptor recognizes a response element in the 5' flanking sequence of the rat acyl CoA oxidase gene. EMBO. J. 11:433-439.

Unoki, H., H. Bujo, M. Jiang, T. Kawamura, K. Murakami, and Y. Saito.2008. Macrophages regulate tumor necrosis factoralpha expression in adipocytes through the secretion of matrix metalloproteinase-3. Int. J. Obes. (London) 32:902-911.

Uysal, K.T., S.M. Wiesbrock, M.W. Marino, and G. S. Hotamisligil. 1997. Protection from obesity-induced insulin resistance in mice lacking TNFalpha function. Nature 389:610-614.

Van Epps-Fung, M., J. Williford, ,A. Wells, and R.W. Hardy. 1997. Fatty-acid induced insulin resistance adipocytes. Endocrinol. 138:4338-4345.

Vernon, R. G. 1976. Effect of dietary fats on ovine adipose tissue metabolism. Lipids 11:662-669 .

Vernon. R. G. 1996. Signal transduction and lipid metabolism during lactation. In T. Muramtasu (ed.), Gene Expression and Nutrition in Animals: From Cell to Whole Body, Research Signpost, Trivandrum, India.

Vernon, R. G. 2005. Lipid metabolism during lactation: a review of adipose tissue-liver interactions and the development of fatty liver. J. Dairy Res. 72:460-469.

Vernon, R. G., M. C. Barber, and E. Finley. 1991. Modulation of the activity of acetyl-CoA carboxylase and other lipogenic enzymes by growth hormone, insulin and dexamethasone in sheep adipose tissue and relationship to adaptations to lactation. Biochem. J. 274:543-548.

Vernon, R. G., and D. J. Flint. 1984. Adipose tissue: metabolic adaptation during lactation. In: Physiological Strategies in Lactation, Symposia 51, Symp. Zool. Soc. Lond. 51:119-146.

Vernon, R. G., and E. Finley. 1988. Roles of insulin and growth hormone in the adaptations of fatty acid synthesis in white adipose tissue during the lactation cycle in sheep. Biochem. J. 256:873-878.

Vernon, R. G., and E. Taylor. 1988. Insulin, dexamethasone and their interactions in the control of glucose metabolism in adipose tissue from lactating and nonlactating sheep. Biochem. J. 256:509-514.

Vernon, R. G., R. A. Clegg, and D. J. Flint. 1981. Metabolism of sheep adipose tissue during pregnancy and lactation. Adaptation and regulation. Biochem. J. 200:307-314.

Vernon, R. G., R. Doris, E. Finley, M. D. Houslay, E. Kilgour, and S. Lindsay-Watt. 1995. Effects of lactation on the signal transduction systems regulating lipolysis in sheep subcutaneous and omental adipose tissue. Biochem. J. 308:291-296.

Visser, M., L. M. Bouter, G. M. McQuillan, M. H. Wener, and T. B. Harris. 1999. Elevated C-reactive protein levels in overweight and obese adults. J. Amer. Med. Assoc. 282:2131-2135.

Weisberg, S.P., D. McCann, M. Desai, M. Rosenbaum, R. L. Leibel, and A. W. Ferrante, Jr.. 2003. Obesity is associated with macrophage accumulation in adipose tissue. J. Clin. Invest. 112: 1796-1808.

Withers, D. J., J. S. Gutierrez, H. Towery, D. J. Burks, J. M. Ren, S. Previs, Y. Zhang, D. Bernal, S. Pons, G. I. Shulman, S. Bonner-Weir, and M. F. White. 1998. Disruption of IRS-2 causes type 2 diabetes in mice. Nature 391:900-904.

Wu, Z., E. D. Rosen, R. Brun, S. Hauser, G. Adelmont, A. E. Troy, C. McKeon, G. J. Darlington, and B. M. Spiegelman. 1999. Cross-regulation of C/EBPa and PPARg controls the transcriptional pathway of adipogenesis and insulin sensitivity. Mol. Cell. 3:151-158.

Wu, Z., N. L. R. Bucher, and S. R. Farmer. 1996. Induction of peroxisome proliferator-activated receptor γ during the conversion of 3T3 fibroblasts into adipocytes is mediated by C/EBPβ, C/EBPδ, and glucocorticoids. Mol. Cell. Biol. 16:4128-4136.

Xu, C., Z. Wang, R. H. Zhang, H. Y. Zhang, S. X. Fu, and C. Xia. 2011. Effect of NEFA and Glucose Levels on CPT-I mRNA Expression and Translation in Cultured Bovine Hepatocytes. J. Vet. Med. Sci. 73:97-101.Xu, H., G. T. Barnes, Q. Yang, G. Tan, D. Yang, C. J. Chou, J. Sole, A. Nichols, J. S. Ross, L. A. Tartaglia, and H. Chen. 2003. Chronic inflammation in fat plays a crucial role in the development of obesity-related insulin resistance. J. Clin. Invest. 112:1821–1830.

Yang Y. T., and R. L. Baldwin. 1973. Preparation and metabolism of isolated cells from bovine adipose tissue. J. Dairy Sci. 56:350-365.

Yang, Q., T. E. Graham, N. Mody, F. Preitner, O. D. Peroni, J. M. Zabolotny, K. Kotani, L. Quadro, and B. B. Kahn. 2005. Serum retinol binding protein 4 contributes to insulin resistance in obesity and type 2 diabetes. Nature 436:356-362.

Zammit, V. A. 1999. The malonyl-CoA and long-chain acyl-CoA axis in the maintenance of mammalian cell function. Biochem. J. 343:505-515.

Zhang, H. H., M. Halbleib, F. Ahmad, V. C. Manganiello, and A. S. Greenberg. 2002. Tumor necrosis factor-alpha stimulates lipolysis in differentiated human adipocytes through activation of extracellular signal-related kinase and elevation of intracellular cAMP. Diabetes 51:2929-2935.

Zhang, Y., R. Proenca, M. Maffei, M. Barone, L. Leopold, and J. M. Friedman. 1994. Positional cloning of the mouse obese gene and its human homologue. Nature 372:425-432.

Zhou, Y. P., and V. E. Grill. 1994. Long-term exposure of rat pancreatic islets to fatty acids inhibits glucose-induced insulin secretion and biosynthesis through a glucose fatty acid cycle. J. Clin. Invest. 93:870-876.

Zhu, Y., C. Qi, J. R. Korenberg, X.-N. Chen, D. Noya, M.S. Rao, and J. K. Reddy. 1995. Structural organization of mouse peroxisome proliferator-activated receptor γ (mPPARγ) gene: Alternative promoter use and different splicing yield two mPPARγ isoforms. Proc. Natl. Acad. Sci. U.S.A. 92:7921-7925.

CHAPTER 2

OVERFEEDING ENERGY UPREGULATES PPARγ-CONTROLLED ADIPOGENIC NETWORKS AND INDUCIBLE ADIPOCYTOKINES IN VISCERAL AND SUBCUTANEOUS ADIPOSE DEPOTS OF HOLSTEIN COWS

ABSTRACT

This experiment was conducted to study the effects of energy overfeeding on gene expression in mesenteric (MAT), omental (OAT), and subcutaneous (SAT) adipose tissue from nonpregnant and nonlactating Holstein cows. Eighteen cows were randomly assigned to either a control (CON, NE_L= 1.35 Mcal/kg DM) or energy-overfed group (OVE, NE_L= 1.62 Mcal/kg DM) for 8 wk. Cows then were euthanized and subsamples of MAT, OAT, and SAT were harvested for transcript profiling via quantitative PCR (qPCR) of 29 genes involved in lipogenesis, triglyceride (TAG) synthesis, lipolysis, transcriptional regulation of lipogenesis, and immune response. The interaction of dietary energy and AT depot was not significant for any gene analyzed. Here, we report differences in gene expression pattern due to energy overfeeding. Overfeeding energy increased ($P < 0.05$) mRNA expression of genes related with *de novo* fatty acid (FA) synthesis (*ACLY, ACACA, FASN, THRSP*), long-chain FA elongation, desaturation, and intracellular trafficking (*ELOVL6, SCD*, and *FABP4*), and TAG synthesis (*GPAM* and *LPIN1*). The transcription regulator *PPARG* was up-regulated ($P < 0.05$) by overfeeding, whereas *SREBF1* was down-regulated ($P < 0.05$). The mRNA expression of *LEP* and *CCL2* was increased in cows overfed energy ($P < 0.05$), while *IL6R* was higher in CON cows ($P < 0.05$). Overall, results indicate that overfeeding energy increases AT mass through stimulation of

transcription of the network encompassing *de novo* FA synthesis and esterification processes. In contrast to other species, PPARγ rather than SREBF1 appears essential for both adipogenesis and lipid filling due to energy overfeeding.

INTRODUCTION

A feature of most mammalian species is their ability to accrete lipid when in positive energy balance. Adipogenesis induced by overfeeding energy can occur via cell proliferation (hyperplasia) or by differentiation of preadipocytes through lipid filling (hypertrophy) (Hausman et al., 2009). Age, physiological status of the animal, and potential limitation of adipocyte size seems to be crucial factors in determining the major pathways driving adipogenesis (Hood and Allen, 1973; Robelin, 1981). In dairy cows there is an obvious trend for greater adipocyte proliferation (i.e,. increase in cells/g tissue) between early and mid-lactation (McNamara et al, 1995). Pre-adipocyte markers such as delta-like 1 homolog (*DLK1*) as well as markers of differentiated adipocytes [e.g., fatty acid binding protein 4 (*FABP4*)] and lipogenic enzymes [e.g., acetyl-CoA carboxylase (*ACACA*), fatty acid synthase (*FASN*)] can be used to evaluate adipogenesis as related to lipid accretion and tissue mass in response to dietary energy intake.

A previous study from our laboratory observed up-regulation of genes involved in FA import (e.g., *CD36*), de novo FA synthesis (e.g., *ACACA*, *FASN*, *SREBF1*), and TAG synthesis (e.g., *LPIN1*, *SCD*) in MacT cells treated with rosiglitazone, which is a potent PPARγ agonist (Kadegowda et al., 2009). In rodents, nuclear (activated) SREBP1c transcriptionally activates lipogenic genes through binding to SREs as well as E-boxes in target gene promoters. Its central role in hepatic lipogenesis has been firmly established in rodents and humans (Horton et al., 2002). Moreover, SREBP1c was identified as a pro-adipogenic basic helix–loop–helix (bHLH)

transcription factor that can induce PPARγ expression and possibly generate an as-yet unknown PPARγ ligand (Kim and Spiegelman, 1996; Kim et al., 1998). It remains unclear whether SREBF1 has a role in bovine adipogenesis or whether it is responsive to dietary energy.

Linear increases in lipogenic activity (greater incorporation rate of acetate) in SAT of hybrid steers (Greathead et al., 2001) and in SAT, MAT, and OAT from growing steers (Baldwin et al., 2007) were observed with increasing metabolizable energy (ME) intake. The stimulatory effect of high carbohydrate intake on lipogenesis is possibly due to (1) increased substrate supply for lipogenesis (e.g., acetate, β-hydroxybutyrate, glucose, and lactate), which in the presence of glucose increases acetate incorporation rate in adipose tissue *in vitro* (Whitehurst et al., 1978); and (2) elevated blood glucose and insulin concentration potentially mediating the induction of lipogenic transcription regulators, e.g. insulin-response elements have been detected in both the promoter regions of *ACACA* and *FASN* in ovine and murine adipocytes (Sul et al., 2000; Travers et al., 2001).

During the dry period pregnant dairy cows can readily over-consume dietary energy and become over-conditioned, which at parturition results in greater susceptibility to fatty liver or ketosis due to the greater amount of non-esterified fatty acids (NEFA) in the circulation (Dann et al., 2006, Douglas et al., 2006, Janovick and Drackley, 2010). Visceral obesity leads to chronic low-grade inflammation due to increased secretion of proinflammatory cytokines from adipose and resident immune cells in human and rodents (Gastaldelli et al., 2002, Shoelson et al., 2006). Whether fat deposition in response to overfeeding energy in dairy cows results in transcriptional changes and a pro-inflammatory status has not been established. The underlying mechanisms whereby dietary energy overfeeding to ruminants regulates lipid metabolism and immune response in visceral and subcutaneous AT are unknown. Our hypothesis was that overfeeding a

moderate-energy diet to dairy cows would enhance fat deposition at least in part through changes in gene expression. Furthermore, different depots possess unique transcriptional signatures, which would make them more susceptible to varied dietary energy intake.

MATERIALS AND METHODS

Experimental Design, Animals, Diets, and Sampling

Experimental Design. Eighteen nonpregnant, nonlactating Holstein cows [body weight (BW) = 656 ± 29; body condition score (BCS) = 3.04 ± 0.25] were randomly assigned to either a moderate-energy diet (OVE; NE_L = 1.62 Mcal/kg DM) or controlled-energy diet (CON; NE_L = 1.35 Mcal/kg DM) provided as a TMR for *ad libitum* intake. The OVE diet contained 73.8% forage without straw and 13.8% ground shelled corn (DM basis); whereas, the CON diet contained 81.7% forage with 40.5% wheat straw and 3.5% ground shelled corn. The TMR were mixed and processed in a Keenan Klassik 140 mixer wagon (Richard Keenan & Co., Ltd., Borris, County Carlow, Ireland) and offered once daily at 0800 h. Straw was not pre-processed before being added to the TMR mixer. Cows had free access to water. Initial and final BW was recorded at the start of wk 1 and end of wk 8. The experiment was conducted in an indoor free-stall barn equipped with Calan gates to monitor individual feed intake. Experimental procedures were approved by the Institutional Animal Care and Use Committee at the University of Illinois (protocol 06194).

DMI, Body Composition, Visceral Adipose Tissue Mass, and Blood Metabolites. These data were collected and analyzed by Nikkhah et al. (unpublished data) and are shown in Table 2.1. Feed intake were recorded daily; feed and TMR samples were collected bi-weekly and composited into 3 pooled samples for nutrient analysis. Blood was sampled at wk 2, 4, and 7 and

serum was obtained by centrifugation at 1800×g for analysis of non-esterified fatty acid (NEFA), β-hydroxybutyrate (BHBA), cholesterol, glucose, and insulin concentrations. Body condition scores (BCS) were assigned at wk 1, 4 and 7. After the 8-wk experiment, cows were euthanized at the University of Illinois College of Veterinary Medicine diagnostic facilities. The weights of visceral organs and visceral AT were recorded on site.

Tissue Sampling. All AT samples were harvested within 20 min of euthanasia and snap-frozen in liquid N_2 until RNA extraction. Subcutaneous AT (SAT) was harvested from the tail-head region on the left side of each cow. Mesenteric, omental, and perirenal AT depots were carefully dissected, weighed, and a subsample collected for RNA extraction.

RNA Extraction and Quality Assessment, Primer Design and Evaluation, Internal Control Gene (ICG) Selection, and Quantitative RT-PCR (qPCR)

RNA Extraction, Quality Assessment, and cDNA Preparation. Adipose tissue was weighted (~2.0 g) and immediately placed into ice-cold TRIzol® Reagent (~15 mL) (Invitrogen, Carlsbad, CA) with 1 µL linear acrylamide (Ambion, Inc., Austin, TX) for extraction of total RNA as previously described (Loor et al., 2005). Total RNA was cleaned using RNeasy mini kit columns and genomic DNA was removed using the RNase-Free DNase Set (Qiagen, Valencia, CA). The RNA concentration was measured with a NanoDrop ND-1000 spectrophotometer (NanoDrop Technologies). The purity of RNA was assessed by ratio of optical density OD260/280, which were above 1.9 for all samples. Integrity of RNA (RIN) was tested by electrophoretic analysis of 28S and 18S rRNA subunits using a 2100 Bioanalyzer (Agilent Technologies), and values were >7.0 for all samples. A portion of the RNA was diluted to 100 ng/µL with DNase-RNase free water prior to RT for cDNA synthesis. The cDNA were synthesized using 100 ng RNA, 1 µg dT18 (Operon Biotechnologies, AL), 1 µL 10 mM dNTP

mix (Invitrogen Corp., CA), 1 µL Random Primers (Invitrogen Corp., CA), and 10 µL DNase/RNase free water. The mixture was incubated at 65°C for 5 min and kept on ice for 3 min. A total of 6 µL of master mix composed of 4.5 µL 5X First-Strand Buffer, 1 µL 0.1 M DTT, 0.25 µL (50 U) of SuperScript™ III RT (Invitrogen Corp.,CA), and 0.25 µL of RNase Inhibitor (10 U, Promega, WI) was added. The reaction was performed in an Eppendorf Mastercycler® Gradient with the following temperature program: 25°C for 5 min, 50°C for 60 min, and 70°C for 15 min. The cDNA was then diluted 1:4 with DNase/RNase free water.

***Primer Design and Evaluation*.** Primers were designed and evaluated as previously described (Bionaz and Loor, 2008). The details of primer sequences and the description of genes are shown in Table 2.3 and Supplemental Table S2.1 and S2.2. Primers were designed using Primer Express 3.0 with minimum amplicon size of 80 bp (amplicons of 100 -120 bp were superior, if possible) and limited 3' G + C percentage (Applied Biosystems, CA). Primer sets were intentionally designed to fall across exon-exon junctions. Then, primers were aligned against NCBI database through BLASTN and UCSC's COW (*Bos taurus*) Genome Browser Gateway to determine the compatibility of primers with already annotated sequences of the corresponding gene in both databases. Prior to qPCR, primers were verified through a 20 µL-PCR reaction, which followed the same procedures of qPCR described below except the dissociation step. A universal reference cDNA amplified from 3 bovine adipose tissues (SAT, mesenteric, and omental AT) was utilized to ensure the identification of genes. Five µL of PCR product was run in a 2% agarose gel stained with ethidium bromide, and the remaining 15 µL were cleaned with a QIAquick® PCR Purification Kit (QIAGEN) and sequenced at the Core DNA Sequencing Facility of the Roy J. Carver Biotechnology Center at the University of Illinois, Urbana (in Supplement Table S2.2). The sequencing product was confirmed through BLASTN at

the National Center for Biotechnology Information (NCBI) database. Only primers that presented a single band of the expected size and the right amplification product were used for qPCR. The accuracy of a pair of primers was evaluated by the presence of a unique peak during the dissociation step at the end of qPCR.

Genes evaluated included: acetyl-Coenzyme A carboxylase alpha (*ACACA*), ATP citrate lyase (*ACLY*), acyl-CoA synthetase long-chain (*ACSL1*), adipose differentiation-related protein (*ADFP* or *PLIN2*), thrombospondin receptor (*CD36*), elongation of long chain fatty acids family member 6 (*ELOVL6*), adipocyte fatty acid binding protein 4 (*FABP4*), fatty acid synthase (*FASN*), mitochondrial glycerol-3-phosphate acyltransferase (*GPAM*), hormone-sensitive lipase (*LIPE*), lipin 1 (*LPIN1*), lipoprotein lipase (*LPL*), stearoyl-CoA desaturase (*SCD*), MLX interacting protein-like (*MLXIPL*), peroxisome proliferator-activated receptor gamma (*PPARG*), sterol regulatory element binding transcription factor 1 (*SREBF1*), thyroid hormone responsive SPOT 14 (*THRSP*), adiponectin (*ADIPOQ*), chemokine (C-C motif) ligand 2 (*CCL2*), chemokine (C-C motif) ligand 5 (*CCL5*), interleukin-1 beta (*IL1B*), interleukin-6 (*IL6*), interleukin-6 receptor (*IL6R*), leptin (*LEP*), acute-phase serum amyloid A1 (*SAA1*), toll-like receptor 4 (*TLR4*), and tumor necrosis factor alpha (*TNF*).

Quantitative PCR (qPCR). qPCR was performed in a MicroAmp^{TM} Optical 384-Well Reaction Plate (Applied Biosystems, CA). Within each well, 4 µL diluted cDNA combined with 6 µL of mixture composed of 5 µL 1×SYBR Green master mix (Applied Biosystems, CA), 0.4 µL each of 10 µM forward and reverse primers, and 0.2 µL DNase/RNase free water were added. Three replicates and a 6 point standard curve plus the non-template control (NTC) were run for each sample to test the relative expression level (User Bulletin #2, Applied Biosystems, CA). qPCR was conducted in ABI Prism 7900 HT SDS instrument (Applied Biosystems, CA)

following these conditions: 2 min at 50 °C, 10 min at 95 °C, 40 cycles of 15 s at 95 °C (denaturation), and 1 min at 60 °C (annealing + extension). The presence of a single PCR product was verified by the dissociation protocol using incremental temperatures to 95 °C for 15 s, then 65 °C for 15 s.

***Internal Control Gene (ICG) Selection and Evaluation*.** A detailed description for the selection criteria of ICG for qPCR has been described previously (Mukesh et al., 2009). Briefly, ICGs are genes that are not coregulated and whose expression does not vary with physiological state or nutritional status (Bionaz and Loor, 2007). Based on previous microarray data for visceral and subcutaneous AT, 11 most stably expressed genes were identified as the candidate ICGs via GeneSpring GX7. The potential co-regulation among these genes was tested using Ingenuity Pathway Analysis (IPA, Ingenuity Systems, Inc., Walnut Creek, CA, USA; released January 7, 2009). Then, all candidate ICGs were tested for expression using the same samples and standard curve samples used in current study. The expression values of candidate ICGs were uploaded into geNorm software to evaluate expression ratio stability (M value), of which the higher stability (expressed as lower M value) between any 2 non-coregulated genes indicates the greater suitability as ICGs. In addition, the optimal number of ICG that should be employed for normalization was determined via geNorm by calculating the pairwise variation (V value) between the normalization factor (NF) obtained using n ICGs and the NF from (n+1) ICGs. The decreased V value in (n+1) ICGs vs. n ICGs indicates the improvement of normalization effect. However, V value below 0.1 should be acceptable for normalization. The geometric mean of the finally selected ICGs was calculated and used as NF for normalization of mRNA expression of the tested genes (Vandesompele et al., 2002).

Data Processing and Statistical Analysis

The threshold cycle (Ct) data were analyzed and transformed using the standard curve with the 7900 HT Sequence Detection System Software (version 2.2.1, Applied Biosystems, CA). Data were then normalized with the geometric mean of the three most stable ICG (Mukesh et al., 2009). Analysis (Supplemental Figure S2.1) revealed that genes encoding kelch-like ECH-associated protein 1 (*KEAP1*), tripartite motif-containing 41 (*TRIM41*), and mitochondrial ribosomal protein 63 (*MRP63*) were the most appropriate to calculate a normalization factor to normalize gene expression data.

The normalized PCR data (relative mRNA expression) were subjected to log transformation in SAS (SAS Inst. Release 8.0) to ensure a normal distribution of residuals. This transformed dataset was analyzed as a 2×3 factorial arrangement (diet and tissue source as the two factors) with the PROC GLM procedure in SAS. No significant interaction between the two factors was detected in the initial analysis; therefore, we excluded the interaction and re-analyzed data simply on main effects. The PDIFF statement of SAS was utilized to evaluate differences with significance declared at $P \leq 0.05$.

Relative mRNA Abundance of Genes within Adipose Tissue

Efficiency of qPCR amplification for each gene was calculated using the standard curve method (Efficiency = $10^{(-1/\text{slope})}$) (See Supplement Table S2.3). Relative mRNA abundance among measured genes was calculated as previously reported (Bionaz and Loor, 2008), using the inverse of PCR efficiency raised to ΔCt (gene abundance = $1/E^{\Delta Ct}$, where ΔCt = Ct of tested gene – geometric mean Ct of 3 internal control genes). Overall mRNA abundance for each gene among all samples of the same adipose tissue was calculated using the median ΔCt, and overall

percentage relative mRNA abundance was computed from the equation: 100 × mRNA abundance of individual gene / sum of mRNA abundance of all genes tested (See Table 2.4).

Gene Network Analysis

Ingenuity Pathway Analysis® software (IPA; Redwood City, CA) was utilized to explore networks among the genes analyzed. This web-based software enables the reconstruction of networks and interactions among genes based on current knowledge (i.e., published literature) among human, mouse and rat genes/proteins. Thus, the software allows for easier interpretation and understanding of the underlying relationships in a biologically relevant context. Prior to uploading data into IPA, relative expression levels of genes in mesenteric and omental adipose from SAS results were transformed to fold-change relative to that in subcutaneous adipose; the same transformation was performed on data from moderate dietary energy to obtain fold-changes compared with data from low dietary energy. One-fold change was set as threshold to depict changes (i.e., genes marked black indicates up-regulation and white for down-regulation) in gene expression between the tissues or treatments.

RESULTS AND DISCUSSION

Except for a tendency for *LPL* (P = 0.085), no statistically significant ($P < 0.05$) interactions were detected between level of dietary energy and fat depot site. Therefore, our data indicate that both VAT and SAT of dairy cows respond in the same fashion to overfeeding energy. In work with beef cattle, Faulconnier et al. (2007) reported a lack of interaction between diet (grass-based or maize silage-based diets) and fat depot (intermuscular, subcutaneous, and perirenal AT) for lipogenic enzymes (glucose-6-phosphate dehydrogenase, malic enzyme, FASN, and glycerol-3-phosphate dehydrogenase) and LPL enzymatic activity. In the subsequent

sections only the main effect of dietary energy level will be discussed. The main effect of adipose depot on transcript profiles is presented in chapter 3.

de novo Fatty Acid Synthesis

Adipose tissues rather than liver are the major site of lipogenesis in non-lactating ruminants (Hood et al., 1980; Bergen and Mersmann, 2005). Expression of 3 genes encoding enzymes that participate in DNS was examined. ATP citrate lyase (*ACLY*) converts citrate to acetyl-CoA in the cytosol and allows glucose and lactate carbon to serve as substrates for DNS. Acetyl-CoA carboxylase (*ACACA*) synthesizes malonyl-CoA from acetyl-CoA derived from either ruminal acetate or glucose, and *FASN* uses malonyl-CoA to initiate a series of elongation reactions leading to the formation of palmitic acid (Vernon, 1980). Overfeeding dietary energy resulted in significantly greater ($P < 0.01$) mRNA expression levels of these 3 genes regardless of fat depot (Figure 2.1). Fold changes in OVE/CON were 1.7, 1.5 and 2.1 (based on mRNA expression of back-transformed data) for *ACLY*, *ACACA*, and *FASN*, respectively. These three genes accounted for ~0.1%, 0.7%, and 4.1% of total genes examined in OVE group, and for ~0.1%, 0.6% and 0.28% in CON (See Table 2.4).

Although acetate, glucose, and lactate could serve as substrates for lipogenesis, acetate has been shown to be the predominant precursor in ruminant adipose (Hanson and Ballard, 1967; Hood et al., 1972; Whitehurst et al., 1978, 1981). Despite the low enzymatic activity of ACLY in growing calf adipose tissues (perirenal, omental, and epididymal) (Ingle et al., 1972b), which may be the same in mature dairy cows as reflected by its low mRNA abundance (~0.1% of all genes tested in both treatment groups), an adaptation of this enzyme to substrate availability has been reported, i.e. there was a substantial increase in lipogenic enzyme activity and glucose-carbon incorporation into fatty acids of dairy cows after infusion of glucose post-ruminally or

intravenously (Bauman, 1976). In a more recent study, activities of ACLY ($P < 0.01$), FASN ($P < 0.05$), and NADP-malate dehydrogenase ($P < 0.01$) were increased in SAT of ad libitum-fed vs. limit-fed steers (Schoonmaker et al., 2004).

A linear increase in lipogenic activity (greater incorporation rate of [1-^{14}C] acetate) in SAT of hybrid steers was observed with increasing metabolizable energy (ME) intake (Greathead et al., 2001), thus confirming that positive energy balance promotes the lipogenic process. The observed up-regulation of *ACLY* by overfeeding energy in the present study may have been due to a sustained increase in the availability of blood glucose and lactate due to greater dietary ground corn grain (13.8% vs. 3.5% of diet DM) and corn silage (50% vs. 28% of DM). The greater expression of *ACACA* and *FASN* in OVE cows indicated that excess energy intake altered adipose lipogenic capacity at least in part through gene transcription. Previous work from our laboratory also found that prepartal energy overfeeding up-regulated lipogenic genes (*ACACA* and *FASN*) and cytosolic isocitrate dehydrogenase 1 (*IDH1*) in SAT (Janovick et al., 2009). IDH1 converts cytoplasmic isocitrate to α-ketoglutarate with the production of NADPH, which is a critical pathway of reducing equivalent supply for DNS in ruminant adipose tissue (Ingle et al., 1972b).

Greater mRNA abundance of lipogenic genes by energy overfeeding in the present study may have been induced by a combination of greater substrate supply and insulin, which is a well-described lipogenic hormone (Sul et al., 2000; Travers et al., 2001). The inclusion of ground corn and easily fermentable corn silage (compared with wheat straw in the CON diet) potentially provided greater amounts of substrates (acetate and glucose derived from either gluconeogenesis or absorbed post-ruminally) for lipogenesis even though no difference in blood glucose concentration was observed between treatments (66.1 and 66.7 mg/dL for CON and OVE) .

Moreover, serum insulin concentration was greater in OVE (23.5 and 29.6 μIU/mL for CON and OVE; Nikkhah et al., 2008).

Long-chain Fatty Acid Uptake, Activation, and Intracellular Trafficking

Gastrointestinal absorption of preformed lipid is relatively small in ruminants as a result of low dietary fat intake, and ruminant liver has limited capability to synthesize and secrete VLDL compared with non-ruminants (Drackley et al., 1999). However, the uptake of preformed LCFA contributes to the intracellular FA pool of AT. In the present study, dietary fat content was nearly doubled in OVE cows due to the inclusion of whole cottonseeds at 5% of dietary DM (Table 2.2). The relative % mRNA abundance of *LPL* accounted for 8.3% and 14.6% in CON and OVE (Table 2.4), which indicated that uptake of LCFA is an important contributor to the intracellular FA pool.

Lipoprotein lipase hydrolyzes LCFA from TAG in chylomicrons or VLDL (Weinstock et al., 1997), and is considered a suitable indicator of energy status in cows (McNamara et al., 1987). The plasma membrane protein CD36 mediates LCFA translocation into the cytosol after their release via LPL (see reviews Hajri and Abumrad, 2002; Thompson et al., 2010). Long-chain acyl-CoA synthases (ACSL) are localized in various subcellular sites including plasma membrane and cytosol and activate FA to acyl-CoA prior to entry into different metabolic pathways (Gargiulo et al., 1999). It was reported that *ACSL1* is the predominant isoform in bovine mammary tissue (Bionaz and Loor, 2008) and AT (Janovick et al., 2009). A study in non-pregnant beef heifers showed that high dietary energy increased LPL activity in SAT (Sprinkle et al., 1998). Bonnet et al. (2000) observed a parallel increase in both LPL activity and mRNA expression in perirenal AT of ewes, which also had greater plasma insulin concentration.

In non-ruminants, insulin regulates *LPL* and *CD36* at the transcriptional level (Thompson et al., 2010) but in our study excess dietary energy consumption (which resulted in greater blood insulin; Nikkhah et al., 2008) did not affect the mRNA expression of these genes ($P > 0.05$, Figure 2.1). We did observe a lower serum glucose:insulin ratio in OVE cows, which may indicate a compromised insulin response by peripherial tissues. Therefore, it is possible that the lack of response of *LPL* and *CD36* to dietary energy overfeeding was the result of impaired insulin sensitivity in AT. This idea is supported by the lower expression of the transcription regulator *SREBF1*, which is a well-established driver of the insulin-induced lipogenic response in non-ruminants (Foufelle and Ferre, 2002). Further discussion of transcription regulators is presented below.

Adipocyte fatty acid-binding protein (encoded by the *FABP4* gene) functions as intracellular LCFA transport protein and helps regulate lipid storage (Hertzel and Bemlohr, 2000). *FABP4* is the best described target gene of the nuclear receptor PPARγ (Lefterova et al., 2008) and is an accepted marker of adipocyte differentiation due to its strikingly increased expression (Hertzel and Bernlohr, 2000). In this study, overfeeding energy significantly increased *FABP4* expression ($P < 0.05$, Figure 2.1), which may be indicative of a sustained degree of adipocyte differentiation. Moreover, *FABP4* accounted for up to ~24% and ~28% of total mRNA abundance in OVE or CON cows, which made it the second most abundant gene in OVE and the most abundant in CON. These data implicate FABP4 as a crucial enzyme in bovine adipocytes. Paradoxically, in non-ruminants this protein was reported to be involved in lipolysis by directly interacting with LIPE (Shen et al., 1999; Smith et al., 2004). Adipocytes obtained from *FABP4*-null mice had markedly reduced efficiency of lipolysis in vivo and in vitro (Coe et al., 1999; Scheja et al., 1999). However, our results do not seem to support such an effect

because no differences were observed in plasma NEFA (0.11 mmol/L for both OVE and CON cows, Nikkhah et al., 2008) or *LIPE* mRNA expression. Macrophages express *FABP4* and its reduced expression resulted in decreased production of a cluster of pro-inflammatory cytokines (Hertzel et al., 2009). Furthermore, disruption of *FABP4* expression alone resulted in alleviation of insulin resistance associated with diet-induced obesity (Hotamisligil et al., 1996). The greater expression of *FABP4* in adipose tissue of OVE cows may have predisposed the animal to insulin insensitivity and a pro-inflammatory state.

Elongation and Desaturation of LCFA

In rodents, isomers of the ELOVL family exhibit tissue- and substrate-specific activity (Ntambi and Miyazaki, 2004). In fact, both ELOVL and SCD are localized in the ER and cooperate during synthesis of 18:0 and *cis*9-18:1 in mice (see review Guillou et al., 2010). ELOVL6 is primarily involved at the ER in the elongation of saturated and monounsaturated FA with 16-carbons, without capacity for elongation beyond 18-carbons (Jakobsson et al., 2006). Janovick et al. (2009) reported that *ELOVL6* was up-regulated together with other lipogenic-related genes (*ACACA*, *FASN*, and *SCD*) in SAT of prepartal dairy cows overfed dietary energy, which may represent a previously-unrecognized step in fatty acid synthesis in bovine AT (Loor, 2010). Loor (2010) proposed that ELOVL6 activity is a 'necessary step' in endogenous formation of 18:0 in adipose, which is then converted to *cis*9-18:1 by SCD. Stearic acid rather than 16:0 is the preferred substrate for SCD in mice, and oleic acid is the predominant isomer of 18:1 in bovine AT (Rukkwamsuk et al., 2000, Webb et al., 1998) and plasma (Loor et al., 2005; Douglas et al., 2007).

In the present study, energy overfeeding markedly increased ($P < 0.01$, Figure 2.1) expression of both *ELOVL6* (1.8 fold-change) and *SCD* (3.5 fold-change) regardless of adipose

depot. Furthermore, the parallel up-regulation of *ELOVL6* and *SCD* and lipogenic genes (*ACACA* and *FASN*), as observed previously in overfed prepartal dairy cows (Janovick et al., 2009), suggests that the lipogenic pathway in ruminant adipose involves elongation of 16:0 and a subsequent desaturation to *cis*9-18:1 and, thus, these joint pathways possibly constitute (as in non-ruminants) the major source of LCFA in bovine AT. More importantly, the expression of these lipogenic enzymes may be subject to the same transcriptional regulators as the 'classical' lipogenic genes. In OVE cows, *SCD* mRNA abundance accounted for ~38.8% of total mRNA compared with ~18% in CON (Table 2.4), which underscores its essential role in the overall process of lipogenesis and esterification in bovine adipocytes as shown in bovine mammary tissue (Bionaz and Loor, 2008).

ELOVL6 was identified as target gene of SREBF1 in rodent liver (Moon et al., 2001; Wang et al., 2005); however, in the present study *ELOVL6* together with other well-established SREBF1 target genes in rodent liver (*ACACA*, *FASN* and *SCD*) were up-regulated by overfeeding energy despite decreased expression of *SREBF1*, which suggests that they may not be regulated by SREBF1 in bovine AT. Results from previous studies also have challenged a putative central role of SREBF1 in lipogenesis in bovine mammary gland (Bionaz and Loor, 2008) and in rat AT (Sekiya et al., 2007).

TAG Synthesis, Lipid Droplet Formation, and Lipolysis

Glycerol-3-phosphate acyltransferase (GPAT) esterifies FA to the *sn*-1 position of glycerol-3-phosphate, which is the first and presumed rate-limiting step of TAG biosynthesis (Takeuchi and Reue, 2009). GPAM is the isoform of GPAT localized on the outer membrane of mitochondria, and the only identified and characterized GPAT in bovine species (see NCBI webpage: http://www.ncbi.nlm.nih.gov/gene/497202). The high mRNA expression in liver and

AT in rodents (Lewin et al., 2001) and in AT in humans (Cao et al., 2006) underscores its critical role in TAG synthesis.

Lipins function as phosphatidate phosphatases (PAP) that convert phosphatidic acid (PA) to diacylglycerol (DAG) during TAG synthesis. *LPIN1* was previously shown to be the most highly-expressed isoform in bovine mammary gland during lactation (Bionaz and Loor, 2008). In the present study, excess dietary energy intake up-regulated both *GPAM* and *LPIN1* ($P < 0.01$, Figure 2.1) and also *ADFP* expression ($P = 0.06$). The latter protein, currently defined as perilipin 2 (NCBI databse), is a lipid droplet membrane protein that functions to protect TAG from basal lipolysis but (paradoxically) also seems to be required for maximal β-adrenergic-stimulated lipolysis (Tansey et al., 2001) (Figure 2.1). Although we did not measure other enzymes (e.g., *AGPAT* and *DGAT* isomers) participating in the step-wise pathway of TAG synthesis, the enhanced expression of *GPAM*, *LPIN1*, and *ADFP* was indicative of an increase in FA channeling towards TAG synthesis. In addition to its PAP activity, *LPIN1* expression is required for induction of PPARγ and C/EBPα expression; both are key transcription factors regulating adipogenesis in non-ruminants (Phan et al., 2004). We found no change in *LIPE* (formerly known as hormone-sensitive lipase; NCBI) expression between the two treatment groups and its % mRNA abundance was lower in OVE than CON (~2.7% vs. ~5.2%, Table 2.3). Such responses seem to be in line with the positive energy balance status of cows even in CON group. However, we cannot exclude posttranslational effects on HSL, which is a demonstrated regulatory point of hormone-stimulated lipolysis (Duncan et al., 2007).

In summary, over consumption of dietary energy increased expression of genes related with FA biosynthesis, elongation and desaturation, and TAG synthesis in a concerted fashion. Thus, the transcriptional changes in these genes partly explain the significant increase in total

visceral fat weight of cows overfed energy (visceral AT weight of OVE vs. CON = 59 kg vs. 35 kg; Nikkhah et al., 2008).

Transcriptional Regulation of Lipogenesis

Adipogenesis induced by overfeeding energy can occur via cell proliferation (hyperplasia) and/or by differentiation of preadipocytes through lipid filling (hypertrophy) (Hausman et al., 2009). Previous work (McNamara et al, 1995) has shown that adipocyte proliferation in SAT (i.e., increase in cells/g tissue) increases between early to mid-lactation, corresponding to the gradual increase in energy balance and the decrease in growth hormone to insulin (Herbein et al., 1985). Although we did not evaluate cell number or cell size in the present study, expression of delta-like 1 homolog (*DLK1*), which is highly-expressed in preadipocytes and functions to inhibit differentiation through suppressing C/EBPδ expression (Smas and Sul, 1993; Sul, 2009), was barely detectable in many of our samples (data not shown), which indicated the presence of few preadipocytes. In other words, differentiation was the predominant event driving adipogenesis and lipid accretion, regardless of diet (Nikkhah et al., 2008). Further, our data underscore that energy overfeeding promoted differentiation and lipid filling, i.e., greater mass deposition (Nikkhah et al., 2008).

Terminal differentiation leads to increased adipocyte size through lipid filling and transformation into a mature adipocyte (Sethi and Vidal-Puig, 2007). The best characterized aspect of differentiation is the sequential cascade regulated by transcription factors that converge at PPARγ and C/EBPα to coordinate expression of adipogenic genes [(e.g. *FABP4* and insulin-induced glucose transporter (*SLC2A4*)] (Spiegelman and Flier, 2001; Lefterova and Lazar, 2009). PPARγ is both necessary and sufficient for differentiation (Rosen and MacDougald, 2006). Ligand activated PPARγ heterodimerizes with retinoid X receptor (RXR) to induce the

expression of adipogenic genes by binding to PPAR response elements (PPRE) (Palmer et al., 1995). In our study *PPARG* expression was up-regulated in AT due to energy overfeeding ($P < 0.05$, Figure 2.2), which was indicative of greater differentiation activity. This also was supported by increased expression of *FABP4*, which is a well-defined PPARγ target gene (Lefterova et al., 2008). Recently, a novel zinc-finger protein encoded by the *Zfp423* gene was identified as a putative transcription regulator that determines differentiation of preadipocytes through control of PPARG expression (Gupta et al., 2010). Whether dietary energy level changes *PPARG* expression through the action of this protein needs further investigation.

Interestingly, except for *FABP4*, other coordinately up-regulated genes are well-established non-ruminant SREBF1 target genes, e.g. *ACACA*, *FASN*, *ELOVL6,* and *SCD* ($P < 0.05$); however, *SREBF1* mRNA expression was significantly lower ($P < 0.05$, Figure 2.2) in cows overfed energy than in CON. Direct transcriptional activation of those genes by PPARγ was the most likely mechanism driving the observed responses, i.e., bovine preadipocytes may be able to differentiate without direct involvement of SREBF1. The murine promoter region of *SCD* contains both SRE (SREBF1 binding site) and a PPAR RE (PPRE; Miller and Ntambi, 1996). Recent studies utilizing chromatin immunoprecipitation (ChIP) coupled with either deep sequencing or whole genome tiling arrays in rodent adipocytes unveiled thousands of PPARγ:RXR binding sites, which are particularly abundant in the vicinity of genes involved in lipid and glucose metabolism (Lefterova et al., 2008; Nielsen et al., 2008).

The opposite expression pattern of *SREBF1* between the treatment groups (lower in OVE than CON) challenges the notion of a central role for SREBF1 in bovine adipocyte lipogenesis. Our results are in accordance with a previous mouse study in which mice deficient in SREBP-1 did not have a significant decrease in the amount of AT (Shimano et al., 1997). Recently, Sekiya

et al. (2007) also reported that SREBP1c did not bind to the functional SRE/E-box site on the *FASN* promoter in adipocytes. Nevertheless, these previous findings do not explain the lower expression of *SREBF1* due to overfeeding energy in our study. *SREBF1* expression was shown to be positively regulated by insulin in vivo and in primary rodent hepatocyte cultures (Shimomura et al., 1999; Azzout-Marniche et al., 2000). Inhibitors of PI3 kinase, an intracellular transducer of insulin- signalling, decreased nuclear and precursor SREBP-1c protein in rodent hepatocytes (Hasty et al., 2000). Thus, the impairment in insulin sensitivity that we inferred from reduced glucose/insulin ratio could be a cause of decreased transcription of *SREBF1* in OVE cows. Because the above-mentioned evidence is from rodent models or hepatocyte culture studies our deduction for bovine AT will have to be confirmed with further studies.

Thyroid hormone (TH) is critical in regulation of energy homeostasis. *THRSP* encodes a nuclear protein that was identified due to its rapid response to thyroid hormone (Kinlaw et al., 1995). It has been implicated in transcriptional regulation of the major lipogenic genes in mammals via an unknown mechanism (Cunningham et al., 1998). *THRSP* is highly expressed in major lipogenic tissues in rodents including liver, AT, and lactating mammary gland (Jump and Oppenheimer, 1985). In lactating bovine mammary gland, however, expression of *THRSP* accounted for only 0.01% of total mRNA abundance and its expression increased modestly after parturition (Bionaz and Loor, 2008). A significant correlation between mRNA of *THRSP* and *FASN* was observed in rat liver (Clarke et al., 1990). Direct evidence of THRSP in regulation of lipogenesis comes from studies with rat hepatocytes, where transfection with THRSP antisense oligonucleotide prevented expression of lipogenic enzymes (Kinlaw et al., 1995; Brown et al., 1997).

In our study, the up-regulation of *THRSP* ($P < 0.05$) paralleled the increase in expression of lipogenic genes in AT of OVE cows. Blood TH is correlated with energy balance of dairy cows (Kunz et al., 1985; Capuco et al., 2001), thus, higher TH secretion may be expected in cows overfed energy with the consequent increase in the transcription of *THRSP* (Cunningham et al., 1998). In the present study, *THRSP* mRNA expression in VAT depots (Chapter 3) was positively correlated with net energy intake in the last 3 wk (shown in Table 2.5). Besides TH, *THRSP* is potentially transcriptionally activated by SREBPs and carbohydrate response element binding protein (formerly-known as ChREBP; encoded by *MLXIPL*) due to the existence of SRE and ChoRE (carbohydrate response element) motifs in its promoter (Jacoby et al., 1989; Jump et al., 2001). It is noteworthy that the % mRNA abundance of *THRSP* in mammary tissue of dairy cows is quite low (0.01% among 45 genes tested, Bionaz and Loor, 2008) compared with other lipogenesis-related genes, but we showed that it was comparatively high in adipose tissue (~4% to 6% mRNA abundance among investigated genes). Together the data clearly indicate a more important role of *THRSP* in bovine AT than mammary tissue. Graugnard et al. (2009) reported a positive correlation between *PPARG* and *THRSP* in longissimus lumborum of fattening beef cattle, which we observed in the present study by overfeeding energy. Whether PPARγ targets *THRSP*, which then could play as a secondary transcription regulator of lipogenic genes or whether they exert a synergistic function needs further study.

At the beginning of this decade, Yamashita et al. (2001) uncovered MLXIPL as a transcription factor regulated via a metabolite produced during glucose oxidation. This discovery was crucial in clarifying earlier observations: (1) besides insulin, glucose is another potent factor inducing transcription of major enzymes in the glycolytic and lipogenic pathways; and (2) several lipogenic genes (including *ACACA* and *FASN*) contain carbohydrate response elements

(ChoRE; Towle et al., 1997) as does THRSP, which in rodents was previously reported to be transcriptionally activated by high-carbohydrate diets (Shih et al., 1995). Despite abundant expression of *MLXIPL* in most lipogenic organs including liver, brown AT, and white AT (Iizuka et al., 2004), most studies have focused on rodent liver, which is the most important organ for lipid and glucose metabolism in non-ruminants. Hence, its function in adipose tissue is still unclear.

Other than a study reporting the expression of *MLXIPL* in growing steers (Graugnard et al., 2010), to our knowledge there is no other documentation of MLXIPL expression and/or activity in bovine tissues. In the present study, *MLXIPL* expression was not affected ($P > 0.05$) by dietary energy level. The low relative % mRNA abundance compared to other TF (*PPARG* and *THRSP*) suggests minor importance of *MLXIPL* in bovine AT, which does not rely on glucose as the primary lipogenic substrate. Activity of MLXIPL appears to be primarily regulated at the post-translational level (phosphorylation/dephosphorylation) (Iizuka and Horikawa, 2008). Liver X receptor (LXR), which was identified as a glucose sensor in non-ruminants (Metro et al., 2007) can regulate transcription of *MLXIPL* in rodent liver (Cha and Repa, 2007). However, only high glucose led to an increase in *MLXIPL* mRNA expression in HepG2 cells (Metro et al., 2007) and 3T3-L adipocytes (Li et al., 2003). Whether MLXIPL is less active in bovine AT or it is only activated trancriptionally during the post-prandial state, i.e. as a result of a transient rise in blood glucose, remains to be determined. Ruminants maintain much lower and less variable blood glucose concentrations thannon-ruminants, which may also challenge its function in ruminants.

In summary, our results highlighted a central role of PPARγ in the transcriptional regulation of adipogenesis and lipid filling process and challengesthe importance of SREBF1 in

bovine AT. The relatively low mRNA abundance of *MLXIPL* in bovine AT was suggestive of a minor involvement in regulation of lipogenic gene expression.

Adipokine Expression

The capability of expressing and secreting various cytokines implicated AT as an active endocrine organ in regulating systemic inflammatory and metabolic disease (Rosen and Spiegelman, 2006). In addition, AT also responds to these cytokines and inflammatory ligands by expressing a wide-variety of receptors (e.g., IL-6R and TLR4), which reflects the autocrine and paracrine characteristics of AT (Schäffler and Schölmerich, 2010). These cytokines include well-defined pro-inflammatory factors, acute-phase proteins, adipocytokines, and chemotactic proteins as signals for immune cell recruitment.

In comparison with non-ruminants, the relationship between AT cytokine expression and excess energy intake has not been documented. Our results (see Figure 2.3) showed that overfeeding energy increased ($P < 0.05$) mRNA expression of *LEP* and *CCL2*, but reduced ($P < 0.05$) expression of *IL6R*. Leptin is mainly produced by white AT and can regulate food intake and energy homeostasis in rodents by binding to specific receptors in the hypothalamus (Friedman and Halaas, 1998). Plasma LEP concentration was reported to be positively related with dietary energy intake (Holtenius et al., 2003) and body fatness (Chilliard et al., 2001), but neither plasma LEP concentration nor mRNA expression of LEP receptor and *LEP* in SAT seemed to be associated with macronutrient composition of the diet or BCS in dairy cows (Duske et al., 2009). As reviewed by Chilliard et al. (2001), insulin increases expression of *LEP* mRNA in bovine AT in vitro. Block et al. (2003) observed a significant increase in plasma LEP after 96 h of hyperinsulinemia/euglycemia clamp in mid-lactating dairy cows. More direct evidence obtained from previous study of our lab (Janovick et al., 2011) showed that, compared with

controlled-energy feeding, overfeeding energy during entire dry period significantly increased plasm insulin concentration prepartum, which was paralleled with higher plasma LEP. In the present study, a numerical increase of blood insulin concentration was found in OVE than CON cows (29.6 vs. 23.5 μIU/mL). Although it is tempting to speculate that insulin may have contributed to the greater *LEP* expression in our study, the fact remains that both *SREBF1* expression and the blood glucose/insulin ratio were lower in OVE cows.

CCL2 encodes a protein that is a member of the C-C motif chemokine family, identified as chemoattractants, which increase macrophage infiltration in AT during obesity and are associated with inflammation and insulin resistance (Kanda et al., 2006). Adipocyte hypertrophy increases *CCL2* expression (Kamei et al., 2006). In the present study, increased *CCL2* expression due to energy overfeeding may be partly explained by greater numbers of differentiated adipocytes, which also was reflected by the greater expression of lipogenic genes (e.g. *ACACA* and *FASN*) and the adipocyte differentiation marker *FABP4*. Enhanced chemotaxis via CCL2 potentially promotes macrophage infiltration and could exacerbate inflammation by promoting the secretion of more pro-inflammatory cytokines. However, mRNA for pro-inflammatory cytokines (*TNF*, *IL1B* and *IL6*) were not differentially expressed between treatments possibly due to the greater *PPARG* expression as PPARγ activity inhibits NFκB, which is the major TF of pro-inflammatory cytokines (Ruan and Pownall, 2009). Despite the lack of difference in *IL6* mRNA expression between dietary treatments, IL6 receptor (*IL6R*) expression was lower due to overfeeding ($P < 0.05$) but the potential mechanisms behind this response are unknown.

Although dietary energy intake in the current study did not affect expression profiles of most adipokines and pro-inflammatory cytokines, overfeeding energy drastically increased fat accumulation in visceral AT depots (Nikkhaha et al., 2008), which had greater expression of

these adipokines and inflammatory mediators, especially in MAT (Ji et al., 2011). Thus, long-term excessive energy intake may indirectly increase production of cytokines by inducing visceral obesity. Drackley and Andersen (2006) proposed that cytokine produced in visceral depots draining directly into liver through the portal vein may induce inflammation and liver dysfunction. However, it remains to be determined whether the higher capacity for cytokine expression is a natural characteristic of adipocytes or whether immune cell infiltration is the primary source of these immune mediators.

SUMMARY AND CONCLUSIONS

Overfeeding energy potentially stimulated lipogenesis to the same extent in both VAT and SAT of dairy cows, which was reflected by the significant up-regulation in expression of genes related with DNS (*ACLY*, *ACACA*, and *FASN*), FA elongation and desaturation (*ELOVL6* and *SCD*), and FA trafficking and TAG synthesis (*FABP4*, *GPAM*, and *LPIN1*). *PPARG* and *THRSP* rather than *SREBF1* were responsive to dietary energy intake and may play more crucial roles in transcriptional regulation of adipogenesis and lipogenesis in bovine AT (see network of transcriptional control in Figure 2.4).

LITERATURE CITED

Azzout-Marniche, D., D. Bécard, C. Guichard, M. Foretz, P. Ferré, and F. Foufelle. 2000. Insulin effects on sterol regulatory-element-binding protein-1c (SREBP-1c) transcriptional activity in rat hepatocytes. Biochem. J. 350:389-393.

Baldwin, R. L. VI, K. R. McLeod, J. P. McNamara, T. H. Elsasser, and R. G. Baumann. 2007. Influence of abomasal carbohydrates on subcutaneous, omental, and mesenteric adipose lipogenic and lipolytic rates in growing beef steers. J. Anim. Sci. 85:2271-2282.

Bauman, D. E. 1976. Intermediary metabolism of adipose tissue. Fed. Proc. 35:2308-2313.

Bergen, W. G., and H. J. Mersmann. 2005. Comparative aspects of lipid metabolism: impact on contemporary research and use of animal models. J. Nutr. 135:2499-2502.

Bionaz, M., and J. J. Loor. 2008. Gene networks driving bovine milk fat synthesis during the lactation cycle. BMC Genomics. 9:366-387.

Block, S. S., R. P. Rhoads, D. E. Bauman, R. A. Ehrhardt, M. A. McGuire, B. A. Crooker, J. M. Griinari, T. R. Mackle, W. J. Weber, M. E. Van Amburgh, and Y. R. Boisclair. 2003. Demonstration of a role for insulin in the regulation of leptin in lactating dairy cows. J. Dairy Sci, 86:3508-3515.

Bonnet, M., C. Leroux, Y. Faulconnier, J. F. Hocquette, F. Bocquier, P. Martin, and Y. Chilliard. 2000. Lipoprotein lipase activity and mRNA are up-regulated by refeeding in adipose tissue and cardiac muscle of sheep. J. Nutr. 130:749-756.

Brown, S. B., M. Maloney, and W. B. Kinlaw. 1997. "Spot 14" protein functions at the pretranslational level in the regulation of hepatic metabolism by thyroid hormone and glucose. J. Biol. Chem. 272:2163-2166.

Cao, J., J. L. Li, D. Li, J. F. Tobin, and R. E. Gimeno. 2006. Molecular identification of microsomal acyl-CoA:glycerol-3-phosphate acyltransferase, a key enzyme in de novo triacylglycerol synthesis. Proc. Natl. Acad. Sci. U.S.A. 103:19695-19700.

Capuco, A. V., D. L. Wood, T. H. Elsasser, S. Kahl, R. A. Erdman, C. P. Van Tassell, A. Lefcourt, and L. S. Piperova. 2001. Effect of somatotropin on thyroid hormones and cytokines in lactating dairy cows during ad libitum and restricted feed intake. J. Dairy Sci. 84:2430-2439.

Cha, J. Y., and J. J. Repa. 2007. The liver X receptor (LXR) and hepatic lipogenesis. The carbohydrate-response element-binding protein is a target gene of LXR. J. Biol. Chem. 282:743-751.

Chilliard, Y., M. Bonnet, C. Delavaud, Y. Faulconnier, C. Leroux, J. Djiane, and F. Bocquier. 2001. Leptin in ruminants. Gene expression in adipose tissue and mammary gland, and regulation of plasma concentration. Domest. Anim. Endocrinol. 21:271-295.

Clarke, S. D., M. K. Armstrong, and D. B. Jump. 1990. Nutritional control of rat liver fatty acid synthase and S14 mRNA abundance. J. Nutr. 120:218-224.

Coe, N. R., M. A. Simpson, and D. A. Bernlohr. 1999. Targeted disruption of the adipocyte lipid-binding protein (aP2 protein) gene impairs fat cell lipolysis and increases cellular fatty acid levels. J. Lipid. Res. 40:967-972.

Cunningham, B. A., J. T. Moncur, J. T. Huntington, and W. B. Kinlaw. 1998. "Spot 14" protein: a metabolic integrator in normal and neoplastic cells. Thyroid 8:815-825.

Dann, H. M., N. B. Litherland, J. P. Underwood, M. Bionaz, A. D'Angelo, J. W. McFadden, and J. K. Drackley. 2006. Diets during far-off and close-up dry periods affect periparturient metabolism and lactation in multiparous cows. J. Dairy Sci. 89:3563-3577.

Douglas, G. N., T. R. Overton, H. G. Bateman, 2nd, H. M. Dann, and J. K. Drackley. 2006. Prepartal plane of nutrition, regardless of dietary energy source, affects periparturient metabolism and dry matter intake in Holstein cows. J. Dairy Sci. 89:2141-2157.

Douglas, G. N., J. Rehage, A. D. Beaulieu, A. O. Bahaa, and J. K. Drackley. 2007. Prepartum nutrition alters fatty acid composition in plasma, adipose tissue, and liver lipids of periparturient dairy cows. J. Dairy Sci. 90:2941-2959.

Drackley, J. K. 1999. Biology of dairy cows during the transition period: the final frontier? J. Dairy Sci. 82:2259-2273.

Drackley, J. K., and J. B. Andersen. 2006. Splanchnic metabolism of long-chain fatty acid in ruminants. Pages 199-218 in Ruminant Physiology: Digestion, Metabolism and Impact of Nutrition on Gene Expression, Immunology and Stress. K. Sejrsen, T. Hvelplund, and M. O. Nielsen, ed. Wageningen Academic Publishers, Wageningen, Netherlands.

Duncan, R. E., M. Ahmadian, K. Jaworski, E. Sarkadi-Nagy, and H. S. Sul. 2007. Regulation of lipolysis in adipocytes. Annu. Rev. Nutr. 27:79-101.

Duske, K., H. M. Hammon, A. K. Langhof, O. Bellmann, B. Losand, K. Nurnberg, G. Nurnberg, H. Sauerwein, H. M. Seyfert, and C. C. Metges. 2009. Metabolism and lactation performance in dairy cows fed a diet containing rumen-protected fat during the last twelve weeks of gestation. J. Dairy Sci. 92:1670-1684.

Faulconnier, Y., I. Ortigues-Marty, C. Delavaud, D. Dozias, R. Jailler, D. Micol, and Y. Chilliard. 2007. Influence of the diet and grazing on adipose tissue lipogenic activities and plasma leptin in steers. Animal 1:1263-1271.

Foufelle, F., and P. Ferre. 2002. New perspectives in the regulation of hepatic glycolytic and lipogenic genes by insulin and glucose: a role for the transcription factor sterol regulatory element binding protein-1c. Biochem. J. 366:377-391.

Friedman, J. M., and J. L. Halaas. 1998. Leptin and the regulation of body weight in mammals. Nature 395:763-770.

Gargiulo, C. E., S. M. Stuhlsatz-Krouper, and J. E. Schaffer. 1999. Localization of adipocyte long-chain fatty acyl-CoA synthetase at the plasma membrane. J. Lipid Res. 40:881-892.

Gastaldelli, A., Y. Miyazaki, M. Pettiti, M. Matsuda, S. Mahankali, E. Santini, R. A. DeFronzo, and E. Ferrannini. 2002. Metabolic effects of visceral fat accumulation in type 2 diabetes. J. Clin. Endocrinol. Metab. 87:5098-5103.

Graugnard, D. E., L. L. Berger, D. B. Faulkner, and J. J. Loor. 2010. High-starch diets induce precocious adipogenic gene network up-regulation in longissimus lumborum of early-weaned Angus cattle. Br. J. Nutr. 103:953-963.

Graugnard, D. E., P. Piantoni, M. Bionaz, L. L. Berger, D. B. Faulkner, and J. J. Loor. 2009. Adipogenic and energy metabolism gene networks in longissimus lumborum during rapid post-weaning growth in Angus and Angus x Simmental cattle fed high-starch or low-starch diets. BMC Genomics. 10:142-157.

Greathead, H. M., J. M. Dawson, N. D. Scollan, and P. J. Buttery. 2001. In vivo measurement of lipogenesis in ruminants using [1-(14)C]acetate. Br. J. Nutr. 86:37-44.

Guillou, H., D. Zadravec, P. G. Martin, and A. Jacobsson. 2010. The key roles of elongases and desaturases in mammalian fatty acid metabolism: Insights from transgenic mice. Prog. Lipid Res. 49:186-199.

Gupta, R. K., Z. Arany, P. Seale, R. J. Mepani, L. Ye, H. M. Conroe, Y. A. Roby, H. Kulaga, R. R. Reed, and B. M. Spiegelman. 2010. Transcriptional control of preadipocyte determination by Zfp423. Nature 464:619-623.

Hajri, T., and N. A. Abumrad. 2002. Fatty acid transport across membranes: relevance to nutrition and metabolic pathology. Annu. Rev. Nutr. 22:383-415.

Hanson, R. W., and F. J. Ballard. 1967. The relative significance of acetate and glucose as precursors for lipid synthesis in liver and adipose tissue from ruminants. Biochem. J. 105:529-536.

Hasty, A. H., H. Shimano, N. Yahagi, M. Amemiya-Kudo, S. Perrey, T. Yoshikawa, J. Osuga, H. Okazaki, Y. Tamura, Y. Iizuka, F. Shionoiri, K. Ohashi, K. Harada, T. Gotoda, R. Nagai, S. Ishibashi, and N. Yamada. 2000. Sterol regulatory element-binding protein-1 is regulated by glucose at the transcriptional level. J. Biol. Chem. 275:31069-31077.

Hausman, G. J., M. V. Dodson, K. Ajuwon, M. Azain, K. M. Barnes, L. L. Guan, Z. Jiang, S. P. Poulos, R. D. Sainz, S. Smith, M. Spurlock, J. Novakofski, M. E. Fernyhough, and W. G. Bergen. 2009. Board-invited review: the biology and regulation of preadipocytes and adipocytes in meat animals. J. Anim. Sci. 87:1218-1246.

Herbein, J. H., R. J. Aiello, L. I. Eckler, R. E. Pearson, and R. M. Akers. 1985. Glucagon, insulin, growth hormone, and glucose concentrations in blood plasma of lactating dairy cows. J. Dairy Sci. 68:320-325.

Hertzel, A. V., and D. A. Bernlohr. 2000. The mammalian fatty acid-binding protein multigene family: molecular and genetic insights into function. Trends Endocrinol. Metab. 11:175-180.

Hertzel, A. V., K. Hellberg, J. M. Reynolds, A. C. Kruse, B. E. Juhlmann, A. J. Smith, M. A. Sanders, D. H. Ohlendorf, J. Suttles, and D. A. Bernlohr. 2009. Identification and characterization of a small molecule inhibitor of Fatty Acid binding proteins. J. Med. Chem. 52:6024-6031.

Holtenius, K., S. Agenas, C. Delavaud, and Y. Chilliard. 2003. Effects of feeding intensity during the dry period. 2. Metabolic and hormonal responses. J. Dairy Sci. 86:883-891.

Hood, R. L., and C. E. Allen. 1973. Cellularity of bovine adipose tissue. J. Lipid Res. 14:605-610.

Hood, R. L., L. J. Cook, S. C. Mills, and T. W. Scott. 1980. Effect of feeding protected lipids on fatty acid synthesis in ovine tissues. Lipids 15:644-650.

Hood, R. L., E. H. Thompson, and C. E. Allen. 1972. The role of acetate, propionate, and glucose as substrates for lipogenesis in bovine tissues. Int. J. Biochem. 3:598-606.

Horton, J. D., J. L. Goldstein, and M. S. Brown. 2002. SREBPs: transcriptional mediators of lipid homeostasis. Cold Spring Harbor Symp. Quant. Biol. 67:491-498.

Hotamisligil, G. S., R. S. Johnson, R. J. Distel, R. Ellis, V. E. Papaioannou, and B. M. Spiegelman. 1996. Uncoupling of obesity from insulin resistance through a targeted mutation in aP2, the adipocyte fatty acid binding protein. Science 274:1377-1379.

Iizuka, K., R. K. Bruick, G. Liang, J. D. Horton, and K. Uyeda. 2004. Deficiency of carbohydrate response element-binding protein (ChREBP) reduces lipogenesis as well as glycolysis. Proc. Natl. Acad. Sci. U.S.A. 101:7281-7286.

Iizuka, K., and Y. Horikawa. 2008. Regulation of lipogenesis via BHLHB2/DEC1 and ChREBP feedback looping. Biochem. Biophys. Res. Commun. 374:95-100.

Ingle, D. L., D. E. Bauman, and U. S. Garrigus. 1972b. Lipogenesis in the ruminant: in vitro study of tissue sites, carbon source and reducing equivalent generation for fatty acid synthesis. J. Nutr. 102:609-616.

Jacoby, D. B., N. D. Zilz, and H. C. Towle. 1989. Sequences within the 5'-flanking region of the S14 gene confer responsiveness to glucose in primary hepatocytes. J. Biol. Chem. 264:17623-17626.

Jakobsson, A., R. Westerberg, and A. Jacobsson. 2006. Fatty acid elongases in mammals: their regulation and roles in metabolism. Prog. Lipid Res. 45:237-249.

Janovick, N. A., and J. K. Drackley. 2010. Prepartum dietary management of energy intake affects postpartum intake and lactation performance by primiparous and multiparous Holstein cows. J. Dairy Sci. 93:3086-3102.

Janovick, N. A., J. J. Loor, P. Ji, R. E. Everts, H. A. Lewin, S. L. Rodriguez-Zas, And J. K. Drackley. 2009. Overfeeding energy prepartum dramatically affects peripartal expression of mRNA transcriptions in subcutaneous adipose tissue compared with controlling energy intake prepartum. J. Dairy Sci. 92(E-Suppl.):557. (Abstr.)

Jump, D. B., and J. H. Oppenheimer. 1985. High basal expression and 3,5,3'-triiodothyronine regulation of messenger ribonucleic acid S14 in lipogenic tissues. Endocrinology 117:2259-2266.

Jump, D. B., A. P. Thelen, and M. K. Mater. 2001. Functional interaction between sterol regulatory element-binding protein-1c, nuclear factor Y, and 3,5,3'-triiodothyronine nuclear receptors. J. Biol. Chem. 276:34419-34427.

Kadegowda, A. K., M. Bionaz, L. S. Piperova, R. A. Erdman, and J. J. Loor. 2009. Peroxisome proliferator-activated receptor-gamma activation and long-chain fatty acids alter lipogenic gene networks in bovine mammary epithelial cells to various extents. J. Dairy Sci. 92:4276-4289.

Kamei, N., K. Tobe, R. Suzuki, M. Ohsugi, T. Watanabe, N. Kubota, N. Ohtsuka-Kowatari, K. Kumagai, K. Sakamoto, M. Kobayashi, T. Yamauchi, K. Ueki, Y. Oishi, S. Nishimura, I. Manabe, H. Hashimoto, Y. Ohnishi, H. Ogata, K. Tokuyama, M. Tsunoda, T. Ide, K. Murakami, R. Nagai, and T. Kadowaki. 2006. Overexpression of monocyte chemoattractant protein-1 in adipose tissues causes macrophage recruitment and insulin resistance. J. Biol. Chem. 281:26602-26614.

Kanda, H., S. Tateya, Y. Tamori, K. Kotani, K. Hiasa, R. Kitazawa, S. Kitazawa, H. Miyachi, S. Maeda, K. Egashira, and M. Kasuga. 2006. MCP-1 contributes to macrophage infiltration into adipose tissue, insulin resistance, and hepatic steatosis in obesity. J. Clin. Invest. 116:1494-1505.

Kim, J. B., and B. M. Spiegelman. 1996. ADD1/SREBP1 promotes adipocyte differentiation and gene expression linked to fatty acid metabolism. Genes Dev. 10:1096-1107.

Kim, J. B., H. M. Wright, M. Wright, and B. M. Spiegelman. 1998. ADD1/SREBP1 activates PPARgamma through the production of endogenous ligand. Proc. Natl. Acad. Sci. U.S.A. 95:4333-4337.

Kinlaw, W. B., J. L. Church, J. Harmon, and C. N. Mariash. 1995. Direct evidence for a role of the "spot 14" protein in the regulation of lipid synthesis. J. Biol. Chem. 270:16615-16618.

Kunz, P. L., J. W. Blum, I. C. Hart, H. Bickel, and J. Landis. 1985. Effects of different energy intakes before and after calving on food intake, performance and blood hormones and metabolites in dairy cows. Anim. Prod. 40:219-231.

Lefterova, M. I., and M. A. Lazar. 2009. New developments in adipogenesis. Trends Endocrinol. Metab. 20:107-114.

Lefterova, M. I., Y. Zhang, D. J. Steger, M. Schupp, J. Schug, A. Cristancho, D. Feng, D. Zhuo, C. J. Stoeckert, Jr., X. S. Liu, and M. A. Lazar. 2008. PPARgamma and C/EBP factors orchestrate adipocyte biology via adjacent binding on a genome-wide scale. Genes Dev. 22:2941-2952.

Lewin, T. M., D. A. Granger, J. H. Kim, and R. A. Coleman. 2001. Regulation of mitochondrial sn-glycerol-3-phosphate acyltransferase activity: response to feeding status is unique in various rat tissues and is discordant with protein expression. Arch. Biochem. Biophys. 396:119-127.

Li, J., K. Takaishi, W. Cook, S. K. McCorkle, and R. H. Unger. 2003. Insig-1 "brakes" lipogenesis in adipocytes and inhibits differentiation of preadipocytes. Proc. Natl. Acad. Sci. U.S.A. 100:9476-9481.

Loor, J. J. 2010. Genomics of metabolic adaptations in the peripartal cow. Animal 4:1110-1139.

Loor, J. J., H. M. Dann, R. E. Everts, R. Oliveira, C. A. Green, N. A. Guretzky, S. L. Rodriguez-Zas, H. A. Lewin, and J. K. Drackley. 2005. Temporal gene expression profiling of liver from periparturient dairy cows reveals complex adaptive mechanisms in hepatic function. Physiol. Genomics. 23:217-226.

Loor, J. J., A. Ferlay, A. Ollier, K. Ueda, M. Doreau, and Y. Chilliard. 2005. High-concentrate diets and polyunsaturated oils alter trans and conjugated isomers in bovine rumen, blood, and milk. J. Dairy Sci. 88:3986-3999.

McNamara, J. P., J. H. Harrison, R. L. Kincaid, and S. S. Waltner. 1995. Lipid metabolism in adipose tissue of cows fed high fat diets during lactation. J. Dairy Sci. 78:2782-2796.

McNamara, J. P., D. C. McFarland, and S. Bai. 1987. Regulation of bovine adipose tissue metabolism during lactation. 3. Adaptations of hormone-sensitive and lipoprotein lipases. J. Dairy Sci. 70:1377-1384.

Metro, N., P. A. Mac, L. Vargas, C. Godio, E. Hampton, V. Molteni, A. Kreusch, and E. Saez. 2007. The nuclear receptor LXR is a glucose sensor. Nature 445:219-223.

Miller, C. W., and J. M. Ntambi. 1996. Peroxisome proliferators induce mouse liver stearoyl-CoA desaturase 1 gene expression. Proc. Natl. Acad. Sci. U.S.A. 93:9443-9448.

Moon, Y. A., N. A. Shah, S. Mohapatra, J. A. Warrington, and J. D. Horton. 2001. Identification of a mammalian long chain fatty acyl elongase regulated by sterol regulatory element-binding proteins. J. Biol. Chem. 276:45358-45366.

Mukesh, M., M. Bionaz, D. E. Graugnard, J. K. Drackley, and J. J. Loor. 2009. Adipose tissue depots of Holstein cows are immune responsive: inflammatory gene expression in vitro. Domest. Anim. Endocrinol. 38:168-178.

Nielsen, R., T. A. Pedersen, D. Hagenbeek, P. Moulos, R. Siersbaek, E. Megens, S. Denissov, M. Borgesen, K. J. Francoijs, S. Mandrup, and H. G. Stunnenberg. 2008. Genome-wide profiling of PPARgamma:RXR and RNA polymerase II occupancy reveals temporal activation of distinct metabolic pathways and changes in RXR dimer composition during adipogenesis. Genes Dev. 22:2953-2967.

Nikkhah, A., J. J. Loor, R. J. Wallace, D. E. Graugnard, J. Vasquez, B. Richards, and J. K. Drackley. 2008. Moderate excesses of dietary energy markedly increase visceral adipose tissue mass in non-lactating dairy cows. J. Dairy Sci. 91(E-Suppl. 1):LB4.

Ntambi, J. M., and M. Miyazaki. 2004. Regulation of stearoyl-CoA desaturases and role in metabolism. Prog. Lipid Res. 43:91-104.

Palmer, C. N., M. H. Hsu, H. J. Griffin, and E. F. Johnson. 1995. Novel sequence determinants in peroxisome proliferator signaling. J. Biol. Chem. 270:16114-16121.

Phan, J., M. Peterfy, and K. Reue. 2004. Lipin expression preceding peroxisome proliferator-activated receptor-gamma is critical for adipogenesis in vivo and in vitro. J. Biol. Chem. 279:29558-29564.

Robelin, J. 1981. Cellularity of bovine adipose tissues: developmental changes from 15 to 65 percent mature weight. J. Lipid Res. 22:452-457.

Rosen, E. D., and O. A. MacDougald. 2006. Adipocyte differentiation from the inside out. Nat. Rev. Mol. Cell. Biol. 7:885-896.

Rosen, E. D., and B. M. Spiegelman. 2006. Adipocytes as regulators of energy balance and glucose homeostasis. Nature 444:847-853.

Ruan, H., and H. J. Pownall. 2009. The adipocyte IKK/NFkappaB pathway: a therapeutic target for insulin resistance. Curr. Opin. Investig. Drugs 10:346-352.

Rukkwamsuk, T., M. J. Geelen, T. A. Kruip, and T. Wensing. 2000. Interrelation of fatty acid composition in adipose tissue, serum, and liver of dairy cows during the development of fatty liver postpartum. J. Dairy Sci. 83:52-59.

Schäffler, A., and J. Schölmerich. 2010. Innate immunity and adipose tissue biology. Trends Immunol. 31:228-235.

Scheja, L., L. Makowski, K. T. Uysal, S. M. Wiesbrock, D. R. Shimshek, D. S. Meyers, M. Morgan, R. A. Parker, and G. S. Hotamisligil. 1999. Altered insulin secretion associated with reduced lipolytic efficiency in aP2-/- mice. Diabetes 48:1987-1994.

Schoonmaker, J. P., F. L. Fluharty, and S. C. Loerch. 2004. Effect of source and amount of energy and rate of growth in the growing phase on adipocyte cellularity and lipogenic enzyme activity in the intramuscular and subcutaneous fat depots of Holstein steers. J. Anim. Sci. 82:137-148.

Sekiya, M., N. Yahagi, T. Matsuzaka, Y. Takeuchi, Y. Nakagawa, H. Takahashi, H. Okazaki, Y. Iizuka, K. Ohashi, T. Gotoda, S. Ishibashi, R. Nagai, T. Yamazaki, T. Kadowaki, N. Yamada, J. Osuga, and H. Shimano. 2007. SREBP-1-independent regulation of lipogenic gene expression in adipocytes. J. Lipid Res. 48:1581-1591.

Sethi, J. K., and A. J. Vidal-Puig. 2007. Thematic review series: adipocyte biology. Adipose tissue function and plasticity orchestrate nutritional adaptation. J. Lipid Res. 48:1253-1262.

Shen, W. J., K. Sridhar, D. A. Bernlohr, and F. B. Kraemer. 1999. Interaction of rat hormone-sensitive lipase with adipocyte lipid-binding protein. Proc. Natl. Acad. Sci. U.S.A. 96:5528-5532.

Shih, H. M., Z. Liu, and H. C. Towle. 1995. Two CACGTG motifs with proper spacing dictate the carbohydrate regulation of hepatic gene transcription. J. Biol. Chem. 270:21991-21997.

Shimano, H., I. Shimomura, R. E. Hammer, J. Herz, J. L. Goldstein, M. S. Brown, and J. D. Horton. 1997. Elevated levels of SREBP-2 and cholesterol synthesis in livers of mice homozygous for a targeted disruption of the SREBP-1 gene. J. Clin. Invest. 100:2115-2124.

Shimomura, I., Y. Bashmakov, S. Ikemoto, J. D. Horton, M. S. Brown, and J. L. Goldstein. 1999. Insulin selectively increases SREBP-1c mRNA in the livers of rats with streptozotocin-induced diabetes. Proc. Natl. Acad. Sci. U.S.A. 96:13656-13661.

Shoelson, S. E., J. Lee, and A. B. Goldfine. 2006. Inflammation and insulin resistance. J. Clin. Invest. 116:1793-1801.

Smas, C. M., and H. S. Sul. 1993. Pref-1, a protein containing EGF-like repeats, inhibits adipocyte differentiation. Cell 73:725-734.

Smith, A. J., M. A. Sanders, B. R. Thompson, C. Londos, F. B. Kraemer, and D. A. Bernlohr. 2004. Physical association between the adipocyte fatty acid-binding protein and hormone-sensitive lipase: a fluorescence resonance energy transfer analysis. J. Biol. Chem. 279:52399-52405.

Spiegelman, B. M., and J. S. Flier. 2001. Obesity and the regulation of energy balance. Cell 104:531-543.

Sprinkle, J. E., C. L. Ferrell, J. W. Holloway, B. G. Warrington, L. W. Greene, G. Wu, and J. W. Stuth. 1998. Adipose tissue partitioning of limit-fed beef cattle and beef cattle with ad libitum access to feed differing in adaptation to heat. J. Anim. Sci. 76:665-673.

Sul, H. S. 2009. Minireview: Pref-1: role in adipogenesis and mesenchymal cell fate. Mol. Endocrinol. 23:1717-1725.

Sul, H. S., M. J. Latasa, Y. Moon, and K. H. Kim. 2000. Regulation of the fatty acid synthase promoter by insulin. J. Nutr. 130:315S-320S.

Takeuchi, K., and K. Reue. 2009. Biochemistry, physiology, and genetics of GPAT, AGPAT, and lipin enzymes in triglyceride synthesis. Am. J. Physiol. Endocrinol. Metab. 296:E1195-1209.

Tansey, J. T., C. Sztalryd, J. Gruia-Gray, D. L. Roush, J. V. Zee, O. Gavrilova, M. L. Reitman, C. X. Deng, C. Li, A. R. Kimmel, and C. Londos. 2001. Perilipin ablation results in a lean mouse with aberrant adipocyte lipolysis, enhanced leptin production, and resistance to diet-induced obesity. Proc. Natl. Acad. Sci. U.S.A. 98:6494-6499.

Thompson, B. R., S. Lobo, and D. A. Bernlohr. 2010. Fatty acid flux in adipocytes: the in's and out's of fat cell lipid trafficking. Mol. Cell. Endocrinol. 318:24-33.

Towle, H. C., E. N. Kaytor, and H. M. Shih. 1997. Regulation of the expression of lipogenic enzyme genes by carbohydrate. Annu. Rev. Nutr. 17:405-433.

Travers, M. T., A. J. Vallance, H. T. Gourlay, C. A. Gill, I. Klein, C. B. Bottema, and M. C. Barber. 2001. Promoter I of the ovine acetyl-CoA carboxylase-alpha gene: an E-box motif at -114 in the proximal promoter binds upstream stimulatory factor (USF)-1 and USF-2 and acts as an insulin-response sequence in differentiating adipocytes. Biochem. J. 359:273-284.

Vandesompele J, K. De Preter, F. Pattyn, B. Poppe, N. Van Roy, A. De Paepe, and F. Speleman. 2002 Accurate normalization of real-time quantitative rt-pcr data by geometric averaging of multiple internal control genes. Genome Biol. 3:RESEARCH0034.

Vernon, R. G. 1980. Lipid metabolism in the adipose tissue of ruminant animals. Prog. Lipid Res. 19:23-106.

Wang, Y., D. Botolin, B. Christian, J. Busik, J. Xu, and D. B. Jump. 2005. Tissue-specific, nutritional, and developmental regulation of rat fatty acid elongases. J. Lipid Res. 46:706-715.

Webb, E. C., S. De Smet, C. Van Nevel, B. Martens, and D. I. Demeyer. 1998. Effect of anatomical location on the composition of fatty acids in double-muscled Belgian Blue cows. Livest. Prod. Sci. 64:61-79.

Weinstock, P. H., S. Levak-Frank, L. C. Hudgins, H. Radner, J. M. Friedman, R. Zechner, and J. L. Breslow. 1997. Lipoprotein lipase controls fatty acid entry into adipose tissue, but fat mass is preserved by endogenous synthesis in mice deficient in adipose tissue lipoprotein lipase. Proc. Natl. Acad. Sci. U.S.A. 94:10261-10266.

Whitehurst, G. B., D. C. Beitz, D. Cianzio, and D. G. Topel. 1981. Fatty acid synthesis from lactate in growing cattle. J. Nutr. 111:1454-1461.

Whitehurst, G. B., D. C. Beitz, M. A. Pothoven, W. R. Ellison, and M. H. Crump. 1978. Lactate as a precursor of fatty acids in bovine adipose tissue. J. Nutr. 108:1806-1811.

Yamashita, H., M. Takenoshita, M. Sakurai, R. K. Bruick, W. J. Henzel, W. Shillinglaw, D. Arnot, and K. Uyeda. 2001. A glucose-responsive transcription factor that regulates carbohydrate metabolism in the liver. Proc. Natl. Acad. Sci. U.S.A. 98:9116-9121.

TABLES AND FIGURES

Table 2.1. DMI, BW, BCS, visceral organ mass, visceral adipost tissue mass, and serum metabolites in cows either overfed energy (OVE, NE_L = 1.62 Mcal/kg DM) or fed the controlled energy diet (CON, NE_L = 1.35 Mcal/kg DM). (Data from Nikkhah et al, unpublished data)

Organs	OVE	CON	SEM	Diet (*P*)
DMI, kg/d	15.7	10.9	0.6	<0.0001
NE_L intake, Mcal/d	25.3	14.7	0.9	<0.0001
Preharvest BW, kg	734.9	736.0	24.0	0.98
Final live BW, kg	805.1	786.8	25.2	0.62
BCS, wk 1	3.26	3.18	0.12	0.66
BCS,wk 4	3.20	3.00	0.13	0.30
BCS, wk 7	3.62	3.55	0.11	0.68
Omental fat, kg	28.07	17.49	1.31	<0.0001
Mesenteric fat, kg	21.99	12.10	2.35	0.01
Perirenal fat, kg	9.86	5.98	1.20	0.04
Total visceral fat[1], kg	59.53	35.57	3.87	0.001
Kidney, kg	1.95	1.78	0.17	0.50
Liver, kg	10.30	9.39	0.59	0.27
Mammary gland, kg	17.40	18.79	1.87	0.61
Carcass[2], kg	511.05	521.0	17.6	0.70
Digestive tract, kg	46.57	45.11	2.94	0.73
Heart, kg	3.92	4.17	0.18	0.34
Glucose, mg/dL	66.7	66.1	2.2	0.85
Insulin, µIU/mL	29.6	23.5	3.2	0.2
Glucose/insulin ratio	2.6	3.5	0.3	0.06
NEFA, mmol/L	0.11	0.11	0.01	0.96
BHBA, mmol/L	0.46	0.35	0.03	0.01
Cholesterol, mmol/L	120.2	99.8	4.5	0.005

[1] Sum of omental, mesenteric, and perirenal adipose tissue
[2] Including carcass, head, hide, hooves and tail

Table 2.2. Ingredients and nutrient composition of diets (% of DM)

	Diet	
Ingredient	**OVE**	**CON**
Alfalfa silage	17.9	10.0
Alfalfa hay	6.0	3.5
Corn silage	50.0	28.0
Wheat straw	0.0	40.5
Ground shelled corn	13.8	3.5
Whole cottonseed	5.0	--
Soybean meal	4.3	11.5
Minerals and Vitamins	3.0	3.0
Nutrient composition		
DM, %	50.0	52.0
NE_L, Mcal/kg	1.62	1.35
CP, %	15.0	12.0
NDF, %	36.7	54.8
Forage NDF, %	33.0	50.1
ADF, %	25.8	36.6
NFC, %	38.7	26.2
Fat, %	3.7	2.2

NFC, non-fiber carbohydrate = 100 – (%CP + %NDF + %Fat + %ash).

Table 2.3. GenBank accession number, hybridization position, sequence, and amplicon size of primers use to analyze gene expression by qPCR

Accession #	Gene	Primers[1]	Primers (5'-3')[2]	bp[3]
AJ132890	*ACACA*	F. 3709	CATCTTGTCCGAAACGTCGAT	101
		R. 3809	CCCTTCGAACATACACCTCCA	
BC108138	*ACLY*	F. 2287	GTTCTCCTCCGAGGTCCAGTT	104
		R. 2390	CAAACACTCCAGCCTCCTTCA	
BC119914	*ACSL1*	F. 1929	GTGGGCTCCTTTGAAGAACTGT	120
		R. 2047	ATAGATGCCTTTGACCTGTTCAAAT	
BC102211	*ADFP*	F. 139	TGGTCTCCTCGGCTTACATCA	81
		R. 219	TCATGCCCTTCTCTGCCATC	
BC140488	*ADIPOQ*	F. 211	GATCCAGGTCTTGTTGGTCCTAA	109
		R. 319	GAGCGGTATACATAGGCACTTTCTC	
BC103112.1	*CD36*	F. 1196	TGATATTTGCAGGTCCATCTATGC	103
		R. 1298	TGGAGATGCAAAAGCAAAGGA	
BC148954.1	*ELOVL6*	F. 439	AGCACCCGAACTAGGAGATACAAT	120
		R. 540	TACCAGGAGTACAGAAGCACAGTGA	
CR552737	*FASN*	F. 6383	ACCTCGTGAAGGCTGTGACTCA	92
		R. 6474	TGAGTCGAGGCCAAGGTCTGAA	
AY515690	*GPAM*	F. 1963	GCAGGTTTATCCAGTATGGCATT	63
		R. 2026	GGACTGATATCTTCCTGATCATCTTG	
BT020625	*LEP*	F. 79	GGCTTTGGCCCTATCTGTCTTA	124
		R. 202	GAGACGGACTGCGTGTGTGA	
EF140760.1	*LIPE*	F. 1674	TCAGTGTCCAAGACAGAGCCAAT	106
		R. 1779	CATGCAGCTTCAGGCTTTTG	
DV797268	*LPIN1*	F. 147	TGGCCACCAGAATAAAGCATG	101
		R. 247	GCTGACGCTGGACAACAGG	
BC118091	*LPL*	F. 327	ACACAGCTGAGGACACTTGCC	101
		R. 427	GCCATGGATCACCACAAAGG	
XM001255565.2	*MLXIPL*	F. 107	TGTCTGACATCTCTGACACACTCTTC	107
		R. 213	TGGCTGGATCATGTCAGCAT	
NM181024	*PPARG*	F. 135	CCAAATATCGGTGGGAGTCG	101
		R. 235	ACAGCGAAGGGCTCACTCTC	
AY241933	*SCD*	F. 665	TCCTGTTGTTGTGCTTCATCC	101
		R. 765	GGCATAACGGAATAAGGTGGC	
XM001790600.1	*SREBF1*	F. 1638	GTGCTGAGGGCAGAGATGGT	106
		R. 1743	ACAAAGAGAAGTGCCAAGGAGAA	
AY656814	*THRSP*	F. 631	CTACCTTCCTCTGAGCACCAGTTC	151
		R. 781	ACACACTGACCAGGTGACAGACA	

1 Primer direction (F: forward; R: reverse) and hybridization position on the sequence
2 Exon-exon junctions are underlined
3 Amplicon size in base pair (bp)

Table 2.4. Gene symbol, name, and percentage of mRNA abundance among all genes investigated in each treatment

Gene Symbol	Gene Name in NCBI	% mRNA in OVE	% mRNA in CON
	Fatty acid and triglyceride metabolism		
ACACA	acetyl-Coenzyme A carboxylase alpha	0.67	0.63
ACLY	ATP citrate lyase	0.09	0.10
ACSL1	acyl-CoA synthetase long-chain	0.38	0.90
ADFP (PLIN2)	adipose differentiation-related protein	2.13	2.74
CD36	thrombospondin receptor	5.61	9.80
ELOVL6	elongation of long chain fatty acids	0.63	0.51
FABP4	adipocyte fatty acid binding protein 4	24.07	28.09
FASN	fatty acid synthase	4.14	2.81
GPAM	glycerol-3-phosphate acyltransferase	0.39	0.50
LIPE	hormone-sensitive lipase	2.67	5.24
LPIN1	lipin 1	0.48	0.40
LPL	lipoprotein lipase	8.33	14.57
SCD	stearoyl-CoA desaturase	38.84	17.99
	Transcription regulators		
MLXIPL	MLX interacting protein-like	0.02	0.03
PPARG	peroxisome proliferator-activated receptor gamma	1.02	1.53
SREBF1	sterol regulatory element binding transcription factor 1	0.28	0.69
THRSP	thyroid hormone responsive SPOT 14	5.80	4.78

Table 2.4. (cont.)

Gene Symbol	Gene Name in NCBI	% mRNA in OVE	% mRNA in CON
	Adipokine and proinflammatory cytokines		
ADIPOQ	adiponectin	3.38	6.65
CCL2	chemokine (C-C motif) ligand 2	0.05	0.04
CCL5	chemokine (C-C motif) ligand 5	0.03	0.03
IL1B	interleukin-1 beta	< 0.01	< 0.01
IL6	interleukin-6	0.02	0.03
IL6R	Interleukin-6 receptor	0.58	1.39
LEP	leptin	0.33	0.41
SAA3	acute-phase serum amyloid A3	0.02	0.04
TLR4	toll-like receptor 4	0.03	0.07
TNF	tumor necrosis factor alpha	0.01	0.02

Table 2.5. Correlation analysis of SCD and THRSP mRNA level with net energy intake. Regardless of treatment assignment, the relative mRNA expression level of SCD in both MAT and OAT was positively correlated with NE_L intake at wk 5 and 6 ($P < 0.05$), and tended to be positively correlated with NE_L intake at wk 7 ($P < 0.1$).

Y-variable	X-variable	Correlation coefficient	*P*-value
NE_L intake at wk5	SCD mRNA in MAT	0.50	0.041
	SCD mRNA in OAT	0.61	0.012
	THRSP mRNA in MAT	0.49	0.046
	THRSP mRNA in OAT	0.52	0.039
NE_L intake at wk6	SCD mRNA in MAT	0.49	0.043
	SCD mRNA in OAT	0.52	0.040
	THRSP mRNA in MAT	0.48	0.049
	THRSP mRNA in OAT	0.44	0.087
NE_L intake at wk7	SCD mRNA in MAT	0.43	0.086
	SCD mRNA in OAT	0.48	0.061
	THRSP mRNA in MAT	0.46	0.061
	THRSP mRNA in OAT	0.49	0.055

Table S2.1. Sequencing results using BLASTN from NCBI (http://blast.ncbi.nlm.nih.gov/Blast.cgi) against nucleotide collection (nr/nt).

Gene	Best hit in NCBI	Score
CCL5	Bos taurus chemokine (C-C motif) ligand 5	96.9
CD36	Bos taurus CD36 molecule (thrombospondin receptor)	64.4
ELOVL6	Bos taurus hypothetical LOC533333	107
IL6R	Bos taurus interleukin 6 receptor (IL6R)	111
LIPE	Bos taurus lipase, hormone-sensitive (LIPE)	114
MLXIPL	Bos taurus similar to Mlx interactor zeta; Mio zeta	63.9
SREBF1	PREDICTED: Bos taurus sterol regulatory element binding transcription factor 1 (SREBF1)	113
TNF	Bos taurus tumor necrosis factor (TNF superfamily, member 2)	93.3

Table S2.2. Sequencing results obtained from PCR products.

Gene	Sequence
CCL5	AGAAGAAGTGGGTGCGAGAGTACATCAACGCTTTGGAGTTGAGCTAGGGTGGACCC
CD36	AAGGAATCCCTGTGTGATAGATTTATTCGTTCCATCCTGTGTGCTGTTTGCATCTCCAAAG
ELOVL6	CAGAAGCTGATCTTCCTGCACTGGTACCACCACATCACTGTGCTTCTGTACTCCTGGTAAA
IL6R	AGGTCGGGAACAAGTCCAGCAACCCCCTAGGATTTGACGGCTACAAACTCCTACAGCCCGACCCAA
LIPE	AGCAGCCCTGACCCGGCCGGAGGGCTCACTGGGAACCGACTCCCTCAAAAGCCTGAAGCTGCATGAA
MLXIPL	AGGATGCCCTACGTGGGCAATGCTGACATGATCCAGCCAAA
SREBF1	CGTCGTCCCCCACTGGTCTGGCTGATGAATGGGCTGCTGGTGCTCTTCTCCTTGGCACTTCTCTTTGTAAA
TNF	TCACTCTCCGGGGCAGCTCCGGTGGTGGGACTCGTATGCCAATGCCCTCATGGAA

Table S2.3. qPCR performances among 29 genes measured in adipose tissues.

Gene	Median Ct[1]	Median Δ Ct[2]	Slope[3]	(R^2)[4]	Efficiency[5]
ACACA	21.9	-3.2	-3.23	0.996	2.04
ACLY	24.5	-0.5	-3.29	0.995	2.01
ACSL1	21.9	-3.1	-3.27	0.998	2.02
ADFP	19.8	-5.4	-3.42	0.995	1.96
ADIPOQ	18.6	-6.4	-3.47	0.995	1.94
CCL2	25.6	0.5	-3.68	0.992	1.87
CCL5	26.4	1.2	-3.64	0.994	1.88
CD36	17.8	-7.4	-3.57	0.996	1.90
ELOVL6	21.5	-3.6	-3.61	0.998	1.89
FABP4	16.2	-9.1	-3.47	0.991	1.94
FASN	18.2	-6.8	-3.71	0.998	1.86
GPAM	22.0	-3.1	-3.74	1.000	1.85
IL1B	29.3	4.2	-3.34	0.986	1.99
IL6	26.6	1.5	-3.22	0.993	2.04
IL6R	21.5	-3.7	-3.36	0.994	1.98
LEP	22.6	-2.6	-3.40	0.997	1.97
LIPE	18.9	-6.2	-3.52	0.998	1.93
LPIN1	22.4	-2.9	-3.30	0.998	2.01
LPL	17.2	-7.9	-3.55	0.992	1.91
MLXIPL	26.4	1.3	-3.08	0.977	2.11
PPARG	20.7	-4.5	-3.44	0.998	1.95
SAA3	26.7	1.4	-3.33	0.995	2.00
SCD	16.5	-8.6	-3.09	0.993	2.11
SREBF1	22.4	-2.7	-3.18	0.995	2.07
THRSP	18.5	-6.7	-3.45	0.999	1.95
TLR4	25.7	0.5	-3.76	0.995	1.84
TNF	27.7	2.5	-3.51	0.986	1.93

[1] The median Ct is the result of Ct values of all samples.

[2] Δ Ct = Ct of gene – geometrical mean of Ct of ICGs, and the median Δ Ct is calculated from Δ Ct of all samples.

[3] Slope of the standard curve.

[4] R^2 means the coefficient of determination of the standard curve.

[5] Efficiency = $10^{(-1/\text{slope})}$.

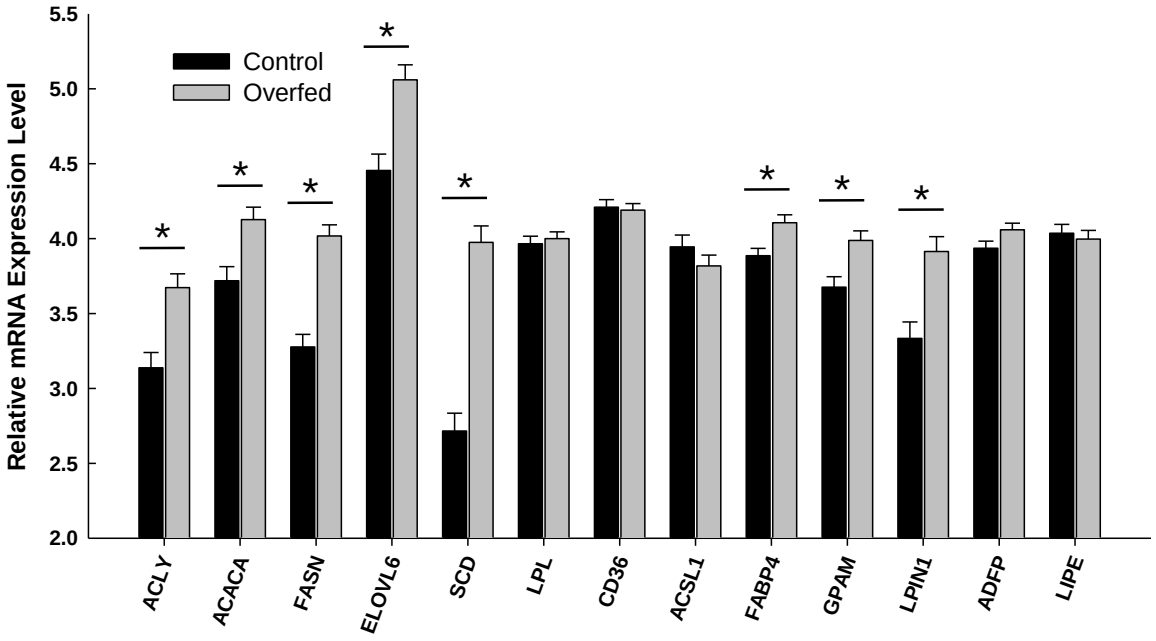

Figure 2.1. Main effect of dietary energy intake on mRNA expression of genes involved in lipid metabolism. Genes marked with asterisk were significantly differentially expressed between treatments ($P < 0.05$). X-axis: official gene symbol from NCBI website. Y-axis: relative mRNA expression value from natural logarithmic transformed data. Black column indicates CON; grey column indicates OVE treatment.

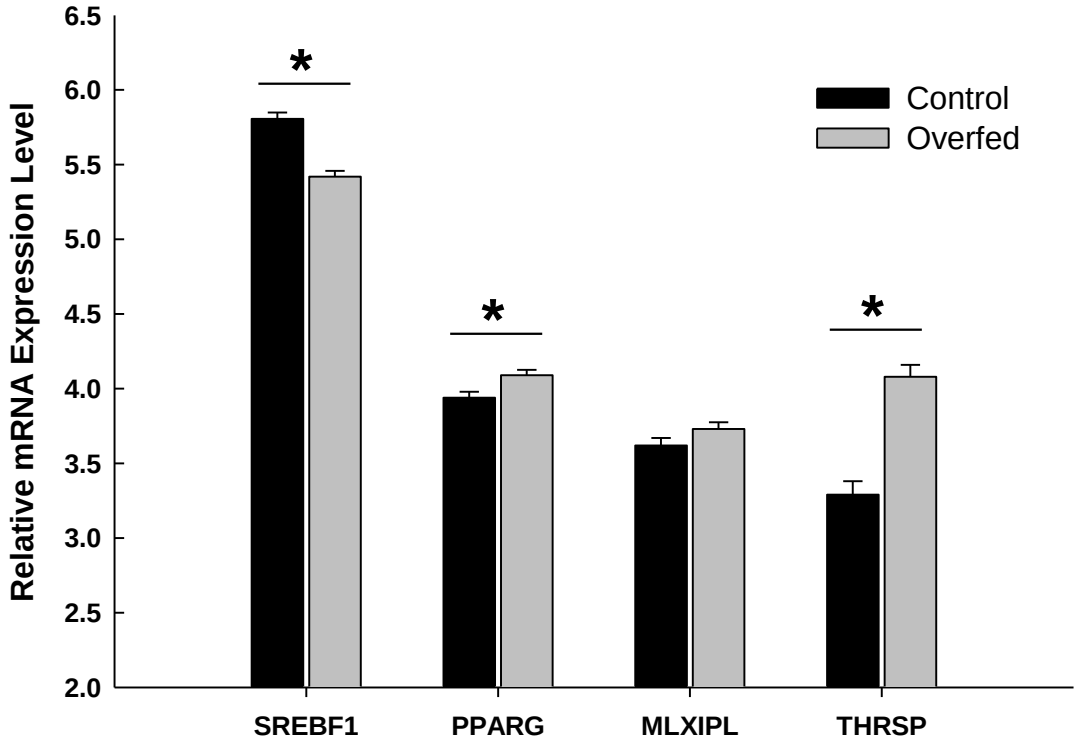

Figure 2.2. Main effect of dietary energy intakeon mRNA expression of transcriptional regulator genes. Genes marked with different letter means significantly differentially expressed among adipose sites ($P < 0.05$). X-axis: official gene symbol from NCBI website. Y-axis: relative mRNA expression value from natural logarithmic transformed data. Black column indicates CON; grey column indicates OVE treatment.

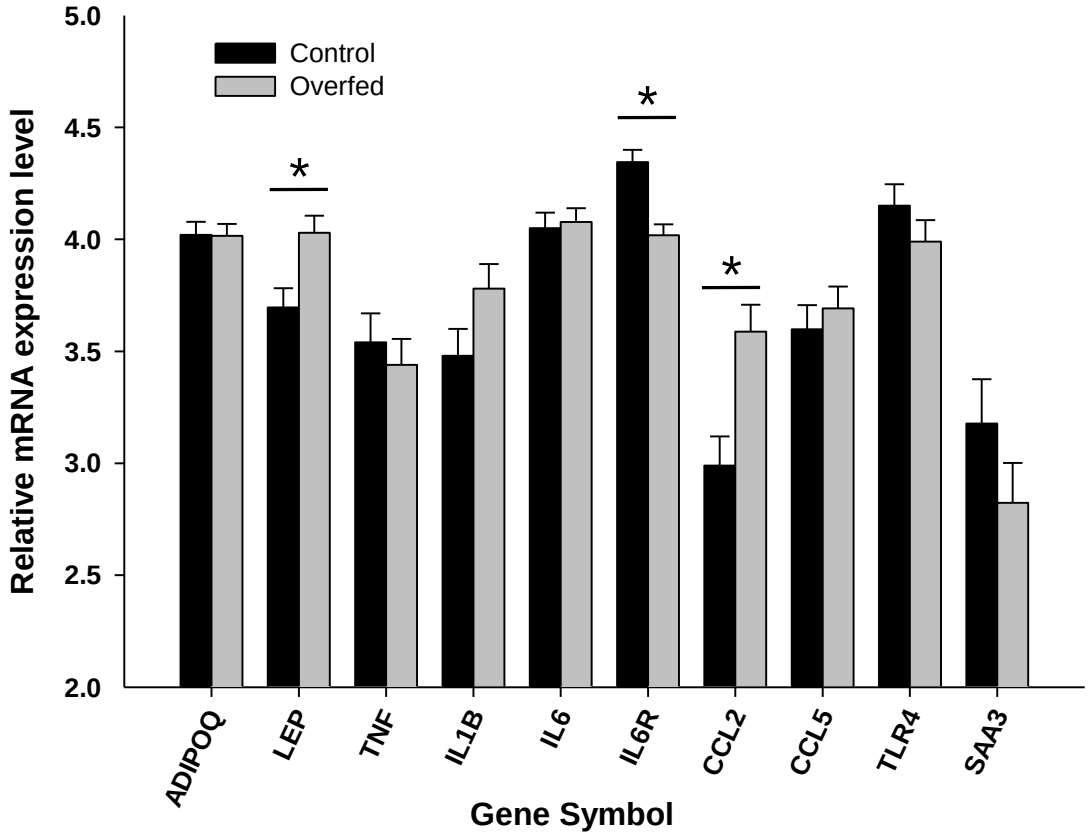

Figure 2.3. Main effect of dietary energy intake on mRNA expression of cytokines. Genes marked with asterisk were significantly differentially expressed between treatments ($P < 0.05$). X-axis: official gene symbol from NCBI website. Y-axis: relative mRNA expression value from natural logarithmic transformed data. Black column indicates CON; grey column indicates OVE treatment.

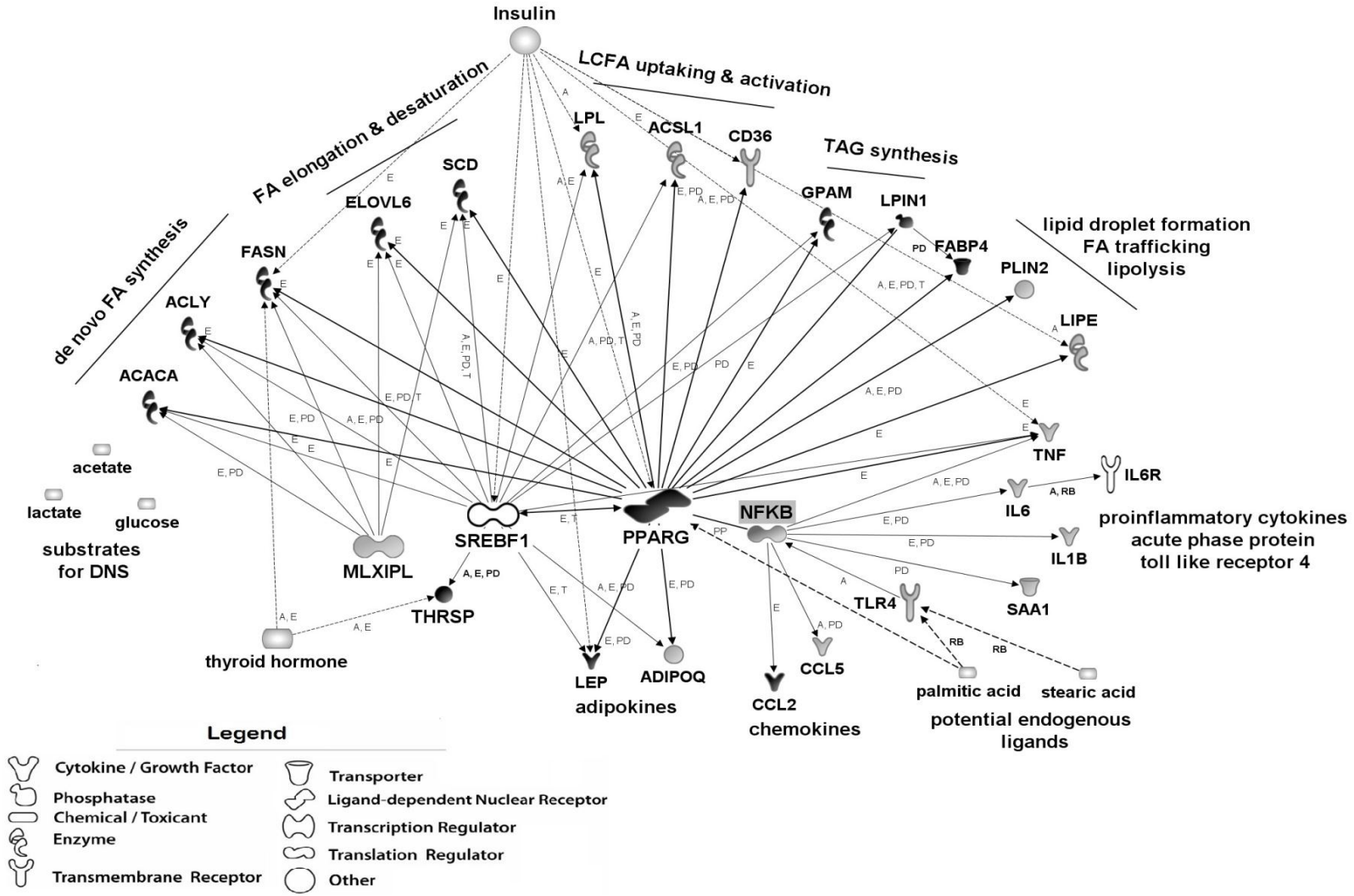
Insulin
LCFA uptaking & activation
FA elongation & desaturation
TAG synthesis
de novo FA synthesis
lipid droplet formation
FA trafficking
lipolysis
LPL
ACSL1
CD36
SCD
ELOVL6
GPAM
LPIN1
FABP4
PLIN2
FASN
ACLY
LIPE
ACACA
TNF
IL6R
IL6
proinflammatory cytokines
acute phase protein
toll like receptor 4
acetate
lactate
glucose
substrates
for DNS
NFKB
SREBF1
PPARG
IL1B
MLXIPL
TLR4
SAA1
THRSP
thyroid hormone
LEP
ADIPOQ
adipokines
CCL5
CCL2
chemokines
palmitic acid
stearic acid
potential endogenous
ligands
Legend
Cytokine / Growth Factor
Phosphatase
Chemical / Toxicant
Enzyme
Transmembrane Receptor
Transporter
Ligand-dependent Nuclear Receptor
Transcription Regulator
Translation Regulator
Other

Figure 2.4.

Figure 2.4. (cont.) Putative network and changes in transcription profile of genes in OVE vs. CON cows. Network was constructed with Ingenuity Pathway Analysis® (IPA) based on IPA knowledge base that derived from published literature of non-ruminant species. Several putative relationships were edited according to recently published literature, which includes LCFA (palmitic and stearic acid) as endogenous ligands of TLR4 (Shi et al., 2006) and PPARγ (Kadegowda et al., 2009). Two hormones (insulin and thyroid hormone) were incorporated due to their potential role in regulation of gene expression. Although not measured, NFκB was included in the network as it has a well-characterized role in regulating transcription of inflammation-related genes. Genes marked in black denote up-regulation and white down-regulation ($P < 0.05$; OVE vs. CON); genes in gray had no statistical change in mRNA expression between treatments. Letters along the edges denote effects on activity (A), expression (E), regulation of binding (RB), protein-DNA binding (PD), and transcription (T).

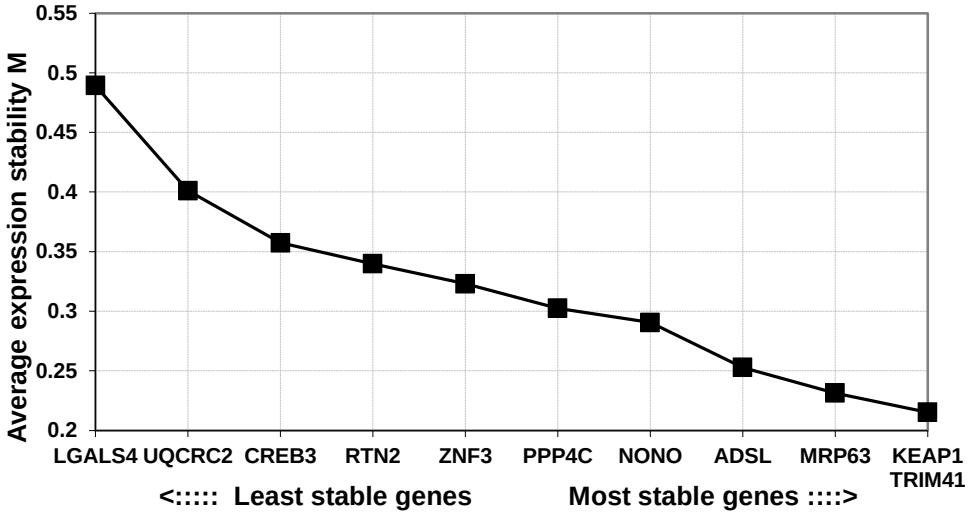

A. Average expression stability values of remaining control genes

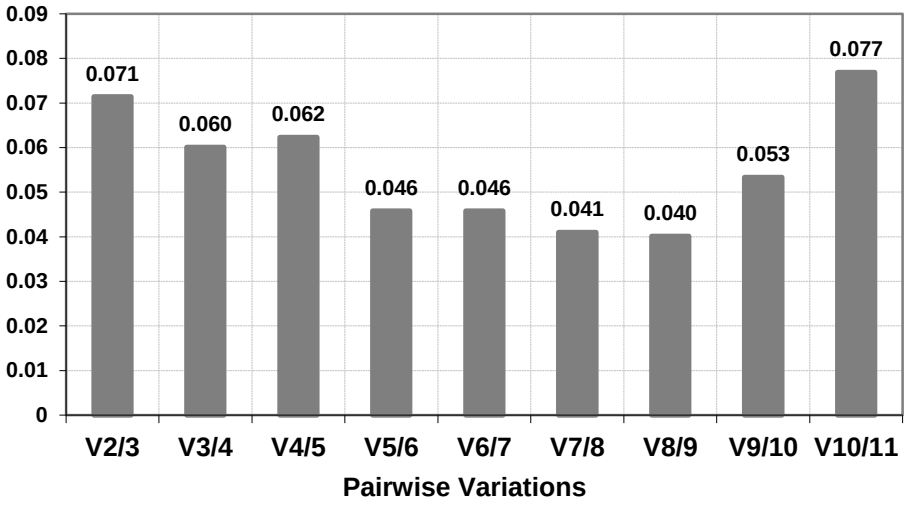

B. Determination of the optimal number of control genes for normalization

Figure S2.1. Panel A, average expression stability M of remaining genes tested in the pairwise comparison. M was calculated by stepwise exclusion of the least stable gene. *KEAP1, TRIM41,* and *MRP63* were the most stable ones; whereas, *LGALS4, UQCRC2,* and *CREB3* were the least stable genes. Panel B, optimal number of ICG for normalization. Y-axis, variation between normalization factor by using *n* ICG (NF_n) and the NF from (*n* + 1) ICG (NF_{n+1}); X-axis, pairwise comparison using (*n* + 1) ICG replacing *n* ICG. Although the analysis indicated that 9 ICG was optimal in our study (panel B), it was evident that using fewer than 9 ICG would still result in a threshold <0.10 which was deemed optimal (Bionaz and Loor, 2007). Thus, on practical grounds we elected to use the geometric mean of the 3 most stable genes, i.e., *KEAP1, TRIM41,* and *MRP63* as ICG.

CHAPTER 3

INFLAMMATION- AND LIPID METABOLISM-RELATED GENE NETWORK SIGNATURES IN VISCERAL AND SUBCUTANEOUS ADIPOSE DEPOTS OF DAIRY COWS

ABSTRACT

We examined mRNA expression of 27 genes in mesenteric (MAT), omental (OAT), and subcutaneous (SAT) adipose tissue from nonpregnant and nonlactating Holstein cows in response to control (CON, NE_L= 1.35 Mcal/kg DM) or overfeeding energy (OVE, NE_L= 1.62/kg DM). Eighteen cows were randomly assigned to one of the two treatment groups. After an 8-wk feeding period, AT were harvested, weighed, and subsamples for RNA extraction were collected from depots immediately after euthanasia. Genes involved in lipogenesis, triglyceride (TAG) synthesis, lipolysis, transcriptional regulation of lipogenesis, and adipose secreted proteins were analyzed via quantitative PCR (qPCR). The interaction of dietary energy and AT depot was not significant for any gene analyzed. In the present work, we report depot-specific differences in gene expression patterns. The mRNA expression of *ACACA* and *FASN* was significantly higher ($P < 0.05$) in SAT than MAT. Expression of *SCD* and *ADFP* was greatest in SAT, intermediate in MAT, and lowest in OAT. However, the two visceral depots had greater expression of *THRSP*, *ACLY*, *LPL*, *FABP4*, *GPAM*, and *LPIN1* in comparison with SAT ($P < 0.05$). The transcription factor *SREBF1* had higher expression in MAT and SAT than OAT ($P < 0.05$). Among AT-secreted proteins, visceral depots had higher ($P < 0.05$) expression of adipokines (leptin and adiponectin) and serum amyloid A3 (*SAA3*) compared with SAT. However, MAT had higher

expression than SAT ($P < 0.05$) of pro-inflammatory cytokines (*IL1B* and *IL6*), IL6 receptor (*IL6R*) and chemokines (*CCL2* and *CCL5*); whereas, *TNF* was higher in SAT than OAT, and intermediate in MAT ($P < 0.05$). Overall results suggested that visceral AT may be more active in uptake of preformed FA than SAT. In contrast, *de novo* FA synthesis could make a greater contribution to the intracellular FA pool in SAT than visceral AT. The visceral AT seemed to have a greater capacity for expressing and likely secreting pro-inflammatory cytokines than SAT; thus, visceral obesity due to overfeeding energy may be detrimental to liver health in dairy cows.
Key words: adipose, gene expression, inflammation, lipogenesis, overfeeding energy, visceral

INTRODUCTION

Adipose tissue (AT) was first recognized to function as an "energy reservoir" in the form of triacylglycerol (TAG) when there was a surplus of nutrients or as provider of energy in the form of long-chain fatty acids (LCFA) during periods of intense lipolysis as it occurs in negative energy balance (NEB). In non-lactating ruminants AT does not only take up preformed FA from blood but is the primary site of *de novo* FA synthesis (DNS) as well (Bergen and Mersmann, 2005). In non-ruminant species (mainly human and rodents) it is well-established that metabolism of visceral AT (VAT) is different from subcutaneous AT (SAT) (Smith and Zachwieja, 1999), e.g., VAT is more sensitive to lipolytic stimuli (e.g. catecholamines) but less so to anti-lipolytic stimulation by insulin (Hellmer et al., 1992; Giorgino et al., 2005); Although, in dairy cows, the metabolic activity of SAT (McNamara, 1995) and VAT (Baldwin et al., 2004) changes with stage of lactation and availability of dietary energy, it is still unclear whether dietary energy intake differentially impacts the metabolism (lipogenesis and lipolysis) of VAT

and SAT. Hence, more research is necessary to further explore fundamental aspects of metabolic regulation in SAT and VAT in ruminants.

The endocrine function of adipose tissue was not recognized until the discovery of leptin (LEP) in 1994, a protein that was initially identified as a feedback signal of AT to regulate food intake and energy expenditure in rodents (Zhang et al., 1994). Subsequent work identified a series of protein products secreted by AT including adiponectin (ADIPOQ), TNF, IL6, resistin, and chemokines (e.g. CCL2) (See review in Sethi and Vidal-Puig, 2007). Many of these products are classical pro-inflammatory cytokines. Studies in humans demonstrated that VAT had greater capability for secretion of these cytokines and is more susceptible to infiltration of macrophages than SAT (Weisberg et al., 2003; Pou et al., 2007). Furthermore, accumulating evidence indicated that obesity and insulin resistance are associated with a chronic proinflammatory response leading to increased cytokine production and activation of inflammatory signaling pathways (See review in Tilg and Moschen, 2008). Although the effect of dietary energy overfeeding on inflammatory status in dairy cows has not been well documented, a recent study provided evidence that SAT and VAT are immunoresponsive (Mukesh et al., 2009). Drackley et al. (2005) proposed that because of direct portal drainage of VAT, an increase in cytokine secretion by this depot might impact negatively the liver.

Lipid metabolism pathways (DNS and TAG synthesis) are composed of multiple stepwise enzymatic reactions. In addition to well-established post-transcriptional and post-translational regulation of enzymatic activity to coordinate AT metabolism (e.g., ACACA), transcriptional regulation represents a long-term mechanism of cellular metabolism (Desvergne et al., 2006). Proteins secreted by AT (e.g., ADIPOQ, LEP) are primarily regulated at the level of transcription (Berger and Moller, 2002). Therefore, evaluation of mRNA expression of genes

encoding enzymes that participate in metabolic pathways, especially the ones catalyzing rate-limiting steps, is of value (Bionaz and Loor, 2008). The objectives of this study were to investigate how overfeeding a moderate-energy diet impacts fat deposition in VAT, and to determine fat depot-specific adipogenic, lipogenic, and immune-related gene expression. Those data were related with blood metabolites and tissue mass in order to gain a more holistic view of the biological phenomena.

MATERIALS AND METHODS

Experimental Design, Animals, Diets, and Sampling

Experimental Design. Eighteen nonpregnant, nonlactating Holstein cows [body weight (BW) = 656 ± 29; body condition score (BCS) = 3.04 ± 0.25] were randomly assigned to either a moderate-energy diet (OVE; NE_L = 1.62 Mcal/kg DM) or controlled-energy diet (CON; NE_L = 1.35 Mcal/kg DM) provided as a TMR for *ad libitum* intake. The OVE diet contained 73.8% forage (without wheat straw) and 13.8% ground shelled corn (DM basis); the CON diet contained 81.7% forage including 40.5% wheat straw and 3.5% ground shelled corn. The TMR was mixed and processed in a Keenan Klassik 140 mixer wagon (Richard Keenan & Co., Ltd., Borris, County Carlow, Ireland) and offered once daily at 0800 h. Cows had free access to water. Initial and final BW was recorded at the start of wk 1 and end of wk 8. The experiment was conducted in an indoor free-stall barn equipped with Calan gates to monitor individual feed intake. Experimental procedures were approved by the Institutional Animal Care and Use Committee at the University of Illinois (protocol 06194).

Tissue Sampling. After the 8-wk experiment, cows were euthanized at the diagnostic facilities of the College of Veterinary Medicine, University of Illinois. . All AT samples were

harvested within 20 min of euthanasia and were snap-frozen in liquid N_2 until RNA extraction. Subcutaneous AT was harvested from the tail-head region on the left side of each cow. Mesenteric, omental, and perirenal AT depots were carefully dissected, weighed, and a subsample collected for RNA extraction.

RNA Extraction and Quality Assessment, Primer Design and Evaluation, Internal Control Gene (ICG) Selection, and Quantitative RT-PCR (qPCR)

RNA Extraction, Quality Assessment, and cDNA Preparation. Adipose tissue was weighed (~2.0 g) and immediately placed into ~15 mL ice-cold TRIzol® Reagent (Invitrogen, Carlsbad, CA) with 1 µL linear acrylamide (Ambion, Inc., Austin, TX) for extraction of total RNA as previously described (Loor et al., 2005). Total RNA was cleaned using RNeasy mini kit columns and genomic DNA was removed using the RNase-Free DNase Set (Qiagen, Valencia, CA). The RNA concentration was measured with a NanoDrop ND-1000 spectrophotometer (NanoDrop Technologies). The purity of RNA was assessed by ratio of optical density OD260/280, which was above 1.9 for all samples. Integrity of RNA (RIN) was tested by electrophoretic analysis of 28S and 18S rRNA subunits using a 2100 Bioanalyzer (Agilent Technologies); values were >7.0 for all samples. A portion of the RNA was diluted to 100 ng/µL with DNase-RNase free water prior to RT for cDNA synthesis. The cDNA were synthesized using 100 ng RNA, 1 µg dT18 (Operon Biotechnologies, AL), 1 µL 10 mM dNTP mix (Invitrogen Corp., CA), 1 µL Random Primers (Invitrogen Corp., CA), and 10 µL DNase/RNase free water. The mixture was incubated at 65°C for 5 min and kept on ice for 3 min. A total of 6 µL of master mix composed of 4.5 µL 5X First-Strand Buffer, 1 µL 0.1 M DTT, 0.25 µL (50 U) of SuperScript™ III RT (Invitrogen Corp.,CA), and 0.25 µL of RNase Inhibitor (10 U, Promega, WI) was added. The reaction was performed in an Eppendorf Mastercycler® Gradient with the

following temperature program: 25°C for 5 min, 50°C for 60 min, and 70°C for 15 min. The cDNA was then diluted 1:4 with DNase/RNase free water.

***Primer Design and Evaluation*.** Primers were designed and evaluated as previously described (Bionaz and Loor, 2008). The details of primer sequences and the description of genes are the same as shown in Table 2.2 and Supplemental Table S2.1 and S2.2. Primers were designed using Primer Express 3.0 with minimum amplicon size of 80 bp (amplicons of 100 -120 bp were preferable, if possible) and limited 3' G + C percentage (Applied Biosystems, CA). Primer sets were intentionally designed to fall across exon-exon junctions. Then, primers were aligned against NCBI database through BLASTN and UCSC's COW (*Bos taurus*) Genome Browser Gateway to determine the compatibility of primers with already annotated sequence of the corresponding gene in both databases. Prior to qPCR, primers were verified through a 20 µL-PCR reaction that followed the same procedures of qPCR described below except the dissociation step. A universal reference cDNA amplified from 3 bovine adipose tissues (SAT, mesenteric, and omental AT) was utilized to ensure the identification of genes. Five µL of PCR product was run in a 2% agarose gel stained with ethidium bromide, and the remaining 15 µL were cleaned with a QIAquick® PCR Purification Kit (QIAGEN) and sequenced at the Core DNA Sequencing Facility of the Roy J. Carver Biotechnology Center at the University of Illinois, Urbana (the same as in Supplement Table S2.2). The sequencing product was confirmed through BLASTN at the National Center for Biotechnology Information (NCBI) database. Only primers that presented a single band of the expected size and the right amplification product were used for qPCR. The accuracy of a pair of primers was evaluated by the presence of a unique peak during the dissociation step at the end of qPCR.

Genes evaluated included: acetyl-Coenzyme A carboxylase alpha (*ACACA*), ATP citrate lyase (*ACLY*), acyl-CoA synthetase long-chain (*ACSL1*), adipose differentiation-related protein (*ADFP* or PLIN2), thrombospondin receptor (*CD36*), elongation of long chain fatty acids family member 6 (*ELOVL6*), adipocyte fatty acid binding protein 4 (*FABP4*), fatty acid synthase (*FASN*), mitochondrial glycerol-3-phosphate acyltransferase (*GPAM*), hormone-sensitive lipase (*LIPE*), lipin 1 (*LPIN1*), lipoprotein lipase (*LPL*), stearoyl-CoA desaturase (*SCD*), MLX interacting protein-like (*MLXIPL*), peroxisome proliferator-activated receptor gamma (*PPARG*), sterol regulatory element binding transcription factor 1 (*SREBF1*), thyroid hormone responsive SPOT 14 (*THRSP*), adiponectin (*ADIPOQ*), chemokine (C-C motif) ligand 2 (*CCL2*), chemokine (C-C motif) ligand 5 (*CCL5*), interleukin-1 beta (*IL1B*), interleukin-6 (*IL6*), interleukin-6 receptor (*IL6R*), leptin (*LEP*), acute-phase serum amyloid A3 (*SAA3*), toll-like receptor 4 (*TLR4*), and tumor necrosis factor alpha (*TNF*).

Quantitative PCR (qPCR). The qPCR analysis was performed in a MicroAmp^{TM} Optical 384-Well Reaction Plate (Applied Biosystems, CA). Within each well, 4 µL diluted cDNA combined with 6 µL of mixture composed of 5 µL 1×SYBR Green master mix (Applied Biosystems, CA), 0.4 µL each of 10 µM forward and reverse primers, and 0.2 µL DNase/RNase free water were added. Three replicates and a 6-point standard curve plus the non-template control (NTC) were run for each sample to test the relative expression level (User Bulletin #2, Applied Biosystems, CA). The qPCR reactions were conducted in an ABI Prism 7900 HT SDS instrument (Applied Biosystems, CA) with the following conditions: 2 min at 50 °C, 10 min at 95 °C, 40 cycles of 15 s at 95 °C (denaturation), and 1 min at 60 °C (annealing + extension). The presence of a single PCR product was verified by the dissociation protocol using incremental temperatures to 95 °C for 15 s, then 65 °C for 15 s.

Internal Control Gene (ICG) Selection and Evaluation. A detailed description for the selection criteria of ICG for qPCR has been provided previously (Mukesh et al., 2009).

Data Processing and Statistical Analysis

The threshold cycle (Ct) data were analyzed and transformed using the standard curve with the 7900 HT Sequence Detection System Software (version 2.2.1, Applied Biosystems, CA). Data were then normalized with the geometric mean of the three most stable ICG (Mukesh et al., 2009). Analysis (Supplemental Figure S2.1) revealed that genes encoding kelch-like ECH-associated protein 1 (*KEAP1*), tripartite motif-containing 41 (*TRIM41*), and mitochondrial ribosomal protein 63 (*MRP63*) were the most appropriate to calculate a normalization factor to normalized gene expression data.

The normalized PCR data (relative mRNA expression) were subjected to log transformation in SAS (SAS Inst. Release 8.0) to ensure a normal distribution of residuals. This transformed dataset was analyzed as a 2 × 3 factorial arrangement (diet and tissue source as as the two factors) with the PROC GLM procedure in SAS. No significant interactions between the two factors were detected in the initial analysis; we excluded the interaction and re-analyzed data with only the main effects. The PDIFF statement of SAS was utilized to evaluate differences with significance declared at $P \leq 0.05$.

Relative mRNA Abundance of Genes within Adipose Tissue

Efficiency of qPCR amplification for each gene (see Table S2.3) was calculated using the standard curve method (Efficiency = $10^{(-1/\text{slope})}$). Relative mRNA abundance among measured genes was calculated as previously reported (Bionaz and Loor, 2008), using the inverse of PCR efficiency raised to ΔCt (gene abundance = $1/E^{\Delta Ct}$, where ΔCt = Ct of tested gene – geometric mean Ct of 3 internal control genes). Overall mRNA abundance for each gene among all samples

of the same adipose tissue was calculated using the median ΔCt, and overall percentage relative mRNA abundance was computed from the equation: 100 × mRNA abundance of individual gene / sum of mRNA abundance of all genes tested (Table 3.2).

RESULTS AND DISCUSSION

In the present study, dietary energy intake exerted a consistent impact on gene expression in both VAT and SAT depots (chapter 2). Except for a tendency for LPL ($P = 0.085$), no interactions were detected ($P > 0.10$) between level of dietary energy and AT depot. Therefore, our data indicate that differential expression of genes among depots was due to unique characteristics of each depot examined. The depot-specific expression pattern of metabolic gene networks in ruminant species has not been documented previously. This manuscript deals exclusively with differences observed between depots. Our results clearly showed that AT from various anatomical sites exhibit different patterns of genes expression.

Lipogenesis, Elongation, and Desaturation

Compared with the two VAT sites, SAT had the highest mRNA expression and % mRNA abundance of the classical lipogenic genes *ACACA*, *FASN* and *SCD* (Figure 3.1). The differences between SAT and MAT for were significant *ACACA* and *FASN* ($P < 0.01$), and among all sites for *SCD* with intermediate response in OAT ($P < 0.02$). However, *ACLY* exhibited the opposite expression pattern with higher mRNA abundance in VAT depots than SAT ($P < 0.05$). Expression of *ELOVL6* was consistent in the three depots ($P > 0.05$). Baldwin et al. (2007) showed that the pattern of acetate incorporation into intracellular FA and TAG was generally greater for SAT as compared with VAT (OAT and MAT). Furthermore, Eguinoa et al. (2003) reported that the activity of glycerol-3-phosphate dehydrogenase and FASN was greater

in SAT than VAT. Because transcriptional regulation is the primary determinant of protein abundance (and likely function) of these genes (Foufelle and Ferre, 2002; Postic et al., 2007), together, our results indicate a potentially greater capacity for *de novo* FA synthesis in SAT than VAT depots.

Studies in humans and rodents have revealed transcriptional differences in a depot-specific manner. In a human study, mRNA expression of *FASN* was 1.7-fold higher in VAT than SAT and these differences corresponded with differences in protein level (Berndt et al., 2007). Higher *FASN* and *SREBF1* expression was found in inguinal AT than in MAT in rats (Palou et al., 2009). Furthermore, Bertile and Raclot (2004) showed delayed and smaller transcriptional changes for lipogenic genes (*FASN* and *ACLY*) in SAT compared with retroperitoneal AT in response to refeeding underfed rats. Despite the above differences among AT depots, in humans and rodents liver rather than AT is the major lipogenic organ (Bergen and Mersmann, 2005) and glucose absorbed from the gastrointestinal (GI) tract is the major substrate for *de novo* lipogenesis. Therefore, glucose delivery to the VAT prior to reaching SAT may result in enhanced transcription of lipogenic genes in VAT. Obvious physiological differences between species make it difficult to compare our data with non-ruminant studies.

Two classical studies at the University of Illinois shed light on site-specific lipogenic activity in ruminants. Ingle et al. (1972a) found that the rate of FA biosynthesis from acetate was higher in internal fat (perirenal and OAT) than in SAT (from rump, abdominal, and backfat) in lambs. However, a shift in lipogenic capacity between the two sites was uncovered in mature animals (sheep and market steers; (Ingle et al., 1972b). Our results supported these early findings at the transcriptional level. We speculate that the opposite expression pattern of *ACLY* between VAT and SAT may have been induced by the relatively greater glucose or lactate carbon

utilization rate through the citrate cleavage pathway, likely for FA synthesis and provision of NADPH. The closer anatomical location of VAT to the GI tract could facilitate absorption of any intestinal glucose and lactate, thus, providing more substrate for lipogenesis.

Correlation analysis revealed significant ($P < 0.05$) positive relationships regardless of dietary treatment between *SCD* expression in SAT and the average pre-harvest cow BCS. Martin et al. (1999) observed that the peak of *SCD* mRNA expression preceded a significant rise in lipogenesis and lipid filling in SAT of yearling steers, and concluded that the level of *SCD* expression was indicative of the extent of terminal differentiation in bovine tail-head SAT. In our study, *SCD* mRNA expression in MAT and OAT was positively correlated with tissue weight. Moreover, *SCD* mRNA expression in VAT was positively correlated ($P < 0.05$) with intake of net energy for lactation (NE_L) at wk 5 and 6, and that relationship also tended ($P < 0.10$) to be significant at wk 7, i.e. prior to slaughter. Hence, overall our results indicate that mRNA expression of *SCD* could be a suitable marker of fat storage in subcutaneous and visceral depots, e.g., the transcriptional change of *SCD* in VAT was more responsive to dietary energy intake than SAT (Ji et al., 2009). A key role of *SCD* in bovine milk fat synthesis has been underscored previously (Bionaz and Loor, 2008).

The SAT exhibited higher expression of *ADFP* than the two VAT depots, with the lowest value in MAT. Thus, lipid droplet synthesis may differ among fat depots.

Long-chain Fatty Acid Uptake, Activation, and Esterification

Interestingly, *LPL*, *GPAM*, and *LPIN1* were more abundant in both VAT depots than in SAT ($P < 0.01$). Expression of *ACSL1* was greater in MAT than in the other two fat depots ($P < 0.05$), while it was numerically higher in OAT than SAT. It appears that VAT has greater capacity for utilizing preformed FA for TAG synthesis than SAT. Such a result is in accordance

with previous studies. For example, Hocquette et al. (1998) reported that both *LPL* mRNA expression and its enzymatic activity were greater in internal fat (perirenal AT and OAT) than in SAT of male calves. Together with our results, this evidence indicates that breed, maturity, and physiological status may influence fat deposition through regulation of major enzymes not only via the provision of substrate but also transcriptionally.

Despite the extensive number of genes we analyzed, it is difficult to make sweeping conclusions about priority for AT deposition among depots studied. For example, despite greater SAT expression of genes for *de novo* FA synthesis (*ACACA*, *FASN*, and *SCD*), VAT could possibly accumulate more lipid through incorporation of preformed FA due to greater expression of *LPL*, *ACSL1*, *GPAM*, and *LPIN1*. We found no difference in expression of *CD36* and *LIPE* among fat depots ($P > 0.05$). The most abundant transcripts among all genes examined were *SCD*, *FABP4*, and *LPL*, which together accounted for ~63.2%, 69.9%, and 71.5% mRNA abundance in MAT, OAT, and SAT, respectively (See Table 3.2). Within lipid metabolic-related genes *SCD* had the greatest fold-change across fat depots; the relative mRNA expression in SAT was 3-fold that in MAT. The different expression patterns of these genes could be indicative of different enrichments of biological processes within AT depots.

Transcriptional Regulation of Lipogenesis

As shown in Figure 3.2, *SREBF1* was more highly expressed in SAT and MAT than in OAT ($P < 0.05$), whereas *PPARG* and *MLXIPL* were consistently expressed among AT depots. The transcription factor MLXIPL was reported to control ca. 50% of hepatic lipogenesis in rodent liver by regulating glycolytic and lipogenic gene expression (Iizuka and Horikawa, 2008) through binding to the carbohydrate response element (ChoRE) in the promoter region of its target genes (Yamashita et al., 2001) including *THRSP* (Shih et al., 1995), *ACACA*, and *FASN*

(Towle et al., 1997). The relative % mRNA abundance of *MLXIPL* (0.02-0.03% of total genes) was much less than that of *SREBF1* (0.3-0.5%) or *PPARG* (0.9-1.5%, shown in Table 3.2) across the three AT depots, from which we deduced that MLXIPL likely plays a minor role in the regulation of lipogenesis in ruminant AT. The consistent mRNA expression level of *PPARG* among all AT sites and its relatively higher mRNA abundance indicated that it may be the key transcription regulator driving adipogenesis and lipid filling (see Table 3.2). We speculate that PPARG activation via dietary LCFA (e.g., saturated and marine PUFA; Kadegowda et al., 2009) could aid in manipulating AT deposition or insulin sensitivity during the transition from pregnancy into lactation, i.e., when insulin sensitivity is markedly impaired (Bauman and Griinari, 2003).

Expression of *THRSP* differed among fat depots with greater values in VAT than in SAT ($P < 0.05$), which underscored its importance in association with other lipogenic genes and potentially the adipocyte differentiation status among depots. This depot-specific expression pattern is possibly induced by differing numbers of thyroid hormone (TH) receptors (TR) and ratios of TR isomers among fat depots, which are required for transcriptional activation of *THRSP* (Cunningham et al., 1998). A recent study revealed a difference in expression of TRα (an isomer of TR) and *THRSP* between SAT and OAT in humans, and a significant correlation of *THRSP* expression with TRα mRNA abundance and with the TRα1/TRα2 ratio (Ortega et al., 2009). However, contrary to our study, they found higher expression of these genes in SAT than in OAT, which could be associated with inherent species differences.

Adipokines and Immune-related Genes

Most of the adipocytokines tested exhibited depot-specific expression patterns (figure 3.3). Adiponectin and *SAA3* mRNA expression was higher in both VAT depots than in SAT ($P <$

0.05), with no statistical difference between MAT and OAT. Leptin was differentially expressed among the three depots ($P < 0.05$), with the highest mRNA abundance in OAT and the lowest in SAT. The MAT had greater mRNA expression of *IL1B* and *IL6R* than the other two depots ($P < 0.05$), while there was no difference between OAT and SAT. A similar expression pattern was detected for *IL6, CCL2,* and *CCL5* of which the mRNA expression profiles were markedly higher in MAT than in SAT ($P < 0.05$) and intermediate in OAT, with no statistical significance between OAT and the other two depots. Expression of *TNF* mRNA was greater in SAT than in OAT ($P < 0.05$) and intermediate in MAT, but differences between MAT and the other two depots were not significant. Visceral AT depots, especially MAT, appear to have greater capacity than SAT to express these adipocytokines, with the exception of *TNF*. Strong evidence of correlative and causative relationships among visceral obesity, systemic low-grade chronic inflammation, hepatic disease, and insulin resistance has been found in human and rodent models and linked to secretion of adipocytokines (Lionetti et al., 2009).

Expression of *TLR4* was did not differ ($P = 0.30$) between SAT and the 2 VAT. Recent evidence seems to support a causative relationship between metabolic phenotype and immune responses of visceral fat, and *TLR4* (at least in non-ruminants) appears to be a key molecular link (Song et al., 2006; Davis et al., 2008; Kopp et al., 2009). This receptor is the best-characterized endogenous sensor for lipopolysaccharide (LPS). Upon binding of LPS to TLR4 and its co-receptors CD14 and MD-2, the adaptor protein myeloid differentiation factor 88 (MyD88) is recruited to the Toll/IL-1 receptor (TIR) domain of the receptor. Interaction of the TIR domain of TLR4 and MyD88 triggers a downstream signaling cascade, leading to activation of the NFκB pathway, which then activates the transcription of many genes encoding pro-inflammatory cytokines, chemokines, and other effectors of the innate immune response (Zuany-Amorim et al.,

2002). In non-ruminant AT, both adipocytes and adipose-resident macrophages express *TLR4* (Lin et al., 2000). Stimulation of non-ruminant adipocytes by LPS induces the release of TNF-a, IL-6, IL-1β, IL-8, and CCL2 (Kopp et al., 2010). Despite the lack of effect of a 2-h in vitro LPS challenge on *TLR4* expression in MAT and SAT from nonlactating cows, Mukesh et al. (2009) observed higher *SAA3*, *CCL5*, and *CCL2* mRNA expression in MAT than in SAT, coupled with markedly increased expression of *TNF* and *IL6* in both sites after LPS challenge; *IL-6* increased more prominently in MAT. Therefore, *CCL2* rather than *TLR4* expression may be a more reliable marker of tissue inflammation. Our data for *CCL2* (along with *IL1B* and *IL6*) seem to support a more prominent proinflammatory potential in MAT than SAT.

SUMMARY AND CONCLUSIONS

Endeavors to decipher the regulatory mechanisms driving metabolism in different AT depots have been largely conducted in human and rodent models. The current study established the different expression patterns of genes that may control lipid accretion between two visceral AT depots and subcutaneous adipose in dairy cows. Thus we have obtained a more holistic evaluation of fundamental differences in dairy cows relative to other species. As suggested by the greater mRNA expression of pro-inflammatory cytokines (*IL1B* and *IL6*), acute phase proteins (*SAA3*), and chemokines (*CCL2* and *CCL5*), our data support the view that increased visceral adiposity may predispose dairy cows to more adverse pathophysiological states (e.g., inflammation and liver damage). Despite the limitations of deducing physiological changes by focusing on transcript profiles, the clear implication of our results supports the hypothesis visceral fat metabolism may impact liver health due to the direct portal drainage, and this may be much more prominent during the transition from late pregnancy to lactation. Future research on

how nutritional management affects the visceral AT metabolism and its endocrine functions during the transition period is warranted.

LITERATURE CITED

Baldwin, R. L., K. R. McLeod, and A. V. Capuco. 2004. Visceral tissue growth and proliferation during the bovine lactation cycle. J. Dairy Sci. 87:2977-2986.

Baldwin, R. L. T., K. R. McLeod, J. P. McNamara, T. H. Elsasser, and R. G. Baumann. 2007. Influence of abomasal carbohydrates on subcutaneous, omental, and mesenteric adipose lipogenic and lipolytic rates in growing beef steers. J. Anim. Sci. 85:2271-2282.

Bauman, D. E., and J. M. Griinari. 2003. Nutritional regulation of milk fat synthesis. Annu. Rev. Nutr. 23:203-227.

Bergen, W. G., and H. J. Mersmann. 2005. Comparative aspects of lipid metabolism: impact on contemporary research and use of animal models. J. Nutr. 135:2499-2502.

Berger, J., and Moller, D. E. 2002. The mechanisms of action of PPARs. Annu. Rev. Med. 53:409-435.

Berndt, J., S. Kralisch, N. Kloting, K. Ruschke, M. Kern, M. Fasshauer, M. R. Schon, M. Stumvoll, and M. Bluher. 2008. Adipose triglyceride lipase gene expression in human visceral obesity. Exp. Clin. Endocrinol. Diabetes 116:203-210.

Bertile, F., and T. Raclot. 2004. mRNA levels of SREBP-1c do not coincide with the changes in adipose lipogenic gene expression. Biochem. Biophys. Res. Commun. 325:827-834.

Bionaz, M., and J. J. Loor. 2008. Gene networks driving bovine milk fat synthesis during the lactation cycle. BMC Genomics. 9:366-387.

Cunningham, B. A., J. T. Moncur, J. T. Huntington, and W. B. Kinlaw. 1998. "Spot 14" protein: a metabolic integrator in normal and neoplastic cells. Thyroid 8:815-825.

Davis, J. E., N. K. Gabler, J. Walker-Daniels, and M. E. Spurlock. 2008. Tlr-4 deficiency selectively protects against obesity induced by diets high in saturated fat. Obesity (Silver Spring) 16:1248-1255.

Desvergne, B., L. Michalik, and W. Wahli. 2006. Transcriptional regulation of metabolism. Physiol. Rev. 86:465-514.

Eguinoa, P., S. Brocklehurst, A. Arana, J. A. Mendizabal, R. G. Vernon, and A. Purroy. 2003. Lipogenic enzyme activities in different adipose depots of Pirenaican and Holstein bulls and heifers taking into account adipocyte size. J. Anim. Sci. 81:432-440.

Foufelle, F., and P. Ferre. 2002. New perspectives in the regulation of hepatic glycolytic and lipogenic genes by insulin and glucose: a role for the transcription factor sterol regulatory element binding protein-1c. Biochem. J. 366:377-391.

Giorgino, F., L. Laviola, and J. W. Eriksson. 2005. Regional differences of insulin action in adipose tissue: insights from in vivo and in vitro studies. Acta Physiol. Scand. 183:13-30.

Hellmer, J., C. Marcus, T. Sonnenfeld, and P. Arner. 1992. Mechanisms for differences in lipolysis between human subcutaneous and omental fat cells. J. Clin. Endocrinol. Metab. 75:15-20.

Hocquette, J. F., B. Graulet, and T. Olivecrona. 1998. Lipoprotein lipase activity and mRNA levels in bovine tissues. Comp. Biochem. Physiol. B. Biochem. Mol. Biol. 121:201-212.

Iizuka, K., and Y. Horikawa. 2008. ChREBP: a glucose-activated transcription factor involved in the development of metabolic syndrome. Endocr. J. 55:617-624.

Ingle, D. L., D. E. Bauman, and U. S. Garrigus. 1972a. Lipogenesis in the ruminant: in vitro study of tissue sites, carbon source and reducing equivalent generation for fatty acid synthesis. J. Nutr. 102:609-616.

Ingle, D. L., D. E. Bauman, and U. S. Garrigus. 1972b. Lipogenesis in the ruminant: in vivo site of fatty acid synthesis in sheep. J. Nutr. 102:617-623.

Ji, P., J. J. Loor, A. Nikkhah, M. Bionaz, N. A. Janovick, and J. K. Drackley. 2009. Changes in deposition of visceral adipose tissues and expression of lipogenesis-related genes induced by diets with different energy levels in non-lactating cows. J. Dairy Sci. 92(E-Suppl.):150. (Abstr.)

Kopp, A., C. Buechler, M. Bala, M. Neumeier, J. Scholmerich, and A. Schaffler. 2010. Toll-like receptor ligands cause proinflammatory and prodiabetic activation of adipocytes via phosphorylation of extracellular signal-regulated kinase and c-Jun N-terminal kinase but not interferon regulatory factor-3. Endocrinol.. 151:1097-1108.

Kopp, A., P. Gross, W. Falk, M. Bala, J. Weigert, C. Buechler, M. Neumeier, J. Scholmerich, and A. Schaffler. 2009. Fatty acids as metabolic mediators in innate immunity. Eur. J. Clin. Invest. 39:924-933.

Lin, Y., H. Lee, A. H. Berg, M. P. Lisanti, L. Shapiro, and P. E. Scherer. 2000. The lipopolysaccharide-activated toll-like receptor (TLR)-4 induces synthesis of the closely related receptor TLR-2 in adipocytes. J. Biol. Chem. 275:24255-24263.

Lionetti, L., M. P. Mollica, A. Lombardi, G. Cavaliere, G. Gifuni, and A. Barletta. 2009. From chronic overnutrition to insulin resistance: The role of fat-storing capacity and inflammation. Nutr. Metab. Cardiovas. 19:146-152.

Loor, J. J., H. M. Dann, R. E. Everts, R. Oliveira, C. A. Green, N. A. Guretzky, S. L. Rodriguez-Zas, H. A. Lewin, and J. K. Drackley. 2005. Temporal gene expression profiling of liver from periparturient dairy cows reveals complex adaptive mechanisms in hepatic function. Physiol. Genomics. 23:217-226.

Martin, G. S., D. K. Lunt, K. G. Britain, and S. B. Smith. 1999. Postnatal development of stearoyl coenzyme A desaturase gene expression and adiposity in bovine subcutaneous adipose tissue. J. Anim. Sci. 77:630-636.

McNamara, J. P. 1995. Role and regulation of metabolism in adipose tissue during lactation. J. Nutr. Biochem. 6:120-129.

Mukesh, M., M. Bionaz, D. E. Graugnard, J. K. Drackley, and J. J. Loor. 2009. Adipose tissue depots of Holstein cows are immune responsive: inflammatory gene expression in vitro. Domest. Anim. Endocrinol. 38:168-178.

Ortega, F. J., J. M. Moreno-Navarrete, V. Ribas, E. Esteve, J. I. Rodriguez-Hermosa, B. Ruiz, B. Peral, W. Ricart, A. Zorzano, and J. M. Fernandez-Real. 2009. Subcutaneous fat shows higher thyroid hormone receptor-alpha1 gene expression than omental fat. Obesity (Silver Spring) 17:2134-2141.

Palou, M., T. Priego, J. Sanchez, A. M. Rodriguez, A. Palou, and C. Pico. 2009. Gene expression patterns in visceral and subcutaneous adipose depots in rats are linked to their morphologic features. Cell. Physiol. Biochem. 24:547-556.

Postic, C., R. Dentin, P. D. Denechaud, and J. Girard. 2007. ChREBP, a transcriptional regulator of glucose and lipid metabolism. Annu. Rev. Nutr. 27:179-192.

Pou, K. M., J. M. Massaro, U. Hoffmann, R. S. Vasan, P. Maurovich-Horvat, M. G. Larson, J. F. Jr Keaney, J. B. Meigs, I. Lipinska, S. Kathiresan, J. M. Murabito, C. J. O'Donnell, E. J. Benjamin, and C. S. Fox. 2007. Visceral and subcutaneous adipose tissue volumes are crosssectionally related to markers of inflammation and oxidative stress: the Framingham heart study. Circulation. 116:1234-1241.

Sethi, J. K., and A. J. Vidal-Puig. 2007. Thematic review series: Adipocyte biology - Adipose tissue function and plasticity orchestrate nutritional adaptation. J. Lipid Res. 48:1253-1262.

Shih, H. M., Z. Liu, and H. C. Towle 1995. Two GACGTG motifs with proper spacing dicate the carbohydrate regulation of hepatic gene transcription. J. Biol. Chem. 270:21991-21997.

Smith, S. R., and J. J. Zachwieja. 1999. Visceral adipose tissue: a critical review of intervention strategies. Int. J. Obesity. 23:329-335.

Song M. J., K. H. K., J. M. Yoon, and J. B. Kim. 2006. Activation of Toll-like receptor 4 is associated with insulin resistance in adipocytes. Biochem. Biophys. Res. Commun. 346:739-745.

Tilg, H., and A. R. Moschen. 2008. Insulin resistance, inflammation, and non-alcoholic fatty liver disease. Trends Endocrin. Metab. 19:371-379.

Towle H. C., E. N. Kaytor, and H. M. Shih. 1997. Regulation of the expression of lipogenic enzyme genes by carbohydrate. Ann. Rev. Nutr. 17:405-433.

Weisberg, S. P. 2003. Obesity is associated with macrophage accumulation in adipose tissue. J.Clin. Invest. 112:1796-1808.

Yamashita, H., M. Takenoshita, M. Sakurai, R. K. Bruick, W. J. Henzel, W. Shillinglaw, D. Arnot, and K. Uyeda. 2001. A glucose-responsive transcription factor that regulates carbohydrate metabolism in the liver. Proc. Natl. Acad. Sci. U. S. A. 98:9116-9121.

Zhang, Y. Y., R. Proenca, M. Maffei, M. Barone, L. Leopold, and J. M. Friedman. 1994. Positional Cloning of the Mouse Obese Gene and Its Human Homolog. Nature. 372:425-432.

Zuany-Amorim, C., J. Hastewell, and C. Walker. 2002. Toll-like receptors as potential therapeutic targets for multiple diseases. Nat. Rev. Drug Discov. 1:797-807.

TABLES AND FIGURES

Table 3.1. Ingredients and nutrient composition of diets (% of DM)

	Diet	
Ingredent	**OVE**	**CON**
Alfalfa silage	17.9	10.0
Alfalfa hay	6.0	3.5
Corn silage	50.0	28.0
Wheat straw	0.0	40.5
Ground shelled corn	13.8	3.5
Whole cottonseed	5.0	--
Soybean meal	4.3	11.5
Minerals and Vitamins	3.0	3.0
Nutrient composition		
DM, %	50.0	52.0
NE_L, Mcal/kg	1.62	1.35
CP, %	15.0	12.0
NDF, %	36.7	54.8
Forage NDF, %	33.0	50.1
ADF, %	25.8	36.6
NFC, %	38.7	26.2
Fat, %	3.7	2.2

NFC, non-fiber carbohydrate = 100 – (%CP + %NDF + %Fat + %ash).

Table 3.2. Gene symbol, name and percentage of mRNA abundance among all genes investigated in each adipose tissue site

Gene Symbol	Gene Name in NCBI	% mRNA in MAT	% mRNA in OAT	% mRNA in SAT
	Fatty acid and triglyceride metabolism			
ACACA	acetyl-Coenzyme A carboxylase alpha	0.41	0.58	0.77
ACLY	ATP citrate lyase	0.10	0.09	0.07
ACSL1	acyl-CoA synthetase long-chain	0.94	0.41	0.41
ADFP (PLIN2)	adipose differentiation-related protein	2.15	2.37	2.44
CD36	thrombospondin receptor	8.54	5.89	6.97
ELOVL6	elongation of long chain fatty acids	0.51	0.58	0.59
FABP4	adipocyte fatty acid binding protein 4	33.44	22.84	18.90
FASN	fatty acid synthase	2.73	4.29	4.25
GPAM	glycerol-3-phosphate acyltransferase	0.52	0.41	0.28
LIPE	hormone-sensitive lipase	4.37	2.91	3.27
LPIN1	lipin 1	0.89	0.44	0.22
LPL	lipoprotein lipase	13.38	10.95	7.15
SCD	stearoyl-CoA desaturase	16.36	36.11	45.37
	Transcriptional regulation of lipogenesis			
MLXIPL	MLX interacting protein-like	0.03	0.02	0.02
PPARG	peroxisome proliferator-activated receptor gamma	1.50	1.10	0.93
SREBF1	sterol regulatory element binding transcription factor 1	0.56	0.35	0.41
THRSP	thyroid hormone responsive SPOT 14	5.79	5.50	4.26

Table 3.2. (cont.)

Gene Symbol	Gene Name in NCBI	% mRNA in MAT	% mRNA in OAT	% mRNA in SAT
	Adipokine and proinflammatory cytokines			
ADIPOQ	adiponectin	6.04	3.85	2.67
CCL2	chemokine (C-C motif) ligand 2	0.07	0.03	0.04
CCL5	chemokine (C-C motif) ligand 5	0.04	0.03	0.02
IL1B	interleukin-1 beta	0.01	< 0.01	< 0.01
IL6	interleukin-6	0.02	0.02	0.02
IL6R	Interleukin-6 receptor	1.11	0.64	0.66
LEP	leptin	0.38	0.50	0.26
SAA3	acute-phase serum amyloid A3	0.03	0.03	< 0.01
TLR4	toll-like receptor 4	0.06	0.04	0.03
TNF	tumor necrosis factor alpha	0.01	0.01	0.01

Table 3.3. Correlation analysis of SCD and LEP mRNA level with BCS and tissue weight.

Y-variable	X-variable	Correlation coefficient	*P*-value
Ave. pre-harvest BCS	SCD mRNA in SAT	0.571	0.021
	LEP mRNA in SAT	0.57	0.022
MAT weight	SCD mRNA in MAT	0.503	0.047
	LEP mRNA in MAT	0.52	0.038
OAT weight	SCD mRNA in OAT	0.607	0.013
	LEP mRNA in OAT	0.44	0.085

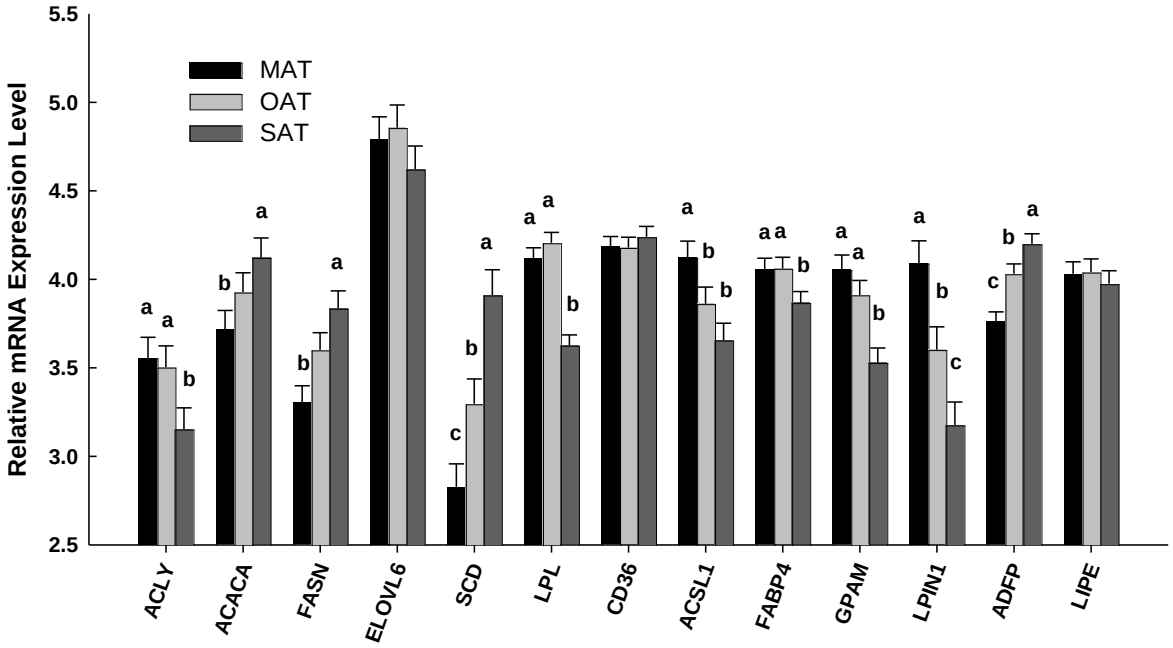

Figure 3.1. Main effect of adipose site on mRNA expression of genes involved in lipid metabolism. Genes marked with different letter means significant differences in expression among adipose sites ($P < 0.05$). X-axis: official gene symbol from NCBI website. Y-axis: relative mRNA expression value from natural logarithmic transformed data. Black column stands for MAT; dark grey column stands for OAT; light grey column stands for SAT.

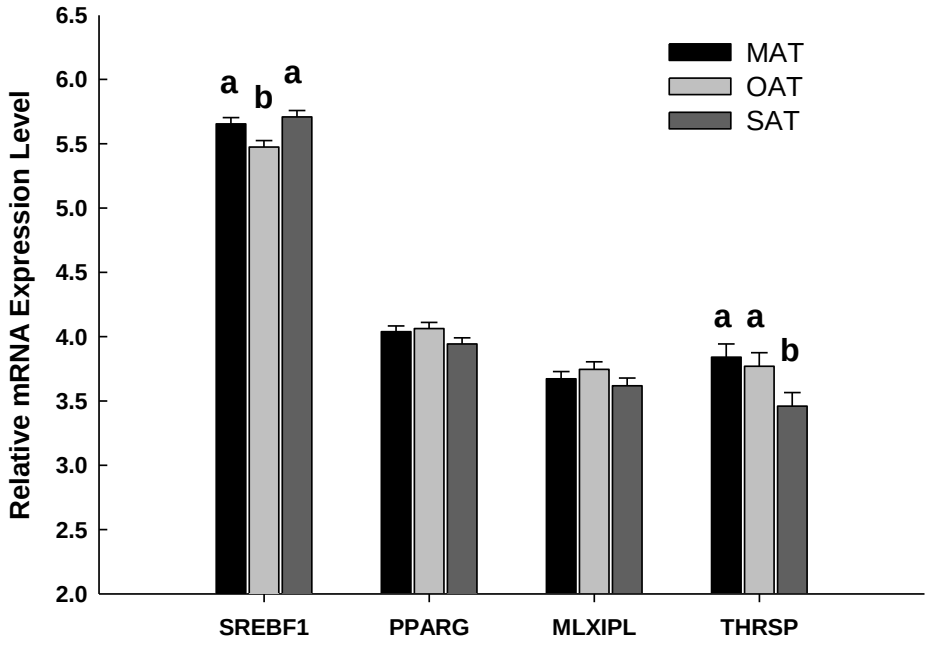

Figure 3.2. Main effect of adipose site on mRNA expression of transcriptional regulator genes. Genes marked with asterisk means significant differences in expression among adipose sites ($P < 0.05$). X-axis: official gene symbol from NCBI website. Y-axis: relative mRNA expression value from natural logarithmic transformed data. Black column stands for MAT; dark grey column stands for OAT; light grey column stands for SAT.

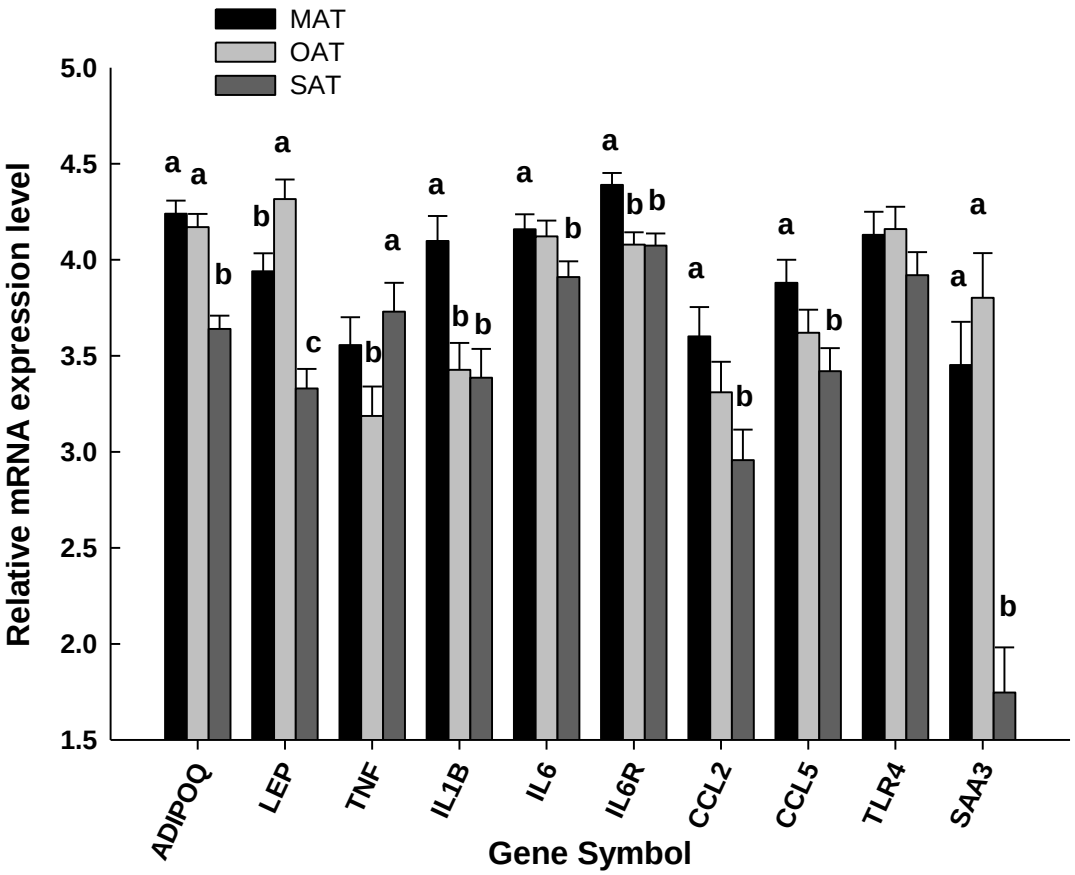

Figure 3.3. Main effect of adipose site on mRNA expression of cytokines. Genes marked with different letter means significant difference in expression among adipose sites ($P < 0.05$). X-axis: official gene symbol from NCBI website. Y-axis: relative mRNA expression value from natural logarithmic transformed data. Black column stands for MAT; dark grey column stands for OAT; light grey column stands for SAT.

CHAPTER 4

TRANSCRIPTIONAL CHANGES IN MESENTERIC AND SUBCUTANEOUS ADIPOSE TISSUE FROM HOLSTEIN COWS IN RESPONSE TO PLANE OF DIETARY ENERGY

ABSTRACT

The transcriptional machinery of cow adipose tissue depots and the role of dietary energy on gene networks remain poorly characterized. Effects of overfeeding (OVE) or controlled (CON) dietary energy on mesenteric (MAT) and subcutaneous (SAT) adipose tissue transcript profiles were assessed in 10 non-pregnant non-lactating cows The RNA from SAT and MES were used for microarray analysis with a 13,000-sequence annotated bovine oligonucleotide microarray. Statistical analysis revealed 409 and 310 differentially expressed genes (DEG) due to tissue sites and diets. Data mining was conducted with GeneSpring GX7 and DAVID Bioinformatics Resources 6.7 for functional analysis (categorized based on Gene Ontology [GO] as biological process [Bp], cellular component [Cc], or molecular function [Mf]) and Dynamic Impact Approach (DIA) for pathway analysis based on KEGG PATHWAY Database. The most enriched functions and pathways were screened based on the DEG and secondary criteria of each analysis. FLUX and IMPACT indices were calculated in DIA analysis with balanced consideration of fold-change, *P*-value and number of DEG participating in the function and pathway. Visual-friendly chart-tables were composed to summarize the most-enriched functions and pathways. Functional analysis from both GeneSpring and DIA analysis revealed that the extracellular region (primarily relating to type I collagen) and cytoskeleton structure (relating to actin filaments) were overrepresented as the signature difference in Cc between SAT and MES depots. Vasculature development, regulation of protein metabolism, and carboxylic acid

metabolism were the most-enriched Bp in the comparison between fat depots, whereas overfeeding energy significantly upregulated the gene sets associated with Bp of cell-substrate and cell-matrix adhesion, response to extracellular stimuli, and Mitogen-activated protein kinase (MAPK) signaling. The most overrepresented and biologically relevant pathways in comparison of adipose sites were extracellular matrix (ECM)-receptor interaction, focal adhesion, adipocytokine signaling, butyrate metabolism, glycolysis/gluconeogenesis, sphingolipid metabolism, and amino acid metabolism. Excess energy consumption significantly impacted the following pathways in AT: immune cell trafficking and signaling, metabolism of xenobiotics by cytochrome P450, and MAPK signaling pathway (not in the list of "top IMPACT", but biologically relevant). Our bioinformatics results unveiled the distinct DEG between subcutaneous and visceral AT, which from a transcriptional perspective may implicate different ECM and cytoskeleton structure, angiogenesis activity, and LCFA metabolism in MES vs. SAT. In addition to potentially increased lipogenesis activity, another prominent consequence in AT induced by long-term energy overfeeding is cell apoptosis, immune cell recruitment, and stimulation of local inflammation. Therefore, we conclude that adipocytes from SAT may respond to external stimuli differently than those from MES due to the distinct ECM and cell skeleton structure, and overfeeding energy may compromise animal health by stimulating local inflammation in AT and secondary systemic inflammation.

INTRODUCTION

Dairy cows can readily overconsume dietary energy during most of the dry period. Studies conducted by different research groups found, in comparison with controlled or restricted energy feeding, excess prepartal energy intake (particularly from high NFC diet) induced higher

prepartal concentrations of insulin and glucose and was associated with greater peripartal lipolysis, which subsequently resulted in greater hepatic lipid accumulation at the onset of lactation and compromised animal health (Holtenius et al., 2003; Dann et al., 2006; Janovick et al., 2011). Obviously, adipose tissue metabolism was differentially regulated in overfed dairy cows in those studies. Furthermore, decreased AT responsiveness to insulin was proposed as the reason for negative effects on animal performance, which is analogous to obesity-induced Type II diabetes in humans and rodent models.

Adipose tissue is not simply a metabolic tissue active in regulating whole body energy homeostasis, but also plays an important endocrine function by secretion of a number of proteins with signaling properties that are involved in regulation of metabolism (e.g., adiponectin, leptin), feed intake (leptin), and immune function and inflammation (TNF-α, IL-1 et al.) (Rosen and MacDougald, 2006). A growing body of literature based on rodents or humans has demonstrated a causal connection between overnutrition-induced obesity (mainly excess energy consumption) and chronic low-grade inflammation, which triggers a variety of metabolic disorders, such as non-alcoholic fatty liver and Type II diabetes (Tilg and Moschen, 2008).

Despite the dominance of mature adipocytes, AT is also composed of immune cells (e.g., macrophages) and stromal-vascular cell fractions containing preadipocytes, endothelial cells, and mesenchymal stem cells, which may vary in their response to external stimuli (such as nutrient supply) and immune activation. Differences between VAT and SAT in proportion of cell types, capillary network, lipid storage capacity, endocrine activity, and responsiveness to lipolytic stimuli have been documented in humans and rodents (Ibrahim, 2010). Excessive visceral obesity was reported to be more detrimental to liver health due to the direct portal drainage of

metabolites and cytokines from VAT (Tiniakos et al., 2010). However, less information is available regarding AT depot-specific metabolism and endocrine traits in dairy cows.

Microarray techniques enable detection of changes in thousands of genes simultaneously, which enables a more holistic picture of tissue metabolic changes from a transcriptional perspective. More than that, the combined utilization of bioinformatics analysis (software and methodology) helps identify the most enriched biological functions, pathways, and physiological changes under certain metabolic states. As case in point, Weisberg et al. (2003) utilized microarray analysis to profile gene expression in perigonadal adipose from mice in which adiposity varied due to sex, diet, and obesity-related mutations. They identified 1304 transcripts that were significantly correlated with body mass. Among the top 100 correlated genes, 30% encode proteins of macrophages.

In the current study, we utilized GeneSpring, DAVID, and KEGG bioinformatics software and the dynamic impact approach (DIA) analysis developed by our group to identify the most enriched GO functions and pathways in MES and SAT of multiparous dairy cows in response to 8 wk of energy overfeeding.

MATERIALS AND METHODS

Animals and Tissue Sample Collection

The study used a subset of 10 cows from a larger study (Nikkhah et al., 2008) consisting of 18 non-pregnant and non-lactating Holstein cows (BW = 656 ± 29; BCS = 3.04 ± 0.25) from the University of Illinois Dairy Research Unit. Cows were fed diets containing either 1.35 Mcal/kg NE_L (DM basis) as a low energy group (CON) or 1.62 Mcal/kg NE_L as a moderate energy group (OVE) for 8 wk before slaughter and tissue collection. Subsamples of subcutaneous and mesenteric adipose were harvested immediately post-slaughter and snap-

frozen in liquid-N until the RNA extraction. All live-animal experimental procedures were approved by the Institutional Animal Care and Use Committee at the University of Illinois.

RNA Extraction

Subsequently, tissue slices (~2 g) were transferred to a tube containing ice-cold Trizol (Invitrogen Corp., San Diego, CA) reagent and immediately subjected to RNA extraction as previously described in chapter 2 and using the method published by Loor et al.(2005). Genomic DNA was removed from RNA with DNase (Qiagen, Valencia, CA) using RNeasy Mini Kit columns (Qiagen). Integrity of RNA (RIN) was assessed by electrophoretic analysis of 28S and 18S rRNA subunits. The RNA concentration was measured using a NanoDrop ND-1000 spectrophotometer (www.nanodrop.com). The purity of RNA (A_{260}/A_{280}) was above 1.9.

Microarray Protocol

We used a 13,257 annotated bovine oligonucleotide microarray containing >10,000 unique elements, which is publicly accessible in the National Center for Biotechnology Information (NCBI) Gene Expression Omnibus (GEO) database (GSE16426) (Loor et al., 2007). Hybridizations were performed in a dye-swap reference design. The reference sample was made by pooling RNA from several bovine adipose tissues (SAT, OAT, and MAT). The cDNA were obtained by reverse transcriptase in a 30 µL reaction containing 8 µg RNA, 2 µL of random hexamer primers (3 µg/µL; Invitrogen Corp., CA), 1 µg oligo dT18 (Operon Biotechnologies, Huntsville, AL), and DNase-RNase-free water to a volume of 17.78 µL. The mixture was incubated at 65°C for 5 min and kept on ice for 3 min. To the mixture were added 12.2 µL solution composed of 6 µL 5X First-Strand Buffer, 3 µL 0.1 M DTT, 0.6 µL 100 mM dNTP mix (Invitrogen Corp.), 0.12 µL of 50 mM 5-(3-aminoallyl)-dUTP (Ambion, CA), 2 µL (100 U) of SuperScriptTM III RT (Invitrogen Corp.), and 0.5 µL of RNase Inhibitor (Promega, Agora, WI).

The reaction was performed at 23 °C for 1 min and 46 °C for 9 h. The cDNA obtained was then treated with 10 µL 1 *M* NaOH and incubated for 15 min at 65 °C to remove residual RNA. The solution was neutralized by adding 10 µL of 1 *M* HCl. The unincorporated 5-(3-aminoallyl)-dUTP and free amines were removed using a Qiagen PCR Purification Kit (Qiagen). Clean cDNA was dried and resuspended in 4.5 µL of 0.1 *M* Na_2CO_3 buffer (pH 9.0) and 4.5 µL of Amersham CyDye™ fluorescent dyes diluted in 60 µL of DMSO (Cy3 or Cy5; GE Healthcare, Waukesha, WI, USA). Binding of Cy dyes with 5-(3-aminoallyl)-dUTP incorporated into cDNA was obtained by incubation at room temperature for 1 h. The unbound dyes were removed using a Qiagen PCR Purification Kit (Qiagen) and clean labelled cDNA was measured by means of a NanoDrop ND-1000 spectrophotometer. Sample and reference were then vacuum-dried in the dark.

Microarray Hybridization and Image Acquisition

Prior to hybridization, slides were re-hydrated, placed in an UV cross-linker, washed with 0.2% SDS solution, thoroughly rinsed with purified water to remove un-bound oligonucleotide, and pre-hybridized using a solution containing 1% albumin, 5 × SCC, and 0.1% SDS at 42 °C for ≥45 min with the aim of decreasing background. After pre-hybridization, slides were rinsed with abundant purified water, immersed in isopropanol for ~10 s, and spin-dried. Dried slides were immediately hybridized in a dye-swap-reference design (i.e., each sample was labeled twice with each of the two dyes and hybridized in each slide with the reference labeled with the opposite dye). Labeled cDNA of the sample was re-hydrated with 80 µL of hybridization buffer #1 (Ambion, Austin, TX) and mixed thoroughly. This solution was used to re-suspend the reference sample labeled with the opposite dye and mixed thoroughly in order to obtain a homogenous solution of the two labeled cDNA. Before hybridization, the labeled cDNA

resuspension of the sample + reference was incubated at 90-95 °C for ca. 3 min to allow for cDNA denaturation to increase the efficiency of binding of oligos to the slide.

Hybridizations were carried out using humidified slide chambers (Corning, Lowell, MA) with cover slips (LifterSlip; Thermo Scientific, Billerica, MA) at 42 °C for ca. 40 hours in the dark. After hybridization, slides were removed from the chamber and washed for 5 min by agitation 3 times with wash buffers in the following order: 1 × SSC and 0.2% SDS solution preheated at 42 °C, 0.1 × SSC and 0.2% SDS solution, and 0.1 × SSC solution. Lastly, slides were inserted into a 50-mL tube, spin-dried and gassed with Argon to preserve dye from bleaching. Arrays were scanned with a ScanArray 4000 (GSI-Lumonics, Billerica, MA) dual-laser confocal scanner and images were processed and edited using GenePix 6.0 (Axon Instruments). Array quality was assessed using an in-house parser written in Perl language as previously described (Loor et al., 2007). Spots that received a -100 flag by GenePix 6.0 were removed from further analysis and background intensity was subtracted from the foreground intensity. Spots on the slide were considered "good" if the median intensity was ≥ 3 × standard deviations above median background for each channel (i.e., dye). Spots were flagged "present" when both dyes passed the criteria, "marginal" if only one dye passed the criteria, or "absent" when both dyes failed to pass the criteria. Statistical analysis was conducted on oligos that were flagged as "present" and "marginal".

Quantitative PCR for Microarray Verification

The protocols for cDNA synthesis, real time RT-PCR, primer design, and testing have been previously described in detail (Bionaz and Loor, 2008; see chapter 4). The relative expression levels of 29 genes whose protein products associate with lipid metabolism, inflammation, and insulin signaling were determined through qPCR. Initial PCR data was

normalized with the geometric mean of 3 pre-determined internal control genes, namely *TRIM41*, *KEAP1,* and *MRP63*. Finally, the LSmean of relative gene expression levels of mesenteric adipose and samples from OVE were transformed to fold-difference relative to subcutaneous adipose and sample from CON group, respectively. Table 4.3 shows the fold change of 29 genes analyzed by qPCR and microarray.

Statistical Analysis

Data from a total of 20 microarrays were normalized for dye and array effects (i.e., Lowess normalization and array centering and scaling) and used for statistical analysis. A mixed effects model was then fitted to the adjusted ratios (adipose/reference) of each oligonucleotide using Proc MIXED (SAS Inst., Cary, NC). The model consisted of the classification factors tissue (SAT, MES), diet (CON, OVE), and dye (Cy3, Cy5) as fixed effects, and cow as a random variable. The overall effect of diet and tissue was computed. The mean of the two spots for each oligonucleotide within each array and between dye-swap arrays was not averaged prior to statistical analysis. Benjamini and Hochberg's false discovery rate (FDR) was used to adjust for the number of comparisons, and significance was declared at FDR ≤ 0.2 (adjusted P-value). For qPCR verification, a 2×2 factorial arrangement in GLM model was used with tissue and diet as the two factors. The significance due to main effects was declared at $P \leq 0.10$.

Data Mining

***Functional Analysis (Gene Ontology (GO)) via GeneSpring GX7*:**

The initial functional analysis was performed by means of GeneSpring GX7 with the annotation updated on March 3, 2009 by the automatic annotation feature in GeneSpring GX7 using GeneBank accession numbers. Out of 13,257 total oligos, the updated GO had 7,710 annotated oligos with a category of Biological process (Bp), 7,765 with a Cellular component

(Cc), and 8,327 with a Molecular function (Mf). The identification of significantly ($P < 0.05$) enriched GO categories was obtained by the calculation of a hypergeometric *P*-value without multiple testing correction, which is a measure of the statistical significance of the overlap between the number of genes in the selected list and all the genes on the array platform assigned to that category (i.e., the likelihood that it is a coincidence that genes in the list were in both the gene list and the category). The statistical results of the microarray data were uploaded into the software and an FDR ≤ 0.2 was set as the criterion to identify the DEG. The following were used to uncover enriched Bp, Cc, and Mf among the DEG: main effect of diet (DEG = 310) and main effect of tissue (DEG = 409); up-regulated DEG in OVE (201) vs. CON (109); and up-regulated DEG in MAT (242) vs. SAT (167).

Criteria Used to Interpret the GO Categories and Build GO Figures:

The GO analysis in GeneSpring GX7 provided a *P*-value and the number of genes in each sub-category to highlight the Bp, Mf, or Cc that were significantly enriched by the genes in the list. A criterion of FDR ≤ 0.2 from the original SAS output was used to declare genes as being significant (DEG). Subsequently, a total of 6 gene lists were uploaded into GeneSpring GX7: the overall DEG in diet and tissue comparison; the up-regulated DEG due to either OVE or CON; and the up-regulated DEG in either MAT or SAT. The most representative list was the overall DEG, which included both up- and downregulated DEG in the comparison, and the final interpretation of the data was based on this. The list of GO categories with associated *P*-values allowed the evaluation of the enrichment of GO categories but did not facilitate the understanding of which tissue or diet contributes more to a biological response. The separate analysis of DEG in each diet and tissue overcame that limitation.

Using the Pivot Table function in Microsoft Excel software we clustered all the GO categories in the overall list and the upregulated DEG lists in separate tissues and diet simultaneously that were significantly enriched (P-value ≤ 0.05) and had more than one DEG. For example, we can conclude that the change in a Bp within the overall tissue effect was primarily due to MES if more DEG that participated in the biological process appeared in MES rather than SAT. We also used different colors to denote different degrees of significance.

***Functional Analysis via DIA Analysis Based on DAVID Bioinformatics Resources 6.7*:**

See Supplemental materials and methods.

Pathway Analysis via Dynamic Impact Approach (DIA) Using KEGG Database:

Preparation of reference KEGG pathway dataset was according to the following steps:

1. The KEGG pathway database for each Entrez gene ID of Bos taurus was downloaded from the KEGG website: http://www.genome.jp/kegg/download/.

2. The total number of molecules present in each pathway and represented in the array platform was calculated. An input file that can work in keggarray.exe was prepared which has the entire list of genes present in the array.

3. The main categories and sub-categories were downloaded from the KEGG website: http://www.genome.jp/kegg/pathway.htmland were Copied and pasted in a new Excel sheet. There were a total of 6 main categories, namely Metabolism, Genetic information processing, Environmental information processing, Cellular processes, Organismal systems, and Human diseases.

DIA analysis of array data was according to the following steps:

1. The original data were copied in separate columns for oligo ID, Entrez gene ID, fold change (FC), FDR, and P-value of each comparison into a new Excel file. FC was expressed in

the form of a ratio, which means all upregulated genes have FC >1 and all downregulated genes have FC < 1. We determined the DEG with FDR cut-off value of 0.2, so all the genes with FDR > 0.2 were removed from dataset.

2. The DEG were matched with KEGG path ID, so that each path ID had a fold change and *P*-value for all DEGs with respect to each of the comparisons (fat depot or dietary energy) in the experiment.

3. The FC and P-value were Log transformed. In order to prevent a bias from the original values while calculating FLUX and IMPACT, FC was subjected to transformation by $\log_2$(FC) and P-value was transformed via –ln(P-value), which will be used in the subsequent calculations.

4. the percentage of number of molecules in each pathway, average FC of DEG in each pathway, and average *P*-value of DEGs in each pathway were calculated.

5. The FLUX and IMPACT were calculated only for the pathways that were represented by at least 30% in our array platform. FLUX: refers to the overall direction in which a term/pathway is impacted after treatment or in the tissue comparison. IMPACT: refers to the absolute perturbation in a biological process or pathway. It gives the magnitude of changes that occur within a term/pathway in either direction weighted by the percentage of DEG that hit the term or pathway.

6. The FLUX and IMPACT were graphed to easily visualize the direction and magnitude. FLUX was depicted with a gradient color change, of which green, yellow, and red were used to denote negative FLUX, 0, and positive FLUX, respectively. The color gradation changed based on the actual calculated value. The IMPACT was expressed with a data bar, of which the length of the bar indicates the magnitude of the perturbation.

$$\text{IMPACT} = \left\{\frac{\text{No. of up regulated DEGs in a specific term/pathway}}{\text{Total no. genes in the term/pathway present in our array}} \text{X100}\right\} \left\{\text{Average } \log_2(\text{Fold change}) \text{ of up regulated gene members in a term/pathway}\right\} \text{X} \left\{\text{Average } -\log_{10}(\text{P-value}) \text{ of up regulated gene members in a term/ pathway}\right\}$$

$$(+)$$

$$\left\{\frac{\text{No. of down regulated DEGs in a specific term/pathway}}{\text{Total no. genes in the term/pathway present in our array}} \text{X100}\right\} \left\{\text{Average } \log_2(\text{Fold change}) \text{ of down regulated gene members in a term/pathway}\right\} \text{X} \left\{\text{Average } -\log_{10}(\text{P-value}) \text{ of down regulated gene members in a term/ pathway)}\right\}$$

$$\text{FLUX} = \left\{\frac{\text{No. of up regulated DEGs in a specific term/pathway}}{\text{Total no. genes in the term/pathway present in our array}} \text{X100}\right\} \left\{\text{Average } \log_2(\text{Fold change}) \text{ of up regulated gene members in a term/pathway}\right\} \text{X} \left\{\text{Average } -\log_{10}(\text{P-value}) \text{ of up regulated gene members in a term/ pathway}\right\}$$

$$(-)$$

$$\left\{\frac{\text{No. of down regulated DEGs in a specific term/pathway}}{\text{Total no. genes in the term/pathway present in our array}} \text{X100}\right\} \left\{\text{Average } \log_2(\text{Fold change}) \text{ of down regulated gene members in a term/pathway}\right\} \text{X} \left\{\text{Average } -\log_{10}(\text{P-value}) \text{ of down regulated gene members in a term/ pathway)}\right\}$$

Pathway analysis via Ingenuity Pathway Analysis (IPA): See Supplemental materials and methods.

Approach for Interpretation and Discussion Among the Significantly Represented Results

Due to the ubiquitous expression of many DEG in various tissues or organs, it is inevitable that the analysis conducted with different software gives obviously irrelevant results for the adipose tissues, such as the significantly impacted biological process of "urinary bladder development" in the DIA analysis of tissue comparisons (MAT vs SAT) and "positive regulation of insulin secretion" in the DIA analysis of diet comparison (OVE vs CON). Thus, only the most biologically relevant results will be interpreted and discussed.

RESULTS

Differentially Expressed Gene (DEG) Induced by Main Effect of Diet and Fat Depot

With the cut-off FDR value of 0.2, results revealed 310 DEGs (257 annotated with Entrez gene ID) affected by the main effect of treatment (OVE vs. CON), among which 201 (164 annotated with Entrez gene ID) and 109 (94 annotated with Entrez gene ID) were up- and down-regulated by overfeeding energy. Regarding tissue site, 409 genes (341 annotated) were differentially expressed between fat depots (MAT vs. SAT), of which 242 (208 annotated) and 167 (133 annotated) were up- and down-regulated in MES vs. SAT. Fifteen DEGs in the comparison between OVE and CON and 45 DEGs in the comparison between MAT and SAT changed by more than 2 fold (as shown in Table 4.1 and 4.2).

Functional Analysis via GeneSpring GX7 Reveals the Most Representative GO Term of Cc, Mf, and Bp

***Most Representative Cc*:** (Shown in Figure 4.1) The most relevant depot specific signature within Cc lies in the extracellular region (GO:5576 extracellular region, $P < 0.05$; GO:31012 extracellular matrix, $P < 0.05$) and the composition of collagen (GO:5583 fibrillar collagen, $P < 0.001$; GO:5584 collagen type I, $P < 0.05$), which were primarily due to the higher expression of relevant genes in SAT than MAT. However, compared with SAT, MAT was characterized by having greater expression of genes associated with actin filaments ($P < 0.05$) and cytoskeleton formation ($P < 0.05$). Despite the high degree of significance within the overall tissue effect for immunological synapse ($P < 0.05$) and MHC class II protein complex ($P < 0.05$), no significant depot difference was uncovered. Within the overall diet effect we found that the cc ribosome ($P < 0.05$), ribosomal subunits ($P < 0.05$), and protein complex of 43S ($P < 0.05$) and 48S ($P < 0.01$) were significantly impacted, which resulted from the greater expression of corresponding genes in CON vs. OVE. In addition, overfeeding energy negatively affected the

immunological synapse and MHC class I protein complex ($P < 0.05$), which was displayed as increased expression of the related genes within the CON treatment.

***Most Representative Mf*:** (Shown in Figure 4.2) A number of Mf were more highly represented in MAT than in SAT, such as cytoskeletal protein binding, magnesium and iron ion binding, signaling kinase activity, and phosphoric ester hydrolase activity. However, SAT had greater expression of genes related with extracellular matrix constituent and transcriptional activator activity. Overfeeding energy potentially enhanced the Mf of transcription coactivator activity, magnesium ion binding, nutrient transporter activity (amino acid and organic acid), and MAPKK kinase activity.

***Most Representative Bp*:** (Shown in Figure 4.3) Compared with SAT, visceral fat exhibited greater expression of genes involved in vasculature development, fatty acid β-oxidation, post-translational modification of protein amino acid residues, and carboxylic acid metabolism. Overconsumption of energy enhanced adipocyte response to external stimulus, nutrient transport (carboxylic acid, amine, and amino acid), and intracellular signaling transduction, such as MAPKKK cascade and protein kinase activity.

KEGG Pathway Analysis via DIA Uncovered the Most Impacted Pathways Either Induced by Different Plane of Dietary Energy or due to the Uniqueness of Fat Depots

***DIA Analysis on Main Category and Sub-Category Regarding Adipose Depot Characteristics*:** (Shown in Figure 4.4) As described in the materials and methods section, only those pathways represented by more than 30% of the genes in our array over the whole genome were eligible for use in calculations of FLUX and IMPACT. The FLUX and IMPACT for each sub-category is the calculated mean FLUX and IMPACT for all the pathways that belong to the same sub-category, based on which the FLUX and IMPACT of each category was calculated.

The most highlighted categories in the comparison between adipose sites were metabolism and organismal systems followed by environmental information processing. In comparison with SAT, the most differentially represented sub-categories within the main category of metabolism in MAT were greater FLUX of carbohydrate, lipid and terpenoids, and polyketides metabolism and lower FLUX of amino acid metabolism and glycan biosynthesis and metabolism.

Xenobiotics biodegradation and metabolism was moderately impacted due to fat depot with greater FLUX in MAT vs. SAT. Regarding the impacted sub-category of organism system we were mainly interested in immune and endocrine system due to the endocrine function of adipocytes and the influence of adipocytokines on function of immune cells. The endocrine function of visceral fat appeared to differ markedly from SAT as indicated by a large IMPACT value, with moderate greater FLUX in MAT. The immune system exhibited the same FLUX pattern in MAT vs. SAT, but in a marginal manner. The most impacted sub-categories within environmental information processing due to tissue source were signaling molecules and interaction and membrane transport, with lower FLUX value in MAT compared with SAT. In addition, the sub-categories of transcription and cell communication were influenced between fat depots with marginally greater FLUX in MAT. Visceral fat is probably more associated with metabolic disease due to the positive value of FLUX compared with SAT.

***DIA Analysis on Main Category and Sub-Category Induced by Dietary Energy Level*:** (Shown in Figure 4.4) Greater plane of dietary energy drastically perturbed and increased FLUX of the main category of metabolism in KEGG. Genetic information processing, organismal system, and human diseases were moderately affected by dietary energy level. Among the most impacted sub-categories, overfeeding energy markedly increased FLUX of metabolism of cofactors and vitamins and xenobiotics biodegradation and metabolism, and moderately

increased FLUX of carbohydrate and lipid metabolism and transcription. Among the moderately impacted sub-categories, adipose from overfed cows exhibited lower FLUX in translation and immune system disease, and greater FLUX in amino acid metabolism and excretory system.

***DIA Analysis of the Most Over-represented Pathways Regarding the Fat Depot Characteristics*:** (Shown in Figure 4.5) There were141 out of the entire 210 KEGG pathways that were substantially represented (> 30%, as described before). However, only the pathways with a $\log_2$IMPACT value > [mean of ($\log_2$IMPACT value of all the pathways) + 1×SD of ($\log_2$IMPACT value of all the pathways)] were considered as "most impacted" and used to focus the discussion. Among all 24 most-impacted pathways in the comparison between fat depots, butanoate metabolism, pentose phosphate pathway, glycolysis/gluconeogenesis, fatty acid elongation in mitochondria, lysine degradation, and limonene and pinene degradation had greater FLUX in MAT vs. SAT. In addition, MAT exhibited higher FLUX in adipocytokine and PPAR signaling pathways and Type II diabetes mellitus compared with SAT. In contrast, greater FLUX was observed in SAT vs. MAT for a number of amino acids metabolism, sphingolipid and ether lipid metabolism, glycosaminoglycan degradation, and ECM-receptor interaction and focal adhesion. Despite a larger IMPACT value, several pathways were deemed biologically meaningless in regard to adipose tissue, including phototransduction and amoebiasis, and will not be discussed here.

***DIA Analysis of the Most Over-represented Pathways Induced by Dietary Treatments*:** (Shown in Figure 4.6) A total of 12 out of 103 substantially represented pathways induced by plane of dietary energy were deemed as the most impacted based on our criteria. Pathways associated with ubiquinone and other terpenoid-quinone biosynthesis, metabolism of xenobiotics by cytochrome P450, sphingolipid and ether lipid metabolism, basal transcription factors, and

type II diabetes were highly enriched in OVE vs. CON due to the positive FLUX value. However, a negative FLUX value was observed for a number of immune function related pathways, such as FC gamma receptor mediated phagocytosis in OVE compared with CON.

DISCUSSION

The Signature Characteristics of Adipose Depots

Physiological differences between visceral and subcutaneous fat depots have long attracted attention. Bioinformatic analysis of our transcriptomic data revealed distinct properties in cellular components, molecular functions, and biological processes between mesenteric and subcutaneous adipose of dairy cows. Such differences seem to underscore the different transcriptional control of genes involved in nutrient metabolism, response to external stimuli and intracellular signaling transduction, endocrine activity, and crosstalk with microenvironments. The SAT exhibited greater expression of genes involved in fibrillar collagen (type I and III) formation (*COL1A1*, *COL1A2* and *COL3A1*). Collagen type I and III are major structural components of extracellular matrix (ECM) in AT (Divoux and Clément, 2011), therefore, the differentially expressed collagen-related genes significantly impacted the ECM-receptor interaction pathway as detected in DIA analysis. In adipose tissue, the ECM does not simply provide architecture for cell anchorage and mitigation, but plays a crucial role in orchestrating adipogenesis and tissue remodeling. Evidence from cellular studies showed that the differentiation of preadipocytes paralleled the increase in type I-VI collagens (Nakajima et al., 2002). During differentiation, the ECM surrounding adipocytes was characterized by a process of degradation of old spiny fibrils and synthesis of thicker new networks (Taleb et al., 2006). The degradation of ECM structural component is mainly executed by metalloproteinases (MMPs) (Christiaens and Lijnen, 2006). The MMP-initiated proteolysis increases the space for cells to

migrate, and MMP-2 was found to release TGF-β, which functions to regulate cell motility and induce ECM expression of collagens (Bouloumie et al., 2001; Yan et al., 2009;). In the current study, we observed greater expression of MMP-2 in SAT than MAT. Therefore, taken together with the greater expression of collagen genes, we speculate that SAT undergoes more active remodeling of ECM, which would preceed preadipocyte differentiation. Bovine adipocytes from SAT are bigger in size and had more differentiation potency than those from visceral depots (personal communication with Häussler S. from University of Bonn, Germany, in July, 2011).

Intriguingly, MAT was characterized by greater expression of gene sets involved in actin cytoskeleton formation (*FGF2, FGF7, ACTN3, MYLK, MYL9, CYFIP2*) (as shown in Figure 4.1. cellular component) and vasculature development and blood vessel morphogenesis (*VEGFA, FGF2*) (as shown in Figure 4.3. biological process). Besides the remodeling of ECM, the reorganization of cytoskeleton and integrin and the development of new capillary networks also are key events of adipocyte differentiation at least in non-ruminant species) (Hausman and Kauffman, 1986; Antras et al., 1989). FGF2 is reported to be a potent stimulator of adipocyte differentiation and proliferation of endothelial cells in mice (Kawaguchi et al., 1998). In the process of angiogenesis, FGF2 stimulates the synthesis of proteinases and integrins to form new capillary structures (Okamura et al., 1991). VEGFA is one of the major angiogenic factors produced and secreted by adipocytes, of which the expression level was believed to be positively correlated with the adipose tissue's angiogenic capacity (Zhang et al., 1997). It can stimulate the proliferation and migration of endothelial cells by binding to its surface VEGF receptor 1 and 2 (VEGFR1 and VEGFR2) (Huusko et al., 2010). Furthermore, we also observed the greater mRNA expression of HIF-3α (*HIF3A*) in MAT vs. SAT. Hypoxia-inducible factor (HIF) is a transcription factor (TF) that plays a central role in oxygen homeostasis in mammalian cells by

stimulating expression of oxygen-regulated genes related to angiogenesis, glucose uptake, and glycolysis (Semenza, 1999). HIF-3α, one subunit of HIF, was demonstrated to be induced and highly-expressed during adipose differentiation and functions as a positive regulator of adipogenesis (Hatanaka et al., 2009).

In addition, MAT expressed higher levels of *CEBPB* and *CEBPD* than SAT, both of which encode the TF that are transiently expressed during early stages of preadipocyte differentiation to stimulate expression of CEBPα and PPARγ (Wu et al., 1995). Since adipose tissue rather than pure adipocytes were used in our study, which consists of mature adipocytes surrounded by a stromal-vascular cell fraction containing preadipocytes, endothelial cells, pericytes, fibroblasts, macrophages, and mesenchymal stem cells, our bioinformatic analysis sheds light on these signature genes and provides evidence that the differentiation process of adipocytes from different depots may follow distinct patterns. Taken together these results allow us to speculate that differentiation of SAT may involve more drastic reconstruction of the ECM structure (collagen); whereas, in MAT adipocyte hypertrophy may require greater expansion of the capillary network to take up more oxygen. Focal adhesion, i.e., cell-matrix adhesion, serves as the mechanical linkage of cells to ECM, which is a process essential for triggering intracellular responses to external stimulus and is mediated by integrins (Zamir and Geiger, 2001). Although the focal adhesion pathway was overrepresented due to a large IMPACT value (as shown in Figure 4.5) the FLUX value was around zero, which may be primarily due to the differentially regulated ECM signaling (higher collagen related gene expression in SAT, greater expression of genes associated with angiogenesis and actin formation in MAT).

The uniqueness of fat depots in terms of nutrient metabolism was also overrepresented in our DIA analysis of KEGG pathways (as shown in Figure 4.5). Sphingolipid metabolism was

one of the pathways altered between MAT and SAT, which was primarily due to differential expression of sphingosine phosphate lyase 1 (*SGPL1*, higher in MAT), sphingosine kinase (*SPHK2*, higher in MAT), sialidase 1 (*NEU1*, higher in SAT), and acid ceramidase 1 (*ASAH1*, higher in SAT). ASAH1 converts ceramides to sphingosine (SP), which is phosphorylated to sphingosine-1-phosphate (S1P) by SPHK2. SGPL1's cleavage of S1P leads to irreversible breakdown of the SP backbone (Spiegel and Milstien, 2003). Ceramides are composed of sphingosine and a fatty acid and serve as one of the major lipids in the lipid bilayer of cell membranes. However, accumulating evidence has demonstrated that ceramides and sphingosine act as important signaling molecules in the regulation of cell proliferation, differentiation, and apoptosis in many cell types (Hannun and Obeid, 2008). In our study, the higher expression of *ASAH1* indicates the potentially greater capacity to produce SP from ceramides. Previous research has demonstrated that SP is an active inducer of apoptosis in various cell types (Cuvillier et al., 2003; Lepine et al., 2004; Suzuki et al., 2004). Suzuki et al. (2004) found that deprivation of SP protects 3T3/A31 cells from apoptosis. Krown et al. (1996) observed that the addition of exogenous SP markedly increased apoptosis of rodent cardiomyocytes *in vitro*. Since SAT had higher expression of *ASAH1* but lower expression of genes associate with catabolism of SP, we speculate that adipocyte from SAT may have greater activity of cell apoptosis compared with that of MAT, which has recently been confirmed by a German research group. They found a higher cell apoptotic rate in SAT than in visceral AT (retroperitoneal fat) of dairy heifers (Häussler et al., 2011).

The DIA pathway analysis revealed greater FLUX of butyrate metabolism and fatty acid elongation in MITO in MAT vs. SAT, which were primarily attributed to the higher mRNA expression of *HADHA* and *ACSM1* in MAT. *HADHA* encodes the alpha subunit of long-chain 3-

hydroxyacyl-CoA dehydrogenase (LCHAD), a part of the mitochondria (MITO) trifunctional protein, which catalyzes the last 3 steps of β-oxidation of long-chain fatty acids (LCFA). The enzyme complex is required for breakdown of the LCFA in MITO. Mutations of *HADHA* in human cause the LCHAD deficiency and result in the dysfunction of MITO to metabolize LCFA (Rinaldo et al., 2002). As we discussed in chapter 3, the MAT had higher expression of *LPL* and *ACSL1* than SAT, together with greater *ACSM1* mRNA in MAT as uncovered in microarray analysis, which indicated a greater uptake and activation of LCFA and medium-chain FA (MCFA) in visceral adipocytes. Thus, the greater FLUX value of these two pathways as represented by higher mRNA level *HADHA* may underscore an adaptive mechanism in MAT to allow for greater influx of preformed LCFA and MCFA for oxidation.

Transcriptomic Modification in Adipose Induced by Energy Overfeeding

Functional analysis revealed that the gene sets associated with cell-substrate adhesion, cell-matrix adhesion, and response to (external) stimulus were the most highly enriched Bp in OVE vs. CON. Such results indicate that over-consumption of dietary energy increased substrate supply to adipose tissue and stimulated the communication between adipocytes and ECM. The altered external stimuli may cause the induction of intracellular signaling, which, as demonstrated in our functional analysis of Bp (shown in figure 4.3, GO analysis), resulted in the enrichment of (MAPK) signaling pathway. The MAPK activity is regulated through three-tiered protein kinase cascade consisted of MAPK, MAPK kinase (MAPKK or MAP2K) and MAPKK kinase (MAPKKK or MAP3K). MAP3K is the first being activated by extracellular stimuli and initiate intracellular signal transduction through phosphorylation of MAP2K (English et al., 1999).

The MAP2K signaling converge onto three subgroups of MAPK, p38, c-Jun N-terminal kinase (JNK), and Extracellular signal-Regulated Kinase (ERK) (Schaeffer and Weber, 1999; Chang and Karin, 2001). The ERK signaling pathways are activated by mitogenic stimuli, whereas JNK and p38 pathways are induced by anti-mitogenic stimuli or stress factors such as environmental or oxidative stress, TGF-β, and the inflammatory cytokines (e.g., IL-1, IL-6, TNF-α and TGF-β) (Ip and Davis, 1998) and free fatty acids (FFA) (Lee et al., 2003). The activation of JNK signaling, particularly in the absence of mitogenic stimuli, has been shown to induce cell apoptosis in many cell types (Chen et al., 1996; Tournier et al., 2001). In cultured adipocytes, the activation of JNK signaling induced by the addition of inflammatory cytokines, FFA or MITO oxidative stress resulted in reduced insulin-stimulated glucose uptake and impaired downstream insulin signaling pathways (Lee et al., 2003; Kim et al., 2009). Several studies demonstrated that the inhibitory effect of JNK on insulin signaling was caused by serine sites on IRS-1, which can blunt tyrosine phosphorylation of IRS-1 required for normal insulin signal transduction (Hirosumi et al., 2002; Sharfi and Eldar-Finkelman, 2008; Sabio et al., 2010).

In the current study, a set of genes involved in MAP3K signaling (*MAP3K4*, *MAP3K5*, *TAOK2*, and *GADD45B*) was overrepresented in OVE compared with CON. The growth arrest and DNA damage-inducible (*GADD*) 45 genes have been found to be induced under various stress conditions such as UV, osmotic and oxidative stress, and cytokines (IL-1, TNFα and TGF-β) (See review in Yang et al., 2009). Their activation may cause growth arrest (Vairapandi et al., 2002), DNA repair (Smith et al., 2000), cell survival or apoptosis (Sheikh et al., 1998), and modulation of the immune response (Lu et al., 2004). Myeloid leukemia cells were rescued from TGFβ-induced apoptosis by blocking the expression of *GADD45B* (Selvakumaran et al., 1994). The link between induced expression of GADD45 proteins by stress factors and stimulated cell

apoptosis was uncovered because all GADD45 proteins (GADD45-α, -β and -γ) activate MAP3K4, which functions exclusively to induce JNK and p38 pathways (Takekawa et al., 1997).

As shown by our results, the coordinated upregulation of *GADD45B* and *MAP3K4* in AT of energy-overfed animals probably indicated the greater induction of JNK signaling in response to energy overfeeding, which may contribute to increased cell apoptosis or growth arrest and insulin resistance in adipocytes. However, we did not observe any difference in expression of pro-inflammatory cytokines (*TNFA*, *IL1B*, and *IL6*) between the two treatment groups using either our array or qPCR, which seems contrary to the suggestion that inflammation induced overexpression of *GADD45B* in AT of OVE cows.

Another *in vitro* study with adipocytes revealed that *GADD45B* is preferentially expressed in differentiated adipocytes and is a target gene of CEBPα, which is one of the major adipogenic transcriptional factors expressed in post-mitotic, differentiated adipocytes (Constance et al., 1996). Temporal mis-expression of CEBPα in undifferentiated adipoblasts leads to mitotic growth arrest, which is mediated by the increased abundance of GADD45 proteins (Constance et al., 1996). Hence, it could be hypothesized that the hypertrophy of adipocytes may be an inducer besides other extracellular stress factors to stimulate the apoptotic pathway .

Despite a lack of difference in mRNA expression of *CEBPA* between the two groups in our array, it does not exclude a greater activity in transcriptional regulation in response to OVE vs. CON. Results from qPCR confirmed that *PPARG*, the master TF of adipogenesis (Rosen and MacDougald, 2006), was highly expressed in OVE vs. CON and in previous studies has been shown to be activated by CEBPα both of which are markers of of the differentiation process (Rosen and MacDougald, 2006). The total visceral AT weight (including mesenteric, omental, and perirenal fat) in OVE cows almost doubled the size of that in the CON group (59.5 vs. 35.5

kg), which partly supports the notion of enhanced adipocyte differentiation. Therefore, our bioinformatics analysis implicated a GADD45-mediated apoptotic pathway (JNK pathway) as being induced in hypertrophic adipocytes by chronic energy overfeeding.

Thousand and one amino acid kinase 2 (*TAOK2*), which had greater mRNA expression in OVE vs. CON, was identified as a key intermediate to activate p38 MAPK cascades in response to DNA damage induced by detrimental stimuli, such as oxidative stress and UV injury (Chen et al., 1999; Raman et al., 2007). As we discussed above, the activation p38 pathway is highly involved in cell apoptosis. Together with the highlighted apoptotic-related genes, in our DIA pathway analysis metabolism of xenobiotics by cytochrome P450 was overrepresented due to the higher expression of *CYP2S1* and *GSTM3* genes in OVE vs. CON. As is well known, the endoplasmic reticulum (ER) contains the majority of cytochrome P450 enzymes involved in xenobiotic metabolism, as well as a number of conjugating enzymes. In addition to its function in bioactivation and detoxification of these cytotoxic compounds, the ER is subject to the damage from reactive intermediates as well, which may lead to cell death (Cribb et al., 2005). Several studies have shown an involvement of the ER stress in the death of hypertrophic adipocytes, leading to adipose insulin resistance (Zinszner et al., 1998; Özcan et al., 2004; Nakatani et al., 2005; Gregor and Hotamisligil, 2007). *GSTM3* encodes a protein of the multigene family of the GST, which catalyzes the conjugation of glutathione with compounds containing an electrophilic center and functions as peroxidase and thiol transferase (Mannervik, 1985). GSTM3 is an antioxidant enzyme involved in the degradation of cytotoxic products in the cell, and the enzyme product of *CYP2S1* was reported to oxidize several carcinogens by using hydrogen peroxide, which is the major contributor to oxidative damage of cells (Bui et al., 2009).

The greater expression of these two genes indicated a greater detoxification activity, which may be a sign of higher risk of ER stress in adipocytes in response to long-term energy overfeeding.

It has been clearly demonstrated *in vitro* that hypertrophy per se promotes adipocyte death and macrophage recruitment and aggregation around individual adipocytes. Such increase in colonies of macrophages is primarily due to the chemoattractant property of adipokines (Cinti et al., 2005). As verified by qPCR, *CCL2* mRNA expression was greater in cows fed OVE vs. CON. Monocyte chemotactic protein-1 (MCP-1), the protein product of *CCL2*, is a chemokine and plays a role in recruitment of monocytes and T lymphocytes to sites of inflammation or to apoptotic cells (Baggiolini, 1998). It is expressed by a number of cell types including endothelial cells (Rollins, 1997) and adipocytes (Gerhardt et al., 2001). Increased expression of MCP-1 has been reported in different adipose depots (visceral, SAT and epicardial fat) in obese patients (Bruun et al., 2005; Yu et al., 2006) with higher expression in visceral than SAT, and closely associated with the enrichment of macrophages (Bruun et al., 2005).

Skurk et al. (2007) clearly illustrated that the secretion of MCP-1 and other adipocytokines (e.g. IL-6, TNF-α) was positively correlated with adipocyte size. *In vitro* addition of MCP-1 to differentiated adipocytes decreased insulin-stimulated glucose uptake, which suggested a causal relationship between MCP-1 and insulin resistance (Sartipy and Loskutoff, 2003). Parallel with greater *CCL2* expression, we found several significantly enriched pathways associated with immune response of monocytes and lymphocytes in response to OVE vs. CON, e.g., natural killer cell mediated cytotoxicity, Fc-gamma receptor-mediated phagocytosis, and T cell receptor signaling. All these enriched pathways underscored the importance of nuclear factor of activated T cells calcineurin-dependent 3 (*NFATC3*), which is a TF central to transactivate TNF expression upon B and T cell receptor engagement (Oh-hora and Rao, 2008). A

recent *in vitro* study showed that the nuclear localization of NFATC3 is also required for TLR-initiated innate immune responses in bone marrow-derived macrophages including TNF expression (Minematsu et al., 2011). The higher expression of *CCL2* and *NFATC3* in AT of cows fed OVE than CON indicated an increase in residency of immune cells in AT of OVE–fed animals, thus, increasing the likelihood of communication between immune cells and adipocytes to induce an immune response and produce the pro-inflammatory cytokines.

Adipocyte death was reported to be remarkably greater in obese mice $^{ob/ob}$ and human individuals (expressed as necrosis rather than apoptosis), and more than 90% of all macrophages (infiltrated and resident) in WAT of these obese subjects were localized to dead adipocytes (Cinti et al., 2005). In addition, accumulating evidence from studies of obese rodent models and humans has demonstrated that macrophages are the predominant source of proinflammatory cytokines (e.g., TNF-α and IL-6) (Weisberg et al., 2003; Fain et al., 2004). As a result, chronic low-grade inflammation has been closely related to subsequent development of insulin resistance in WAT (Xu et al., 2003; see review in Tilg and Moschen, 2008). In the current study, we observed an increase in insulin to glucose ratio, which may indicate lower efficiency of insulin-stimulated glucose uptake in peripheral tissues. Taken together, our results and the evidence from rodent and humans allow us to hypothesize that a series of events may be induced sequentially in response to energy overfeeding. Overfeeding energy increased adipocytes differentiation and apoptotic gene expression, which may result in ER-stress, adipocyte death, and subsequently increase the recruitment of immune cells. The increased infiltration of macrophages augments the production of proinflammatory cytokines, which may finally trigger the insulin resistance in WAT of overfed animals.

In conclusion, the transcriptomics results highlighted a depot-specific regulation of cytoskeleton formation, ECM structure, and blood vessel morphology, which potentially induces different responses to extracellular stimuli including substrate and oxygen supply in visceral vs. SAT adipocytes. Long-term overfeeding energy could stimulate adipocyte hypertrophy which may activate apoptosis through MAPK-JNK pathway and subsequently result in the recruitment of immune cells. The aggregation of immune cells on adipocytes may induce inflammation by promoting secretion of pro-inflammatory cytokines, and the drainage of cytokines either produced by adipocyte or immune cells via the circulation may cause inflammation of other organs such as the liver.

LITERATURE CITED

Antras, J, F. Hilliou, G. Redziniak, and J. Pairault. 1989. Decreased biosynthesis of actin and cellular fibronectin during adipose conversion of 3T3-F442A cells. Reorganization of the cytoarchitecture and extracellular matrix fibronectin. Biol. Cell. 66:247-254.

Baggiolini, M. 1998. Chemokines and leukocyte traffic. Nature 392:565-568.

Bouloumie, A., C. Sengenes, G. Portolan, J. Galitzky, and M. Lafontan. 2001. Adipocyte produces matrix metalloproteinases 2 and 9: involvement in adipose differentiation. Diabetes 50:2080-2086.

Bruun, J. M., A. S. Lihn, S. B. Pedersen, and B. Richelsen. 2005. Monocyte chemoattractant protein-1 release is higher in visceral than subcutaneous human adipose tissue (AT): implication of macrophages resident in the AT. J. Clin. Endocrinol. Metab. 90:2282-2289.

Bui, P. H., E. L. Hsu, and O. Hankinson. 2009. Fatty acid hydroperoxides support cytochrome P450 2S1-mediated bioactivation of benzo[a]pyrene-7,8-dihydrodiol. Mol. Pharmacol. 76:1044-1052.

Chang, L., and M. Karin. 2001. Mammalian MAP kinase signaling cascades. Nature 410:37-40.

Chen, Y. R., C. F. Meyer, and T. H. Tan. 1996. Persistent activation of c-Jun N-terminal kinase 1 (JNK1) in γ radiation-induced apoptosis. J. Biol. Chem. 271:631-634.

Chen, Z., M. Hutchison, and M. H. Cobb. 1999. Isolation of the protein kinase TAO2 and identification of its mitogen-activated protein kinase/extracellular signal-regulated kinase kinase binding domain. J. Biol. Chem. 274:28803-28807.

Christiaens, V., and H. R. Lijnen. 2006. Role of the fibrinolytic and matrix metalloproteinase systems in development of adipose tissue. Arch. Physiol. Biochem. 112:254-259.

Cinti, S., G. Mitchell, G. Barbatelli, I. Murano, E. Ceresi, E. Faloia, S. Wang, M. Fortier, A. S. Greenberg, and M. S. Obin. 2005. Adipocyte death defines macrophage localization and function in adipose tissue of obese mice and humans. J. Lipid Res. 46:2347-2355.

Constance, C. M., J. I. 4th. Morgan, and R. M. Umek. 1996. C/EBPalpha regulation of the growth-arrest-associated gene gadd45. Mol. Cell Biol. 16:3878-3883.

Cribb, A. E., M. Peyrou, S. Muruganandan, and L. Schneider. 2005. The endoplasmic reticulum in xenobiotic toxicity. Drug Metab. Rev. 37:405-442.

Cuvillier, O., and T. Levade. 2003. Enzymes of sphingosine metabolism as potential pharmacological targets for therapeutic intervention in cancer. Pharmacol. Res. 47:439-445.

Dann, H. M., N. B. Litherland, J. P. Underwood, M. Bionaz, A. D'Angelo, J. W. McFadden, and J. K. Drackley. 2006. Diets during far-off and close-up dry periods affect periparturient metabolism and lactation in multiparous cows. J. Dairy Sci. 89:3563-3577.

Divoux, A., and K. Clément. 2011. Architecture and the extracellular matrix: the still unappreciated components of the adipose tissue. Obes. Rev. 12:e494-503.

English, J., G. Pearson, J. Wilsbacher, J. Swantek, M. Karandikar, S. Xu, and M. H. Cobb. 1999. New insights into the control of MAP kinase pathways. Exp. Cell Res. 253:255-270.

Fain, J., S. Bahouth, and A. Madan. 2004. TNF-alpha release by the nonfat cells of human adipose tissue. Int. J. Obes. Relat. Metab. Disord. 28:616-622.

Gerhardt, C. C., I. A. Romero, R. Cancello, L. Camoin, and A. D. Strosberg. 2001. Chemokines control fat accumulation and leptin secretion by cultured human adipocytes. Mol. Cell Endocrinol. 175:81-92.

Gregor, M. G., and G. S. Hotamisligil. 2007. Adipocyte stress: the endoplasmic reticulum and metabolic disease. J. Lipid Res. 48:1905-1914.

Hannun, Y. A., and L. M. Obeid. 2008. Principles of bioactive lipid signalling: lessons from sphingolipids. Nature Rev.: Mol. Cell Biol. 9:139-150.

Hatanaka, M., S. Shimba, M. Sakaue, Y. Kondo, H. Kagechika, K. Kokame, T. Miyata, and S. Hara. 2009. Hypoxia-inducible factor-3alpha functions as an accelerator of 3T3-L1 adipose differentiation. Biol. Pharm. Bull. 32:1166-1172.

Hausman, G. J., and R. G. Kauffman. 1986. The histology of developing porcine adipose tissue. J. Anim. Sci. 63:642-658.

Hirosumi, J., G. Tuncman, L. Chang, C. Z. Gorgun, K. T. Uysal, K. Maeda, M. Karin, and G. S. Hotamisligil. 2002. A central role for JNK in obesity and insulin resistance. Nature 420:333-336.

Holtenius, K., S. Agenäs, C. Delavaud, and Y. Chilliard. 2003. Effects of feeding intensity during the dry period. 2. Metabolic and hormonal responses. J. Dairy Sci. 86:883-891.

Huusko, J., M. Merentie, M. H. Dijkstra, M. M. Ryhänen, H. Karvinen, T. T. Rissanen, M. Vanwildemeersch, M. Hedman, J. Lipponen, S. E. Heinonen, U. Eriksson, M. Shibuya, and S. Ylä-Herttuala. 2010. The effects of VEGF-R1 and VEGF-R2 ligands on angiogenic responses and left ventricular function in mice. Cardiovasc. Res. 86:122-130.

Ibrahim, M. M. 2010. Subcutaneous and visceral adipose tissue: structural and functional differences. Obes. Rev. 11:11-18.

Ip, Y. T., and R. J. Davis. 1998. Signal transduction by the c-Jun N-terminal kinase (JNK)-from inflammation to development. Curr. Opin. Cell Biol. 10:205-219.

Janovick, N. A., Y. R. Boisclair, and J. K. Drackley. 2011. Prepartum dietary energy intake affects metabolism and health during the periparturient period in primiparous and multiparous Holstein cows. J. Dairy Sci. 94:1385-1400.

Kawaguchi, N., K. Toriyama, E. Nicodemou-Lena, K. Inou, S. Torii, and Y. Kitagawa. 1998. *De novo* adipogenesis in mice at the site of injection of basement membrane and basic fibroblast growth factor. Proc. Natl. Acad. Sci. U.S.A. 95:1062-1066.

Kim, T., J. Wayne Leitner, R. Adochio, and B. Draznin. 2009. Knockdown of JNK rescues 3T3-L1 adipocytes from insulin resistance induced by mitochondrial dysfunction. Biochem. Biophys. Res. Commun. 378:772-776.

Lee, Y. H., J. Giraud, R. J. Davis, and M. F. White. 2003. c-Jun N-terminal kinase (JNK) mediates feedback inhibition of the insulin signaling cascade. J. Biol Chem. 278:2896-2902.

Lepine, S., B. Lakatos, M. P. Courageot, H. Le Stunff, J. C. Sulpice, and F. Giraud. 2004. Sphingosine contributes to glucocorticoid-induced apoptosis of thymocytes independently of the mitochondrial pathway. J. Immunol. 173:3783-3790.

Lepine, S., B. Lakatos, P. Maziere, M. P. Courageot, J. C. Sulpice, and F. Giraud. 2002. Involvement of sphingosine in dexamethasone-induced thymocyte apoptosis. Ann. N.Y. Acad. Sci. 973:190-193.

Lu, B., A. F. Ferrandino, and R. Flavell. 2004. Gadd45beta Is Important for Perpetuating Cognate and Inflammatory Signals in T Cells. Nature Immunol. 5:38-44.

Mannervik, B. 1985. Glutathione peroxidase. Methods Enzymol. 113:490-495.

Minematsu, H., M. J. Shin, A. B. Celil Aydemir, K. O. Kim, S. A. Nizami, G. J. Chung, and F. Y. Lee. 2011. Nuclear presence of nuclear factor of activated T cells (NFAT) c3 and c4 is required for Toll-like receptor-activated innate inflammatory response of monocytes/macrophages. Cell Signal. 2011 Jun 25. [Epub ahead of print]

Nakajima, I., S. Muroya, R. Tanabe, and K. Chikuni. 2002. Extracellular matrix development during differentiation into adipocytes with a unique increase in type V and VI collagen. Biol. Cell 94:197-203.

Nakatani, Y., H. Kaneto, D. Kawamori, K. Yoshiuchi, M. Hatazaki, T. A. Matsuoka, K. Ozawa, S. Ogawa, M. Hori, Y. Yamasaki, and M. Matsuhisa. 2005. Involvement of endoplasmic reticulum stress in insulin resistance and diabetes. J. Biol. Chem. 280:847-851.

Oh-hora, M., and A. Rao. 2008. Calcium signaling in lymphocytes. Curr. Opin. Immunol. 20:250-258.

Okamura, K., Y. Sato, T. Matsuda, R. Hamanaka, M. Ono, K. Kohno, and M. Kuwano. 1991. Endogenous basic fibroblast growth factor-dependent induction of collagenase and interleukin-6 in tumor necrosis factor-treated human microvascular endothelial cells. J. Biol. Chem. 266:19162-19165.

Özcan, U., Q. Cao, E. Yilmaz, A. H. Lee, N. N. Iwakoshi, E. Ozdelen, G. Tuncman, C. Görgün, L. H. Glimcher, and G. S. Hotamisligil. 2004. Endoplasmic reticulum stress links obesity, insulin action, and type 2 diabetes. Science. 306:457-461.

Raman, M., S. Earnest, K. Zhang, Y. Zhao, and M. H. Cobb. 2007. TAO kinases mediate activation of p38 in response to DNA damage. EMBO J. 26:2005-2014.

Rinaldo, P., D. Matern, and M. J. Bennett. 2002. Fatty acid oxidation disorders. Annu. Rev. Physiol. 64:477-502.

Rollins, B. J. 1997. Chemokines. Blood. 90:909-928.

Rosen, E. D., and O. A. MacDougald. 2006. Adipocyte differentiation from the inside out. Nat. Rev. Mol. Cell Biol. 7:885-896.

Sabio, G., N. J. Kennedy, J. Cavanagh-Kyros, D. Y. Jung, H. J. Ko, H. Ong, T. Barrett, J. K. Kim, and R. J. Davis. 2010. Role of muscle c-Jun NH2-terminal kinase 1 in obesity-induced insulin resistance. Mol. Cell. Biol. 30:106-115.

Sartipy, P., and D. J. Loskutoff. 2003. Monocyte chemoattractant protein 1 in obesity and insulin resistance. Proc. Natl. Acad. Sci. USA. 100:7265-7270.

Schaeffer, H. J., and M. J. Weber. 1999. Mitogen-Activated Protein Kinases: Specific Messages from Ubiquitous Messengers. Mol. Cell. Biol. 19:2435-2444.

Selvakumaran, M., H. K. Lin, R. Tjin Tham Sjin, J. Reed, D. A. Liebermann, and B. Hoffman. 1994. The novel primary response gene Myd118 and the roto-ncogenes Myb, Myc and Bcl-2 modulate transforming growth factor B1-induced apoptosis of myeloid leukemia cells. Mol. Cell. Biol. 14:2352-2360.

Semenza, G. L. 1999. Regulation of mammalian O_2 homeostasis by hypoxia-inducible factor 1. Annu. Rev. Cell. Dev. Biol. 15:551-578.

Sharfi, H., and H. Eldar-Finkelman. 2008. Sequential phosphorylation of insulin receptor substrate-2 by glycogen synthase kinase-3 and c-Jun NH2-terminal kinase plays a role in hepatic insulin signaling. Am. J. Physiol. Endocrinol. Metab. 294:E307-E315.

Sheikh, M. S., M. C. Hollander, and A. J. Fornace. 2000. Role of Gadd45 in apoptosis. Biochem. Pharm. 59:43-45.

Skurk, T., C. Alberti-Huber, C. Herder, and H. Hauner. 2007. Relationship between adipocyte size and adipokine expression and secretion. J. Clin. Endocrinol. Metab. 92:1023-1033.

Smith, M. L., J. M. Ford, M. C. Hollander, R. A. Bortnick, S. A. Amundson, Y. R. Seo, C. Deng, P. C. Hanawalt, and A. J. Jr. Fornace. 2000. P53-Mediated DNA repair responses to UV radiation: Studies of mouse cells lacking P53, P21, and/or Gadd45 genes. Mol. Cell. Biol. 20:3705-3714.

Spiegel, S., and S. Milstien. 2003. Sphingosine-1-phosphate: An enigmatic signalling lipid. Nat. Rev. Mol. Cell. Biol. 4:397-407

Suzuki, E., K. Handa, M. S. Toledo, and S. Hakomori. 2004. Sphingosine-dependent apoptosis: a unified concept based on multiple mechanisms operating in concert. Proc. Natl. Acad. Sci. U. S. A. 101:14788-14793.

Takekawa, M., F. Posas, and H. Saito. 1997. A human homolog of the yeast Ssk2/Ssk22 map kinase kinase kinases, MTK1, mediates stress-induced activation of the P38 and JNK pathways. EMBO J. 16:4973-4982.

Taleb, S., R. Cancello, K. Clement, and D. Lacasa. 2006. Cathepsin s promotes human preadipocyte differentiation: possible involvement of fibronectin degradation. Endocrinol. 147:4950-4959.

Tilg, H., and A. R. Moschen. 2008. Insulin resistance, inflammation, and non-alcoholic fatty liver disease. Trends Endocrinol. Metab. 19:371-379.

Tiniakos, D. G., M. B. Vos, and E. M. Brunt. 2010. Nonalcoholic fatty liver disease: pathology and pathogenesis. Annu. Rev. Pathol. 5:145-171.

Tournier, C., C. Dong, T. K. Turner, S. N. Jones, R. A. Flavell, and R. J. Davis. 2001. MKK7 is an essential component of the JNK signal transduction pathway activated by proinflammatory cytokines. Genes Dev. 15:1419-1426.

Vairapandi, M., A. G. Balliet, B. Hoffman, and D. A. Liebermann. 2002. Gadd45β and Gadd45γ are Cdc2/cyclinb1 kinase inhibitors with a role in S and G2/M cell cycle checkpoints induced by genotoxic stress. J. Cell. Physiol. 192:327-338.

Weisberg, S. P., D. McCann, M. Desai, M. Rosenbaum, R. L. Leibel, and Jr. A. W. Ferrante. 2003. Obesity is associated with macrophage accumulation in adipose tissue. J. Clin. Invest. 112:1796-1808.

Weisberg, S., D. McCann, M. Desai, M. Rosenbaum, R. Leibel, and A. Ferrante. 2003. Obesity is associated with macrophage accumulation in adipose tissue. J. Clin. Invest. 112:1796-1808.

Wu, Z., Y. Xie, N. L. Bucher, and S. R. Farmer. 1995. Conditional ectopic expression of C/EBP beta in NIH-3T3 cells induces PPAR gamma and stimulates adipogenesis. Genes Dev. 9:2350-2363.

Xu, H., G. T. Barnes, Q. Yang, G. Tan, D. Yang, C. J. Chou, J. Sole, A. Nichols, J. S. Ross, L. A. Tartaglia, and H. Chen. 2003. Chronic inflammation in fat plays a crucial role in the development of obesity-related insulin resistance. J. Clin. Invest. 112:1821-1830.

Yan, J. D., S. Yang, J. Zhang, and T. H. Zhu. 2009. BMP6 reverses TGF-beta1- induced changes in HK-2 cells: implications for the treatment of renal fibrosis. Acta. Pharmacol. Sin. 30:994-1000.

Yang, Z., L. Song, and C. Huang. 2009. Gadd45 proteins as critical signal transducers linking NF-kappaB to MAPK cascades. Curr. Cancer Drug Targets. 9:915-930.

Yu, R., C. S. Kim, B. S. Kwon, and T. Kawada. 2006. Mesenteric adipose tissue-derived monocyte chemoattractant protein-1 plays a crucial role in adipose tissue macrophage migration and activation in obese mice. Obesity (Silver Spring) 14:1353-1362.

Zamir, E., and B. Geiger. 2001. Molecular complexity and dynamics of cell–matrix adhesions. J. Cell Sci. 114:3583-3590.

Zhang, Q. X., C. J. Magovern, C. A. Mack, K. T. Budenbender, W. Ko, and T. K. Rosengart. 1997. Vascular endothelial growth factor is the major angiogenic factor in omentum:mechanism of the omentum-mediated angiogenesis. J. Surg. Res. 67:147-154.

Zinszner, H., M. Kuroda, X. Wang, N. Batchvarova, R. T. Lightfoot, H. Remotti, J. L. Stevens, and D. Ron. 1998. CHOP is implicated in programmed cell death in response to impaired function of the endoplasmic reticulum. Genes Dev. 12:982-995.

TABLES AND FIGURES

Table 4.1. DEG (FDR ≤ 0.2) with expression difference ≥ 2-fold between dietary treatments (OVE vs. CON). Positive fold-difference means DEG were more highly expressed in OVE than CON, whereas negative fold-difference indicates DEG had lower expression in OVE than CON.

Oligo ID	GenBank	Gene Symbol	Gene Name	Fold-Difference	P-value	FDR
Up-regulated in OVE vs. CON						
OLIGO_11285	NM_005063	SCD	stearoyl-CoA desaturase	3.50	0.0023	0.132
OLIGO_00815	NM_000245	MET	met proto-oncogene	2.52	0.0001	0.065
OLIGO_05066		MGC143330	endoplasmic reticulum-golgi intermediate compartment	2.45	0.0032	0.187
OLIGO_07313	NM_017986	GPR172B	G protein-coupled receptor 172B	2.44	0.0011	0.124
OLIGO_04905	XM_595298	LOC517135	chromosome 22 open reading frame 13 ortholog	2.40	0.0042	0.196
OLIGO_09862	NM_004521	KIF5B	kinesin family member 5B	2.32	0.0043	0.196
OLIGO_02993		CN439798		2.31	0.0010	0.115
OLIGO_10679	NM_002370	MAGOH	mago-nashi homolog, proliferation-associated (Drosophila)	2.25	0.0002	0.065
OLIGO_00533		SERINC3	serine incorporator 3	2.24	0.0002	0.065
OLIGO_01279	NM_001015892	TAF9	TAF9 RNA polymerase II, TATA box binding protein (TBP)-associated factor	2.21	0.0021	0.159
OLIGO_00123	NM_003251	THRSP	thyroid hormone responsive SPOT14 homolog	2.20	0.0025	0.132
OLIGO_00906	NM_004291	CARTPT	CART prepropeptide	2.17	0.0049	0.203
OLIGO_02892	NM_001012669	FASN	fatty acid synthase	2.10	0.0014	0.128
Down-regulated in OVE vs. CON						
OLIGO_11220	NM_181689	NNAT	neuronatin	-2.73	2.1×10^{-5}	0.040
OLIGO_09664	NM_001014988	LAT	linker for activation of T cells	-2.00	0.0013	0.130

Table 4.2. DEG (FDR ≥ 0.2) with expression difference ≥ 2-fold between tissues (MAT vs. SAT). Positive fold-difference means DEG had higher expression in MAT than SAT, whereas negative fold-difference indicates DEG had lower expression in MAT than SAT.

Oligo ID	GenBank	Gene Symbol	Gene Name	Fold-Difference	P-value	FDR
Up-regulated in MAT vs. SAT						
OLIGO_05586	NM_199161	SAA3	serum amyloid A 3	5.45	0.0025	0.170
OLIGO_12174	NM_004797	ADIPOQ	adiponectin	3.23	0.0021	0.127
OLIGO_11220	NM_181689	NNAT	neuronatin	2.95	9.2×10^{-6}	0.011
OLIGO_09217	NM_005252	FOS	FBJ murine osteosarcoma viral oncogene homolog	2.81	0.0001	0.037
OLIGO_09413	NM_145693	LPIN1	lipin 1	2.55	0.0023	0.144
OLIGO_10000	DR749338	DR749338		2.52	1.1×10^{-6}	0.007
OLIGO_06440	NM_005327	HADH	hydroxyacyl-Coenzyme A dehydrogenase pseudogene	2.37	0.0003	0.058
OLIGO_03834	NM_004040	RHOB	ras homolog gene family, member B	2.27	3.9×10^{-6}	0.007
OLIGO_09127	NM_006744	RBP4	retinol binding protein 4, plasma	2.25	0.0022	0.127
OLIGO_10552	NM_001063	TF	transferrin	2.17	0.0026	0.138
OLIGO_08595	NM_018100	EFHC1	EF-hand domain (C-terminal) containing 1	2.16	1.9×10^{-6}	0.007
OLIGO_12171	NM_002591	PCK1	phosphoenolpyruvate carboxykinase 1	2.15	0.0017	0.113
OLIGO_06738	NM_002612	PDK4	pyruvate dehydrogenase kinase, isozyme 4	2.06	0.0044	0.169
OLIGO_04502	NM_144641	PPM1M	protein phosphatase 1M	2.06	2.9×10^{-5}	0.020
OLIGO_11884	NM_002006	FGF2	fibroblast growth factor 2	2.04	0.0002	0.054
Down-regulated in MAT vs. SAT						
OLIGO_10483	NM_000089	COL1A2	collagen, type I, alpha 2	-4.53	2.9×10^{-5}	0.020
OLIGO_02891	NM_000071	CBS	cystathionine-beta-synthase	-3.17	6.8×10^{-6}	0.010
OLIGO_00934	NM_001075435	MGC143401	myosin binding protein H	-2.97	0.0034	0.153
OLIGO_07817	NM_017703	FBXL12	F-box and leucine-rich repeat protein 12	-2.95	0.0001	0.037
OLIGO_13133	NM_001982	ERBB3	v-erb-b2 erythroblastic leukemia viral oncogene homolog 3	-2.87	0.0063	0.200

Table 4.2. (cont.)

Oligo ID	GenBank	Gene Symbol	Gene Name	Fold-Difference	P-value	FDR
OLIGO_02728	NM_001005367	TTYH1	tweety homolog 1 (Drosophila)	-2.76	0.0001	0.037
OLIGO_11285	NM_005063	SCD	stearoyl-CoA desaturase	-2.72	0.0020	0.180
OLIGO_00835	NM_003014	SFRP4	secreted frizzled-related protein 4	-2.66	0.0041	0.166
OLIGO_09430	XM_614120	LOC534369	ATPase type 13A1	-2.66	0.0007	0.074
OLIGO_04894	XM_001126181	MGC142346	aurora kinase A interacting protein 1	-2.64	0.0005	0.070
OLIGO_02697	XM_172995	LOC255809	chromosome 19 open reading frame 38	-2.63	0.0002	0.047
OLIGO_09832	NM_018250	RC74	integrator complex subunit 9	-2.57	0.0016	0.108
OLIGO_06101	NM_024578	OCEL1	occludin/ELL domain containing 1	-2.53	0.0002	0.047
OLIGO_06643	NM_005827	SLC35B1	solute carrier family 35, member B1	-2.51	0.0049	0.177
OLIGO_09048	NM_000355	TCN2	transcobalamin II	-2.45	0.0002	0.045
OLIGO_12570	NM_015221	DNMBP	dynamin binding protein	-2.41	0.0010	0.087
OLIGO_02864	NM_022716	PRRX1	paired related homeobox 1	-2.38	0.0001	0.025
OLIGO_10599	NM_002046	GAPDH	glyceraldehyde-3-phosphate dehydrogenase	-2.31	0.0012	0.095
OLIGO_04103		LOC519222	DIS3 mitotic control homolog (S. cerevisiae)-like 2	-2.30	0.0027	0.138
OLIGO_07055	NM_002961	S100A4	S100 calcium binding protein A4	-2.29	0.0022	0.127
OLIGO_10553	NM_000090	COL3A1	collagen, type III, alpha 1	-2.27	0.0040	0.163
OLIGO_08952	NM_007159	SLMAP	sarcolemma associated protein	-2.22	0.0005	0.070
OLIGO_07207	NM_004887	CXCL14	chemokine (C-X-C motif) ligand 14	-2.21	0.0001	0.024
OLIGO_02231	XM_910489	2310004N24Rik	RIKEN cDNA 2310004N24 gene	-2.20	0.0018	0.116
OLIGO_05794	NM_002009	FGF7	fibroblast growth factor 7	-2.18	0.0011	0.089
OLIGO_02155	NM_014048	MKL2	MKL/myocardin-like 2	-2.12	0.0030	0.146
OLIGO_11084	NM_000088	COL1A1	collagen, type I, alpha 1	-2.10	0.0001	0.024
OLIGO_12335	NM_015429	ABI3BP	ABI family, member 3 (NESH) binding protein	-2.00	0.0002	0.047

Table 4.3. Fold change consistency of genes investigated in qPCR and microarray

Gene	Description	Fold-Difference			
		MAT vs SAT		OVE vs CON	
		Microarray	qPCR	Microarray	qPCR
	Lipid metabolism, fatty acid import				
ACLY	ATP citrate lyase	1.11	1.52*	1.18	1.71**
ACACA	acetyl-Coenzyme A carboxylase alpha	-1.09	-1.50*	1.51	1.52*
FASN	fatty acid synthase	-1.10	-1.67**	1.90	2.10**
ELOVL6	elongation of long chain fatty acids	-1.08	1.17	1.55	1.78**
SCD	stearoyl-CoA desaturase	-1.60	-2.72**	4.36	3.50**
GPAM	glycerol-3-phosphate acyltransferase	1.80	1.63**	1.48	1.33*
LPL	lipoprotein lipase	1.57	1.65**	-1.09	1.04
CD36	thrombospondin receptor	1.31	-1.04	-1.12	-1.01
ACSL1	acyl-CoA synthetase long-chain	1.38	1.55*	-1.27	-1.09
ADFP	adipose differentiation-related protein	-1.06	-1.60**	1.22	1.13
LPIN1	lipin 1	1.72	2.55**	1.09	1.79**
LIPE	hormone-sensitive lipase	1.50	1.04	1.17	-1.04
LEP	leptin	1.02	1.78**	1.14	1.39
ADIPOQ	adiponectin	3.23	1.82**	-1.06	-1.01
	Transcription regulation				
THRSP	thyroid hormone responsive SPOT 14	2.02	1.46*	2.53	2.20**
PPARG	peroxisome proliferator-activated receptor gamma	1.21	1.13	1.19	1.15
SREBF1	sterol regulatory element binding transcription factor 1	1.13	-1.04	-1.07	-1.41**
MLXIPL	MLX interacting protein-like	1.01	1.08	1.07	1.11
NR2F2	nuclear receptor	1.08	1.40**	-1.20	-1.08
	Immune response, acute-phase response, inflammation and insulin sensitivity				
TNF	tumor necrosis factor	-1.11	-1.15	-1.52	-1.05
IL-1B	interleukin-1 beta	1.04	1.87**	1.15	1.33
IL-6	interleukin-6	-1.11	1.20	-1.13	1.02
IL-6R	Interleukin-6 receptor	1.21	1.38**	-1.08	-1.36**
AKT2	thymoma viral proto-oncogene	-1.18	1.25*	-1.09	-1.27**
SAA3	acute-phase serum amyloid A1	-1.29	5.45**	1.07	-1.48
TLR4	toll-like receptor 4	-1.03	1.22	-1.20	-1.18
CCL2	chemokine (C-C motif) ligand 2	1.22	1.83	1.09	1.78*
CCL5	chemokine C-C motif ligand 5	-1.07	1.51	-1.03	1.08
INSR	insulin receptor	1.21	1.22	1.02	1.01

** $P \leq 0.05$; * $P \leq 0.10$.

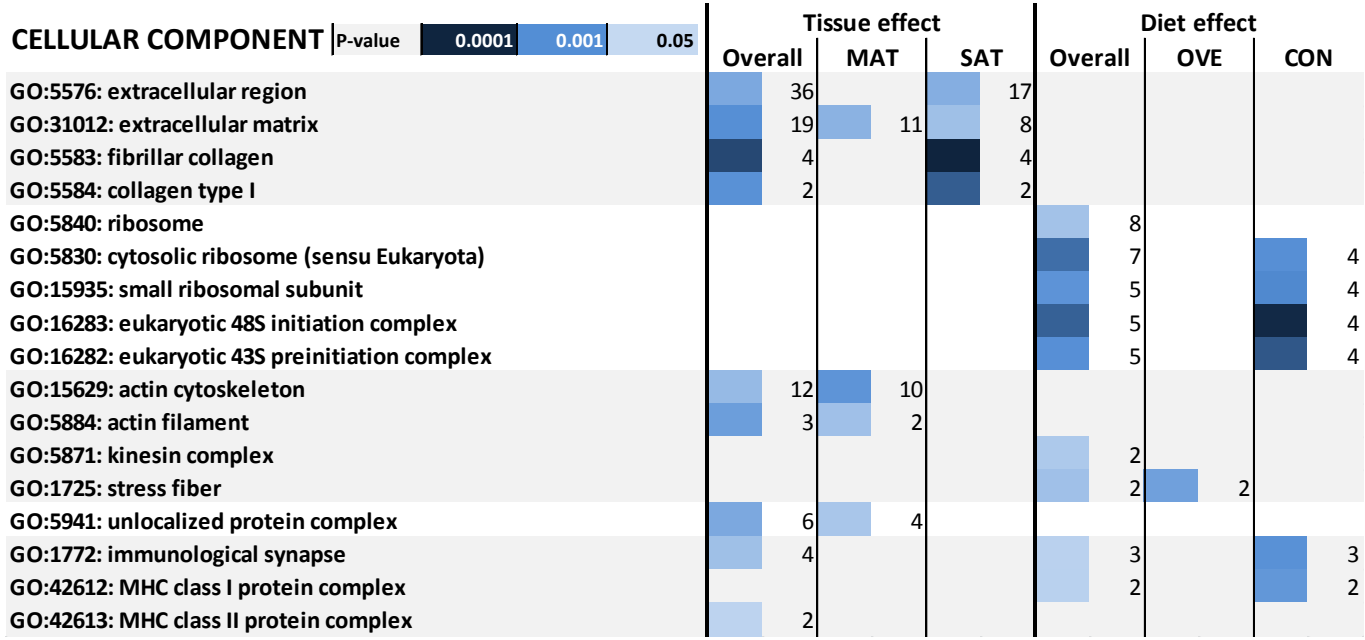

Figure 4.1. Most representative cellular component (Cc) in GO analyses among DEG in either diet or tissue comparison.
Most representative GO Cc among significantly impacted Cc with unadjusted *P*-value ≤ 0.05 in the 6 analyses (described in materials and methods). The Cc were grouped and shown by different background colors (grey or white). The color gradation in the left column of each analysis denotes the degree of reliability of this Cc being influenced or the range of the *P*-value (criteria shown on the top row of the figure), and no color means not significant in this analysis ($P > 0.05$); The number in the right column of each analysis means how many DEG (FDR ≤ 0.2) exerted an effect on this Cc. MAT: mesenteric adipose tissue; SAT: subcutaneous adipose tissue; OVE: moderate energy diet; Strw or CON: controlled energy diet.

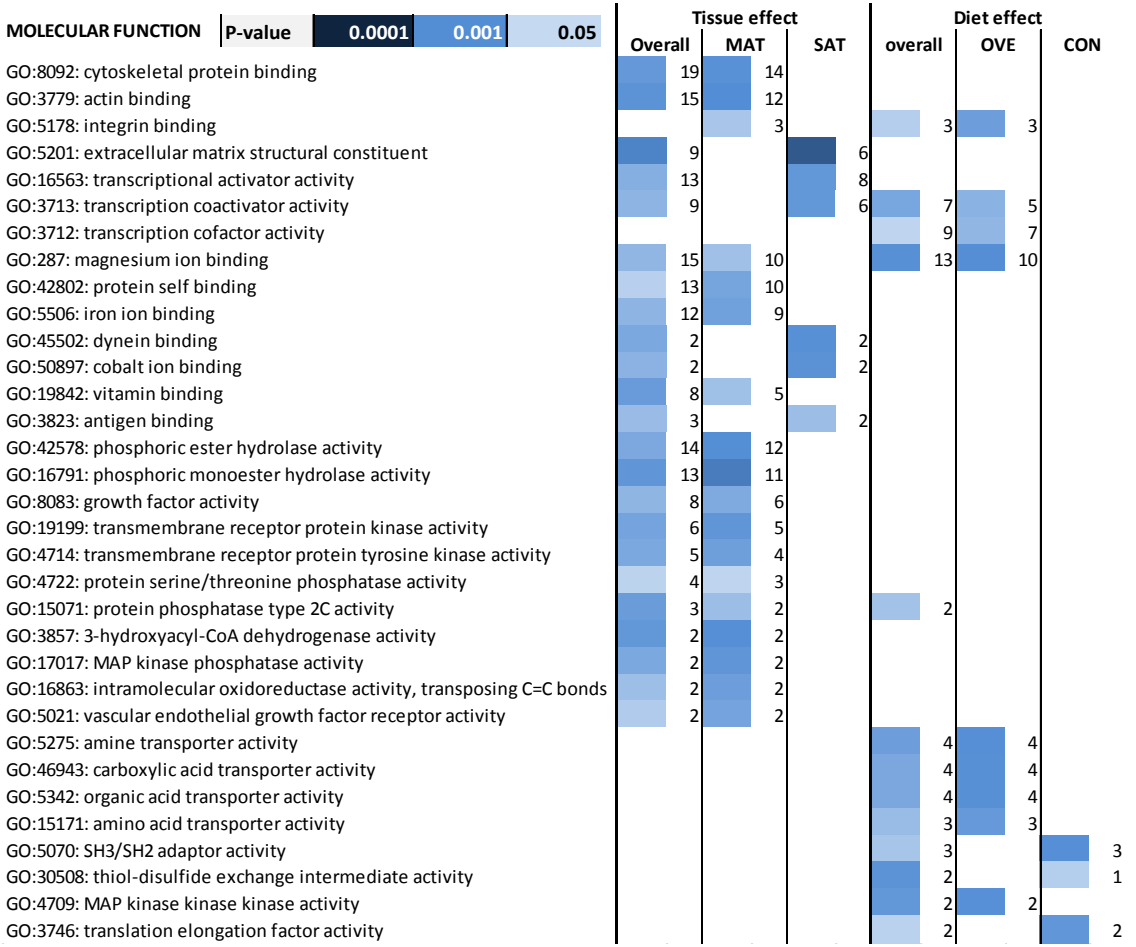

Figure 4.2. Most representative molecular functions (Mf) in GO analyses among DEG in either diet or tissue comparison.
Most representative GO Mf among significantly impacted Mf with unadjusted *P*-value ≤ 0.05 in the 6 analyses (described in materials and methods). The color gradation in the left column of each analysis denotes the degree of reliability of this Mf being influenced or the range of the *P*-value (criteria showed on the top row of the figure), and no color means not significant in this analysis ($P > 0.05$); The number in the right column of each analysis means how many DEG (FDR ≤ 0.2) participated in the Mf. MAT: mesenteric adipose tissue; SAT: subcutaneous adipose tissue; OVE: moderate energy diet; Strw or CON: controlled energy diet.

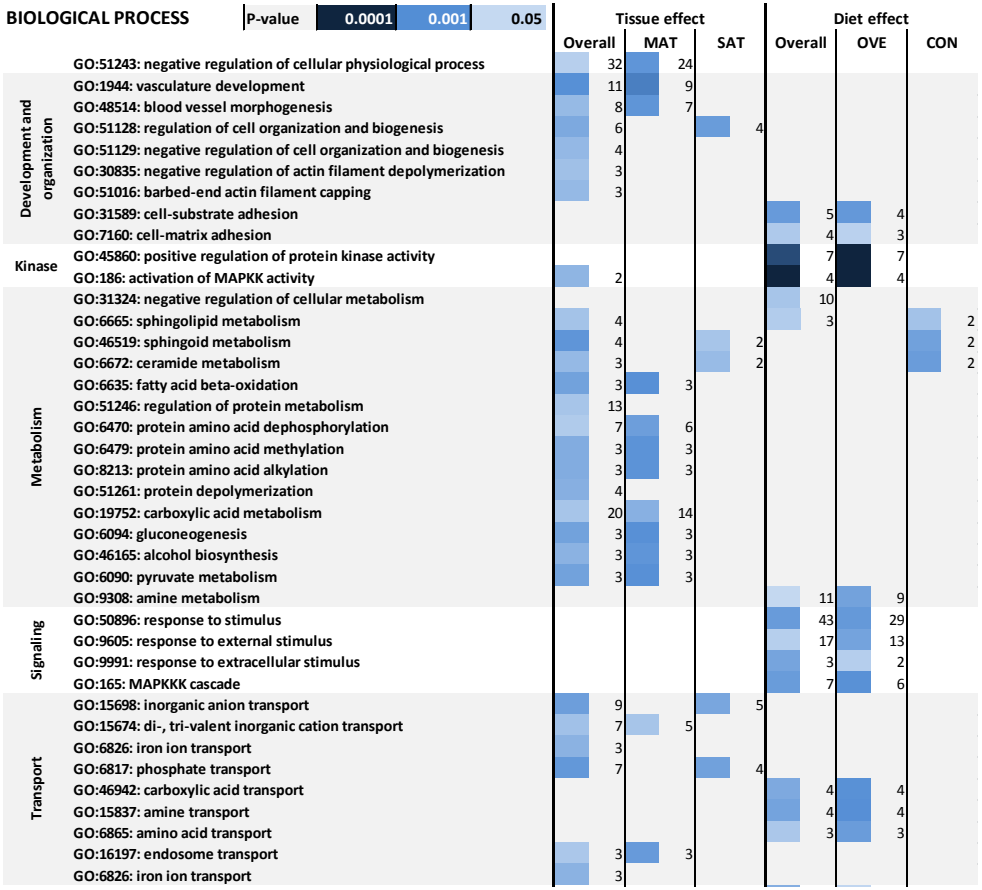

Figure 4.3. Most representative biological process (Bp) in GO analyses among DEG in either diet or tissue comparison**.**
Most representative GO Bp among significantly impacted Bp with unadjusted *P*-value ≤ 0.05 in the 6 analyses (described in materials and methods). The Bp were grouped by the overall function that they belong to and showed by different background colors (grey or white). The color gradation in the left column of each analysis denotes the degree of reliability of this Bp being influenced or the range of the *P*-value (criteria showed on the top row of the figure), and no color means not significant in this analysis ($P > 0.05$); The number in the right column of each analysis means how many DEG (FDR ≤ 0.2) participated in this Bp. MAT: mesenteric adipose tissue; SAT: subcutaneous adipose tissue; OVE: moderate energy diet; Strw or CON: controlled energy diet.

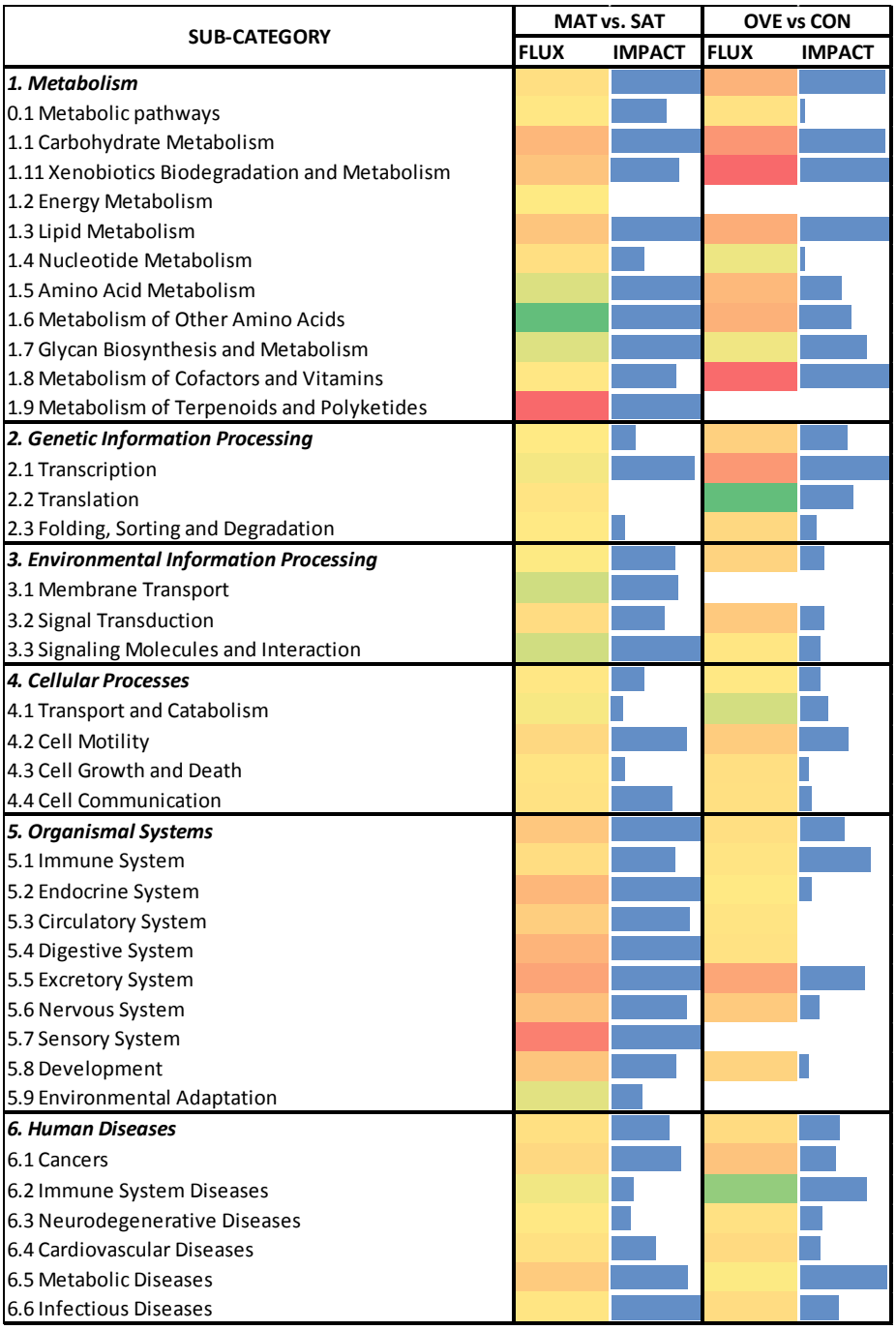

Figure 4.4. The FLUX and IMPACT of main- and sub-categories of KEGG PATHWAY database due to main effects of fat depots (SAT vs. MAT) or dietary energy plane (OVE vs. CON). The FLUX value ranges from -25.9 (greenest, pathway: Metabolism of other amino acids) to 26.5 (reddest, pathway: Metabolism of terpenoids and polyketides) for fat depot comparison, and -6.7 to 14.6 for diet comparison. IMPACT bar length ranges from 2 to 10+ for all comparison, which means any IMPACT value that is more than 10 will be expressed as the same full bar length (Maximum for fat depot comparison: 35.4, Metabolism of other amino acids; Maximum for diet comparison: 19.9, Metabolism of cofactor and vitamins).

SUB-CATEGORY	PATHWAY NAME	MAT vs SAT			
		FLUX	IMPACT	Up-regulated	Down-regulated
Carbohydrate Metabolism	Butanoate metabolism			HADHA; ACSM1	
	Glycolysis / Gluconeogenesis			PCK1; FBP1; PGM1	GAPDH
	Pentose phosphate pathway			FBP1; PGM1	
Lipid Metabolism	Ether lipid metabolism				PAFAH1B1; PAFAH1B2; PLA2G7
	Fatty acid elongation in mitochondria			HADHA	
	Sphingolipid metabolism			SGPL1; SPHK2	NEU1; ASAH1
Amino Acid Metabolism	Cysteine and methionine metabolism				CBS
	Glycine, serine and threonine metabolism				CBS; AGXT
	Lysine degradation			HADHA; PLOD2	SETD2
Metabolism of Other Amino Acids	Selenoamino acid metabolism				
Glycan Biosynthesis and Metabolism	Glycosaminoglycan degradation				GNS
Metabolism of Terpenoids and Polyketides	Limonene and pinene degradation				
Signal Transduction	Phosphatidylinositol signaling system			ITPR2; CALM1; CALM3; CDS2;	INPP1; PIK3C2A
Signaling Molecules and Interaction	ECM-receptor interaction				COL1A1; COL1A2; COL3A1
Cell Communication	Focal adhesion			VEGFA; MYLK; MYL9; SHC1; ACTN3; PARVA	COL1A1; COL1A2; COL3A1
Endocrine System	Adipocytokine signaling pathway			PCK1; ADIPOQ; RXRG	CAMKK1; PRKAB2
	PPAR signaling pathway			PCK1; ADIPOQ; RXRG	
Digestive System	Gastric acid secretion			MYLK; CALM1; CALM3; ITPR2	
Excretory System	Proximal tubule bicarbonate reclamation			PCK1	
Sensory System	Phototransduction			GNB1; GUCY2D; CALM1; CALM3	
Cancers	Bladder cancer			VEGFA	MMP2
	Melanoma			FGF2; FGF7	MITF
Metabolic Diseases	Type II diabetes mellitus			ADIPOQ	
Infectious Diseases	Amoebiasis			CSF2; ACTN3	COL1A1; COL1A2; COL3A1

Figure 4.5. The FLUX, IMPACT and the DEGs for the most over-represented KEGG pathway in comparison of fat depots (MAT vs. SAT). The most over-represented pathways were screened from a complete list of over-represented pathways that is based on DEGs in comparison of fat depot and contains more than 30% of genes presented in genome as in our array. The threshold value for "most over-represented pathway" has the Log_2(IMPACT of this pathway) > [Mean of Log_2(IMPACT of every pathway) + SD of (IMPACT of every pathway)]. The FLUX value ranges from -61.4 (the greenest, pathway: Selenoamino acid metabolism) to 33.1 (the reddest, pathway: phototransduction). The IMPACT bar length stands for the value that ranges from 16.7 (pathway: Gastric acid secretion) to 30+ (Maximum is 61.4 for pathway: Selenoamino acid metabolism), which means any IMPACT value that more than 30 will be expressed as the same full bar length.

SUB-CATEGORY	PATHWAY	OVE vs CON			
		FLUX	IMPACT	Up-regulated	Down-regulated
Carbohydrate Metabolism	Glyoxylate and dicarboxylate metabolism			GLYCTK;	
Xenobiotics Biodegradation and Metabolism	Metabolism of xenobiotics by cytochrome P450			CYP2S1; GSTM3	
Lipid Metabolism	Sphingolipid metabolism			NEU1; PPAP2A	ASAH1
	Ether lipid metabolism			PAFAH1B1; PPAP2A	
Glycan Biosynthesis and Metabolism	Other glycan degradation			NEU1	
Metabolism of Cofactors and Vitamins	Ubiquinone and other terpenoid-quinone biosyn			COQ3	
Transcription	Basal transcription factors			TAF9	
Immune System	Fc gamma R-mediated phagocytosis			PIK3R1; PPAP2A	LAT; VAV3
	Fc epsilon RI signaling pathway			PIK3R1	LAT; VAV3
	Natural killer cell mediated cytotoxicity			PIK3R1; NFATC3	LAT; VAV3
	T cell receptor signaling pathway			PIK3R1; NFATC3	LAT; VAV3
Metabolic Diseases	Type II diabetes mellitus			PIK3R1	SOCS1

Figure 4.6. The FLUX, IMPACT and the DEGs for the most over-represented KEGG pathway in comparison of dietary energy plane (OVE vs. CON). The most over-represented pathways were screened from a complete list of over-represented pathways that is based on DEGs in comparison of diets and contains more than 30% of genes presented in genome as in our array. The threshold value for "most over-represented pathway" has the Log_2(IMPACT of this pathway) > [Mean of Log_2(IMPACT of every pathway) + SD of (IMPACT of every pathway)]. The FLUX value ranges from -5.2 (the greenest, pathway: Fc epsilon RI signaling pathway) to 34.5 (the reddest, pathway: Ubiquinone and other terpenoid-quinone biosynthesis). The IMPACT bar length stands for the value that ranges from 10.2 (pathway: T cell receptor signaling) to 20+ (Maximum is 34.5 for pathway: Ubiquinone and other terpenoid-quinone biosynthesis), which means any IMPACT value that more than 30 will be expressed as the same full bar length.

CHAPTER 5

PREPARTAL PLANE OF DIETARY ENERGY CHANGED INSULIN SIGNALING TRANSDUCTION AND TRANSCRIPTIONAL ADAPTATION OF ADIPOSE TISSUE OF DAIRY COWS DURING THE TRANSITION PERIOD

ABSTRACT

Reduced peripheral insulin responsiveness is a hallmark of physiological adaptation in late pregnancy and early lactation in dairy cows. Previous studies demonstrated prepartum overfeeding dietary energy seemed to predispose animals to a more severe insulin-resistant state, which resulted in enhanced postpartum lipolysis of dairy cows. In an attempt to evaluate the mechanism for the effect of prepartum overfeeding in regulation of adipose metabolism and insulin sensitivity during transition period, 14 Holstein cows ($\geq 2^{nd}$ parity) were dried off at -50 d relative to expected parturition date and offered a controlled-energy diet (NE_L = 1.24 Mcal/kg DM) that contained 36% of DM as wheat straw until -21 d. Then animals were randomly assigned to either the same controlled-energy diet (controlled or CON) or a moderate-energy diet (overfed or OVE, NE_L = 1.47 Mcal/kg DM) during the close-up dry period (-21 d to parturition). Both groups were fed the same lactation diet (NE_L = 1.65 Mcal/kg DM) after calving. Blood samples were collected before the morning feeding twice weekly from -21 to 30 d relative to parturition. Subcutaneous adipose tissue (AT) was biopsied from the tail-head region at -10, 7, and 21 d. Adipose explants from part of the AT collected at -10 and 7 d were used to determine the IRS1 tyrosine phosphorylation (IRS1-pY) level with or without insulin challenge in vitro. Total RNA was extracted from the rest of the AT from all 3 biopsies. Quantitative RT-PCR was

utilized to analyze mRNA expression of 24 genes associated with lipid metabolism and insulin signaling. Overfeeding energy markedly increased DMI ($P = 0.05$), NE_L intake ($P < 0.01$), and serum insulin concentration ($P < 0.01$) during the close-up period. Compared with OVE group, serum NEFA levels of CON cows were numerically higher and lower in close-up period and postpartum, respectively. However, OVE animals experienced a more drastic increase of circulating NEFA after calving than the CON group ($P = 0.04$) and tended to have higher serum BHBA postpartum ($P = 0.06$). As a consequence, postparturient hepatic lipid and triglyceride accumulation was significantly greater in OVE vs. CON cows. No difference in any aspect of performance was detected between the two groups, except the tendency for greater milk protein percentage ($P = 0.10$) in CON group. Adipose IRS1-pY, either without or with insulin challenge was significantly lower at 7 vs. -10 d for both groups. The AT biopsied at -10 d in OVE animals had greater IRS1-pY in response to insulin challenge than that in CON group. The mRNA expression of genes involved in fatty acid biosynthesis, fatty acid uptake and activation, NADPH production, and triglyceride synthesis were all up-regulated at -10 d by overfeeding energy compared with CON. However, the expression of these genes was remarkably suppressed post-calving in both groups. Despite the decrease in both groups, genes encoding adipose triglyceride lipase (*ATGL*) and its activator protein (*ABHD5*) were more highly expressed in OVE vs. CON at -10 and +7 d. *PPARG* exhibited the same expression pattern as *ATGL* and *ABHD5*, whereas *CEBPA* showed the same change as those of lipogenic genes. In conclusion, the sharply increased postparturient lipolysis in OVE cows may not be the consequence of insulin resistance induced by preparturient overfeeding. Overfeeding increased lipolytic gene expression, which may contribute to the greater body fat mobilization in early lactation. Prepartum overfeeding regulates adipose tissue metabolism at least from the transcriptional level.

INTRODUCTION

Insulin is a major anabolic hormone in ruminants as in human and rodents. The classic mechanism of insulin action on adipose tissue includes stimulation of adipogenesis and glucose utilization and inhibition of lipolysis. "Insulin resistance" has been defined as either decreased sensitivity (the insulin concentration to induce half-maximal response) or responsiveness (the maximal response) of insulin-sensitive tissues (primarily adipose and skeletal muscle) to insulin (Kahn, 1978).

The periparturient period in ruminants has long been thought to represent a physiological state of increased peripheral insulin resistance (IR), which was considered an important homeorhetic adaptation to shift energy from peripheral tissues to the fetus and mammary gland (Bauman and Currie, 1980). Measurements of glucose utilization in vivo revealed that late-pregnant ewes exhibit reduced insulin sensitivity (Petterson et al., 1993), and also had compromised responsiveness to insulin's antilipolytic effect (Petterson et al., 1994). I*n vitro* insulin-stimulated glucose and acetate uptake were almost completely suppressed in subcutaneous adipose tissue from early lactating ewes (Vernon and Taylor, 1988). However, the underlying molecular mechanism for peripartal IR remains unclear. Vernon and Taylor (1988) were unable to attribute the apparent IR to changes in receptor number or insulin-receptor binding affinity, and they suggested the possibility of "post-receptor" defects, which have not been evaluated in ruminants so far.

With regard to insulin's antilipolytic effect, besides the hypoinsulinemia during early lactation (Bell, 1995), the apparent IR in adipose during the transition period is linked with the sharp increase in circulating NEFA around parturition. Whereas intrajugular infusion of the

insulin-sensitizing drug thiazolidinedione (TZD) during the close-up dry period was found to decrease postpartal serum NEFA linearly with increased dose administered (Smith et al., 2009).

The "steam-up" dietary approach during the last few weeks of gestation, i.e., feeding a higher-energy diet primarly by increasing cereal grains, has been used in the field for a number of years. On the one hand such a management approach was designed to compensate for the normal reduction in voluntary feed intake as parturition approaches, and was thought to be useful in priming the cow for greater appetite postpartum (Grummer, 1995); on the other hand, the high level of non-fiber carbohydrate (NFC) in the steam-up approach was expected to stimulate ruminal propionate production and consequently hepatic gluconeogenesis, which would trigger insulin secretion and suppress adipose tissue lipolysis during the periparturient period (Ingvartsen and Andersen, 2000).

However, studies from different research groups demonstrated that prepartal overfeeding of energy from grains with greater NFC has often resulted in prepartal hyperglycemia and hyperinsulinemia and marked adipose tissue mobilization (i.e., greater blood NEFA concentration) at the initiation of lactation (Rukkwamsuk et al., 1999; Holtenius et al., 2003; Dann et al., 2006; Douglas et al., 2006; Janovick et al., 2011). As a consequence of increased lipolysis, energy-overfed cows had greater hepatic lipid accumulation and were more subject to metabolic disorders postpartum (Dann et al., 2006; Janovick et al., 2011). The observed signs resemble those of obesity-induced Type II diabetes, which is primarily due to dysfunctional insulin signaling in adipose tissue and skeletal muscle metabolism (McGarry, 2002). In comparison with the steam-up approach, physical control of prepartal energy consumption to meet but not greatly exceed energy requirements by inclusion of bulky forages (e.g., wheat straw, low-quality hay) stabilizes DMI around parturition, and has resulted in more "moderate"

increases in blood NEFA during early lactation (Janovick et al., 2010). Thus, uncovering the mechanisms whereby dry period energy nutrition affects adipose tissue metabolism is of great importance.

The metabolic effects of insulin are initiated upon binding of the hormone to the α-subunit on its receptor (INSR), which induces a conformational change and activates the tyrosine kinase activity of the β-subunit. This event stimulates recruitment of insulin receptor substrate (IRS) proteins causing phosphorylation on multiple tyrosine residues (IRS-p-Y). Those phosphorylated residues serve as docking sites for a number of downstream proteins (Virkamäki et al., 1999). The tyrosine phosphorylation of IRS1 is linked with activation of thymoma viral protooncogene (AKT), which finally triggers the translocation of insulin-sensitive glucose transporter (GLUT4) (Foran et al., 1999) and activation of phosphodiesterase 3B leading to the initiation of insulin's antilipolytic effect in adipocytes (Kitamura et al., 1999).

Accumulating evidence from rodent and human studies has revealed that defects in IRS1 tyrosine phosphorylation are causal of peripheral insulin resistance either during late pregnancy (Sevillano et al., 2007) or in cases of obesity induced by Type II diabetes (Esposito et al., 2001; Sesti et al., 2001). Hence, IRS1-p-Y could be used as parameter to determine insulin responsiveness in adipose tissue of transition dairy cows. More importantly, linking phosphorylation with transcriptomics could be valuable in expanding our mechanistic knowledge of nutritional regulation of peripartal adipose tissue metabolism and. The study of longitudinal changes in gene expression as it relates to insulin signaling could shed light on the long-term dynamic metabolic adaptations to physiological and nutritional status.

The hypotheses that we sought to test in the present research were that prepartal energy overfeeding 1) exacerbates subcutaneous adipose tissue IR by compromising the tyrosine

phosphorylation of IRS-1, and 2) changes adipose tissue metabolism through alterations in expression of genes encoding the major functional enzymes involved in adipogenesis, lipogenesis, and lipolysis.

MATERIALS AND METHODS

Experimental Design, Diet, and Animals

All procedures were conducted under protocols approved by the University of Illinois Institutional Animal Care and Use Committee. Fourteen multiparous Holstein cows were used in this study. All cows were dried off at d -50 relative to expected parturition and fed a controlled-energy diet (NE_L = 1.24 Mcal/kg DM; Table 5.1) containing wheat straw at 36% of DM for ad libitum intake during the far-off period (i.e. d -50 to d -21). During the close-up period (i.e. d -21 to parturition), cows were randomly assigned either to a moderate-energy diet (Overfed or OVER; NE_L = 1.47 Mcal/kg DM) or continuously fed the same controlled-energy diet (Controlled or CON) for ad libitum intake. The same lactation diet (NE_L = 1.65 Mcal/kg DM) was provided for all animals postpartum until 30 days in milk (DIM).

Managements, Sampling, and Analyses

Both pre- and postpartum diets were mixed daily and fed as TMR. All cows were individually fed once daily at 0630 h. Individual feed offered and feed refusals were recorded daily from the initiation of dry period through 30 d postpartum. Cows were housed in a free stall barn with Calan gates during the dry period (dry-off at -50 d relative to expected parturition). At 3 d before expected parturition, cows were moved to individual maternity pens until parturition. After parturition, cows were housed in tie stall barn and milked 3 times daily and milk yields were recorded. When cows were > 6 DIM, milk samples were taken at each milking of the same

day once weekly and analyzed for fat, protein, lactose, and urea N, as well as SCC (Dairy Lab Services, Dubuque, IA). Cow BW was recorded once weekly for all cows after the morning milking and before the morning feeding. Additionally, cows were weighed after parturition and calf birth weight was recorded. Body condition score (BCS) (Wildman et al., 1982) was independently evaluated by 2 individuals once per week and the mean score was used for each cow. Individual feed ingredients were sampled weekly and DM content (AOAC, 1995) was determined for each component. Rations were adjusted for DM of ingredients on a weekly basis. Weekly feed ingredient samples were dried and frozen at −20°C and then composited monthly for analysis of DM, CP, NDF, and ADF by wet chemistry techniques at a commercial laboratory (Dairy One, Ithaca, NY). For energy calculations, Dairy One used the Ohio State summative energy equation to predict total digestible nutrients (TDN) at maintenance and the NRC (2001) equations to calculate NE_L at 3× maintenance, with the Van Soest variable discount system used for forages. Blood was sampled from the coccygeal vein or artery every Monday and Thursday before morning feeding from -21 to 30 d. Samples were collected into evacuated serum tubes containing clot activator. Serum was obtained by centrifugation at 1,300 × g for 15 min and frozen at -20°C until later analysis. Serum insulin concentration was analyzed by a commercial bovine insulin ELISA kit (cat. #10-1201-01; Mercodia AB). Concentrations of BHBA and NEFA were analyzed using commercial kits at the Veterinary Diagnostics Laboratory, College of Veterinary Medicine, University of Illinois.

AT Biopsy and Tissue Handling

Adipose biopsies were collected from alternate sides of the tail-head region at -10, 7, and 21 d before the morning feeding. The hair of the surgical area was cut closely with clippers and washed with an iodine disinfectant mixture. Lidocaine-HCl (5 ml; Agri Laboratories) was given

intramuscularly to anaesthetize the biopsy area 10 min before performing a ~2 cm incision. Adipose tissue was collected with scalpel and forceps. The incision was then closed with surgical staples (Multi-Shot Disposable Skin Stapler, Henry Schein) and iodine ointment was applied to the wound. The wound was carefully watched for the following 7 d, and treated accordingly if any inflammation or swelling were observed. A 2-4 g of tissue was harvested by blunt dissection. Half of the tissue was quickly blotted with sterile gauze to remove residual blood and snap-frozen in liquid N_2 until RNA extraction for gene expression analysis. The remaining ~2 g of tissue was prepped for culture (only conducted with samples from -10 and 7 d) by quickly rinsing in pre-warmed (~37°C) sterile 1× PBS solution and coarsely minced to minimize risk of hypoxia. Subsequently, tissue samples were quickly transported (within 30 min after biopsy) back to the laboratory in pre-warmed (~37°C) 1× Dulbecco's Modified Eagle Medium (DMEM; Cat. #12320-032, Invitrogen).

AT Explants and Protein Assay

All of the following procedures, except weighing, were carried out under a laminar flow hood using sterile techniques. Tissue was carefully processed to remove adjacent non-adipose tissue, and chopped into small pieces of ca. 10 mg. Evenly distributed pieces of tissue were placed into sterile petri dishes (Cat. #5662-7161, Fisher Scientific) and weighed to make sure each culture dish contained ~100 mg tissue. Subsequently, all samples were quickly washed with 5 mL 37°C 1× DMEM to remove lipid released from tissue during cutting. Samples were then transferred into 12-well culture plate (Cat. #CLS3512, Sigma-Aldrich), which contained 1.5 mL 37°C 1× DMEM in each well. Tissue was pre-incubated in a water-jacketed CO_2 incubator (at 37°C with 5% CO_2) for 30 min for adaptation.

After 30-min adaptation, two samples were taken out and served as duplicate negative controls, i.e. the 0 min sample before insulin challenge. The remaining samples were transferred into a new culture plate, which contained 1.5 mL 37°C 1× DMEM in each well with or without addition of 1 µmol/L bovine insulin (Cat. #I0516, Sigma-Aldrich; 10 mg/mL bovine insulin in 25 mM HEPES, pH 8.2, sterile-filtered). Culture plates were then incubated with the same conditions as listed above. Duplicate samples with or without insulin were removed from plates at 15, 30, and 60 min of incubation,.

After removal tissue samples were immediately immersed into 1.5 mL ice-cold 1× cell lysis buffer (Cat. #9803, Cell Signaling Technology®) containing 1 mM phenylmethylsulfonyl fluoride (PMSF; protease inhibitor, Cat. #P7626, Sigma-Aldrich) and were quickly homogenized. After homogenization tissue was sonicated in an ice bath 2 times for ca. 10 sec/time right to break down the nuclear membrane. Samples were then centrifuged at 8984 × g at 4°C for 10 min and the supernant was carefully transferred into 1.5 mL tubes without disturbing lipid layer, and stored at -80°C until protein analysis.

Total protein was analyzed with the BCA protein assay kit (Cat. #23227, Thermo Scientific). Total IRS-1 and IRS-1 pan-tyrosine phosphorylation (IRS1-pY) were analyzed with PathScan® Total IRS-1 Sandwich ELISA kit (Cat. #7328, Cell Signaling Technology®) and PathScan® Phospho-IRS-1(pan Tyr) Sandwich ELISA kit (Cat. #7133, Cell Signaling Technology®) according to manufacturer's instructions. Phosphorylation level of IRS1 was calculated according to the manufacturer's protocol by dividing absorbance values of IRS1-pY at 450 nm by absorbance values of total IRS1 at 450 nm.

RNA Extraction, Primer Design and Evaluation, Internal Control Gene (ICG) Selection, and Real-time RT-PCR (qRT-PCR)

RNA extraction, cDNA synthesis, primer design and evaluation, and real-time PCR (qPCR) were conducted as presented previously (Bionaz and Loor, 2008; the same as described in chapter 3 materials and methods). The information for primers used in this study is listed in Table S5.2. The criteria for ICG selection was described in Bionaz and Loor, 2007. In this study, 8 candidate ICGs were evaluated using GeNorm software (for detail see chapter 3 materials and methods). Analysis revealed that genes encoding beta actin (*ACTB*), ribosomal protein S9 (*RPS9*) and glyceraldehyde-3-phosphate dehydrogenase (*GAPDH*) were the most stably expressed and were finally used as ICG. Relative mRNA abundance was calculated for each gene to demonstrate the proportion of mRNA expression level of each gene in total mRNA abundance of all genes tested (for detail information on calculation of mRNA abundance, see chapter 3 materials and methods).

Statistical Analysis

To avoid problems with fitting covariance structure, pre and postpartal data for DMI, NE_L intake, energy balance, serum concentration of insulin, BHBA, and NEFA were analyzed separately as a completely randomized design using the MIXED procedure of SAS (version 9.1, SAS Institute Inc.) The fixed effects in the model were close-up diet (Trt), day or week, and Trt × day (or week) for each variable analyzed. The REPEATED statement was used for variables measured over time (DMI, NE_L intake, energy balance, milk yield, milk components, and serum insulin, BHBA and NEFA). Autoregressive covariance structure was the best fit for these data. Significance was declared when $P < 0.05$, and tendencies when $P < 0.15$.

Phosphorylation level of IRS1-pY from the negative control samples was analyzed as a 2 × 2 factorial in CRD using PROC MIXED procedure of SAS to evaluate the effects of close-up diets (Trt) and day relative to parturition (Day) on IRS1 tyrosine phosphorylation. The data from samples after insulin challenge were analyzed as 2 × 2 × 3 in CRD with the same SAS program to evaluate the main effects of Trt, Day and insulin challenge time (Time) and all the interactions of IRS1-pY.

The relative mRNA abundance data of the tested genes were normalized with the geometric mean of 3 ICGs. To ensure normal distribution of residuals, normalized data were subjected to square root transformation. This final dataset was analyzed as 2 (Trt) × 3 (Day) factorial in CRD using PROC MIXED model. Significant difference was declared at $P \leq 0.05$, and tendency of significance at $P \leq 0.10$. Contrasts were conducted for genes with significant interactions and declared significant at $P < 0.05$.

RESULTS

Performance, Serum Hormone and Metabolites, and Hepatic Lipid Accumulation

As expected, compared with CON, OVE cows had greater DMI ($P = 0.05$), NE_L intake ($P < 0.01$), energy balance ($P < 0.01$), serum insulin concentration ($P < 0.01$), and numercially lower serum NEFA concentration ($P = 0.16$) during the close-up period. In comparison with CON, close-up energy overfeeding had no effect on postpartal (within 30 DIM) DMI, NE_L intake, energy balance, serum insulin concentration ($P > 0.10$). However, OVE animals had a tendency for greater circulating BHBA ($P = 0.06$) and numercially higher serum NEFA concentration post-calving ($P = 0.15$). When comparing serum NEFA changes postpartum vs. the close-up

period between the two groups, energy overfeeding resulted in significantly higher NEFA change post-calving ($P = 0.04$) (shown in Table 5.2, Figure 5.1-5.3 and 5.5).

Close-up energy overfeeding did not affect milk production, fat-corrected milk yield (3.5% FCM), energy corrected milk yield (ECM), or any milk components either expressed as percentage or as yields ($P > 0.10$) . There was a tendency for lower milk protein percentage in OVE cows ($P = 0.10$). Both groups had greater hepatic lipid and TAG concentration postpartum ($P < 0.01$). However, prepartum energy overfeeding resulted in a more pronounced increase in both indices in early lactation. Particularly at 21 d post-calving, OVE cows still had greater TAG and lipid contents in liver compared to 7 d, whereas CON cows tended to decrease TAG and lipid between 7 and 21 d as expressed by tendency and significance of interactions of treatment and day relative to parturition (Figure 5.4).

Gene Expression

Insulin Signaling Pathawy

As shown in Figure 5.6, no treatment effect was detected for *INSR* mRNA expression ($P = 0.77$), perhaps due to the large variation observed. Overfeeding tended to increase *IRS1* expression ($P = 0.08$), which appeared to be due to the difference at 21 d post-calving. Expression of *IRS1* mRNA increased markedly in both groups at 21 d compared with -10 and 7 d ($P < 0.01$). Cows fed OVE had greater mRNA expression of *GLUT4* at -10 d ($P < 0.05$), but the expression was sharply downregulated postpartum in both groups ($P < 0.05$). In comparison with OVE cows, controlled energy feeding resulted in greater *PDE3B* expression primarily at -10 and 7 d ($P = 0.02$). The mRNA expression of this gene was lower in late pregnancy in both groups, but increased at 7 d postpartum followed by a drastic decreased at 21 d of lactation ($P < 0.01$).

de novo Lipogenesis and Desaturation

A coordinated upregulation was observed for genes involved in *de novo* FA synthesis and desaturation (*ACLY*, *ACACA*, *FASN*, and *SCD*), FA uptake and activation (*LPL*, *ACSS2*, and *ACSL1*), NADPH production and glyceroneogenesis (*G6PD*, *IDH1*, and *PCK1*), and TAG synthesis (*GPAM* and *DGAT2*) in response to close-up energy overfeeding at -10 d relative to expected parturition ($P < 0.05$). However, the mRNA expression of all these genes regardless of prepartal diet was drastically downregulated to the same expression at 7 d postpartum, and remained unchanged through 21 d of lactation ($P < 0.05$) (shown in Figure 5.7 and 5.8).

Lipolysis

Prepartal energy overfeeding led to greater mRNA expression of adipose triglyceride lipase (*ATGL*), and its activator protein *ABHD5*, at -10 and 7 d compared with controlled energy feeding ($P < 0.05$). At 21 d after calving, the expression profiles of these two genes were similar in both groups. The mRNA expression of the gene encoding the major β-adrenergic receptor in adipocyte, *ADRB2*, was increased at 21 d compared with its level at -10 d in both groups ($P < 0.01$). A numerically higher expression of *HSL* and *ADRB2* was found in OVE vs. CON cows at 7 d (shown in Figure 5.9).

Transcritpion Regulators, GHR and ANGPTL4

As shown in Figure 5.10, a significant main effect of prepartal dietary energy level was detected for the mRNA expression of the major transcription factors (TF) regulating adipogenesis, *CEBPA* ($P = 0.04$) and *PPARG* ($P = 0.03$). However, this main effect was primarily due to the remarkably higher expression of *CEBPA* and *PPARG* at -10, and PPARG at 7 d in cows fed OVE vs. CON. However, OVE cows had lower adipose *SREBF1* mRNA expression at -10 d than CON group ($P < 0.05$). A significant interaction of prepartal dietary

level and day relative to parturition was observed for the mRNA expression of *ANGPTL4* ($P < 0.05$), recognized as fasting-induced adipose factor (Kersten et al., 2000). Controlled energy feeding during the close-up period led to greater mRNA expression in AT at -10 and 21 d relative to parturition compared with overfeeding energy; whereas, the expression of this gene was sharply increased to the similar level at 7 d postpartum in both groups. The mRNA of *GHR* displayed the same expression pattern as *PPARG*.

IRS1 Tyrosine Phosphorylation

In the absence of the insulin challenge in vitro, no significant difference of prepartal overfeeding on IRS1 phosphorylation level was observed. at -10 and 7 d was However, decreased IRS1-pY was observed for both groups at 7 vs. -10 d relative to parturition. In tissue challenged with supraphysiological amounts of bovine insulin across the different time points, phosphorylation level was significantly lower in postpartal than prepartal tissue. Furthermore, adipose from OVE or CON cows responded to the same in vitro insulin challenge differently in pre- and postpartum, i.e. IRS1-pY level was greater at -10 d and lower at 7 d in OVE vs. CON cows (shown in Figure 5.11).

DISCUSSION

Production Data

Similar to what we found in previous studies (Janovick et al., 2010), CON successfully controlled the DMI during the entire dry period and limited NE_L intake close to predicted requirements. This was probably due to the bulkiness from wheat straw and the ensuing rumen fill response. Since OVE contained 9% more of ground shelled corn (GSC) than CON diet, those cows consumed ca. 1.4 kg more of GSC daily than CON animals, which may have resulted in

greater propionate production prepartum. Thus, it is reasonable to assume that hepatic gluconeogenesis was quantitatively greater in OVE animals, thus stimulating greater pancreatic insulin secretion as we found in OVE cows. Although we did not analyze serum glucose concentration in the current study, the repeatable data from two recently finished studies (Richards et al., 2009; Vasquez et al., unpublished data), which utilized the same dry period feeding strategy as the present study, showed that hyperinsulinemia due to close-up overfeeding energy was always paralleled with hyperglycemia. Regardless of treatment duration (either in far-off or close-up or the entire dry period), this and previous research from our laboratory (Dann et al., 2006; Janovick et al., 2011) and others (Holtenius et al., 2003; Rabelo et al., 2005) clearly showed that overfeeding energy by increasing NFC content resulted in higher blood concentrations of insulin and glucose level, which was analogous to the IR state found in patients with Type II diabetes.

It is noteworthy that in all studies mentioned above, circulating insulin and glucose concentrations affected only by current feeding level, and no carryover effect was observed when cows were switched to another dietary energy plane. It has long been established that late-pregnant dairy cows experience a state of peripheral insulin resistance as a mechanism to spare glucose for fetal growth (Bauman and Currie, 1980). Uterine tissues take up ca. 46% of maternal glucose supply in an insulin-independent manner in late-pregnant cows (Bell, 1995). Hence, the alternative explanation for this period of energy-overfeeding IR state is that an increase in gluconeogenesis may have exceeded the maximal disposal rate of glucose by peripheral tissues during the late pregnant period.

The same pre- and postpartal patterns as in the current study with significant differences in circulating NEFA between OVE and CON cows have been observed in previous studies in

which overfeeding was implemented for the whole dry period (Janovick et al., 2011) or during the close-up period (Vasquez et al., 2011; significant difference in pre- and numerical difference in postpartum from Richards et al., unpublished data). Relative to previous studies, the smaller number of animals (7 in each treatment) likely precluded us from detecting statistical significance in serum NEFA concentration between the two groups.

Rukkwamsuk et al. (1998) reported that adipose tissue cows overfed energy during the entire dry period collected at -1 wk relative to parturition had lower basal lipolytic rate in vitro, but tended to have greater noradrenaline-stimulated lipolysis at -1 and 3 wk in comparison with energy restricted animals. A second study from the same group demonstrated that adipose tissue from the same overfed cows had greater in vitro rates of basal esterification at -1 wk (Rukkwamsuk et al., 1999), which probably helped recycle mobilized NEFA into TAG and helps explain the lower prepartal adipose lipolytic rate in overfed cows. Thus, such responses also may partly explain the lower circulating prepartal NEFA in overfed cows in the current and previous studies (Dann et al., 2006; Janovick et al., 2010).

The greater postpartal hepatic lipid and TAG concentration and greater serum BHBA in overfed animals provide indirect evidence of greater lipolytic activity after calving. Fasting has been linked with higher NEFA mobilization and reduced peripheral response to insulin and glucose uptake (Oikawa and Oetzel, 2006). However, even though the postparturient DMI and energy balance were not different between the two groups in the current study, OVE cows still experienced a more prominent increase of serum NEFA after calving. This phenomenon does not seem to be specific to the periparturient period. Dann et al. (2006) found that cows that overconsumed higher energy in the far-off dry period and were energy restricted in the close-up period had the highest close-up serum NEFA concentrations than groups receiving CON or ca.

80% of estimated NEL requirements in the far-off and were energy restricted in the close-up period. Thus, our data and those from previous studies indicated that prepartal plane of energy nutrition impacted the mechanisms controlling lipolysis or lipolytic activity, the sensitivity to lipolytic stimulation, or a combination of these aspects.

Both prepartal dietary groups had relatively low postpartal serum insulin concentrations, thus, as adipose tissue is subjected to antilipolytic regulation by insulin, it was of great importance to determine whether prepartal overfeeding of energy predisposes animals to an exacerbated IR state resulting in greater mobilization of body fat. In the current study, close-up energy overfeeding had no benefit on milk production or component yields, yet resulted in greater postpartal NEFA which underscored the lower efficiency of such feeding strategy. Such results are consistent with the recent findings from two studies in our group, in which the same dietary treatments with larger groups of animals were employed (Richards et al., 2009; Vasquez et al., 2011).

In ruminants, hepatic uptake of circulating NEFA is in proportion to its circulating concentrations (Bell, 1979) and, relative to other species, the cow has limited capacity to synthesize VLDL in liver (Emery et al., 1992; Bauchart et al., 1996). Hence, the increased accumulation of hepatic lipid is the consequence of uncontrolled increases in blood NEFA at the onset of lactation. This phenomenon is more pronounced when cows are fed with high-energy density, high-starch diets during the dry period (current study; Grum et al., 1996; Holtenius et al., 2003; Janovick et al., 2011). Hepatic metabolic adaptations to periparturient nutritional plane was not the focus of current study, and readers are referred to recent reviews (Drackley et al., 2001; Friggens et al., 2004) for more detailed information on that aspect.

IRS1 Tyrosine Phosphorylation and Expression of Insulin Signaling Genes

The underlying mechanisms of IR during the transition period are still unclear. Using the euglycemic hyperinsulinemic clamp, Petterson et al. (1993) demonstrated that IR during late pregnancy was primarily due to impaired peripheral insulin sensitivity, which suggested that mechanisms involved reduction in INSR binding or defects in early post-receptor signal transduction. Early studies regarding alterations of INSR numbers and binding affinity were mainly conducted with ewes and failed to give conclusive results (Vernon et al., 1981; Vernon and Taylor, 1988; Guesnet et al., 1991). Guesnet et al. (1991) reported a 62% decrease of INSR accompanied by markedly decreased insulin-stimulated lipogenesis in omental AT of early lactating ewes. Vernon and Taylor (1988) showed that, compared with non-lactating controls, SAT from early lactation ewes had both reduced sensitivity and response to insulin stimulated glucose uptake and FA synthesis in vitro. However, neither number nor binding affinity of INSR differed between the two physiological states. Recently, a similar study showed that the mRNA expression of INSR in SAT of periparturient dairy cows remained unchanged from 8 wk pre- to 5 wk postpartum (Sadri et al., 2010). In the current study, with greater degree of variation, *INSR* expression was not affected during the transition period, which seems to highlight a weak association with transition period IR.

Vernon and Taylor (1988) attributed lactational IR to defects in intracellular insulin signaling transduction at the post-receptor level. At the molecular level, insulin receptor substrates (IRS) are the proteins that carry out the first intracellular step mediating insulin signaling. IRS1, rather than the other isoforms, is preferentially involved in insulin-induced metabolic actions including glucose uptake (Saltiel and Kahn, 2001). Phosphorylation of IRS1

on tyrosine residues is required for insulin stimulated glucose uptake. A substantial body of research demonstrated a causal relationship between compromised tyrosine phosphorylation of IRS1 (IRS1-pY) and adipose IR in either late pregnant rodents (Sevillano et al., 2007) or in cases of obesity-induced Type II diabetis (Esposito et al., 2001; Sesti et al., 2001; Smith, 2002).

IRS1-pY was shown to be relatively sustained due to less dephosphorylation by phosphatase (Ogihara et al., 1997), so we assume that the phosphorylation level of IRS1 in adipose tissue that adapted to the culture medium without bovine insulin for 30 min was still representative of its basal physiological state. As shown in Figure 5.11, IRS1-pY was significantly reduced at 7 d postpartum compared with 10 d before calving, which suggested a lower degree of insulin signaling postpartum. However, we do not believe that this result alone was indicative of exacerbated an IR state in early lactation because lower IRS1-pY also may be due to the postpartal hypoinsulinemia observed. Similarly, the numerically lower prepartal IRS1-pY in cows fed CON may have resulted from lower serum insulin concentration in those animals.

A supraphysiological challenge with bovine insulin should have elicited maximal response in IRS-pY, which was clearly reflected by the much higher phosphorylation level after insulin challenge. After insulin stimulation and regardless of prepartal diet, the IRS1-pY was still much lower in postpartal than prepartal tissue. Thus, we speculate that animals experienced more severe peripheral IR early post-calving to spare more glucose for milk synthesis. At the transcriptional level, no significant dietary treatment difference was observed in *IRS1* mRNA expression between -10 and 7 d, which suggests that defects in posttranslational modification of IRS1 is likely the major mechanism exacerbating IR at the initiation of lactation. The concomitant decrease of *GLUT4* expression also represented a reduction in the capacity of glucose uptake by adipose during early lactation. If a similar scenario was prevailing in goats, it

may help to interpret the diminished whole-body glucose utilization in response to insulin in lactating vs. nonlactating goats (Debras et al., 1989). This may at least in part also be responsible for the loss of lipogenic activity in subcutaneous adipose tissue of early lactating cows (McNamara et al., 1995), as glucose is an important source of cytosolic NADPH required for FA biosynthesis (Bauman, 1976). The increase in mRNA expression of IRS1 in both groups from 7 to 21 d postpartum suggests that transcriptional regulation may be involved in the process of restoration of insulin responsiveness after calving.

Contrary to our hypothesis, OVE cows had higher insulin-stimulated IRS1-pY and *GLUT4* mRNA expression than CON cows prepartum, and no significant difference was observed between the two groups postpartum, i.e., close-up energy overfeeding did not predispose animals to a more IR status but rather if anything seemed to have enhanced insulin sensitivity. Holtenius et al. (2003) reported a greater glucose clearance rate (GCR) after a glucose tolerance test (GTT) in overfed vs. underfed cows at 3 wk prior to calving. Therefore, the higher GCR may have reflected the real peripheral response to GTT in overfed cows. Ruminants have lower peripheral insulin responsiveness in terms of glucose utilization relative to humans and rodents (e.g. maximal insulin-stimulated glucose utilization rate for sheep or bovine was 50-75% and 15-20% of the rate for human and rats; Hocquette et al, 1996), and insulin had insufficient inhibitory effect on propionate-derived hepatic gluconeogenesis (Brockman, 1990; Donkin and Amentano, 1995). The higher prepartal serum insulin and glucose concentration in overfed cows as observed in the current study (glucose was not measured) and other studies (Holtenius et al., 2003; Dann et al., 2006; Janovick et al., 2011) may be due to the fact that the increase in gluconeogenesis induced by energy overfeeding overwhelmed the mechanisms of

peripheral tissue glucose utilization in late pregnancy, rather than contributed to an exacerbated insulin resistance.

Insulin antagonizes cAMP-mediated lipolytic signaling downstream of IRS signaling pathway through activation of PDE3B in an AKT-dependent manner (Kitamura et al., 1999; Degerman et al., 2003). Upon insulin-stimulated phosphorylation, PDE3B catalyzes metabolism of cAMP into AMP, which in turn reduces the activation of PKA and consequently blunts hormone-stimulated lipolysis in adipocytes. The lower prepartal serum NEFA in OVE cows may have been caused by higher circulating insulin and greater adipose insulin sensitivity. Interestingly, adipose from CON cows, which had greater prepartal NEFA level, also had greater mRNA expression of *PDE3B* at -10 and 7 d. Those responses suggested the existence of a feedback-regulating mechanism that was activated in response to a blunted anitlipolytic response by insulin (i.e., signaling may have been "impaired") through upregulation of *PDE3B* expression. Such mechanism was more pronounced for both groups at 7 d and coincided with a marked increase in serum NEFA and exacerbated IR postpartum. Hence, the prolonged upregulation of *PDE3B* postpartum as a consequence of controlled energy feeding during the dry period may be one of the factor that contributes to lower postpartal lipolysis relative to OVE cows.

Lipogenesis

Recent studies in ruminants has provided compelling evidence that transcriptional regulation in response to different nutritional planes and physiological status is an important control mechanism of lipid metabolism in mammary gland (Bauman et al., 2008; Bionaz and Loor, 2008), skeletal muscle (Graugnard et al., 2009), liver (Loor et al., 2005, 2006), and adipose tissue (Loor, 2010). In non-lactating ruminants, adipose tissue is the principal site of lipogenesis (Bergen and Mersmann, 2005). Previous studies showed that cows overconsuming energy during

the dry period gained more weight and body condition before calving (Dann et al., 2006; Janovick et al., 2010). In the current study, expression of *ACACA*, *FASN*, and *SCD*, encoding the major enzymes involved in *de novo* fatty acid synthesis (DNS), was upregulated in OVE cows at -10 d likely as a result of excessively positive energy balance. As acetate is the major precursor for DNS in ruminant adipose tissue (Hood et al., 1972), the higher expression of *ACSS2* indicated that OVE cows had the potential to activate and channel more acetate from blood towards adipogenesis during the dry period. Although classic in vitro studies showed low activity of ATP-citrate lyase (ACLY) in ruminant adipose (Ingle et al., 1972a), which indicated minimal contribution of glucose-derived carbon for lipogenesis, we still observed a more than 2-fold increase in mRNA expression of *ACLY* at -10 d in response to OVE vs. CON. Thus, data indicate potentially greater glucose use for lipogenesis in those cows and also that this enzyme is adaptable, at least at the transcriptional level, to nutrient availability and particularly dietary starch content as was observed previously in beef skeletal muscle (Graugnard et al., 2010).

In ruminant adipose tissue, the cytosolic isocitrate dehydrogenase (IDH1) and pentose phosphate pathway were highlighted as the predominant sources for NADPH production to support DNS (Ingle et al., 1972b). Both *IDH1* and *G6PD*, the rate limiting enzymes controlling each pathway, were coordinately upregulated along with the other lipogenic genes in OVE vs. CON cows in the prepartal period. Those responses support the notion that lipogenesis was enhanced by energy overfeeding. In fact, not only was DNS apparently increased but the process of uptake of preformed FA also was probably enhanced prepartum by energy overfeeding as reflected by greater expression of *LPL* and *ACSL1* in OVE vs. CON cows.

Lastly, the greater expression of *GPAM* and *DGAT2* in OVE vs. CON group at -10 d seems to be in agreement with the greater prepartal basal adipose esterification rates found

previously in energy-overfed vs. restricted-fed cows (Rukkwamsuk et al., 1999), which also supports our hypothesis that lower prepartal serum NEFA in OVE vs. CON cows may have partially resulted from greater recycling of NEFA within adipose tissue through re-esterification. Overall, the data discussed here strongly indicate that adipose lipogenesis was stimulated by enhanced plane of energy nutrition in late pregnancy and, at the transcriptional level, the entire process was synchronized, i.e., there was likely a strong degree of co-regulation via a transcription factor or nuclear receptor.

In the current study, the remarkable and coordinated downregulation of lipogenic genes after calving explains the nearly complete loss of in vitro lipogenic enzyme activity in adipose tissue from early lactating dairy cows (McNamara et al. 1995). No carryover effects of prepartal plane of nutrition were detectable postpartum for any of these genes, indicating that the well-established physiological changes (NEB, hormonal environment, stress) around parturition override the impact of dry period nutritional management on adipose lipogenesis.

Insulin, the principal anabolic hormone that stimulates transcription of lipogenic genes in adipocytes, mediates parts of its response through activation of transcriptional regulators (Kersten, 2001; Griffin and Sul, 2004; Rosen and MacDougald, 2006). In the present study, the expression pattern of lipogenic genes during the transition period matched well the changes observed in serum insulin concentration and insulin sensitivity assessed by IRS1-pY, regardless of plane of nutrition prepartum. Therefore, we speculate that postparturient hypoinsulinemia and exaggerated IR directly cause the suppression of mRNA expression of lipogenic genes.

Lipolysis

The classic lipolytic pathway in response to β-adrenergic stimulation and HSL is well-established. Not until recently has accumulating evidence indicated the existence of another

lipolytic enzyme, adipose triglyceride lipase (ATGL), that is highly expressed in white adipose tissue and is primarily responsible for basal and β-adrenergic-stimulated TAG hydrolysis (Miyoshi et al., 2007 and 2008). The complete activation of ATGL requires binding to its activator protein ABHD5 after it dissociates from perilipin following phosphorylation induced by β-adrenergic stimulation (see review by Zechner et al., 2009). Due to the specificity or preference of its substrate (triacylglycerol), ATGL is now considered the rate-limiting enzyme of lipolysis in mammals (Haemmerle et al., 2006). The anti-lipolytic effect of insulin reduces the activity of PKA by stimulating PDE3B, which increases catabolism of cytosolic cAMP, thereby preventing phosphorylation of PLIN and effectively reversing the dissociation of PLIN and ABHD5 (Subramanian et al., 2004).

Based on the known roles of ATGL and ABDH5, it was interesting that OVE cows had both lower prepartal serum NEFA and higher mRNA expression of *ATGL* and *ABHD5*. Despite the well-characterized posttranslational modification of lipolytic enzyme activities, the amount of available enzyme, which is regulated at the transcriptional level, may also affect the magnitude of lipolytic reactions. As discussed previously OVE cows had higher prepartal serum insulin and likely undiminished insulin sensitivity compared with CON cows, i.e. lower lipolytic capacity. In addition, transcriptional adaptations in these cows likely resulted in greater potential for re-esterification of NEFA released from either basal or stimulated lipolysis. Thus, despite the greater mRNA expression of *ATGL* and *ABHD5*, it is possible that lipolysis was still tightly controlled in OVE cows prepartum.

Postpartum, both *ATGL* and *ABHD5* mRNA expression were decreased in both groups, which agrees with the reduced adipose ATGL protein expression in early lactating vs. late pregnant dairy cows observed recently (Koltes and Spurlock, 2011). Both mRNA and protein

expression of *ATGL* in AT were reduced in individuals with obesity-induced insulin resistance compared with insulin-sensitive subjects (Jocken et al., 2007). The parallel postpartal decrease of *ATGL* mRNA expression with IRS1-pY implicates that insulin sensitivity is required to maintain *ATGL* expression in bovine adipocytes. However, the carryover effect of close-up energy overfeeding was maintained because both genes were upregulated at 7 d postpartum in OVER cows compared with. CON cows. Interestingly, the mRNA expression of *HSL* and *ADRB2* (the major isoform of β-adrenergic receptor in adipocytes, Table 5.3) also was greater in OVE than CON cows at 7 d. Such response indicated that OVE cow may have been more sensitive to lipolytic stimulation, e.g. via norepinephrine, postpartum. On the other hand, adipose insulin sensitivity and responsiveness (assessed by decreased IRS1-pY and *GLUT4* mRNA expression) and esterification capacity (assessed by decreased mRNA of *GPAM*, *DGAT2* and *PCK1*) appeared to have been depressed to the same extent in both dietary groups.

The sympathetic nervous system in AT appears to be more active during early lactation (McNamara and Murray, 2001). Koltes and Spurlock (2010) found increased phosphorylation of HSL early post-calving compared with late pregnancy, despite unchanged HSL protein expression, which supported the notion of greater postparturient β-adrenergic stimulated lipolysis. Together, these data allow a better mechanistic explanation of the greater circulating NEFA in OVE cows early postpartum as has been repeatedly observed in recent studies (Holtenius et al., 2003; Dann et al., 2006; Janovick et al., 2011). The greater expression of lipolytic genes (*ATGL*, *HSL*, and *ADRB2*) also provides answers for the greater in vitro noradrenaline-stimulated lipolysis in adipose tissue from cows that were overfed energy during the dry period compared with restricted-fed cows (Rukkwamsuk et al., 1998). In comparison with d -10, the mRNA expression of the major adipose β-adrenergic receptor *ADRB2* was increased in both groups,

indicating that the increased lipolysis during early lactation is not simply a cause of decreased insulin responsivennes but also increased sensitivity to lipolytic stimulation.

Transcriptional Regulation

One of the well-established functions of insulin is to stimulate adipogenesis, the differentiation process of preadipocyte into lipid-loaded mature adipocytes. This process is initialized by activating the sequential expression of a series of transcription regulators; PPARγ and C/EBPα induced by "early" transcription regulators (mainly C/EBPβ and C/EBPδ) are considered the "master regulators" mediating insulin signals to activate transcription of most lipogenic genes (Rosen and MacDougald, 2006). In comparison with CON cows, the coordinated upregulation of lipogenic genes at -10 d in OVE-fed cows paralleled the greater expression of *PPARG* and *CEBPA*. Despite a lack of direct evidence in bovine adipocytes, Kadegowda et al. (2009) found increased mRNA expression of *ACACA*, *FASN*, *DGAT1*, *LPIN1*, and *AGPAT6* in bovine mammary epithelial cells when the culture medium was supplemented with the PPARγ agonist rosiglitazone. Thus, we suggest from our data that expression of lipogenic genes was probably subject to PPARγ transcriptional regulation.

The accumulating literature has defined multiple roles of C/EBPα in adipogenesis. First, the presence of C/EBPα was required for maintaining PPARγ expression during adipocyte differentiation in non-ruminants (Farmer, 2006). Furthermore, blunting *CEBPA* expression led to markedly lower expression of *PPARG*, *FABP4*, *GLUT4* and *DGAT2* in 3T3-L1 preadipocytes even after culture in differentiation-stimulating medium for 5 d (Payne et al., 2010). Mice deficient in C/EBPα have defective development of white AT (Linhart et al., 2001). Our data revealed an expression pattern of *CEBPA* identical to that of lipogenic genes in response to dietary treatment and the change in physiological state during transition period; whereas, despite

a moderate decrease after calving, *PPARG* expression was still significantly greater in AT of overfed vs. control cows at 7 d postpartum. Thus, our results seem to implicate that the presence of C/EBPα is required to sustain the expression of lipogenic genes. The presence of C/EBPα is also required for acquisition of insulinsensitivity in adipocytes. Differentiated C/EBPα(-/-) fat cells (induced by ectopic expression of PPARγ) completely lost insulin-stimulated glucose uptake, which is primarily due to reduced gene expression and tyrosine phosphorylation of *INSR* and *IRS1* (Wu et al., 1999). Whether the reduced adipose IRS1-pY postpartum observed in the current study resulted from the decreased expression of *CEBPA* warrants further research.

The transcription factor SREBF1c has well-documented importance in stimulating hepatic lipogenic gene expression in humans and rodents (Foufelle and Ferré, 2002). It also has been reported as another important pro-adipogenic transcription factor (Eberle et al., 2004), partly due to the production of an as-yet unknown endogenous PPARγ ligand in adipocytes (Kim and Spiegelman, 1996; Kim et al., 1998). However, in our study, *SREBF1* expression was lower in energy-overfed vs. control cows at -10 d, which is the opposite of the expression of lipogenic genes and *PPARG*. Thus, our data do not support a key role of *SREBF1* in lipogenesis of subcutaneous AT at least from a transcriptional standpoint.

In the present study, we observed the same expression pattern of *PPARG* and *ATGL* in response to energy overfeeding. In fully-differentiated 3T3-L1 adipocytes, both *ATGL* mRNA and protein expression are induced by PPARγ agonists in a dose- and time-dependent manner (Kershaw et al., 2007). The same response of *ATGL* was observed in WAT of either lean or obese mice following oral treatment with the PPARγ agonist rosiglitazone (Kershaw et al., 2007). Such transcriptional regulation of *ATGL* by PPARγ was supported by another study as well (Kim et al., 2006). Therefore, we postulate that increased prepartal insulin in response to overfeeding

energy stimulated *PPARG* expression and its activity as a transcription factor, which. in turn increased transcription of *ATGL*. However, the carryover effect of overfeeding energy seems to have maintained a greater expression of *PPARG* (and probably its activity) only through the first few days post-calving. As a consequence, the *ATGL* mRNA expression remained higher in OVE cows in early lactation. That effect likely contributed to the greater magnitude of lipolysis in OVE cows. The transcriptional regulation of PPARγ on *ATGL* warrants further research.

Other Factors Involved in the Regulation of Lipid Homeorhesis During the Periparturient Period

Besides insulin, growth hormone (GH) also plays an important role in orchestrating the metabolic adaptation and nutrient partitioning (Bauman and Vernon, 1993). Growth hormone stimulates hepatic synthesis and secretion of IGF-1, which serves as feedback signal to control GH release (Le Roith et al., 2001). However, early lactation was characterized as a period of uncoupling of the GH – IGF-1 axis (Lucy, 2008). The plasma concentration of GH of dairy cows was increased during early lactation, when animals were experiencing NEB (Bell, 1995). Growth hormone targeting of AT functionally antagonizes insulin's effects by amplifying the lipolytic response to β-adrenergic signals and inhibiting lipogenesis (Etherton and Bauman, 1998). Thus, the greater circulating GH concentration contributes to increased lipolysis postpartum. Rhoads et al. (2004) reported that the abundance of GHR protein in AT of dairy cows fell in paralleled the decrease of plasma insulin concentration from late pregnancy (-28 d) to early lactation (10 d). Administration of exogenous insulin increased adipose GHR protein expression in both late pregnancy and early lactation (Rhoads et al., 2004). In the current study, close-up overfeeding increased adipose mRNA expression of *GHR* at -10 d, which may have been mediated by the increased plasma insulin concentration in OVE cows. Despite decreased postpartal expression in

both groups, the carryover effect of energy overfeeding maintained greater *GHR* mRNA in OVE cows vs. CON cows at 7 d postpartum. Hence, the OVE cows may be more responsive to increased GH postpartum and have greater lipolytic activity in AT.

Adipose tissue also serves as an active endocrine organ to affect metabolic homeostasis by secreting an array of adipocytokines. Both mRNA and protein,of ANGPTL4 (fasting-induced adipose factor), are highly expressed in WAT and liver of rodents (Kersten et al., 2000) and humans (Kersten et al., 2009) as well as in cattle (Mamedova et al., 2010). A growing body of literature demonstrated that *ANGPTL4* is upregulated in adipose tissue by fasting and inhibits LPL activity with a consequent increase in lipolysis (see reviews by Kersten, 2005 and Hato et al., 2008). Mice lacking ANGPTL4 (Angptl4$^{-/-}$) have increased ability to gain weight (Bäckhed et al., 2004); whereas, mice overexpressing this protein in WAT have a remarkably limited capability for TAG accumulation and have increased concentrations of circulating TAG and NEFA (Mandard et al., 2006).

In the present study, changes in adipose mRNA expression of *ANGPTL4* during the periparturient period coincided with changes of circulating NEFA concentration in both groups. Particularly prepartum, the OVE cows had lower expression of *ANGPTL4*, greater *LPL* mRNA, and lower serum NEFA than CON cows. However, such a relationship did not seem to apply at 21 d postpartum. Despite being identified as a target gene of PPARγ in preadipocytes in mice (Yoon et al., 2000), our study does not support such abrelationship at least from the *PPARG* standpoint. Further research is required to clarify the function of *ANGPTL4* in the regulation of lipid homeostasis in peripartal cows.

CONCLUSIONS

The results of the present study provide evidence that moderately overfeeding energy during the last 3 wk of the prepartal period facilitates rather than compromises the pathway of insulin signaling in subcutaneous adipose tissue of dairy cows. This may contribute to the increase in lipogenic gene expression and, potentially, lipid deposition in adipose tissue both in subcutaneous and internal depots. Adipose insulin resistance may be exacerbated postpartum vs. prepartum due to both reduced circulating insulin and increased lipolytic stimuli. Physiological adaptations around parturition overwhelmed the transcriptional adaptations of adipose lipogenic genes induced by prepartal energy overfeeding. However, the sustained higher expression of lipolytic-related genes including *ATGL* and *ABHD5* and the lower mRNA expression of *PDE3B* may contribute to the parallel and remarkably increased rates of lipolysis that were apparent in overfed animals at the initiation of lactation. Our study highlighted the presumed pivotal role of PPARγ and CEBPα as the major transcriptional regulators of lipogenic gene expression during the preparturient period. In addition, we speculate that PPARγ may transcriptionally activate *ATGL* expression as well and serve as the link between lipogenesis (and adipogenesis) and lipolysis.

LITERATURE CITED

AOAC. 1995. Official Methods of Analysis. 16th ed. AOAC International, Arlington, VA.

Bäckhed, F., H. Ding, T. Wang, L. V. Hooper, G. Y. Koh, A. Nagy, C. F. Semenkovich, and J. I. Gordon. 2004. The gut microbiota as an environmental factor that regulates fat storage. Proc. Natl. Acad. Sci. U.S.A. 101:15718–15723.

Bauman, D. E. 1976. Intermediary metabolism of adipose tissue. Fed. Proc. 35:2308-2313.

Bauman, D. E., and W. B. Currie. 1980. Partitioning of nutrients during pregnancy and lactation: a review of mechanisms involving homeostasis and homeorhesis. J. Dairy Sci. 63:1514-1529.

Bauman, D. E., and R. G. Vernon. 1993. Effects of exogenous bovine somatotropin on lactation. Annu. Rev. Nutr. 13:437-461.

Bauman, D. E., J. W. Perfield II, K. J. Harvatine, and L. H. Baumgard. 2008. Regulation of fat synthesis by conjugated linoleic acid: Lactation and the ruminant model. J. Nutr. 138:403-409.

Bauchart, D., D. Gruffat, and D. Durand. 1996. Lipid absorption and hepatic metabolism in ruminants. Proc. Nutr. Soc. 55:39–47.

Bell, A. W. 1979. Lipid metabolism in liver and selected tissues and in the whole body of ruminant animals. Prog. Lipid Res. 18:117-164.

Bell, A. W. 1995. Regulation of organic nutrient metabolism during transition from late pregnancy to early lactation. J. Anim. Sci. 73:2804-2819.

Bergen, W. G., and H. J. Mersmann. 2005. Comparative aspects of lipid metabolism: impact on contemporary research and use of animal models. J. Nutr. 135:2499-2502.

Bionaz, M., and J. J. Loor. 2007. Identification of reference genes for quantitative real-time PCR in the bovine mammary gland during the lactation cycle. Physiol. Genomics. 29:312-319.

Bionaz, M., and J. J. Loor. 2008. Gene networks driving bovine milk fat synthesis during the lactation cycle. BMC Genomics. 9:366-387.

Brockman, R. P. 1990. Effect of insulin on the utilization of propionate in gluconeogenesis in sheep. Br. J. Nutr. 64:95-101.

Dann, H. M., N. B. Litherland, J. P. Underwood, M. Bionaz, A. D'Angelo, J. W. McFadden, and J. K. Drackley. 2006. Diets during far-off and close-up dry periods affect periparturient metabolism and lactation in multiparous cows. J. Dairy Sci. 89:3563-3577.

Debras, E., J. Grizard, E. Aina, S. Tesseraud, C. Champredon, and M. Arnal. 1989. Insulin sensitivity and responsiveness during lactation and dry period in goats. Am. J. Physiol. 256:E295–E302.

Degerman, E., T. R. Landström, L. S. Holst, O. Göransson, L. Härndahl, F. Ahmad, Y. –H. Choi, S. Masciarelli, H. Liu, and V. Manganiello. 2003. Role for Phosphodiesterase 3B in Regulation of Lipolysis and Insulin Secretion. In Diabetes Mellitus: A Fundamental and Clinical Text. D. LeRoith, J. M. Olefsky, and S. I. Taylor, eds. Philadelphia: Lippincott Williams & Wilkins, pp.374–381.

Donkin, S. S., and L. E. Armentano. 1995. Insulin and glucagon regulation of gluconeogenesis in preruminating and ruminating bovine. J. Anim. Sci. 73:546-551.

Douglas, G. N., T. R. Overton, H. G. Bateman 2nd, H. M. Dann, and J. K. Drackley. 2006. Prepartal plane of nutrition, regardless of dietary energy source, affects periparturient metabolism and dry matter intake in Holstein cows. J. Dairy Sci. 89:2141-2157.

Drackley, J. K., T. R. Overton, and G. N. Douglas. 2001. Adaptations of glucose and long-chain fatty acid metabolism in liver of dairy cows during the periparturient period. J. Dairy Sci. 84(E. Suppl.):E100-E112.

Eberle, D., B. Hegarty, P. Bossard, P. Ferre, and F. Foufelle. 2004. SREBP transcription factors: master regulators of lipid homeostasis. Biochimie 86:839-848.

Emery, R. S., J. S. Liesman, and T. H. Herdt. 1992. Metabolism of long chain fatty acids by ruminant liver. J. Nutr. 122:832–837.

Esposito, D. L., Y. Li, A. Cama, M. J. Quon. 2001. Tyr(612) and Tyr(632) in human insulin receptor substrate-1 are important for full activation of insulin-stimulated phosphatidylinositol 3-kinase activity and translocation of GLUT4 in adipose cells. Endocrinology 142:2833-2840.

Etherton, T. D., and D. E. Bauman. 1998. Biology of somatotropin in growth and lactation of domestic animals. Physiol. Rev. 78:745-761.

Farmer, S. R. 2006. Transcriptional control of adipocyte formation. Cell Metab. 4:263-273.

Foran, P. G., L. M. Fletcher, P. B. Oatey, N. Mohammed, J. O. Dolly, and J. M. Tavare. 1999. Protein kinase B stimulates the translocation of GLUT4 but not GLUT1 or transferrin receptors in 3T3-L1 adipocytes by a pathway involving SNAP-23, synaptobrevin-2, and/or cellubrevin. J. Biol. Chem. 274:28087-28095.

Foufelle, F., and P. Ferré. 2002. New perspectives in the regulation of hepatic glycolytic and lipogenic genes by insulin and glucose: a role for the transcription factor sterol regulatory element binding protein-1c. Biochem. J. 366:377-391.

Friggens, N. C., J. B. Andersen, T. Larsen, O. Aaesb, and R. J. Dewhurst. 2004. Priming the dairy cow for lactation: a review of dry cow feeding strategies. Anim. Res. 53:453-473.

Graugnard, D. E., L. L. Berger, D. B. Faulkner, and J. J. Loor. 2010. High-starch diets induce precocious adipogenic gene network up-regulation in longissimus lumborum of early-weaned Angus cattle. Br. J. Nutr. 103:953-963.

Graugnard, D. E., P. Piantoni, M. Bionaz, L. L. Berger, D. B. Faulkner, and J. J. Loor. 2009. Adipogenic and energy metabolism gene networks in longissimus lumborum during rapid post-weaning growth in Angus and Angus x Simmental cattle fed high-starch or low-starch diets. BMC Genomics. 10:142-157.

Griffin, M. J., and H. S. Sul. 2004. Insulin regulation of fatty acid synthase gene transcription: roles of USF and SREBP-1c. IUBMB Life 56:595-600.

Grum, D. E., J. K. Drackley, R. S. Younker, D. W. LaCount, and J. J. Veenhuizen. 1996. Nutrition during the dry period and hepatic lipid metabolism of periparturient dairy cows. J. Dairy Sci. 79:1850-1864.

Grummer, R. R. 1995. Impact of changes in organic nutrient metabolism on feeding the transition dairy cow. J. Anim. Sci. 73:2820-2833.

Guesnet, P. M., M. J. Massoud, and Y. Demarne. 1991. Regulation of adipose tissue metabolism during pregnancy and lactation in the ewe: the role of insulin. J. Anim. Sci. 69:2057-2065.

Haemmerle, G., A. Lass, R. Zimmermann, G. Gorkiewicz, C. Meyer, J. Rozman, G. Heldmaier, R. Maier, C. Theussl, S. Eder, D. Kratky, E. F. Wagner, M. Klingenspor, G. Hoefler, and R. Zechner. 2006. Defective lipolysis and altered energy metabolism in mice lacking adipose triglyceride lipase. Science 312:734-737.

Hato, T., M. Tabata, and Y. Oike. 2008. The role of angiopoietin-like proteins in angiogenesis and metabolism. Trends Cardiovasc. Med. 18:6-14.

Häussler, S., S. Dänicke, K. Friedauer, D. Germeroth, D. von Soosten, and H. Sauerwein. 2011. Dynamics of fat cell turnover in visceral and subcutaneous fat tissue in dairy cows. J. Dairy Sci. 94(E-suppl.):345.

Hocquette, J. F., M. Balage, and P. Ferré. 1996. Facilitative glucose transporters in ruminants. Proc. Nutr. Soc. 55:221-236.

Holtenius, K., S. Agenäs, C. Delavaud, and Y. Chilliard. 2003. Effects of feeding intensity during the dry period. 2. Metabolic and hormonal responses. J. Dairy Sci. 86:883-891.

Hood, R. L., E. H. Thompson, and C. E. Allen. 1972. The role of acetate, propionate and glucose as substrates for lipogenesis in bovine tissues. Int. J. Biochem. 3:598-606.

Ingle, D. L., D. E. Bauman, and U. S. Garrigus. 1972a. Lipogenesis in the ruminant: in vivo site of fatty acid synthesis in sheep. J. Nutr. 102:617-623.

Ingle, D. L., D. E. Bauman, and U. S. Garrigus. 1972b. Lipogenesis in the ruminant: in vitro study of tissue sites, carbon source and reducing equivalent generation for fatty acid synthesis. J. Nutr. 102:609-616.

Ingvartsen, K. L., and J. B. Andersen. 2000. Integration of metabolism and intake regulation: a review focusing on periparturient animals. J. Dairy Sci. 83:1573–1597.

Janovick, N. A., and J. K. Drackley. 2010. Prepartum dietary management of energy intake affects postpartum intake and lactation performance by primiparous and multiparous Holstein cows. J. Dairy Sci. 93:3086-3102.

Janovick, N. A., Y. R. Boisclair, and J. K. Drackley. 2011. Prepartum dietary energy intake affects metabolism and health during the periparturient period in primiparous and multiparous Holstein cows. J. Dairy Sci. 94:1385-1400.

Jocken, J. W., D. Langin, E. Smit, W. H. Saris, C. Valle, G. B. Hul, C. Holm, P. Arner, and E. E. Blaak. 2007. Adipose triglyceride lipase and hormone-sensitive lipase protein expression is decreased in the obese insulin-resistant state. J. Clin. Endocrinol. Metab. 92:2292-2299.

Kadegowda, A. K., M. Bionaz, L. S. Piperova, R. A. Erdman, and J. J, Loor. 2009. Peroxisome proliferator-activated receptor-gamma activation and long-chain fatty acids alter lipogenic gene networks in bovine mammary epithelial cells to various extents. J. Dairy Sci. 92:4276-4289.

Kershaw, E. E., M. Schupp, H. P. Guan, N. P. Gardner, M. A. Lazar, and J. S. Flier. 2007. PPARgamma regulates adipose triglyceride lipase in adipocytes in vitro and in vivo. Am. J. Physiol. Endocrinol. Metab. 293:E1736-E1745.

Kersten, S. 2005. Regulation of lipid metabolism via angiopoietin-like proteins. Biochem. Soc. Trans. 33:1059-1062.

Kersten, S., L. Lichtenstein, E. Steenbergen, K, Muddle, H. F. Hendriks, M. K. Hesselink, P. Schrauwen, and M. Müller. 2009. Caloric restriction and exercise increase plasma ANGPTL4 levels in humans via elevated free fatty acids. Arterioscler. Thromb. Vasc. Biol. 29:969–974.

Kersten, S., S. Mandard, N. S. Tan, P. Escher, D. Metzger, P. Chambon, F. J. Gonzalez, B. Desvergne, and W. Wahli. 2000. Characterization of the fasting-induced adipose factor FIAF, a novel peroxisome proliferator-activated receptor target gene. J. Biol. Chem. 275:28488–28493.

Kersten, S. 2001. Mechanisms of nutritional and hormonal regulation of lipogenesis. EMBO Rep. 2:282-286.

Kim, J. B., and B. M. Spiegelman. 1996. ADD1/SREBP1 promotes adipocyte differentiation and gene expression linked to fatty acid metabolism. Genes Dev. 10:1096–1107.

Kim, J. B., H. M. Wright, M. Wright, and B. M. Spiegelman. 1998. ADD1/SREBP1 activates PPARγ through the production of endogenous ligand. Proc. Natl. Acad. Sci U.S.A. 95:4333–4337.

Kim, J. Y., K. Tillison, J. H. Lee, D. A. Rearick, and C. M. Smas. 2006. The adipose tissue triglyceride lipase ATGL/PNPLA2 is downregulated by insulin and TNF-alpha in 3T3-L1 adipocytes and is a target for transactivation by PPARgamma. Am. J. Physiol. Endocrinol. Metab. 291: E115-E127.

Kitamura, T., Y. Kitamura, S. Kuroda, Y. Hino, M. Ando, K. Kotani, H. Konishi, H. Matsuzaki, U. Kikkawa, W. Ogawa, and M. Kasuga.1999. Insulin-induced phosphorylation and activation of cyclic nucleotide phosphodiesterase 3B by the serine-threonine kinase Akt. Mol. Cell Biol. 19:6286-6296.

Koltes, D. A., and D. M. Spurlock. 2011. Coordination of lipid droplet-associated proteins during the transition period of Holstein dairy cows. J. Dairy Sci. 94:1839-1848.

Le Roith, D., C. Bondy, S. Yakar, J. L. Liu, and A. Butler. 2001. The somatomedin hypothesis: 2001. Endocr. Rev. 22:53-74.

Linhart, H. G., K. Ishimura-Oka, F. DeMayo, T. Kibe, D. Repka, B. Poindexter, R. J. Bick, and G. J. Darlington. 2001. C/EBPalpha is required for differentiation of white, but not brown, adipose tissue. Proc. Natl. Acad. Sci. U S A. 98:12532-12537.

Loor, J. J. 2010. Genomics of metabolic adaptations in the peripartal cow. Animal. 4:1110–1139.

Loor, J. J., H. M. Dann, R. E. Everts, R. Oliveira, C. A. Green, N. A. Guretzky, S. L. Rodriguez-Zas, H. A. Lewin, and J. K. Drackley. 2005. Temporal gene expression profiling of liver from periparturient dairy cows reveals complex adaptive mechanisms in hepatic function. Physiol. Genomics. 23:217-226.

Loor, J. J., H. M. Dann, N. A. Guretzky, R. E. Everts, R. Oliveira, C. A. Green, N. B. Litherland, S. L. Rodriguez-Zas, H. A. Lewin, and Drackley JK. 2006. Plane of nutrition prepartum alters hepatic gene expression and function in dairy cows as assessed by longitudinal transcript and metabolic profiling. Physiol. Genomics. 27:29-41.

Lucy, M. C. 2008. Functional differences in the growth hormone and insulin-like growth factor axis in cattle and pigs: implications for post-partum nutrition and reproduction. Reprod. Domest. Anim. 43 Suppl 2:31-39.

Mamedova, L. K., K. Robbins, B. J. Johnson, and B. J. Bradford. 2010. Tissue expression of angiopoietin-like protein 4 in cattle. J. Anim. Sci. 88:124-130.

Mandard, S., F. Zandbergen, E. van Straten, W. Wahli, F. Kuipers, M. Müller, and S. Kersten. 2006. The fasting-induced adipose factor/angiopoetin-like protein 4 is physically associated with lipoproteins and governs plasma lipids levels and adiposity. J. Biol. Chem. 281:934–944.

McGarry, J. D. 2002. Dysregulation of fatty acid metabolism in the etiology of type 2 diabetes. Diabetes 51:7-18.

McNamara, J. P., and C. E. Murray. 2001. Sympathetic nervous system activity in adipose tissues during pregnancy and lactation of the rat. J. Dairy Sci. 84:1382-1389.

McNamara, J. P., J. H. Harrison, R. L. Kincaid, and S. S. Waltner. 1995. Lipid metabolism in adipose tissue of cows fed high fat diets during lactation. J. Dairy Sci. 78:2782-2796.

Miyoshi, H., J. W. Perfield 2nd, M. S. Obin, and A. S. Greenberg. 2008. Adipose triglyceride lipase regulates basal lipolysis and lipid droplet size in adipocytes. J. Cell. Biochem. 105:1430–1436.

Miyoshi, H., J. W. Perfield 2nd, S. C. Souza, W. J. Shen, H. H. Zhang, Z. S. Stancheva, F. B. Kraemer, M. S. Obin, and A. S. Greenberg. 2007. Control of adipose triglyceride lipase action by serine 517 of perilipin A globally regulates protein kinase A-stimulated lipolysis in adipocytes. J. Biol. Chem. 282:996–1002.

Ogihara, T., B. C. Shin, M. Anai, H. Katagiri, K. Inukai, M. Funaki, Y. Fukushima, H. Ishihara, K. Takata, M.Kikuchi, Y. Yazaki, Y. Oka, and T. Asano. 1997. Insulin receptor substrate (IRS)-2 is dephosphorylated more rapidly than IRS-1 via its association with phosphatidylinositol 3-kinase in skeletal muscle cells. J. Biol. Chem. 272:12868–12873.

Oikawa, S., and G. R. Oetzel. 2006. Decreased insulin response in dairy cows following a four-day fast to induce hepatic lipidosis. J. Dairy Sci. 89:2999-3005.

Payne, V. A., W. S. Au, C. E. Lowe, S. M. Rahman, J. E. Friedman, S. O'Rahilly, and J. J. Rochford. 2010. C/EBP transcription factors regulate SREBP1c gene expression during adipogenesis. Biochem. J. 425:215-223.

Petterson, J. A., F. R. Dunshea, R. A. Ehrhardt, and A. W. Bell. 1993. Pregnancy and undernutrition alter glucose metabolic responses to insulin in sheep. J. Nutr. 123:1286-1295.

Petterson, J. A., R. Slepetis, R. A. Ehrhardt, F. R. Dunshea, and A. W. Bell. 1994. Pregnancy but not moderate undernutrition attenuates insulin suppression of fat mobilization in sheep. J. Nutr. 124:2431-2436.

Rabelo, E., R. L. Rezende, S. J. Bertics, and R. R. Grummer. 2005. Effects of Pre- and Postfresh Transition Diets Varying in Dietary Energy Density on Metabolic Status of Periparturient Dairy Cows. J. Dairy Sci. 88:4375-4383.

Rhoads, R. P., J. W. Kim, B. J. Leury, L. H. Baumgard, N. Segoale, S. J. Frank, D. E. Bauman, and Y. R. Boisclair. 2004. Insulin increases the abundance of the growth hormone receptor in liver and adipose tissue of periparturient dairy cows. J. Nutr. 134:1020-1027.

Richards, B. F., N. A. Janovick, K. M. Moyes, D. E. Beever, and J. K. Drackley. 2009. Comparison of a controlled-energy high-fiber diet fed throughout the dry period to a two-stage far-off and close-up dietary strategy. J. Dairy Sci. 92(E-Suppl.):140 (Abstract).

Rosen, E. D., and O. A. MacDougald. 2006. Adipocyte differentiation from the inside out. Nat. Rev. Mol. Cell Biol. 7:885-896.

Rukkwamsuk, T., T. Wensing, and M. J. Geelen. 1998. Effect of overfeeding during the dry period on regulation of adipose tissue metabolism in dairy cows during the periparturient period. J. Dairy Sci. 81:2904-2911.

Rukkwamsuk, T., T. Wensing, and M. J. Geelen. 1999. Effect of overfeeding during the dry period on the rate of esterification in adipose tissue of dairy cows during the periparturient period. J. Dairy Sci. 82:1164-1169.

Sadri, H., R. M. Bruckmaier, H. R. Rahmani, G. R. Ghorbani, I. Morel, and H. A. van Dorland. 2010. Gene expression of tumour necrosis factor and insulin signalling-related factors in subcutaneous adipose tissue during the dry period and in early lactation in dairy cows. J. Anim. Physiol. Anim. Nutr. (Berlin). 94:e194-e202.

Saltiel, A. R., and C. R. Kahn. 2001. Insulin signalling and the regulation of glucose and lipid metabolism. Nature 414:799–806.

Sesti, G., M. Federici, M. L. Hribal, D. Lauro, P. Sbraccia, and R. Lauro. 2001. Defects of the insulin receptor substrate (IRS) system in human metabolic disorders. FASEB J. 15:2099–2111.

Sevillano, J., J. de Castro, C. Bocos, E. Herrera, and M. P. Ramos. 2007. Role of insulin receptor substrate-1 serine 307 phosphorylation and adiponectin in adipose tissue insulin resistance in late pregnancy. Endocrinology 148:5933-5942.

Smith, K. L., W. R. Butler, and T. R. Overton. 2009. Effects of prepartum 2,4-thiazolidinedione on metabolism and performance in transition dairy cows. J Dairy Sci. 92:3623-3633.

Smith, U. 2002. Impaired (‘diabetic’) insulin signaling and action occur in fat cells long before glucose intolerance—is insulin resistance initiated in the adipose tissue? Int. J. Obes. Relat. Metab. Disord. 26:897–904.

Subramanian, V., A. Rothenberg, C. Gomez, A. W. Cohen, A. Garcia, S. Bhattacharyya, L. Shapiro, G. Dolios, R. Wang, M. P. Lisanti, and D. L. Brasaemle. 2004. Perilipin A mediates the reversible binding of CGI-58 to lipid droplets in 3T3-L1 adipocytes. J. Biol. Chem. 279: 42062-42071.

Vasquez, J. A., K. L. Perfield, H. B. Green, and J. K. Drackley. 2011. Effects of close-up dietary energy strategy and prepartal dietary monensin on production and metabolism in Holstein cows. J. Dairy Sci. 94 (E-Suppl. 1):690. (Abstract)

Vernon, R. G., R. A. Clegg, and D. J. Flint. 1981. Metabolism of sheep adipose tissue during pregnancy and lactation. Biochem. J. 200:307-314.

Virkamäki, A., K. Ueki, and C. R. Kahn. 1999. Protein-protein interaction in insulin signaling and the molecular mechanisms of insulin resistance. J. Clin. Invest. 103:931–943.

Wildman, E. E., G. M. Jones, P. E. Wagner, R. L. Boman, H. F. Troutt, and T. N. Lesch. 1982. A dairy cow body condition scoring system and its relationship to selected production characteristics. J. Dairy Sci. 65:495–501.

Wu, Z., E. D. Rosen, R. Brun, S. Hauser, G. Adelmant, A. E. Troy, C. McKeon, G. J. Darlington, and B. M. Spiegelman. 1999. Cross-regulation of C/EBP alpha and PPAR gamma controls the transcriptional pathway of adipogenesis and insulin sensitivity. Mol. Cell. 3:151-158.

Yoon, J. C., T. W. Chickering, E. D. Rosen, B. Dussault, Y. Qin, A. Soukas, J. M. Friedman, W. E. Holmes, and B. M. Spiegelman. 2000. Peroxisome proliferator-activated receptor gamma target gene encoding a novel angiopoietin-related protein associated with adipose differentiation. Mol. Cell Biol. 20:5343-5349.

Zechner, R., P. C. Kienesberger, G. Haemmerle, R. Zimmermann, and A. Lass. 2009. Adipose triglyceride lipase and the lipolytic catabolism of cellular fat stores. J. Lipid Res. 50:3-21.

TABLES AND FIGURES

Table 5.1. Ingredient and chemical composition of diets

	Diet[1]		
Component	**CON**	**OVE**	**Lactation**
Ingredient, % of DM			
Alfalfa silage	12.00	8.20	5.00
Alfalfa hay	---	3.50	4.00
Corn silage	33.00	35.90	33.00
Wheat straw	36.00	15.40	4.00
Cottonseed	---	---	3.50
Wet brewers grains	---	6.00	10.00
Ground shelled corn	4.00	13.00	22.20
Soy hulls	2.00	4.00	4.00
Soybean meal, 48% CP	7.94	3.10	3.30
Expeller soybean meal[2]	---	2.00	6.20
SoyChlor	0.15	3.80	---
Blood meal 85%	1.00	1.00	0.30
Urea	0.45	0.30	0.14
Rumen-inert fat[3]	---	---	1.00
Limestone	1.30	1.30	1.18
Salt (plain)	0.32	0.30	0.27
Sodium bicarbonate	---	---	0.75
Potassium carbonate	---	---	0.10
Calcium sulfate	---	---	0.10
Dicalcium phosphate	0.12	0.18	0.27
Magnesium oxide	0.21	0.08	0.14
Magnesium sulfate	0.91	0.97	---
Mineral-vitamin mix[4]	0.20	0.20	0.20
Vitamin A[5]	0.015	0.015	---
Vitamin D[6]	0.025	0.025	---
Vitamin E[7]	0.38	0.38	---
Biotin	---	0.35	0.35
Chemical Analysis			
DM of diet, %	47.1 ± 2.0	46.6 ± 0.8	45.2 ± 1.5
NE_L, Mcal/kg	1.24	1.47	1.65
CP, % DM	14.6	15.6	16.3
ADF, % DM	36.2	30.2	24.1
NDF, % DM	52.7	44.7	37.9

[1] Controlled diet was provided for all animals during the far-off dry period (-50 d to -21 d relative to expected calving). During close-up dry period (-21 d to calving), one group of animals continued to be fed the controlled diet for ad libitum intake and another group was fed the overfed diet for ad libitum intake. After calving, all animals were fed the lactation diet for ad libitum intake.

[2]SoyPLUS (West Central Soy, Ralston, IA)

[3]Energy Booster 100® (MSC, Carpentersville, IL)

[4]Contained a minimum of 5% Mg, 10% S, 7.5% K, 2.0% Fe, 3.0% Zn, 3.0% Mn, 5,000 mg/kg of Cu, 250 mg/kg of I, 40 mg/kg of Co, 150 mg/kg of Se, 2,200 kIU/kg of vitamin A, 660 kIU/kg of vitamin D3, and 7,700 IU/kg of vitamin E.

[5]Contained 30,000 kIU/kg.

[6]Contained 5,009 kIU/kg.

[7]Contained 44,000 IU/kg.

Table 5.2. Effect of close-up overfeeding energy on DMI, NE_Lintake, blood metabolites, and production of dairy cows

Variable	CON	OVE	*P*-value		
			Trt	Week	T×W
DMI, kg/d[1]					
Close-up	12.6 ± 0.70	14.8 ± 0.72	0.05	0.02	0.53
Postpartum, d 1 - 7	13.0 ± 1.84	15.3 ± 1.85	0.39	< 0.01	0.12
Postpartum, d 1 - 28	16.7 ± 1.84	17.0 ± 1.84	0.92	< 0.01	0.02
NE_L intake, MJ/d[1]					
Close-up	65.4 ± 4.07	91.1 ± 4.070	< 0.01	< 0.01	0.22
Postpartum	115.4 ± 12.5	117.8 ± 12.5	0.89	< 0.01	0.05
Energy balance, % of req.					
Close-up	107.9 ± 4.60	139.9 ± 4.11	< 0.01	0.03	0.23
Postpartum	63.7 ± 6.59	67.7 ± 6.56	0.67	< 0.01	0.13
Serum insulin, µg/L					
Close-up	0.37 ± 0.04	0.58 ± 0.03	< 0.01	< 0.01	0.10
Postpartum	0.14 ± 0.03	0.21 ± 0.03	0.12	0.09	0.65
Serum NEFA, mEq/mL					
Close-up	0.39 ± 0.05	0.27 ± 0.05	0.16	< 0.01	0.23
Postpartum	0.79 ± 0.09	1.01 ± 0.09	0.15	0.03	0.24
Change in Post- vs. Pre-[2]	+ 0.40±0.09	+ 0.68±0.09	0.04	--	--
Serum BHBA, mmol/L					
Close-up	0.47 ± 0.04	0.44 ± 0.04	0.53	0.02	0.42
Postpartum	0.88 ± 0.11	1.20 ± 0.11	0.06	< 0.01	0.40
Milk yield, kg/d[3]	41.7 ± 2.23	41.2 ± 2.23	0.82	< 0.01	0.85
3.5% FCM yield, kg/d[4]	46.4 ± 2.67	47.4 ± 2.45	0.79	< 0.01	0.09
ECM yield, kg/d[5]	47.7 ± 2.43	45.9 ± 2.39	0.61	0.15	0.87
Milk Fat					
%	4.47 ± 0.21	4.43 ± 0.19	0.86	0.07	0.94
kg/d	1.78 ± 0.11	1.81 ± 0.10	0.83	0.10	0.27
Milk protein					
%	3.26 ± 0.09	3.04 ± 0.09	0.10	< 0.01	0.63
kg/d	1.32 ± 0.07	1.21 ± 0.07	0.32	0.09	0.26
Milk lactose					
%	4.60 ± 0.09	4.71 ± 0.09	0.42	< 0.01	< 0.01
kg/d	1.89 ± 0.12	1.93 ± 0.12	0.78	< 0.01	< 0.01

[1]DMI and NE_L intake were analyzed based on daily data.
[2]Estimates and contrast were made to compare the effect of close-up dietary energy planes on serum NEFA change of postpartum vs. close-up period. Dataset is composed of serum NEFA concentrations at -14, -8, and -3 d for close-up period and 2, 8, 14, and 21 d postpartum of each animal with 7 cows per treatment.
[3]Milk yield was analyzed based on daily data.
[4]Fat-corrected milk = 0.4324 × (milk yield) + 16.2162 × (fat yield). Milk samples from the first week were not used to calculate FCM.
[5]Energy-corrected milk = (0.327 × milk yield) + (12.95 × fat yield) + (7.2 × protein yield).

Table S5.1. Gene symbol, full name and subcellular localization and mRNA abundance for genes investigated, genes were categorized with the major function involved

Gene Symbol	Full Gene Name from NCBI	Subcellular Localization[1]	mRNA Abundance[2]		
			d -10	d +7	d +21
***de novo* FA synthesis**					
ACLY	ATP citrate lyase	CP	12.39	5.28	2.99
ACACA	acetyl-Coenzyme A carboxylase alpha	CP/MIT	11.68	0.86	2.49
FASN	fatty acid synthase	CP	147.96	3.24	14.85
SCD	stearoyl-CoA desaturase	ER/ME	586.87	5.34	5.93
LCFA uptake					
LPL	lipoprotein lipase	EM/PM	24.85	1.93	15.2
ACSS2	acyl-CoA synthetase short-chain family member 2	CP	35.65	1.07	2.07
ACSL1	acyl-CoA synthetase long-chain	ER/MOM/PEM	3.62	0.72	36.4
Cytosolic NADPH and glycerol production					
G6PD	glucose-6-phosphate dehydrogenase	CP	18.73	3.06	17.67
IDH1	isocitrate dehydrogenase 1 ($NADP^+$)	CP	15.58	1.82	9.91
PCK1	phosphoenolpyruvate carboxykinase 1	CP	0.56	0.12	0.01
TAG synthesis					
GPAM	glycerol-3-phosphate acyltransferase	ME/MIM/MOM	36.04	2.55	1.02
DGAT2	diacylglycerol O-acyltransferase 2	ER	118.46	7.72	3.9
Lipolysis					
PNPLA2	patatin-like phospholipase domain containing 2	CP/LP/PM	13.52	5.92	80.72
ABHD5	abhydrolase domain containing 5	CP/LP	0.6	0.26	0.61
LIPE	hormone-sensitive lipase	CP/MIT/PM	20.17	10.2	37.47
ADRB1	adrenergic receptor, beta 1	ME/PM	0.02	0.04	0.19
ADRB2	adrenergic receptor, beta 2	ME/PM	1.32	1.9	5.17

Table S5.1. (cont.)

Gene Symbol	Full Gene Name from NCBI	Subcellular Localization[1]	mRNA Abundance[2]		
			d -10	d +7	d +21
Transcriptional regulation					
CEBPA	CCAAT/enhancer binding protein, alpha	NU	0.26	0.23	3.25
SREBF1	sterol regulatory element binding transcription factor 1	ER/NU	3.14	0.79	3.5
PPARG	peroxisome proliferator-activated receptor gamma	NU/CP	9.38	4.01	4.93
Insulin signaling pathway					
INSR	insulin receptor	PM	0.36	0.32	2.55
IRS1	insulin receptor substrate 1	CP/PM	0.49	0.16	<0.01
SLC2A4	solute carrier family 2 (facilitated glucose transporter), member 4	CP/PM	1.24	0.37	2.14
PDE3B	phosphodiesterase 3B, cGMP-inhibited	CP/ER/ME/GO	4.95	2.26	4.64
Receptors, adipokine and signaling proteins					
ANGPTL4	angiopoietin-like 4	EM	8.99	28.15	6.72
Total mRNA abundance of tested genes			**1076.8**	**88.3**	**264.3**

[1] Subcellular localization abbreviations: CP = cytoplasm; EM = extracellular matrix; ER = endoplasmic reticulum; GO = golgi apparatus; LP: lipid droplet; ME = membrane; MIM = mitochondrial inner membrane; MIT = mitochondrion; MOM = mitochondrial outer membrane; NU = nucleus; PEM = peroxisomal membrane; PM = plasma membrane.

[2] Calculation of relative mRNA abundance refered to Chapter 2; the mRNA abundance of each gene at every biopsy day was listed instead of the percentage of mRNA abundance of each gene among all the genes tested.

Table S5.2. GenBank accession number, hybridization position, sequence, and amplicon size of primers used to analyze gene expression in qPCR.

Accession #	Gene	Primers[1]	Sequence (5'-3')[2]	Size[3]
NM_001076063.1	*ABHD5*	F: 1141	CTGCAGATGATGTGGGAAAGC	100
		R: 1240	GACTGCCTGGTTCTCGTGTCA	
AJ132890	*ACACA*	F: 3709	CATCTTGTCCGAAACGTCGAT	101
		R: 3809	CCCTTCGAACATACACCTCCA	
BC108138	*ACLY*	F: 2287	GTTCTCCTCCGAGGTCCAGTT	104
		R: 2390	CAAACACTCCAGCCTCCTTCA	
BC119914	*ACSL1*	F: 1929	GTGGGCTCCTTTGAAGAACTGT	120
		R: 2047	ATAGATGCCTTTGACCTGTTCAAAT	
BC134532	*ACSS2*	F: 1881	GGCGAATGCCTCTACTGCTT	100
		R: 1970	GGCCAATCTTTTCTCTAATCTGCTT	
BC140488	*ADIPOQ*	F: 211	GATCCAGGTCTTGTTGGTCCTAA	109
		R: 319	GAGCGGTATACATAGGCACTTTCTC	
AF188187	*ADRB1*[4]	F:	CAGAACTCACGGAAGACGAGC	
		R:	AAGGTGGCGCTGGACC	
Z86037	*ADRB2*[5]	F:	TCAAAAGCCACGGACCCC	
		R:	ACTATCGTAACTAAGTGTTCCCT	
DY208485	*AGPAT6*	F: 171	AAGCAAGTTGCCCATCCTCA	101
		R: 271	AAACTGTGGCTCCAATTTCGA	
NM_173986	*AKT1*	F: 1565	CACGTGCTCTGGACGCTTC	102
		R: 1666	ATGGCGAGGTTCCACTCAAAC	
XM_864913.3	*AKT2*	F: 4646	GCCTCCAGCCGCTTCAC	100
		R: 4745	GCAGCAAACTGGAGACCAGAT	
DQ355521.1	*ANGPTL4*	F: 28	AGGAAGAGGCTGCCCAAGAT	108
		R: 136	CCCTCTCTCCCTCTTCAAACAG	
X91503	*CD36*	F: 743	GTACAGATGCAGCCTCATTTCC	81
		R: 823	TGGACCTGCAAATATCAGAGGA	
NM_176784.2	*CEBPA*	F:	GCAAAGCCAAGAAGTCCG	
		R:	GGCTCAGTTGTTCCACCCGCTT	
BT030532.1	*DGAT2*	F: 389	CATGTACACATTCTGCACCGATT	100
		R: 488	TGACCTCCTGCCACCTTTCT	
BC148954.1	*ELOVL6*	F: 439	AGCACCCGAACTAGGAGATACAAT	102
		R: 540	TACCAGGAGTACAGAAGCACAGTGA	
DV778074	*FABP4*	F: 402	TGGTGCTGGAATGTGTCATGA	101
		R: 502	TGGAGTTCGATGCAAACGTC	
CR552737	*FASN*	F: 6383	ACCTCGTGAAGGCTGTGACTCA	92
		R: 6474	TGAGTCGAGGCCAAGGTCTGAA	
XM_583090.4	*FOXO1*	F: 716	GCTCCTGGTGGATGCTCAAT	105
		R: 820	GGCCTCGGCTCTTAGCAAAT	
XM_583628.4	*G6PD*	F: 408	CAACCAGCTGTCCAACCACAT	100
		R: 507	CACCATGAGGTTCTGGACCAT	
AY748827.1	*GHR*	F: 156	ATCCAGTCCTAGAGACAAATTCTTCTG	100
		R: 255	TTAGCCCCATCTGTCCAGTGA	
AY515690	*GPAM*	F: 1963	GCAGGTTTATCCAGTATGGCATT	63
		R: 2026	GGACTGATATCTTCCTGATCATCTTG	
DQ403090.1	*IDH1*	F: 1061	ATGGCTCTCTTGGCATGATGA	100
		R: 1161	CATTCGGTAGTGACGGGTTACA	

Table S5.2. (cont.)

Accession #	Gene	Primers[1]	Sequence (5'-3')[2]	Size[3]
XM_589325	*INSIG1*	F: 438	AAAGTTAGCAGTCGCGTCGTC	120
		R: 557	TTGTGTGGCTCTCCAAGGTGA	
XM_614207	*INSIG2*	F: 494	TCCAGTGTGATGCGGTGTGTA	109
		R: 602	TGGATAGTGCAGCCAGTGTGA	
AY574999	*INSR*	F: 245	CCCTTCGAGAAAGTGGTGAACA	84
		R: 328	AGCCTGAAGCTCGATGCGATAG	
CR551751	*IRS1*	F: 73	TGTTGACTGAACTGCACGTTCT	112
		R: 184	CATGTGGCCAGCTAAGTCCTT	
EF140760.1	*LIPE*	F: 1674	TCAGTGTCCAAGACAGAGCCAAT	106
		R: 1779	CATGCAGCTTCAGGCTTTTG	
DV797268	*LPIN1*	F: 147	TGGCCACCAGAATAAAGCATG	101
		R: 247	GCTGACGCTGGACAACAGG	
BC118091	*LPL*	F: 327	ACACAGCTGAGGACACTTGCC	101
		R: 427	GCCATGGATCACCACAAAGG	
XM_001255565.2	*MLXIPL*	F: 2529	CCTGACGGATCCAGACTGTATACC	91
		R: 2619	AGGGTCTGTCCAGCACTATAAAGATT	
XM_612999.4	*NR3C1*	F: 395	AAGCACCCCCAGTAGAGAAGAA	100
		R: 494	CACAGTAGCTCCTCCCCTTAGG	
XM_618666.4	*PDE3B*	F: 2235	CGTCCTACATGCTGTTTGGTATCT	100
		R: 2334	AGGGTTAATTGCTGTTTCATTTCC	
DV814745	*PLIN1*	F: 443	GATCGCCTCTGAGCTGAAGG	108
		R: 550	AGAGCGGCCCCTAGGATTT	
NM_001046005.1	*PNPLA2*	F: 765	CACCAGCATCCAGTTCAACCT	102
		R: 866	CTGTAGCCCTGTTTGCACATCT	
NM_181024	*PPARG*	F: 135	CCAAATATCGGTGGGAGTCG	101
		R: 235	ACAGCGAAGGGCTCACTCTC	
DV935188	*SCAP*	F: 990	CCATGTGCACTTCAAGGAGGA	108
		R: 1097	ATGTCGATCTTGCGTGTGGAG	
AY241933	*SCD*	F: 665	TCCTGTTGTTGTGCTTCATCC	101
		R: 765	GGCATAACGGAATAAGGTGGC	
NM_001033625	*SLC27A1*	F: 861	GGCAAGGGCATGGATGATC	96
		R: 951	GCGGTAGTACCTGCTGTGCAC	
M60448	*SLC2A1*	F: 275	CCCCCAGAAGGTGATTGAAG	135
		R: 409	GAACCAATCATGCCTCCCAC	
AY458600.1	*SLC2A4*	F: 79	CCTTGGTCCTTGCCGTATTC	102
		R: 180	TGTAGCTCTGTTCAATCACCTTCTG	
TC263657	*SREBF1*	F: 143	CCAGCTGACAGCTCCATTGA	67
		R: 209	TGCGCGCCACAAGGA	
AY656814	*THRSP*	F: 631	CTACCTTCCTCTGAGCACCAGTTC	151
		R: 781	ACACACTGACCAGGTGACAGACA	
NM_001101893.1	*ZFP423*	F: 4490	CGTGATGTGATTGCTTGGCTATT	119
		R: 4599	CATAGTTTTAATCACTGTCCGGTGAA	

[1] F: forward primer; R: reverse primer; number: start of hybridization position

[2] Exon-exon junctions are underlined

[3] Amplicon size expressed as base pair (bp)

[4 and 5] Primer sequence cited from: Sumner JM, McNamara JP. Expression of lipolytic genes in the adipose tissue of pregnant and lactating Holstein dairy cattle. J Dairy Sci. 2007; 90:5237-5246.

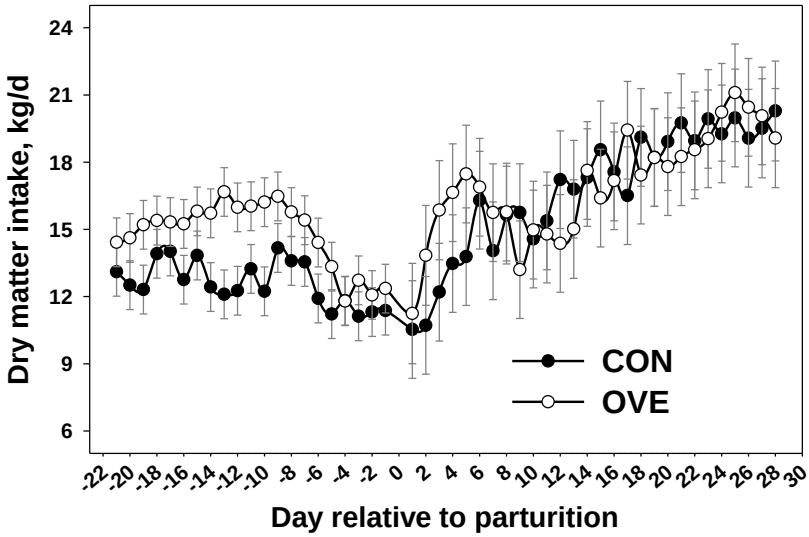

Figure 5.1. Daily DMI (kg/d) from -21 to 28 d relative to parturition for cows either fed controlled energy diet (CON, n = 7) or moderate energy diet (OVE, n = 7) during close-up dry period (-21 d to parturition). All animals were given controlled energy diet during far-off dry period (-50 to -22 d) and the same lactation diet for ad libitum intake post-calving. Values are expressed as mean ± SE. Data from far-off, close-up and postpartum periods were analyzed separately. Far-off (data not shown): Group difference, $P = 0.57$; *d*ay, $P = 0.2$; G×D, $P = 0.15$. Close-up: Trt, $P = 0.05$; day, $P = 0.02$; T×D, $P = 0.53$. Postpartum: Trt, $P = 0.92$; day, $P < 0.01$; T×D, $P < 0.02$.

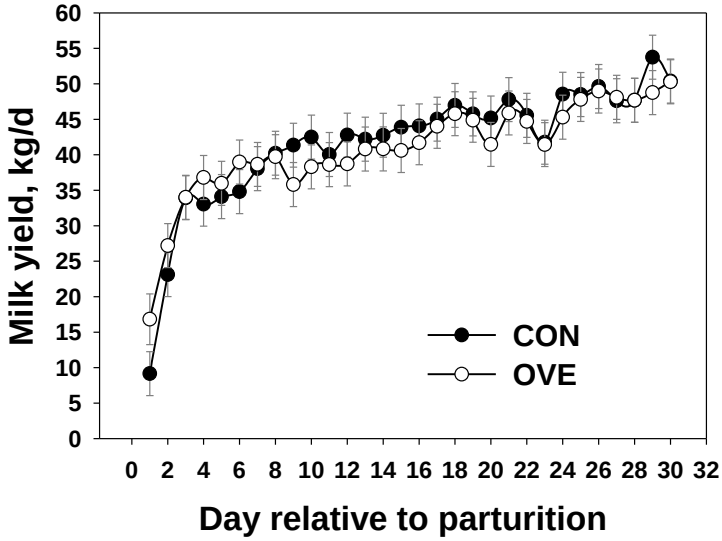

Figure 5.2. Daily milk yield (kg/d) from parturition until 30 d in lactation. Data from 7 animals of each treatment were included. Values are expressed as mean ± SE. Trt, $P = 0.82$; day, $P < 0.01$; T×D, $P = 0.85$.

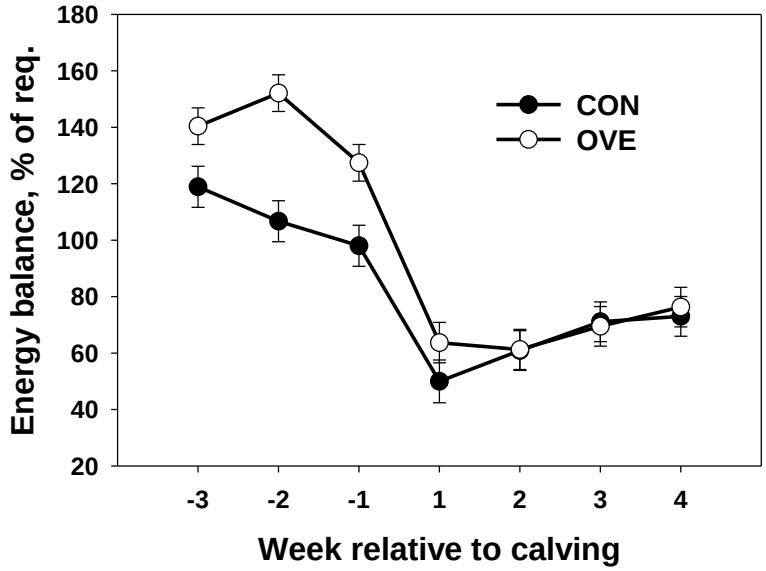

Figure 5.3. Weekly whole-body energy balance (% of requirements) from -3 to 4 wk relative to parturition. Data from 7 animals of each treatment were included. Values are expressed as mean ± SE. Data from close-up and postpartum were analyzed separately. Close-up period: Trt, $P < 0.01$; week, $P = 0.03$; T×W, $P = 0.23$. Postpartum: Trt, $P = 0.67$; week, $P < 0.01$; T×W, $P = 0.13$.

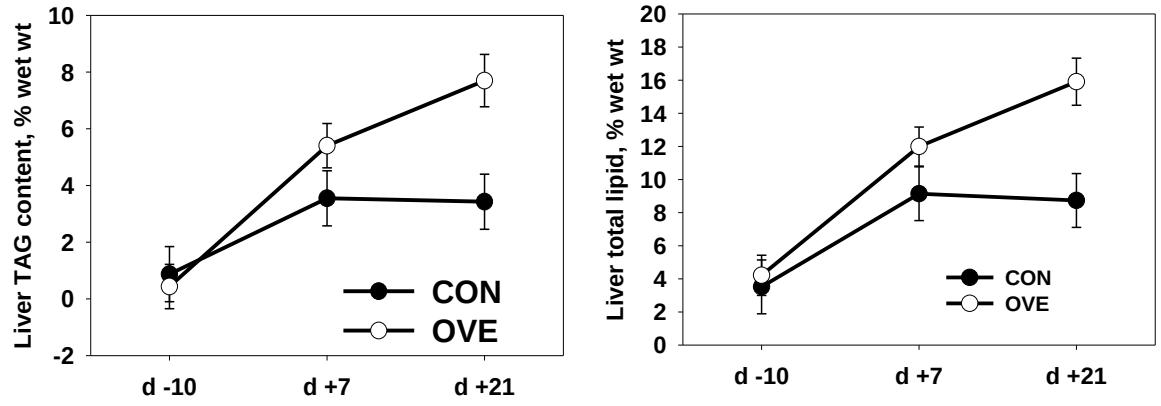

Figure 5.4. Liver lipid and triglyceride content (wt % of the wet tissue wt) at -10, 7 and 21 d relative to parturition. Data from 7 animals of each treatment were included. Values are expressed as mean ± SE. (A) Liver total lipid content. Trt, $P = 0.02$; week, $P < 0.01$; T×W, $P = 0.08$. (B) Liver triglyceride content. Trt, $P = 0.02$; week, $P < 0.01$; T×W, $P < 0.04$.

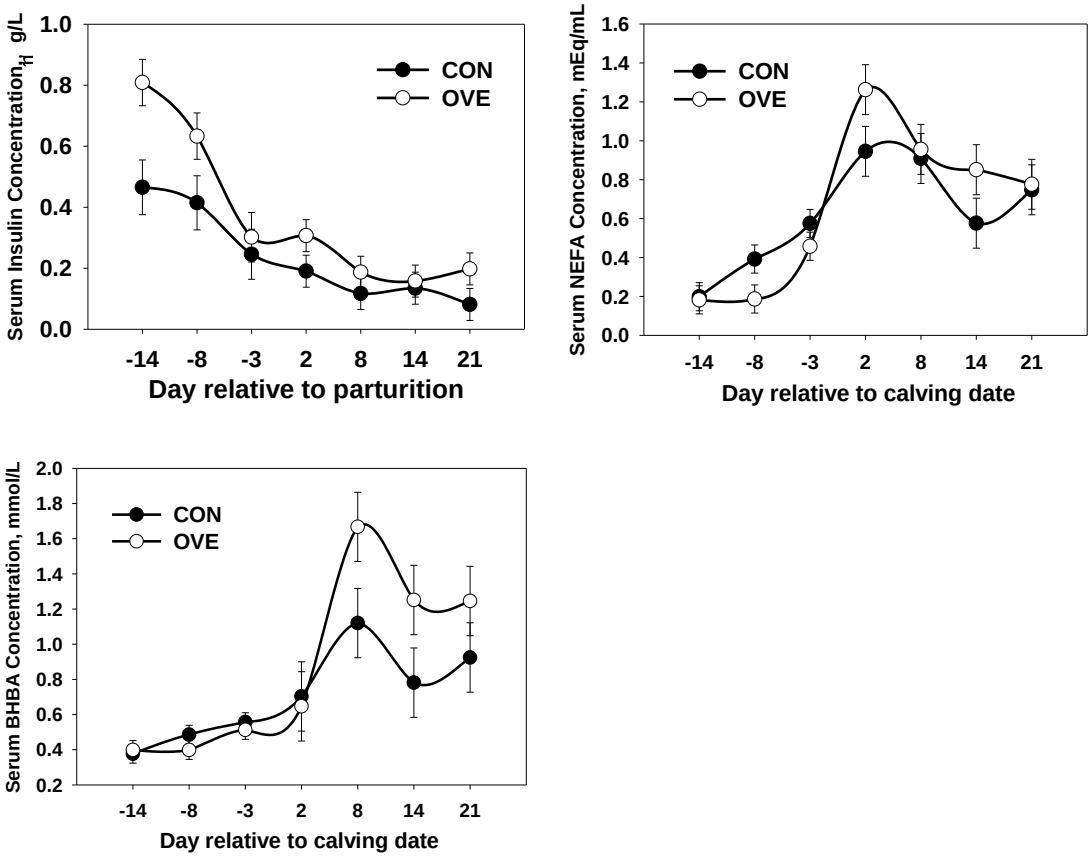

Figure 5.5. Temporal concentrations of serum insulin and metabolites from -14 to 21 d relative to parturition. Data from 7 animals of each treatment were included. Values are expressed as mean ± SE. Data of prepartum and postpartum were analyzed separately. (A) serum insulin concentration (μg/L). Prepartum: Trt, $P < 0.01$; day, $P < 0.01$; T×D, $P = 0.10$. Postpartum: Trt, $P = 0.12$; day, $P = 0.09$; T×D, $P = 0.65$.

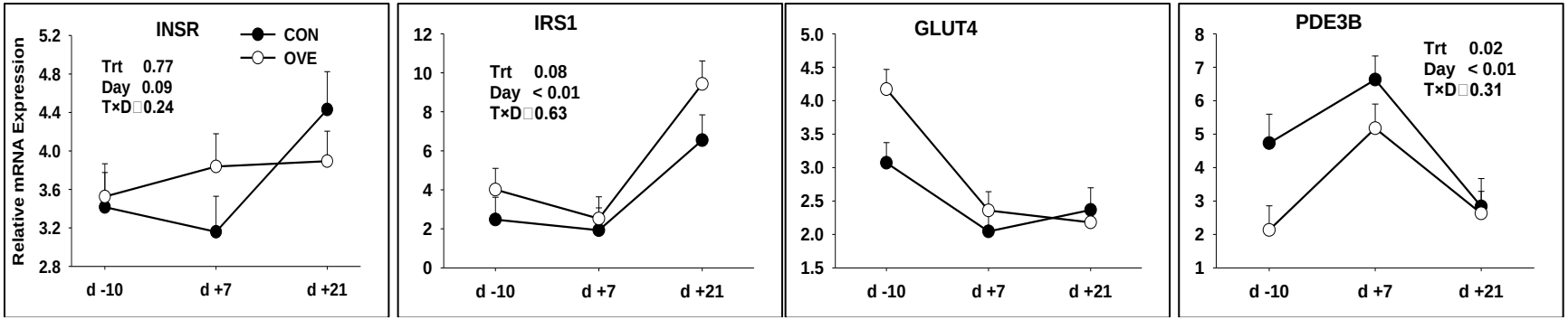

Figure 5.6. Relative mRNA expressions of genes involved in insulin signaling pathway in adipose tissue of transition dairy cows in response to close-up energy overfeeding. Each treatment contains 7 animals. Values are expressed as mean ± SE. The *P* values for main effect of treatment (Trt) and day and interaction of treatment and day (T×D) were listed only for those genes without significant interaction effect ($P > 0.05$). For genes with sigificant interaction effect ($P < 0.05$), contrasts were made between two treatments at the same biopsy date and significant difference ($P < 0.05$) were marked with lowercase (a and b). Contrast were also made between any two biopsy dates in the same treatment and significant difference ($P < 0.05$) between d -10 and d +7 or d +21 were marked with asterisks (*****), and pond mark indicates significant difference ($P < 0.05$) between d +7 and d +21 for within each treatment.

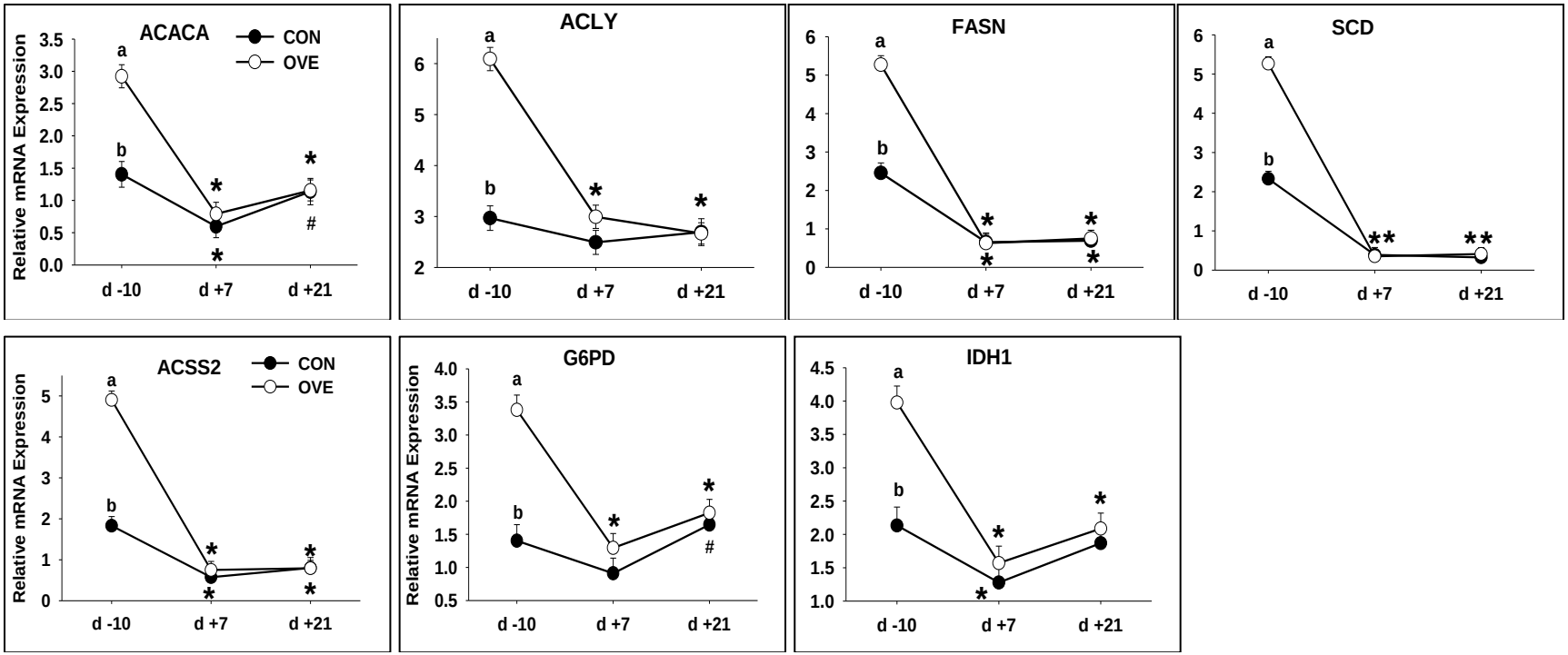

Figure 5.7. Relative mRNA expressions of genes associated with *de novo* FA synthesis (*ACLY*, *ACACA*, *FASN*, and *SCD*), cytosolic acetate activation (*ACSS2*) and cytosolic NADPH production (*G6PD* and *IDH1*) in adipose tissue of transition dairy cows in response to close-up energy overfeeding. Each treatment contains 7 animals. Values are expressed as mean ± SE. See Figure 5.6 for significance mark explanation.

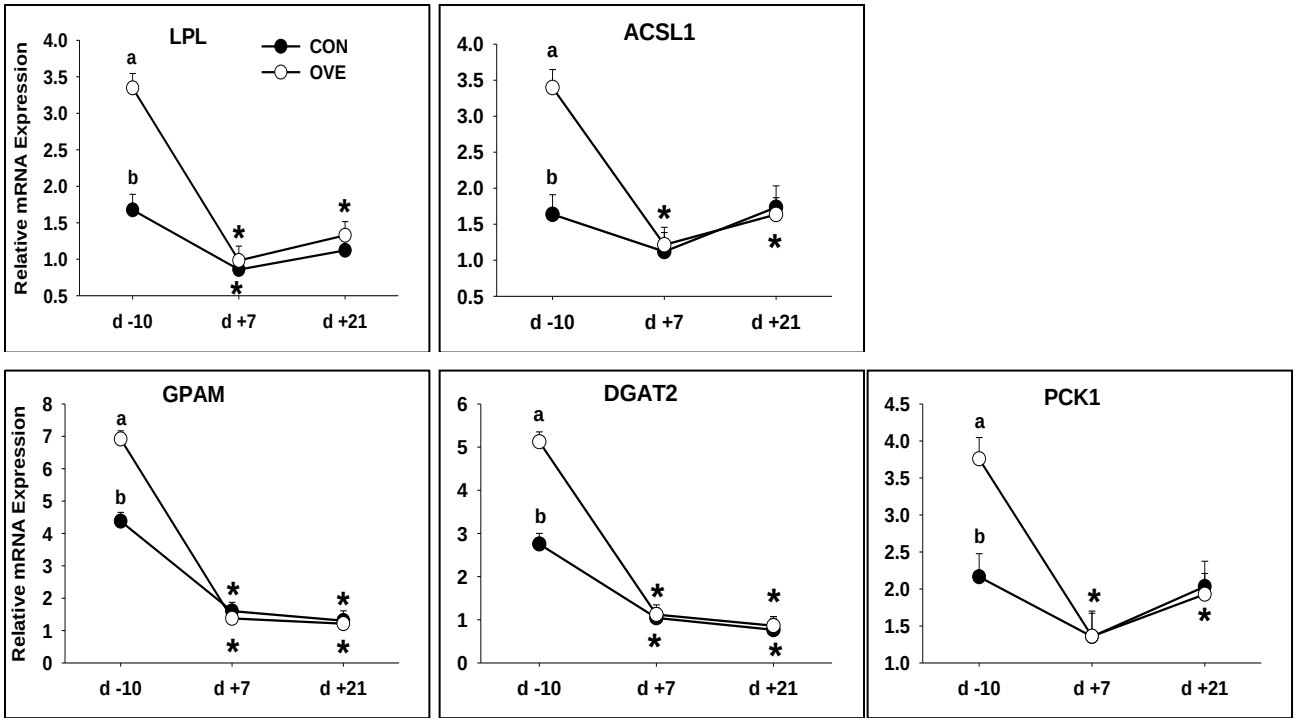

Figure 5.8. Relative mRNA expressions of genes associated with LCFA import and activation (*LPL* and *ACSL1*), TAG synthesis (*GPAM* and *DGAT2*) and glyceroneogenesis (*PCK1*) in adipose tissue of transition dairy cows in response to close-up energy overfeeding. Each treatment contains 7 animals. Values are expressed as mean ± SE. See Figure 5.6 for significance mark explanation.

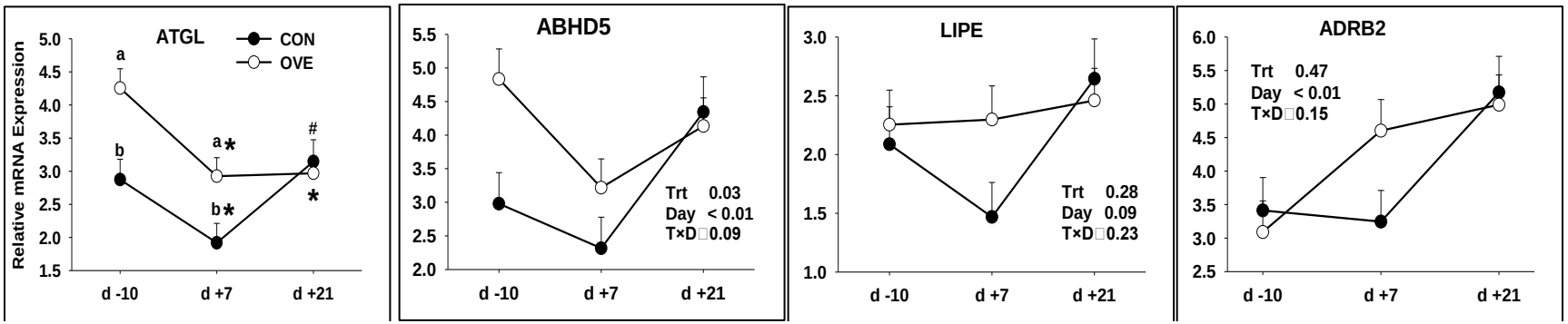

Figure 5.9. Relative mRNA expressions of genes associated with lipolysis in adipose tissue of transition dairy cows in response to close-up energy overfeeding. Each treatment contains 7 animals. Values are expressed as mean ± SE. See Figure 5.6 for significance mark explanation.

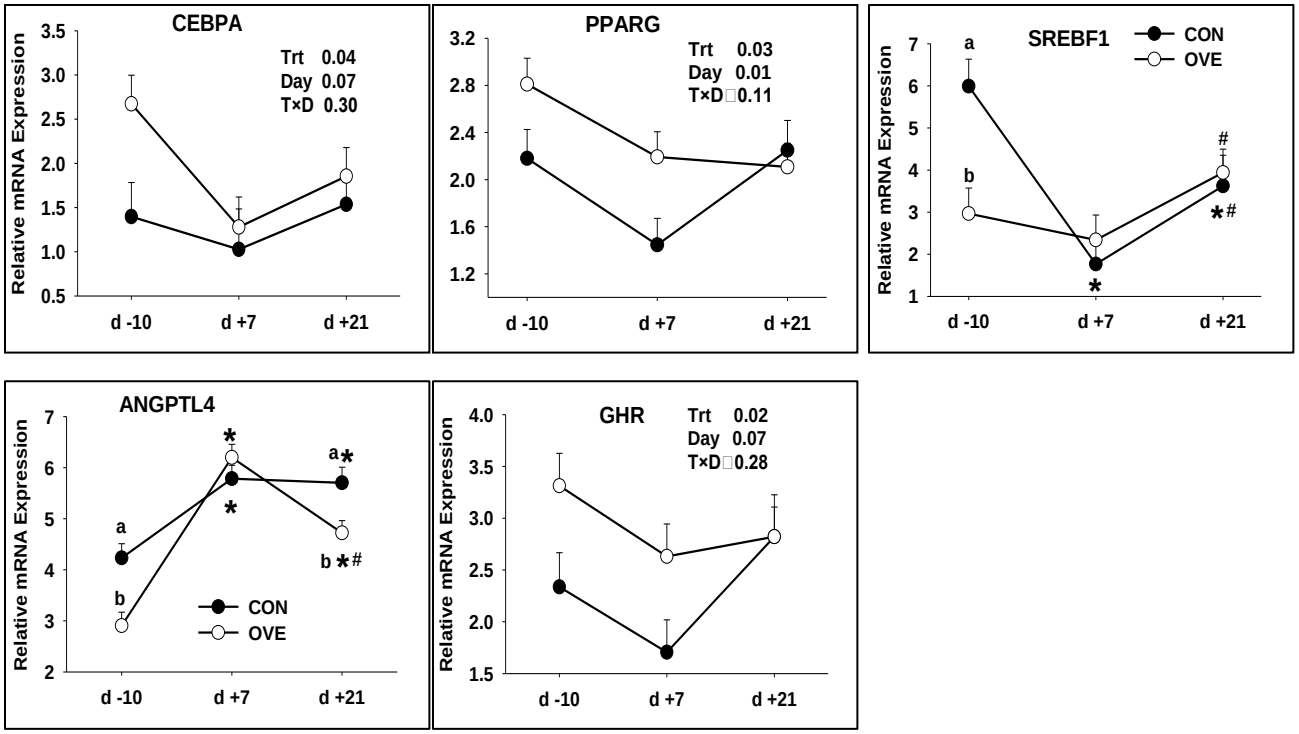

Figure 5.10. Relative mRNA expressions of transcriptional factors (*CEBPA*, *PPARG*, and *SREBF1*), fasting induced adipose factor (*ANGPTL4*) and growth hormone receptor (GHR) in adipose tissue of transition dairy cows in response to close-up energy overfeeding. Each treatment contains 7 animals. Values are expressed as mean ± SE. See Figure 5.6 for explanations of significance mark.

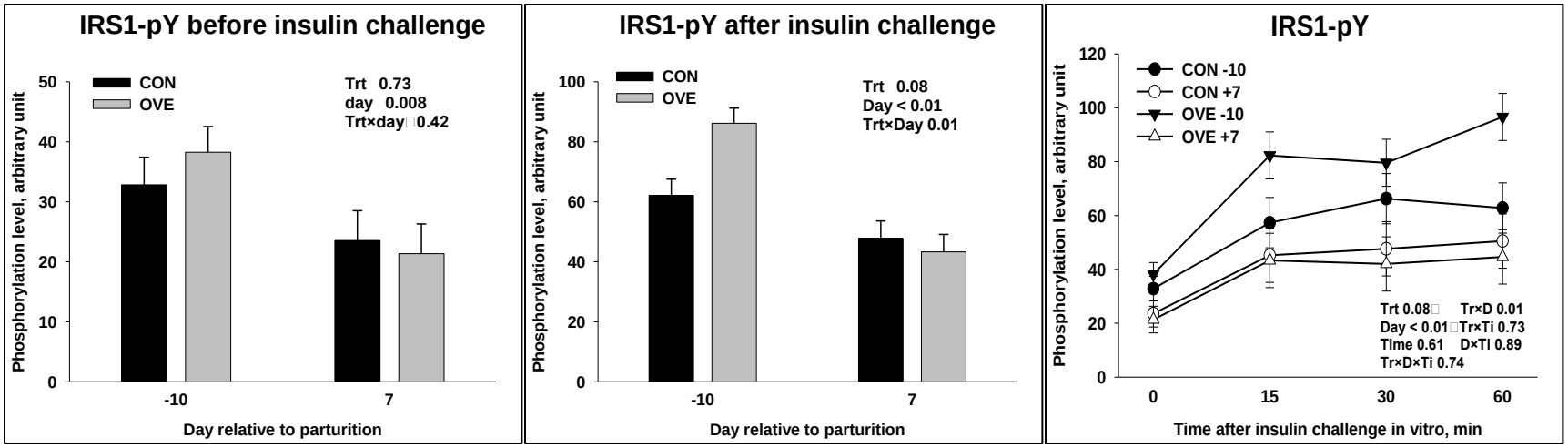

Figure 5.11. IRS1 tyrosine phosphorylation (IRS1-pY) in vitro. Phosphorylation level, expressed as arbitrary units, is calculated by dividing the absorption value of IRS1 tyrosine phosphorylation by absorption value of total IRS1. Data for d -10 are from 7 animals of each treatment, and data for d +7 are from 6 animals of each treatment. *P* values of main effect and interactions are listed in each panel. (A) IRS1-pY level without insulin challenge. Phosphorylation level are determined in adipose tissues that were minced and incubated in culture medium at 37°C for 30 min; (B) IRS1-pY level after insulin challenge. Phosphorylation level were determined in minced adipose tissue that were challenged with hyperphysiological bovine insulin for 15, 30, and 60 min. (C) Temporal tyrosine phosphorylation level of IRS1 before and after insulin challenge. All the *P* values for main effects and interactions are based on the data of IRS1-pY after insulin challenge. Least significant mean for 0 min are the values shown in (A).

CHAPTER 6

SUMMARY AND CONCLUSIONS

Experiment 1and 2 (chapters 3, 4, and 5) were conducted to evaluate the effect of dietary energy plane (moderate energy diet, OVE vs. controlled energy diet, CON) on transcriptomic change of mesenteric (MAT), omental (OAT), and subcutaneous (SAT) adipose tissues (AT) of multiparous non-pregnant non-lactating Holstein dairy cows through either quantitative PCR (qPCR) or microarray techniques (only for MAT and SAT in microarray), respectively.

In experiment 1 (chapters 3 and 4), no significant interaction of main effects (energy level and AT site) was detected in gene expression, hence only main effects were discussed. Overfeeding energy significantly increased gene expression associated with *de novo* fatty acid synthesis (*ACLY*, *ACACA*, *FASN*, *ELOVL6* and *SCD*), triglyceride synthesis (*GPAM* and *LPIN1*), fatty acid transportation (*FABP4*) transcriptional factors (*PPARG* and *THRSP*) and adipokines (*LEP* and *CCL2*). There was no treatment effect on mRNA profiles of genes related to uptake of preformed fatty acid (*LPL*, *CD36* and *ACSL1*), lipolysis (*HSL*) and other pro-inflammatory cytokines (*TNF*, *IL6* and *IL1B*), chemokine (*CCL5*) and acute phase protein (*SAA3*). The expression of *SREBF1*, of which the protein product was well-established lipogenic transcriptional factor in rodent liver, was decreased in response to energy overfeeding in AT. Visceral AT (MAT and OAT) exhibited higher expression genes involved in LCFA uptake, activation and transport (*LPL*, *ACSL1* and *FABP4*) and esterification (*GPAM*, *LPIN1*) than those in SAT, whereas the mRNA expression of most genes participated in DNS (*ACACA*, *FASN* and *SCD*) were higher in SAT compared with visceral AT. Generally, visceral AT, particularly MAT,

showed higher expression of adipocytokines (*ADIPOQ*, *LEP*, *IL1B*, *IL6*, *CCL2*, *CCL5* and *SAA3*) than SAT. In summary, overfeeding dietary energy may stimulate lipid accumulation (reflected by increased expression lipogenic and triglyceride synthesis genes) and adipocyte differentiation (represented by increased expression of classic mature adipocyte gene *FABP4*) equivalently in both visceral AT and SAT. The genes in DNS pathway showed greater sensitivity in response to increased energy intake in form of non-fiber carbohydrate (NFC) feeds. Our results highlight the central role of PPARγ, at least from mRNA level, in transcriptional regulation of lipogenic gene expression in bovine adipose tissue. The increased expression LEP may indicate the increased feedback signal from AT to inhibit feed intake. Most adipocytokines were not differentially expressed due to energy over-consumption, except higher expression of *CCL2*, which may contribute to increased chemotaxis of macrophage recruitment into AT and subsequently increased inflammation status. In comparison with the other, visceral AT may be more prone to utilize preformed fatty acid, whereas SAT may accumulate more lipids through DNS pathways. Visceral AT may have greater endocrine activity by secreting various adipokines including pro-inflammatory cytokine, chemokine and acute phase protein, which may be more detrimental to animal health, especially hepatic integrity, due to the direct portal drainage to liver.

In experiment 2, MAT and SAT from a subset of animals in Exp. 1 and 2 (5 animal from each dietary treatment) were analyzed for transcriptional adaptation of AT to over-consumption of energy through microarray technique. The statistics analysis revealed 409 and 310 differentially expressed genes (DEG) (FDR ≤ 0.2; unadjusted $P < 0.007$) due to AT depot and dietary energy level, respectively. The bioinformatics analysis via dynamic impact approach (DIA) based on KEGG Pathway database uncovered that the most represented pathway in comparison between fat depots were extracellular matrix (ECM)-receptor interaction, focal

adhesion, adipocytokine signaling, butyrate, sphingolipid and amino acid metabolism, whereas overfeeding energy significantly impacted immune cell trafficking, metabolism of xenobiotics by cytochrome P450, and MAPK signaling pathway in AT of dairy cows. Consistently, functional analysis via GeneSpring GX 7 unveiled that extracellular region and cytoskeleton structure, blood vessel morphology, and regulation of protein and carboxylic acid metabolism were the most enriched cellular component (Cc) and biological process (Bp) in comparison of fat depot. Excess energy intake markedly impacted the functions of cell-substrate and cell-matrix adhesion, response to external stimuli and MAPK signaling in AT compared with controlled energy feeding.

By looking into the DEG sets involved in the over-represented pathways and functions and the established connections among these DEGs primarily based on molecular studies cell culture, and rodent model and human subjects, we deducted that the signature difference between SAT and MAT may lie in the ECM component, angiogenic activity, cytoskeleton structure and endocrine functionality. SAT may be more active in modification of ECM components, particularly in collagen synthesis, whereas MAT may have greater potential in development of capillary network, cytoskeleton structure and be more subjected to the infiltration of immune cells. Compared with CON, overfeeding may induce adipocyte apoptosis by stimulating differentiation and hypertrophy of the cells, which can subsequently induce the recruitment of immune cells, the production of pro-inflammatory cytokines and exacerbate inflammation status. The transcriptomic evidence of current study highly implicated the involvement of MAPK-JNK pathway in energy overfeeding induced adipocyte differentiation and apoptosis.

In experiment 3, 14 (a subset from a large herd study) Holstein dairy cows (≥ 2 parity) were used to study the effect of prepartal dietary plane of energy (close-up overfeeding energy,

Overfed vs. controlled energy feeding, Controlled) on physiological changes and milking performance of animals and transcriptional adaptation of SAT during transition period. Insulin sensitivity of SAT in periparturient period was evaluated by measuring the IRS1-tyrosine phosphorylation (IRS1-pY) in vitro after challenging with hyperphysiological bovine insulin. Compared with Controlled group, Overfed cows had greater prepartal energy balance due to the higher DMI, greater prepartal serum insulin and numerically lower prepartal and higher postpartal serum NEFA, but significant increase of postpartal serum NEFA, which indicated the greater lipolytic activity postpartum. Close-up overfeeding energy did not benefit milking performance (neither milk production nor milk components production or percentage), but increase hepatic lipid accumulation. The mRNA expression of lipogenic genes in AT were higher in Overfed than in Controlled at -10 d, but decreased to the similar level in both groups postpartum (7 and 21 d). Overfed cows had greater transcriptional profiles of lipolytic gene expression (*ATGL* and *ABHD5*) and lower in *PDE3B* mRNA at -10 and 7 d. A significant interaction of prepartal dietary energy plane (Overfed vs. Controlled) and time relative to parturition (-10 vs. 7 d) was detected *in vitro* for insulin-stimulated IRS1-pY in AT, of which Overfed had higher and lower IRS1-pY in pre- (-10 d) and early postpartum (7 d) than Controlled group. Furthermore, for both groups, the IRS1-pY was significantly depressed at 7 d than that in -10 d. Our results suggested that overfeeding did not compromise the AT insulin sensitivity in prepartum, hence the higher circulating insulin may stimulate lipogenesis (as supported by higher expression of lipogenic gene in AT) and help reduce lipolysis in late pregnancy (lower prepartal NEFA). The same expression pattern of *ATGL* and *PPARG* support the evidence from rodent AT study that *ATGL* is PPARγ target gene. Hence, we speculate that overfeeding increased adipogenesis, which is paralleled with increased expression of lipolytic

gene. Despite the greater expression of triglyceride lipase (*ATGL*), the potentially higher re-esterification process and insulin's anti-lipolytic activity may override the lipolytic effects prepartum. In early lactation, the AT insulin sensitivity was markedly reduced in both groups as well as the lipogenic activitiy, which may be due to the overwhelming homeorhetic adaptation. The shift of metabolism from anabolism to catabolism during transition period favors mobilization of body reserves. The greater expression of *ATGL* and *ABHD5*, and lower expression of *PDE3B* in Overfed early postpartum may contribute to significantly increased lipolysis and reduced anti-lipolytic capacity in those animals. It turned out that increased lipolysis in response to prepartal overfeeding gives no benefit in milk production, but potentially compromise liver integrity and being detrimental to animal health postpartum.

Overall Conclusion

Dairy cow can easily over-consume energy during dry period, which resulted in increased BW and BCS. Our results clearly demonstrated the increased BCS was, at least partly, due to increased mRNA expression of lipogenic genes in AT. However, minor different response was observed when overfeeding energy in non-pregnant non-lactating cows (NPNL) compared with preparturient dairy cows. in NPNL, only genes associated with DNS (*ACLY*, *ACACA*, and *FASN*) was upregulated in response to energy overfeeding, whereas genes involved in both DNS and uptaking preformed FA (*LPL* and *ACSL1*) were increased prepartum in OVE vs. CON. Thus, such difference may associate with specific physiological state, which is characterized as altered hormonal environment and metabolic status. The signal of greater dietary energy plane that leads to increased mRNA expression of lipogenic genes is transducted by several "mediators". Our results, from transcriptional perspective, highlighted the importance of PPARγ and CEBPα as the major transcriptional factor inducing lipogenic gene expression in bovine adipocyte. Prepartum

overfeeding energy in from of greater NFC feed ingredients was found to increase (despite numerically) propionate production in rumen fermentation (Richards et al., unpublished data), which results in increased hepatic glucogenesis and stimulates greater insulin secretion subsequently. We speculate the greater blood insulin concentration in OVE vs. CON serves as the external mediator induce the transactivity of PPARγ and CEBPα, and triggers lipogenesis in perparturient period.

Reduced insulin response and utilization of glucose is an important metabolic adaptation of peripheral tissues in transition dairy cows (Bauman and Currie, 1980). Previous study from our group showed preparturient overfeeding energy resulted in increased blood insulin and glucose concentration prepartum and increase mobilization of body fat postpartum, which leads us to the hypothesis of exacerbated insulin resistance in peripheral tissue of transition dairy cows by energy overfeeding. In current study, we utilized IRS1-pY as an indicator for insulin effectiveness in AT. However, our results indicated that two stage feeding program (far-off CON and close-up OVE) did not comparomised AT insulin sensitivity in window from -10 to 7 d relative to parturition, but actually facilitated preparturient insulin signaling in AT as demonstrated by higher IRS-pY in OVE than CON at -10 d. Nevertheless, such results does not warrant us to exclude the possibility of incurred insulin resistance in dairy cows induced by long-term energy overfeeding (such as 8 wk overfeeding in experiment 1, in which we found the reduced insulin-to-glucose ratio in OVE group), which maybe more resemble to obesity induced insulin resistance in non-ruminant animals. I speculate, at cellular level, the adipocyte differentiation induced by close-up OVE is still in the normal stage, whereas long-term OVE may cause the over-enlargement of adipocyte and resulted in pathogenesis of insulin resistance which should be deemed as the self-protection behavior to adipocyte per se.

Our result of IRS1-pY also clearly showed that AT is more insulin resistant in early lactation (at least in window < 7 DIM) than in late pregnancy (at least in window < -10 d), which, we speculate, contributes to sharply increase postparturient lipolysis in AT. Hence, any nutritional management (in pre- and/or postpartum) that can improve insulin sensitivity postpartum may rescue animal from over-mobilization of body fat, which triggers ketosis, fatty liver and other metabolic disorders in early lactation.

Absolutely, our IRS1-pY results needs to be confirmed in futher research, and should be extended to more molecules involved in insulin signaling pathway, such as upstream INSR tyrosine kinase activity and downstream kinase activities.

Another important finding of our research is the increased *ATGL* and *ABHD5* expression in AT of OVE cows prepartum (-10 d) and early postpartum (7 d), which gave partial explanation of greater serum NEFA in OVE cow postpartum. Evidence from rodent study showed that *ATGL* is one of target gene of PPARγ (Kershaw et al., 2007). Our results showed the same expression pattern of *ATGL* and *PPARG*, hence, I propose that OVE increased PPARγ activity, which, in turn, stimulated *ATGL* mRNA expression. Certainly, such hypothesis needs to be tested in cellular study of bovine adipocytes in futher.

Unlike our hypothesis, we did not find prevailing evidence that overfeeding increased mRNA expression of pro-inflammatory cytokines in AT (SAT, MAT and OAT). However, our results supported that overfeeding may result in increased portal drainage of pro-inflammatory cytokines produced from visceral AT to liver by increasing visceral AT mass, which is characterized by greater expression of gene encoding pro-inflammatory cytokines and chemokines (either due to visceral adipocyte or resident macrophages) than SAT.

In general, as supported by our results, we suggest that continues controlled feeding during dry period did not compromise production performance postpartum and is more beneficial to animal health postpartum by decreasing metabolic disorders.

LITERATURE CITED

Bauman, D. E., and W. B. Currie. 1980. Partitioning of nutrients during pregnancy and lactation: a review of mechanisms involving homeostasis and homeorhesis. J. Dairy Sci. 63:1514-1529.

Kershaw, E. E., M. Schupp, H. P. Guan, N. P. Gardner, M. A. Lazar, and J. S. Flier. 2007. PPARgamma regulates adipose triglyceride lipase in adipocytes in vitro and in vivo. Am. J. Physiol. Endocrinol. Metab. 293:E1736-E1745.

APPENDIX A

STUDY OF HEPATIC LIPID ACCUMULATION, FIBROSIS, AND AGGREGATION OF MATURE MACROPHAGES VIA HISTOCHEMICAL AND IMMUNOHISTOCHEMICAL TECHNIQUE

ABSTRACT

To evaluate the histological and pathological changes in liver of transition dairy cows, repeated liver biopsies were conducted in 17 Holstein dairy cows (≥ 2 parity) at -10, 7, and 21 d relative to parturition date (3 cows had all 3 biopsy samples, 7 cows had 2 samples, the remaining cows had only 1 sample). Formalin-fixed and paraffin-embedded liver sections were processed for hematoxylin and eosin (H&E) staining, and Masson's trichrome (MT) staining and counter-stained with hematoxylin. The H&E staining section gives the shape of hepatocyte and intracellular lipid droplets, and enables the observation for ballooning degree, Mallory body, and the aggregation of monocytes (primarily neutrophils and leukocytes), which indicates the different stages of progression of pathological development and hepatocyte apoptotic activity. Staining with MT distinguishes the hepatocytes from surrounding connective tissues by dying the collagen blue, which implicates hepatic fibrosis degree as a sign of increased cirrhosis. The whole slide (containing triplicate sections of each slice) was scanned using a NanoZoomer Digital Pathology (NDP) System (Hamamatsu Co., Bridgewater, NJ). ImageJ imaging software was used in attempt to calculate the lipid droplet area as the percentage of total section area from the scanned whole slide image. Immunohistochemistry was utilized to detect mature macrophage (including resident Kupffer cells and infiltrated macrophages) in formalin-fixed and paraffin-embedded liver section (rat monoclonal F4/80 as primary antibody and rat ABC staining system: sc-2019; Santa Cruz Biotechnology, inc.). The image of the entire H&E stained section clearly

showed almost no lipid accumulation in hepatocyte at -10 d prepartum, but large occupation of intracellular lipid droplets was witnessed at 7 d postpartum (macrovesicular steatosis), which was sustained, and probably increased, at 21 d postpartum. Intriguingly, the most macrovesicularity was located in the perivenous area and exhibited a radiatial shape surrounding the central vein. In periportal zone, the hepatocytes were characterized by the formation of numerous small lipid droplets (microvesicularity) postpartum. The hepatocytes located in the intermediate zone had the least lipid storage. The infiltration of monocytes and suspected Mallory bodies in lipid-accumulated area was observed in a few samples of 21 d postpartum. Furthermore, no MT-stained collagen was observed in samples. We failed to detect mature macrophages in the liver sections. Although the exact reason for this is unknown, we speculate that incompatibility of the primary antibody may account for the failure of the experiment. Preliminary conclusions based on the limited number of replicates indicate that most postpartal fatty liver (non-clinical) in response to sharply increased lipid mobilization from peripheral tissues may develop into the macrovesicular stage. The correlations among lipid content, immune cell infiltration and activation, hepatocyte apoptosis, cirrhosis, and the clinical signs of the whole animal warrant further researches. The intention to quantify the lipid content by analyzing the surface lipid droplet area in hepatic section via ImageJ software requires future work to correlate the results given by ImageJ with the actual quantity analyzed through chemical method.

INTRODUCTION

Triglyceride (TAG) accumulation is commonly seen in early lactating dairy cows, particularly for high producing cows, which may be more vulnerable to develop into pathological conditions such as ketosis and fatty liver disease. Practically, the ratio of hepatic lipid to

glycogen exceeding 2:1 is considered as the alarm of pathological disorders (Grummer, 1993; Drackley et al., 2001). However the underlying mechanism for hepatic metabolic disorders induced by increased infiltration of lipid is still unclear. Accumulating evidence from studies of non-alcoholic fatty liver disease (NAFLD) with rodent models implicates the causative connection between hepatocyte lipid accumulation and endoplasmic reticulum (ER) stress, activation of immune cells, inflammation, and, consequently, steatohepatitis (Mollica et al., 2011). In addition, chronic over-nutrition has been shown to induce liver inflammation due to increased release of pro-inflammatory cytokines from adipocytes (Tilg, 2010). Previous research from our research group demonstrated that cows overfed dietary energy during the dry period had increased postpartal hepatic lipid accumulation and were more susceptible to insults of ketosis and other metabolic disorders compared with cows fed controlled or restricted energy diets (Dann et al., 2006; Janovick et al., 2011). Therefore, we speculate that in addition to increased lipid infiltration per se, other mechanisms may also contribute to postpartal hepatic pathogenesis.

In rodent models, hepatic steatosis histologically manifests as the accumulation of macrovesicular or microvesicular lipid droplets inside hepatocytes. The appearance of ballooning hepatocytes, Mallory bodies in swollen hepatocytes, and recruitment and activation of immune cells are closely associated with hepatic pathogenesis (Reddy and Rao, 2006). Kupffer cells represented more than 80% of tissue-resident macrophages in rats (Bouwens et al., 1986), the activation of which is the hallmark of inflammation (Baffy, 2009). Fibrosis of hepatic tissues is linked with liver cirrhosis (Paradis and Bedossa, 2008). Hepatocytes located in each zone (periportal, transition, and perivenous zones) are functionally different. From periportal to perivenous zone, there is a gradient decrease of oxygen concentration. Periportal hepatocytes are

more prominent in oxidative function, such as β-oxidation of fatty acids, whereas the perivenous zone is characterized by higher lipogenic activity (cited from Wikipedia website, refer to Bacon et al., 2006). Therefore, each zone may play different roles in pathological development of hepatosteatosis.

To our knowledge, there is very limited literature recording hepatic histological changes of transition dairy cows. In the current study, we characterized the hepatic morphological alterations with focus on lipid accumulation and pathogenesis in periparturient dairy cows using the grading system from study of hepatic steatosis in a rodent animal model.

MATERIALS AND METHODS

Experimental Design, Diets, Animals, and Liver Biopsy

This study used a subset of animals from a large herd study. Experimental design and dietary treatment were the same as described in Chapter 6. Liver biopsy was conducted at -10, 7, and 21 d relative to parturition date. However, the insufficient number of animal replicates and incomplete biopsies (only one or two biopsies were available) for several animals did not allow us to make any statistical analyses.

Preparation for Tissue Section: Fixation, Dehydration, and Embedding

An aliquot of liver tissue (ca. 0.5 × 0.5 × 0.5 cm^3) was dissected immediately after biopsy, and immersed into 10% formalin solution (equivalent to 4% formaldehyde solution) for fixation of cellular morphology overnight (preferred) or longer. Then, the sample was put blocked into a cassette (with the sample number marked on cassette with pencil) and subjected to the dehydration process by sequentially passing through a series of increasing alcohol concentration solutions: 30%, 50%, 70%, 80%, 90%, 95%, and 100% for ca. 2 h for each step. After dehydration, tissue was cleared with xylene solution 3 × 10 min and finally embedded with

melting paraffin and cooled down for 60 min to be ready for sectioning. Multiple 5-micron sections were sliced, and triplicates of sections were placed on each glass slide (Histology Lab, College of Veterinary Medicine at University of Illinois at Urbana-Champaign).

Hematoxylin and Esion (H&E) Staining

Hematoxylin colors the nuclei blue, whereas counterstaining with eosin marks the cytoplasm pink. The empty original lipid droplet areas are not stained, hence it appears white in light microscope. The glass slides containing liver tissue sections were dipped into the following solutions sequentially as below (protocol provided by Histology Lab, College of Veterinary Medicine at University of Illinois at Urbana-Champaign):

1) De-paraffinizaion and re-hydration section:

   Xylene solution: 3 × 2 min each; 100% ethanol: 2 × 2 min each; 95% ethanol: 2 min; 70% ethanol: 2 min; wash in running tap water: 2 min

2) Hematoxylin (from Surgipath) staining: 2 min;

   Wash in running tap water: 2 min; dip in Define ca. 6 seconds; wash in running tap water: 1 min; 95% ethanol: 2 × 1 min each

3) Eosin/Phloxine (from Richard Allen) staining: 30 sec

4) Dehydration and clearance

   95% ethanol: 2 × 1 min each; 100% ethanol: 2 × 2 min each; xylene: 3 × 2 min each;

5) Mount with xylene based mounting medium and coverslip slides.

Masson's Trichrome (MT) Staining

MT is a tri-color staining, which is generally utilized to differentiate cells from surrounding connective tissues. Due to its coloration of collagen with blue, it is used histologically to determine the fibrosis development in hepatic tissue. H&E stained slides were

counterstained with MT in the current study, of which the nuclei were dark blue and cytoplasm dark pink (The protocol is provided by Histology Lab, College of Veterinary Medicine at University of Illinois at Urbana-Champaign).

Solutions required: 1) Bouin's solution: 75 mL Picric acid (saturated aqueous solution), 25 mL Formaldehyde (37 – 40%), 5 mL Glacial acetic acid; 2) Weigert's iron hematoxylin working solution: mixture of equal volume of solution A and B (make working solution just before use); solution A: 5 g Hematoxylin in 500 mL 95% ethanol; solution B: 20 mL Ferric chloride (29% aqueous solution), 5 mL Glacial acetic acid, 475 mL deionized water; 3) Biebrich Scarlet-Acid Fuchsin solution: 180 mL Biebrich scarlet (1% aqueous solution), 20 mL acid fuchsin (1% aqueous solution), 2 mL Glacial acetic acid; 4) phosphomolybdic/phosphotungstic acid solution (PPA): 5 g phosphomolybdic acid and 5 g phosphotungstic acid dissolved in 200 mL deionized water; 5) Aniline Blue solution: 2.5 g Aniline blue, 2 mL Glacial acetic acid, 100 mL deionized water; 6) Acetic water: 1 mL Glacial acetic acid, 99 mL deionized water.

The slides were dipped into the following solutions sequentially as listed below:

1) Bouin's solution: 1 hr at 60°C;
2) Rinse in running water;
3) Weigert's iron hematoxylin: 10 min;
4) Biebrich scarlet-Acid fuchsin solution: 2 min;
5) Rinse in distilled water (dH_2O);
6) PPA solution: 10 min;
7) Quick rinse in dH_2O;
8) Aniline blue solution: 5 min;
9) Rinse in dH_2O;

10) 1% acetic water solution: 2-3 min;

11) Following step 4) and 5) described in H&E staining

Determination of Hepatic Mature Macrophages via Immunohistochemical Technique

The Emr1 (designated F4/80, EGF-like molecule containing mucin-like hormone receptor 1) was characterized by an extracellular region with several N-terminal epidermal growth factor (EGF) domains, and predominantly expressed on surface of macrophages and serves as a marker for tissue-resident mature macrophage (Baud et al., 1995). In the current study, rat monoclonal F4/80 antibody (Ab) was utilized as primary Ab (catalogue #: sc-52664; Santa Cruz biotechnology, Inc.) combined using immunoperoxidase staining (ImmunoCruz^{TM} rat ABC staining system, catalogue #: sc-2019; Santa Cruz biotechnology, Inc.) to delineate bovine Kupffer cells. The principle for ABC staining is biotinylated secondary Ab that binds to primary Ab was connected to biotinylated horseradish peroxidase (HRP) by bridging of avidin, which is a tetrameric biotin-binding protein. With the addition of peroxidase substrate and chromogenic substance (3, 3'-Diaminobenzidine, DAB, is used), the peroxidase connected to compound of F4/80-primary Ab-secondary Ab can catalyze the reaction and produce the colored products for visualization and quantification of the marked Kupffer cells.

In prevention of masked antigen by formalin fixation and paraffin embedding, unmasking steps (heat treatment) were performed prior to application of primary antibody. Briefly, slides were placed in a container, covered with 10 mM sodium citrate buffer (pH 6.0), and heated at 95°C for 5 min. Slides were allowed to cool in the buffer for approximately 20 min. Slides were washed in deionized water three times for 3 min each. Excess liquid was aspirated from slides.

After antigen restoration, slides were incubated in primary Ab PBS solutions of differentially diluted concentrations (1:50, 1:100, and 1:200) to obtain the maximal signal. All

the following immunoperoxidase staining steps was carried out following the kit's protocol (ImmunoCruz^{TM} rat ABC staining system, catalogue #: sc-2019; Santa Cruz biotechnology, Inc.)

RESULTS AND DISCUSSION

We use cow 7979 as an example (shown in Figure A.1) to demonstrate the histological change and progression of lipid accumulation during transition period (biopsied at -10, 7, and 21 d). By comparison with other cows, this cow had a very low grade of lipid accumulation postpartum, but the postpartal distribution of lipid droplet was still representative of the common situation as we found in other liver sections of most cows in current study. In the top picture of Figure A.1 (biopsy at -10 d), no visible lipid droplet was found in the whole section, which is consistent with the low circulating NEFA in cows at this time (refer to chapter 6, cows used here were from the same study as described in chapter 6). At 7 d postpartum (middle picture in Figure A.1), sporadic hepatocytes with single macro-lipid vesicle (macrovesicle) were observed in perivenious area, whereas the hepatocytes surround the periportal area was almost free of the lipid infiltration. Despite no excessive increase of lipid storage at 21 d postpartum (bottom pic. in Figure A.1), it is still obvious that the number of macrovesicular hepatocytes increased surrounding the hepatic vein together with the population of hepatocytes with a number of micro-lipid droplets in both perivenious and, to a less extent, periportal zone. Three pictures in Figure A.2 showed the liver sections of cow 8189 from biopsy at -10 (top), 7 (middle) and 21 d (bottom), respectively. Cow 8189 received the same dietary treatment as cow 7979 from dry-off until 30 days of lactation, but this cow experienced more drastic increase of hepatic lipids postpartum that can be visually determined very easily. Despite the substantial variation of lipid content between the two cows, the distribution and progression of hepatic lipid showed the same pattern as cow 7979.

In Figure A.3, we demonstrated the section (cow 8159, 21 d postpartum) of the most excessive postpartal lipid infiltration (visually determined) among all the samples in the current study. Intriguingly, the holistic view of section (top pic. in Figure A.3) clearly showed transition zone (intermediate area between perportal and perivenous area) colored the pinkest compared with other areas, which indicated the lowest fat storage in these hepatocytes. Furthermore, we observed the two colonies of aggregated immune cells (mostly neutrophils and lymphocytes) in the perivenous area of the greatest macrovesicular hepatocytes (bottom pic. in Figure A.3 and lower pic. in Figure A.4). A suspected Mallory body, which is considered an important hallmark of non-alcoholic steatohepatitis (NASH) in human individuals (Machado and Cortez-Pinto, 2011), was observed in a remarkably enlarged hepatocyte in the perivenous area (upper picture in Figure A.4).

No obvious MT-stained collagen was observed in slides under light microscope, hence we speculate that these animals did not progressed into fibrosis stage, the marker of liver cirrhosis (liver slides stained with MT were not scanned).

We failed to mark Kupffer cell by using rat F4/80 primary Ab. In this experiment, we tried two methods to unmask antigen, which may be caused by formalin fixation and paraffin embedding, and three concentrations of primary Ab on several liver slides from different dairy cows; thus, we speculate the compatibility of primary Ab may be the reason for our lack of success.

Based on the results from these individual cows, it seems that hepatic lipid infiltration initiated from perivenous zone with formation of numerous micro vacuoles of lipid droplets, which fused into a macro vacuole with continuation of higher circulating NEFA postpartum. The lipid occupation may start to extend to the periportal zone with the same progression pattern as

most hepatocytes in perivenous zone appeared to contain a single large lipid droplet. The transition zone is the area of the least vulnerability to accumulating lipid compared with other two zones. Such prioritized lipid storage pattern may result from zone-specific distribution of enzymes involved in TAG synthesis, which determines functional differences. We were not able to detect where Kupffer cells are primarily located, which requires further research. In addition, how hepatic lipid accumulation, infiltration and activation of immune cells, and inflammation status are correlated with the appearance of pathological disorders in cows should be the subject of further studies.

LITERATURE CITED

Bacon, B. R., J. G. O'Grady, A. M. Di Bisceglie, and J. R. Lake. 2006. Comprehensive Clinical Hepatology. Elsevier Health Sciences. ISBN 0323036759.

Baffy, G. 2009. Kupffer cells in non-alcoholic fatty liver disease: The emerging view. J. Hepatol. 51:212-223.

Baud, V., S. L. Chissoe, E. Viegas-Pequignot, S. Diriong, V. C. N'Guyen, B. A. Roe, and M. Lipinski. 1995. EMR1, an unusual member in the family of hormone receptors with seven transmembrane segments. Genomics 26:334-344.

Bouwens, L., M. Baekeland, R. De Zanger, and E. Wisse. 1986. Quantitation, tissue distribution and proliferation kinetics of Kupffer cells in normal rat liver. Hepatology 6:718-722.

Drackley, J. K., T. R. Overton, and G. N. Douglas. 2001. Adaptations of glucose and long-chain fatty acid metabolism in liver of dairy cows during periparturient period. J. Dairy Sci. 84: E100-E112.

Grummer, R. R. 1993. Etiology of lipid-related metabolic disorders in periparturient dairy cows. J. Dairy Sci. 76:3882-3896.

Machado, M. V., and H. Cortez-Pinto. 2011. Cell death and nonalcoholic steatohepatitis: where is ballooning relevant? Expert Rev. Gastroenterol. Hepatol. 5:213-222.

Mollica, M. P., L. Lionetti, R. Putti, G. Cavaliere, M. Gaita, and A. Barletta. 2011. From chronic overfeeding to hepatic injury: role of endoplasmic reticulum stress and inflammation. Nutr. Metab. Cardiovasc. Dis. 21:222-230.

Paradis, V., and P. Bedossa. 2008. Definition and natural history of metabolic steatosis: histology and cellular aspects. Diabetes Metab. 34:638-642.

Reddy, J. K., and M. S. Rao. 2006. Lipid metabolism and liver inflammation. II. Fatty liver disease and fatty acid oxidation. Am J Physiol Gastrointest Liver Physiol. 290:G852-858.

Tilg, H. 2010. The role of cytokines in non-alcoholic fatty liver disease. Dig. Dis. 28:179-185.

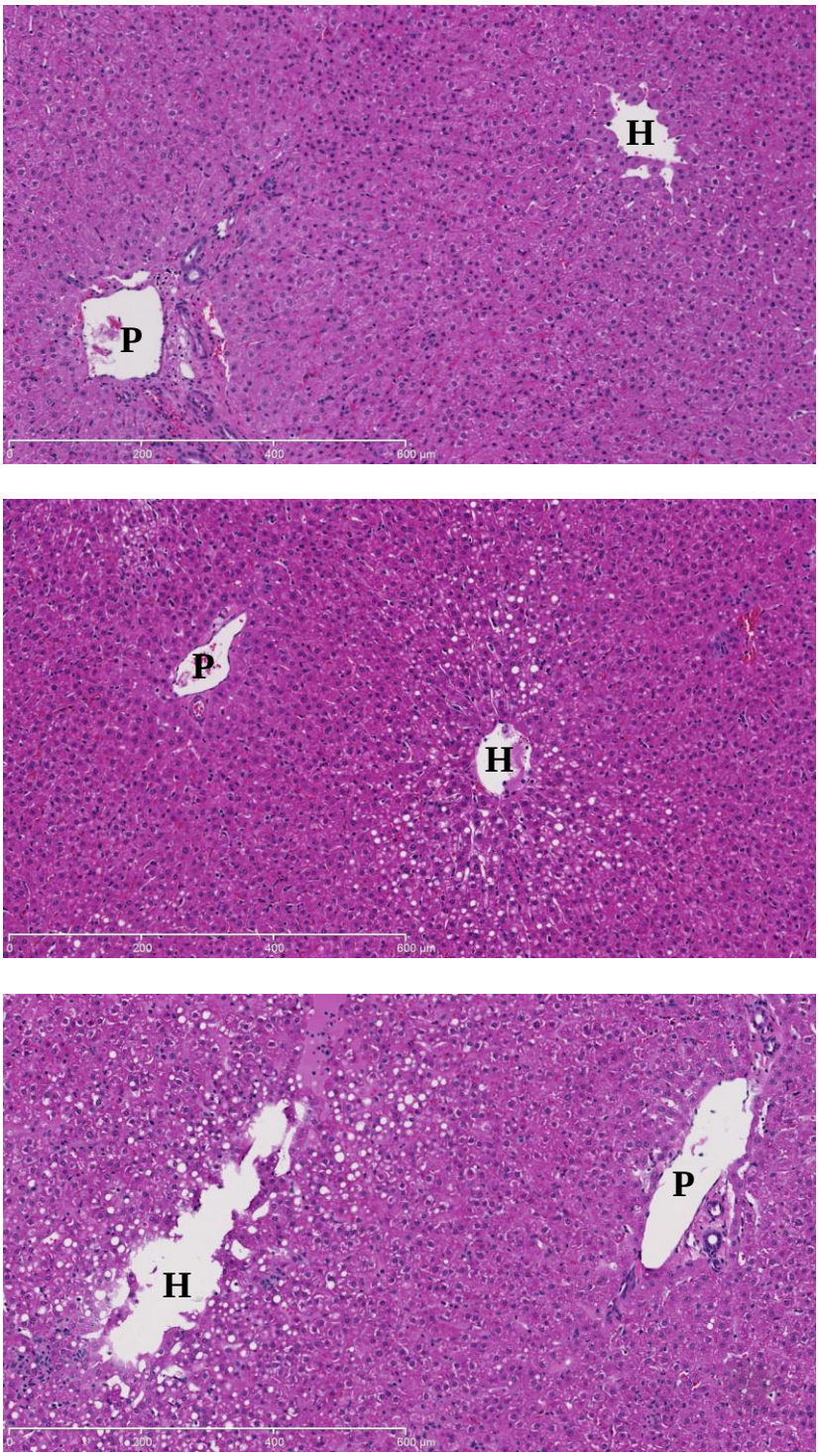

Figure A.1. Mild progression of hepatic lipid accumulation in liver sections of cow 7979 biopsied at -10, 7 and 21 d relative to parturition. (in each figure, H: central vein; P: portal vein) Top: -10 d sample; middle: 7 d sample; bottom: 21 d sample (H&E, 10×). These samples were not analyzed for lipid and TAG content through chemical method.

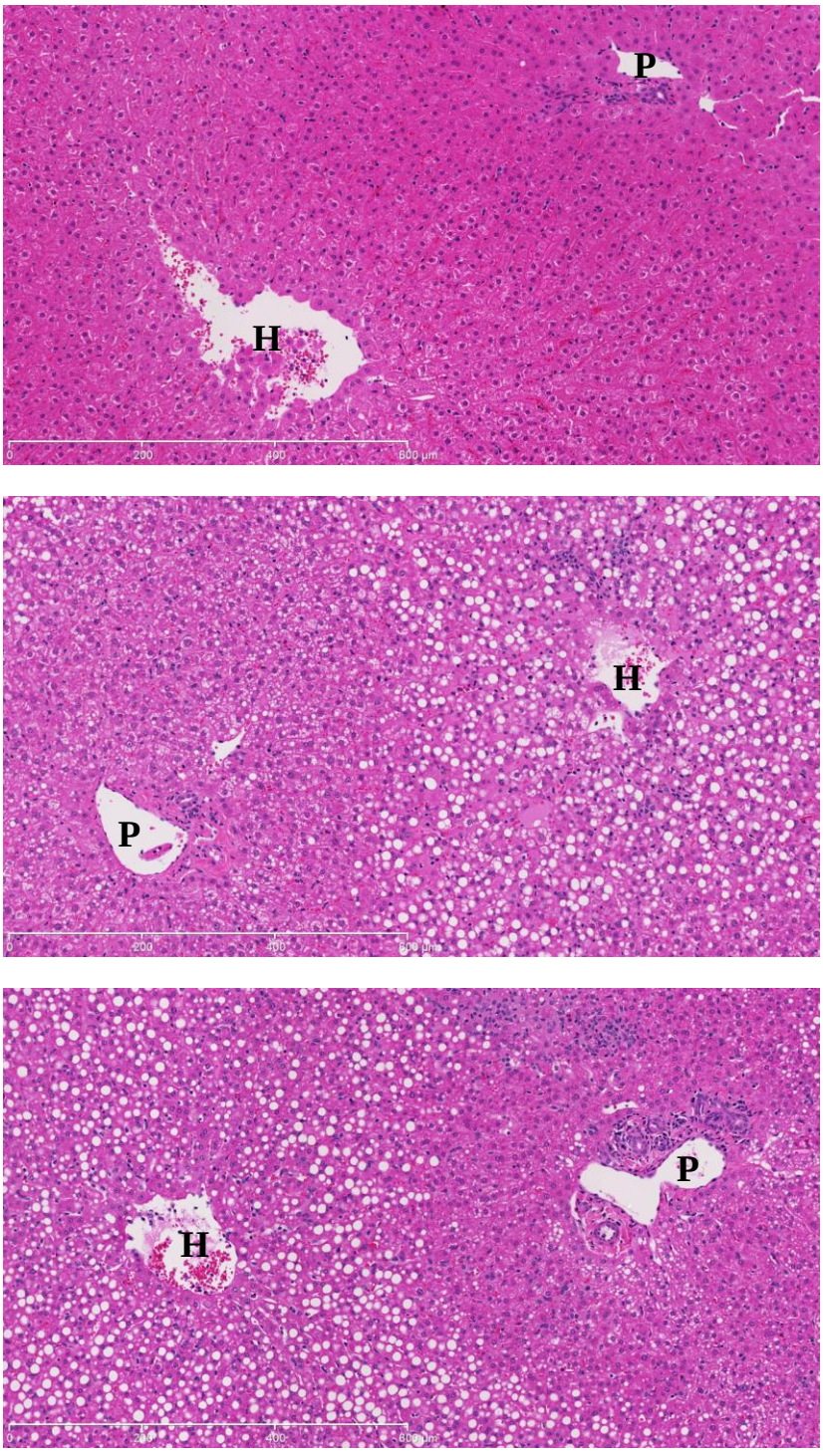

Figure A.2. Progressive increase of lipid accumulation in liver sections of cow 8189 biopsied at -10, 7, and 21 d relative to parturition. (in each figure, H: central vein; P: portal vein) Top: -10 d sample; middle: 7 d sample; bottom: 21 d sample (H&E, 10×). Chemical analysis for sample of this cow at -10, 7 and 21 d were 4.0, 15.1 and 12.6% for lipid content and 0.41, 1.09 and 8.93% for TAG content.

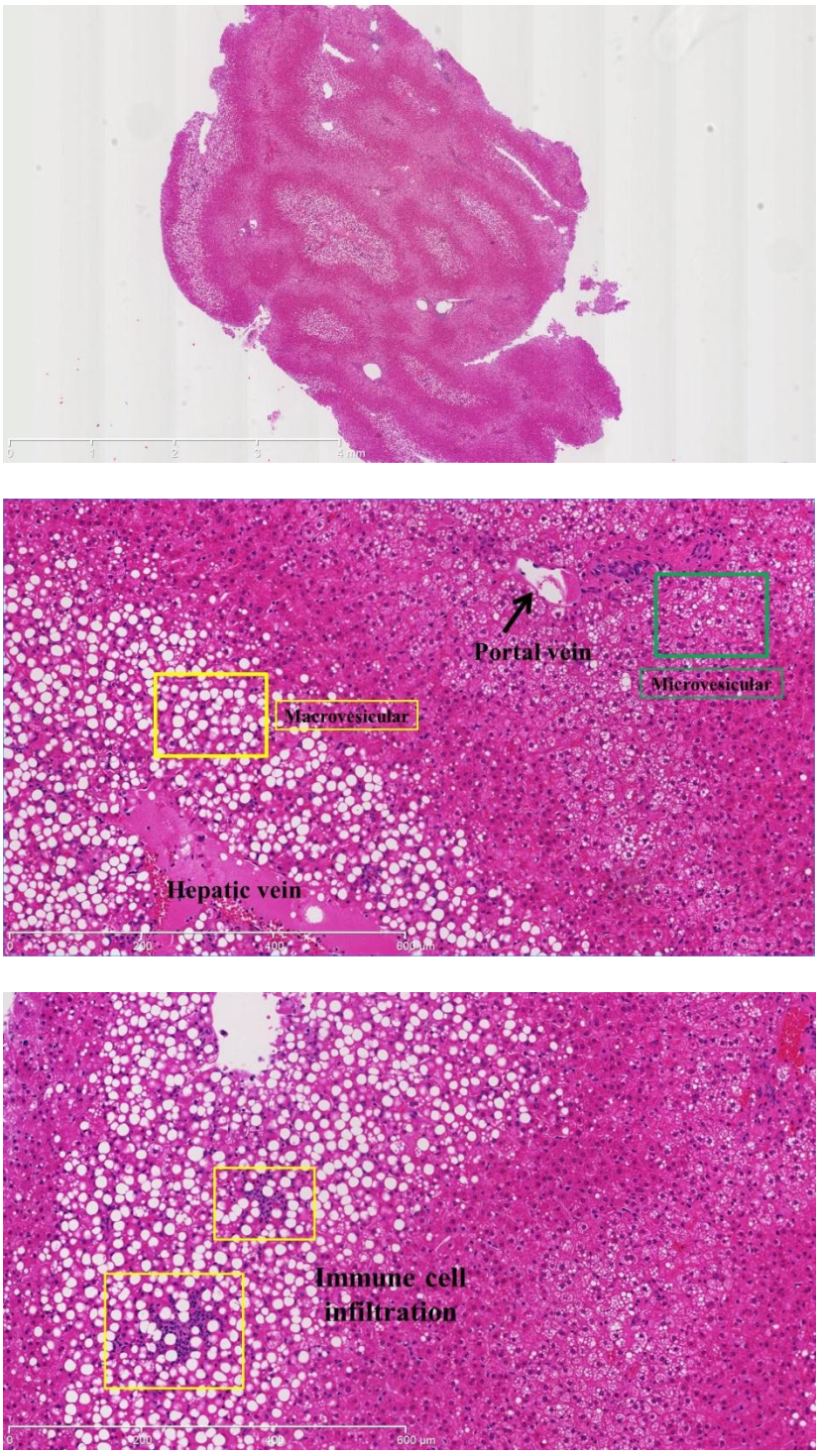

Figure A.3. Liver section of cow 8159 biopsied at 21 d postpartum (H&E). Top: holistic view of lipid distribution (1.25×); middle: pattern of intracellular lipid storage (macrovesicular vs. microvesicular) and the distribution of each pattern (10×); bottom: immune cell infiltration (10×). Chemical analysis for sample of this cow at -10, 7 and 21 d were 3.9, 16.3 and 17.4% for lipid content and 0.32, 1.61 and 6.51% for TAG content.

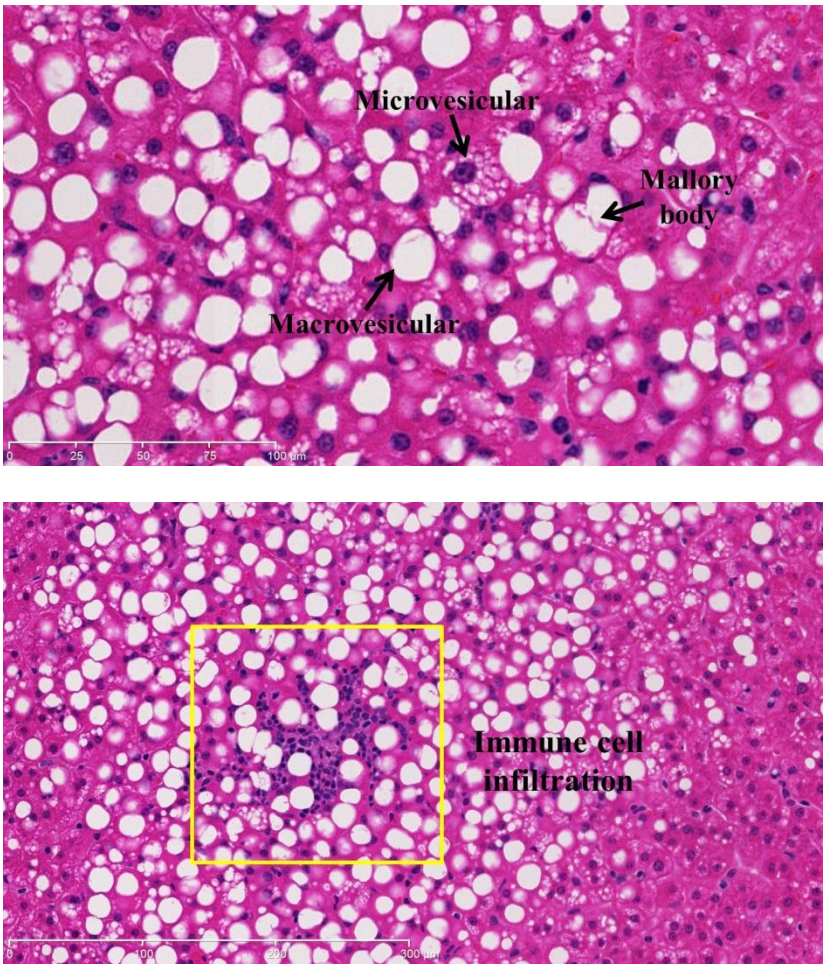

Figure A.4. Liver sample section of cow 8159 biopsied at 21 d postpartum (H&E). Upper: Macro- vs. microvesicular lipid storage in hepatocytes and suspected Mallory body (40×). Lower: immune cell infiltration (40×)

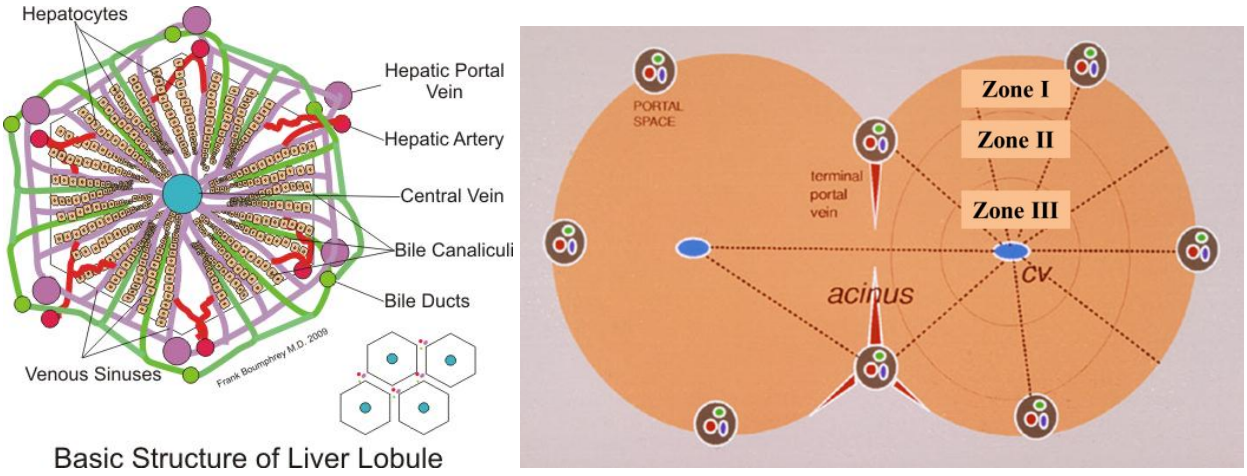

Figure A.5. Basic structure and zonation of liver acinus lobule. The picture on the left showed the basic structure of liver lobule. In the picture on the right, CV: central vein, Z I: periportal zone, Z II: transition zone, Z III: perivenous zone.

VITA

Peng Ji was born in Jilin City, Jilin province, China on June 3, 1982. He graduated from Jilin First High School in 2001. Peng attended Shenyang Agricultural University and received a Bachelor of Science degree in Animal Nutrition and Feed Sciences in 2005. Then, he started his graduate study in China Agricultural University with Dr. Sheng-Li Li as his advisor, and Peng received a Master of Science degree in Animal Science in 2008. After graduation, Peng joined Dr. James K. Drackley's laboratory and was co-advised by Dr. Juan J. Loor for his Ph.D. research.